

**Interaction of *Chlamydia trachomatis* with the host cell  
MHC class I antigen presentation pathway during  
active and persistent infection**

Dissertation

zur Erlangung des akademischen Grades  
„doctor rerum naturalium“ (Dr. rer. nat.)

vorgelegt dem Rat der Biologisch-Pharmazeutischen Fakultät  
der Friedrich-Schiller-Universität Jena

von Diplom-Biologin  
Christina Große  
geboren am 10. Januar 1982  
in Jena.

**Interaction of *Chlamydia trachomatis* with the host cell  
MHC class I antigen presentation pathway during  
active and persistent infection**

Dissertation

Submitted in partial fulfilment  
of the requirements for the degree of  
“doctor rerum naturalium” (Dr. rer. nat.)

Submitted to the council of the Faculty of Biology and Pharmacy  
at the Friedrich Schiller University, Jena

by Christina Große  
with degree in biology (Dipl.-Biol.)  
born on 10th January 1982  
in Jena.

Reviewers:

Prof. Dr. Eberhard Straube,  
Institute for Medical Microbiology,  
University Hospital, Jena, Germany

Prof. Dr. Axel A. Brakhage,  
Leibniz Institute for Natural Product Research and Infection Biology e.V.  
Hans-Knöll-Institute, Jena, Germany

Prof. Dr. Andreas Essig,  
Institute for Medical Microbiology and Hygiene,  
University Hospital, Ulm, Germany

Date of the public disputation: 17th October 2012

# Contents

<b>Index of figures .....</b>	<b>V</b>
<b>Index of tables .....</b>	<b>VII</b>
<b>Abstract .....</b>	<b>VIII</b>
<b>Zusammenfassung .....</b>	<b>X</b>
<b>Abbreviations .....</b>	<b>XII</b>
<b>1 Introduction .....</b>	<b>1</b>
<b>1.1 Chlamydia .....</b>	<b>1</b>
1.1.1 The family of <i>Chlamydiaceae</i> .....	1
1.1.2 The chlamydial developmental cycle .....	2
1.1.3 Interaction of <i>Chlamydia</i> with the host cell .....	3
1.1.4 The role of the chlamydial protease CPAF in <i>Chlamydia</i> host cell interaction ....	5
1.1.5 Chlamydial persistence.....	6
1.1.6 Immune response to <i>C. trachomatis</i> genital infection.....	8
1.1.7 <i>Chlamydia</i> -induced reactive arthritis .....	9
<b>1.2 MHC class I antigen presentation during chlamydial infection .....</b>	<b>10</b>
1.2.1 The MHC class I antigen presentation pathway.....	10
1.2.2 MHC class I presentation of chlamydial antigens to CD8+ T cells .....	12
<b>1.3 The aim of the present study .....</b>	<b>14</b>
<b>2 Material and Methods.....</b>	<b>15</b>
<b>2.1 Material .....</b>	<b>15</b>
2.1.1 Mammalian cells and bacterial strains .....	15
2.1.2 Material.....	15
<b>2.2 Methods .....</b>	<b>15</b>
2.2.1 Cell culture .....	15
2.2.2 Propagation of <i>C. trachomatis</i> .....	16
2.2.3 Infection procedure.....	16
2.2.4 Determination of inclusion number, IFUs and burst size.....	16
2.2.5 Preparation of cells for transmission electron microscopy.....	17
2.2.6 Confocal laser scanning microscopy of immunofluorescently stained cells.....	17
2.2.7 RNA isolation and reverse transcription .....	18
2.2.8 Analysis of gene expression with real-time quantitative PCR .....	19
2.2.9 ELISA for IFN- $\beta$ quantitation .....	20
2.2.10 siRNA transfection of fibroblasts.....	20
2.2.11 SDS-PAGE and immunoblotting .....	21
2.2.12 Flow cytometry.....	22
2.2.13 Cell-free cleavage assay .....	23

2.2.14	Immunoprecipitation of CPAF .....	24
2.2.15	Endoglycosidase H treatment .....	25
2.2.16	Fluorescence in situ hybridisation (FISH).....	25
2.2.17	Sample preparation for two dimensional (2D) gel electrophoresis .....	26
2.2.18	2D gel electrophoresis of chlamydial RBs .....	27
2.2.19	Statistics.....	27
<b>3</b>	<b>Results.....</b>	<b>28</b>
<b>3.1</b>	<b>Characterisation of the persistent-like growth state of <i>C. trachomatis</i> in fibroblasts.....</b>	<b>28</b>
3.1.1	Comparison of the replication cycle of <i>C. trachomatis</i> between epithelial cells and fibroblasts .....	28
3.1.2	<i>IDO</i> expression in <i>C. trachomatis</i> -infected fibroblasts .....	33
3.1.3	Role of <i>IDO</i> in growth inhibition of <i>C. trachomatis</i> in fibroblasts .....	35
3.1.4	Expression of selected chlamydial genes in epithelial cells and fibroblasts infected with <i>C. trachomatis</i> .....	37
3.1.5	Influence of <i>IDO</i> expression on chlamydial gene expression in fibroblasts infected with <i>C. trachomatis</i> .....	40
3.1.6	Differences in the expression of the chlamydial protease CPAF between active and persistent infection in epithelial cells and in fibroblasts .....	41
<b>3.2</b>	<b>Influence of <i>C. trachomatis</i> infection on the MHC class I antigen presentation pathway .....</b>	<b>43</b>
3.2.1	Surface expression of MHC class I in <i>C. trachomatis</i> infected cells .....	43
3.2.2	Influence of <i>C. trachomatis</i> infection on expression of key proteins involved in MHCI antigen processing and presentation .....	45
3.2.3	TAP2 degradation during active infection with <i>C. trachomatis</i> .....	49
<b>3.3</b>	<b>Role of Golgi fragmentation in the downregulated MHCI surface expression in actively <i>C. trachomatis</i> infected epithelial cells.....</b>	<b>51</b>
3.3.1	Fragmentation of the Golgi apparatus in <i>C. trachomatis</i> infected cells .....	51
3.3.2	Degradation of GM130 and Golgin-245 during active <i>C. trachomatis</i> infection.....	55
3.3.3	Role of CPAF in degradation of GM130 and Golgin-245 .....	56
3.3.4	MHCI co-localisation with GM130 in <i>C. trachomatis</i> infected cells .....	59
3.3.5	Change in sensitivity of MHCI molecules to Endoglycosidase H cleavage after active infection with <i>C. trachomatis</i> .....	62
<b>3.4</b>	<b><i>C. trachomatis</i> mediated degradation of the host cell mRNA export factor NXF1.....</b>	<b>63</b>
3.4.1	Influence of active <i>C. trachomatis</i> infection on NXF1 expression in HeLa cells.....	63
3.4.2	The role of CPAF in degradation of NXF1 .....	65
3.4.3	Analysis of NXF1 degradation during IFN- $\gamma$ mediated chlamydial persistence and chlamydial infection of fibroblasts .....	68
3.4.4	Examination of poly(A) <sup>+</sup> RNA distribution in <i>Chlamydia</i> -infected cells .....	69

<b>4</b>	<b>Discussion .....</b>	<b>71</b>
<b>4.1</b>	<b>Persistent growth of <i>C. trachomatis</i> in fibroblasts .....</b>	<b>72</b>
4.1.1	Chlamydial growth arrest in fibroblasts at the stage of RB-to-EB re-differentiation .....	72
4.1.2	Different efficiencies of IFN to induce <i>IDO</i> expression between the three infection models .....	74
4.1.3	Role of <i>IDO</i> in chlamydial persistence in fibroblasts .....	75
4.1.4	Comparison of chlamydial gene expression in fibroblasts with other persistence models .....	77
4.1.5	Expression of the chlamydial protease CPAF in fibroblasts .....	79
<b>4.2</b>	<b>Impact of chlamydial infection on MHC class I antigen presentation .....</b>	<b>80</b>
4.2.1	Expression of the TAP transporter and immunoproteasome subunits in <i>Chlamydia</i> -infected cells .....	81
4.2.2	Role of RFX5 in MHCI antigen presentation in <i>Chlamydia</i> -infected cells .....	82
4.2.3	Differences in interference of <i>C. trachomatis</i> with MHC class I antigen presentation during active and persistent infection .....	83
4.2.4	Correlation of CPAF expression with chlamydial interference with MHCI antigen presentation .....	84
4.2.5	Degradation of TAP2 through <i>C. trachomatis</i> .....	85
4.2.6	Role of Golgi fragmentation and Golgi protein degradation in inhibition of intracellular MHCI trafficking in actively <i>Chlamydia</i> -infected cells .....	88
4.2.7	Golgi fragmentation and Golgi protein degradation during chlamydial persistence and fibroblast infection .....	90
4.2.8	Other mechanisms of <i>C. trachomatis</i> to escape immune recognition by T cells	91
4.2.9	Chlamydial proteins that may elicit a CD8+ T cell response and their different expression during active and persistent infection .....	93
4.2.10	Role of CPAF mediated golgin degradation in <i>Chlamydia</i> -host cell interaction .....	93
<b>4.3</b>	<b><i>C. trachomatis</i> mediated degradation of the host cell mRNA export factor NXF1 .....</b>	<b>96</b>
<b>4.4</b>	<b>Summary and outlook .....</b>	<b>97</b>
<b>5</b>	<b>References .....</b>	<b>100</b>
<b>6</b>	<b>Appendix .....</b>	<b>112</b>
<b>6.1</b>	<b>Material .....</b>	<b>112</b>
6.1.1	Chemicals .....	112
6.1.2	Kits .....	113
6.1.3	Proteins, enzymes and standards .....	114
6.1.4	Buffers and media .....	114
6.1.5	Nucleic acids .....	116
6.1.6	Antibodies .....	118
6.1.7	Material .....	120
6.1.8	Devices .....	121

6.1.9	Software.....	121
6.2	<b>Comparative 2D gel electrophoresis of chlamydial RB proteins from infected HeLa cells and fibroblasts .....</b>	<b>122</b>
7	<b>Acknowledgement.....</b>	<b>128</b>
8	<b>Curriculum vitae .....</b>	<b>129</b>
9	<b>Publications .....</b>	<b>130</b>
9.1	<b>Journal publications .....</b>	<b>130</b>
9.2	<b>Conference contributions.....</b>	<b>130</b>
10	<b>Statement.....</b>	<b>131</b>
10.1	<b>Selbständigkeitserklärung .....</b>	<b>131</b>
10.2	<b>Erklärung zur Dissertation.....</b>	<b>131</b>

## Index of figures

Fig. 1: The chlamydial developmental cycle. ....	2
Fig. 2: Mechanisms of chlamydial persistence induction. ....	7
Fig. 3: The MHC class I antigen presentation pathway. ....	11
Fig. 4: Immunofluorescent staining of <i>C. trachomatis</i> inclusions in HeLa cells and fibroblasts. ....	29
Fig. 5: Burst size of <i>C. trachomatis</i> in epithelial cells and fibroblasts. ....	31
Fig. 6: <i>C. trachomatis</i> inclusions visualised by transmission electron microscopy. ....	32
Fig. 7: Influence of <i>C. trachomatis</i> infection on <i>IDO</i> gene expression in fibroblasts. ....	34
Fig. 8: Influence of <i>C. trachomatis</i> infection on <i>IDO</i> gene expression in HeLa cells. ....	34
Fig. 9: Efficiency of <i>IDO</i> siRNA knockdown in <i>C. trachomatis</i> infected fibroblasts. ....	36
Fig. 10: Effect of <i>IDO</i> siRNA knockdown on <i>C. trachomatis</i> growth in fibroblasts. ....	36
Fig. 11: Expression of <i>C. trachomatis</i> genes in the three different infection models. ....	38
Fig. 12: Protein expression of chlamydial CPAF, HSP60 and MOMP in the three infection models. ....	42
Fig. 13: Influence of <i>C. trachomatis</i> infection on MHCI surface expression. ....	44
Fig. 14: Expression of proteins involved in the MHC I antigen presentation pathway in <i>C. trachomatis</i> infected cells. ....	48
Fig. 15: Effect of inhibition of eukaryotic and prokaryotic translation on TAP2 expression in HeLa cells actively infected with <i>C. trachomatis</i> . ....	49
Fig. 16: Cell-free cleavage assay of TAP2. ....	50
Fig. 17: Impact of inhibition of CPAF activity with lactacystin on the degradation of TAP2. ....	50
Fig. 18: Immunofluorescent staining of Golgi proteins in <i>C. trachomatis</i> infected cells. ....	52
Fig. 19: Expression of GM130 and Golgin-245 after infection with <i>C. trachomatis</i> . ....	55
Fig. 20: Effect of inhibition of eukaryotic and prokaryotic translation on GM130 and Golgin-245 expression in <i>C. trachomatis</i> infected cells. ....	56
Fig. 21: Role of CPAF in degradation of GM130 and Golgin-245 during active chlamydial infection. ....	57

Fig. 22: Impact of inhibition of CPAF activity with lactacystin on cleavage of GM130 and Golgin-245. ....	58
Fig. 23: Co-localisation of MHCI with the Golgi apparatus during chlamydial infection.....	61
Fig. 24: Differences in sensitivity of MHCI molecules to cleavage with Endo H between the different infection models. ....	63
Fig. 25: NXF1 is degraded upon active <i>C. trachomatis</i> infection in HeLa cells.....	64
Fig. 26: Cleavage of NXF1 and other nuclear proteins in a cell-free cleavage assay.....	66
Fig. 27: Effect of inhibition of CPAF with lactacystin on NXF1 cleavage.....	67
Fig. 28: Degradation of NXF1 during IFN- $\gamma$ mediated persistent infection and in infected fibroblasts. ....	69
Fig. 29: Influence of <i>C. trachomatis</i> infection on intracellular distribution of poly(A)+ RNA.....	70
Fig. 30: Hypothetical model of <i>C. trachomatis</i> interference with the MHC class I antigen presentation pathway. ....	87
Fig. 31: 2D gel of purified proteins from RBs grown in HeLa cells for 24 h. ....	123
Fig. 32: 2D gel of purified proteins from RBs grown in fibroblasts for 24 h. ....	124

## Index of tables

Table 1: Replication efficiency of <i>C. trachomatis</i> in epithelial cells and fibroblasts: inclusion numbers, IFUs and burst size.....	30
Table 2: IFN- $\beta$ production in HeLa cells and fibroblasts.....	33
Table 3: Influence of <i>IDO</i> siRNA knockdown on expression of chlamydial genes in fibroblasts. ....	40
Table 4: Influence of <i>C. trachomatis</i> infection on MHCI surface expression. ....	45
Table 5: Gene expression of components of the MHCI antigen presentation pathway in <i>C. trachomatis</i> infected cells. ....	46
Table 6: Composition of buffers and solutions .....	115
Table 7: Primer for human genes .....	117
Table 8: Primer for <i>C. trachomatis</i> D genes.....	117
Table 9: Primer for detection of mycoplasma contamination .....	118
Table 10: Primary antibodies.....	118
Table 11: Proteins from HeLa gel identified with MS (*MS/MS).....	125
Table 12: Proteins from fibroblast gel identified with MS (*MS/MS) .....	127

## Abstract

The growth of obligate intracellular bacteria of the genus *Chlamydia* strictly depends on nutrients and energy delivered from the host cell, usually an epithelial cell, to an intracellular vacuole in which the bacteria are able to multiply. This interaction with the host cell largely is promoted by chlamydial effector proteins interfering with host cell pathways by cleaving or binding host cell proteins. Infection with the human pathogen *Chlamydia trachomatis* often leads to chronic infection, with the bacteria being assumed to be in a persistent growth state. Chlamydial persistence is characterised by atypical, metabolically active, but non-dividing bacteria and can be elicited by different factors such as nutrient depletion, antibiotic treatment or cytokines. One important means of the immune system to combat infection with this pathogen is the presentation of chlamydial antigens through major histocompatibility complex I (MHCI) molecules on the surface of infected cells, which in turn activates cytotoxic T cells to kill *Chlamydia*-infected cells.

In the present study, the MHCI antigen presentation pathway was examined during active and persistent infection in order to find out whether or not *C. trachomatis* interferes with this pathway dependent on its growth state. When analysing the expression of different components of the MHCI pathway, it was found that active *C. trachomatis* infection of epithelial cells leads to degradation of the endoplasmic reticulum-resident antigen transporter subunit TAP2, which is essential for peptide delivery from the cytosol into the ER for loading onto MHCI. This correlated with abnormal MHCI trafficking and reduced MHCI surface expression in these cells. During IFN- $\gamma$  induced persistent *C. trachomatis* infection of epithelial cells degradation of TAP2 could not be observed, and MHCI trafficking and surface expression were not compromised in these cells. As another model for *Chlamydia*-host cell interaction fibroblasts were analysed as additional host cell type. *C. trachomatis* showed atypical growth and some characteristics of chlamydial persistence in these cells, in part, this was a result of the induction of indoleamine 2,3-dioxygenase expression due to an infection-induced endogenous IFN- $\beta$  production. However, chlamydial gene and protein expression during persistence within fibroblasts was completely different from the IFN- $\gamma$  induced persistence model. Nevertheless, MHCI expression was also found to be functional and even upregulated in fibroblasts during chlamydial infection.

Furthermore, the *Chlamydia*-induced Golgi fragmentation, which was accompanied by degradation of the two Golgi proteins GM130 and Golgin-245 through the secreted chlamydial protease CPAF, was analysed as a second interference mechanism for the

MHCI trafficking through the cell. Strong CPAF expression was only found during active, but not persistent and fibroblast infection. This correlated with degradation of GM130, Golgin-245, TAP2 and the mRNA export factor NXF1, which was found as another newly discovered target for chlamydial cleavage activity, during active infection, whereas cleavage of these proteins was reduced both during persistent and fibroblast infection.

Altogether, the results show that the ability of *Chlamydia* to interact with host cell pathways, such as the MHCII antigen presentation pathway, largely depends on host cell conditions that promote productive chlamydial growth and thus expression of CPAF and other chlamydial effector proteins. During chlamydial persistence an interference with MHCII antigen presentation was not detected, which suggests that elimination of persistently infected cells through the host immune system principally should be possible in vivo. An interference with the MHCII presentation pathway during active *C. trachomatis* infection may reduce recognition through cytotoxic T cells and thus represent a mechanism to escape the immune response in order to complete chlamydial development.

## Zusammenfassung

Das Wachstum obligat intrazellulärer Bakterien der Gattung *Chlamydia* hängt strikt von Nährstoffen und Energie ab, die sie von der Wirtszelle – normalerweise einer Epithelzelle – erwerben. Dies geschieht durch Rekrutierung der Nährstoffe zu einer intrazellulären Vakuole, in der sich die Bakterien vermehren. Diese Interaktion mit der Wirtszelle wird im Wesentlichen durch chlamydiale Effektor-Proteine, die Wirtszell-Signalwege durch Spaltung oder Bindung von Wirts-Proteinen beeinträchtigen, vermittelt. Die menschliche Infektion mit dem Erreger *Chlamydia trachomatis* führt häufig zu chronischer Infektion, bei der angenommen wird, dass die Bakterien in einem persistenten Zustand vorliegen. Die chlamydiale Persistenz ist durch atypische, Stoffwechsel-aktive Bakterien, die die Zellteilung eingestellt haben, gekennzeichnet und kann unter anderem durch Nährstoffmangel, Behandlung mit Antibiotika oder Zytokine ausgelöst werden. Ein wichtiger Teil des Immunsystems zur Bekämpfung der Infektion mit diesem Krankheitserreger ist die Präsentation von Chlamydien-Antigenen durch Moleküle des Haupthistokompatibilitätskomplex I (MHCI) auf der Oberfläche infizierter Zellen. Dies führt zur Aktivierung zytotoxischer T-Zellen, welche Chlamydien-infizierte Zellen daraufhin abtöten.

In der vorliegenden Arbeit wurde der MHCI-Antigenpräsentations-Weg während aktiver und persistenter Infektion untersucht, um herauszufinden, ob *C. trachomatis* diesen zellulären Weg in Abhängigkeit seines Wachstumszustandes behindert. Die Analyse der Expression verschiedener Komponenten des MHCI-Weges zeigte, dass die aktive Infektion von Epithelzellen mit *C. trachomatis* zur Degradierung der TAP2-Untereinheit des Antigentransporters TAP führt. Dieser Transporter ist für die Lieferung von Peptiden in das Endoplasmatische Retikulum und somit für die Beladung von MHCI-Molekülen notwendig. Die TAP2-Degradierung korrelierte mit einem abnormalen MHCI-Transport und reduzierter MHCI-Oberflächenexpression in diesen Zellen. Während der IFN- $\gamma$  vermittelten persistenten *C. trachomatis*-Infektion von Epithelzellen wurde keine TAP2-Degradierung gefunden, und der Transport und die Oberflächenexpression von MHCI waren in diesen Zellen nicht beeinträchtigt. Als weiteres Model für die Chlamydien-Wirtszell-Interaktion wurde mittels Chlamydien-Infektion von Fibroblasten ein weiterer Wirtszell-Typ untersucht. Das Wachstum von *C. trachomatis* in diesen Zellen war atypisch, zeigte Merkmale der Persistenz und war zum Teil das Ergebnis einer Aktivierung der Indolamin-2,3-Dioxygenase-Expression aufgrund einer endogenen, durch Infektion verursachten IFN- $\beta$ -Produktion. Allerdings unterschied sich das Expressionsmuster

chlamydialer Gene und Proteine während der Persistenz in Fibroblasten deutlich von dem während der IFN- $\gamma$  induzierten Persistenz. Dennoch war auch hier die MHCI-Oberflächenexpression während der Infektion nicht beeinträchtigt sondern sogar hochreguliert.

Des Weiteren wurde die Chlamydien-induzierte Golgi-Fragmentierung als zweiter Interferenz-Mechanismus für den intrazellulären MHCI-Weg untersucht. Dabei wurde eine Degradierung der Golgi-Proteine GM130 und Golgin-245 durch die sezernierte chlamydiale Protease CPAF beobachtet. Eine hohe CPAF-Expression kam nur während der aktiven, nicht aber persistenten und Fibroblasten-Infektion vor. Dies korrelierte mit der Degradierung von GM130, Golgin-245, TAP2 und einem weiteren, neu entdeckten Ziel-Protein, welches von *C. trachomatis* gespalten wird, dem mRNA Exportfaktor NXF1, während der aktiven Infektion. Die Degradierung dieser Proteine war sowohl während der persistenten als auch der Fibroblasten-Infektion reduziert.

Insgesamt zeigen die Ergebnisse, dass die Fähigkeit der Chlamydien mit zellulären Wegen wie dem MHCI-Antigenpräsentations-Weg zu interagieren stark von solchen Wirtszell-Bedingungen abhängt, die das produktive Wachstum von Chlamydien und somit auch die Expression von CPAF und anderen chlamydialen Effektor-Proteinen begünstigen. Da während der Chlamydien-Persistenz keine Beeinträchtigung des MHCI-Weges beobachtet werden konnte, sollte die Entfernung von persistent infizierten Zellen durch das Immunsystem in vivo prinzipiell möglich sein. Die Interferenz mit dem MHCI-Weg während der aktiven Infektion hingegen könnte dazu führen, dass infizierte Zellen durch zytotoxische T-Zellen schlechter erkannt werden. Dies würde einen Mechanismus darstellen, um der Immunantwort zu entkommen und somit die Vervollständigung des Entwicklungszyklus der Chlamydien zu gewährleisten.

## Abbreviations

2D	two dimensional
AB	aberrant body
AMV	Avian Myeloblastosis Virus
APS	ammonium persulfate
ATP	adenosine triphosphate
$\beta_2$ M	beta-2 microglobulin
bp	base pairs
BGM	Buffalo Green Monkey
BSA	bovine serum albumin
$\text{Ca}^{2+}$	calcium ion
Cap1	class I accessible protein-1
CE	cytosolic extract
CD	Cluster of differentiation
cDNA	complementary deoxyribonucleic acid
CiReA	<i>Chlamydia</i> -induced reactive arthritis
CMV	Cytomegalovirus
$\text{CO}_2$	carbon dioxide
CPAF	Chlamydial Protease/proteasome-like Activity Factor
CT	cycle threshold
C-terminal	carboxyl-terminal
Cy3	Cyanine 3
DAPI	4',6-diamidino-2-phenylindole
DMSO	dimethyl sulfoxide
DNA	deoxyribonucleic acid
dNTP	deoxynucleoside triphosphate
DTT	dithiothreitol
EB	elementary body
EBV	Epstein-Barr virus
ELISA	Enzyme-linked immunosorbent assay
Endo H	Endoglycosidase H
ER	endoplasmic reticulum
ERAD	endoplasmic reticulum associated protein degradation
Fig.	figure
FISH	Fluorescence in situ hybridisation
FITC	Fluorescein isothiocyanate
FCS	fetal calf serum
g	symbol for gravitational acceleration
GAPDH	Glyceraldehyde 3-phosphate dehydrogenase

GM130	Golgi matrix protein 130
GTP	guanosine triphosphate
H <sub>2</sub> O	chemical formula for water
HLA-ABC	Human leukocyte antigen A, B and C corresponding to the three genes HLA-A, HLA-B and HLA-C
HSP60	Heat Shock Protein 60
HSV	Herpes simplex virus
IB	intermediate body
IDO	Indoleamine 2,3-dioxygenase
IFNAR	Interferon-alpha/beta receptor
IFNB	gene name for Interferon-beta
IFN	Interferon
IFU	inclusion forming unit
IgG	Immunoglobulin G
IL	interleukin
IRF-1	Interferon regulatory factor 1
ISGF3	Interferon stimulated gene factor 3
kDa	kilo-Dalton
LGV	Lymphogranuloma venereum
LMP	Large multifunctional peptidase
LPS	Lipopolysaccharide
MECL1	Multicatalytic Endopeptidase Complex-Like 1
MHC	major histocompatibility complex
MEM	minimal essential medium
min	minutes
MOI	multiplicity of infection
MOMP	Major outer membrane protein
mRNA	messenger ribonucleic acid
mRNP	messenger ribonucleoprotein
MTOC	Microtubule Organizing Centre
MALDI TOF	Matrix-assisted laser desorption/ionization time of flight
mW	milliwatt
NBD	nucleotide binding domain
NE	nuclear extract
NF-κB	Nuclear factor kappa-light-chain-enhancer of activated B cells
NKT cells	natural killer T cells
nm	nanometre
NPC	nuclear pore complex
N-terminal	amino-terminal
NXF1	Nuclear RNA export factor 1
PARP-1	Poly (ADP-ribose) polymerase 1

PBS	phosphate buffered saline
PLC	peptide loading complex
OD	optical density
Oligo(dT) <sub>50</sub>	oligonucleotide consisting of 50 molecules deoxyribosylthymine
PC7	proprotein convertase 7
PCR	polymerase chain reaction
p.i.	post infection
PE	phycoerythrin
pH	symbol for negative decimal logarithm of hydrogen ion activity
RB	reticulate body
RNA	ribonucleic acid
RNase	ribonuclease
rRNA	ribosomal ribonucleic acid
RFX5	Regulatory Factor X 5
ROI	region of interest
RT	room temperature
RT-PCR	reverse transcription polymerase chain reaction
SDS-PAGE	sodium dodecyl sulphate polyacrylamide gel electrophoresis
siRNA	small interfering RNA
SNARE	<u>S</u> oluble <u>N</u> -ethylmaleimide-sensitive factor <u>A</u> ttachment <u>P</u> rotein <u>R</u> eceptor
SSC buffer	saline-sodium citrate buffer
16SrRNA	16S ribosomal ribonucleic acid
TAP	Transporter associated with antigen processing
TBS	Tris-buffered saline
TCA	trichloroacetic acid
TGN	<i>trans</i> -Golgi network
TNF- $\alpha$	Tumor necrosis factor-alpha
TTSS	type III secretion system

# 1 Introduction

## 1.1 *Chlamydia*

### 1.1.1 The family of *Chlamydiaceae*

The class *Chlamydiae* with the single order *Chlamydiales* represents one branch of the bacteria domain that consists merely of obligate intracellular bacteria. They are well-adapted parasites of different eukaryotic host cells ranging from single-cellular amoebae to highly differentiated epithelial cells of the mammalian mucosa. All members have a biphasic developmental cycle with alternation between an infectious, extracellular form and an intracellular, replicating form. The family of *Chlamydiaceae* currently holds several species that are pathogens of different vertebrates. Of these *Chlamydia trachomatis* is a species that is highly adapted to humans, and it consists of several serovars causing different diseases. Serovars A – C are the agents of trachoma, a tropical disease that is characterised by an ocular infection often leading to scarring and blindness (reviewed in Burton & Mabey, 2009). Serovars D – K usually cause a sexually transmitted urogenital tract infection, which can be asymptomatic. However, in some cases infection with these serovars can lead to pelvic inflammatory disease, an ascending infection of the upper parts of the female genital tract, with severe sequelae like ectopic pregnancy and tubal infertility (reviewed in Carey & Beagley, 2010). Lymphogranuloma venereum (LGV) is a sexually transmitted disease elicited by serovars L1 – L3 that, in contrast to serovars D – K, are able to invade and multiply in the local lymph-nodes resulting in severe lymphadenopathy (reviewed in Sary & Sary, 2008).

Further chlamydial species that are known to cause disease in humans are *Chlamydia pneumoniae*, *Chlamydia psittaci* and *Chlamydia abortus*. *C. pneumoniae* is a ubiquitous human pathogen and usually infects the upper and lower respiratory tract which can lead to pneumonia, bronchitis, sinusitis and pharyngitis. Previous studies further revealed an association of *C. pneumoniae* infection with chronic diseases like intrinsic asthma, chronic obstructive pulmonary disease, multiple sclerosis, atherosclerosis and Alzheimer's disease (reviewed in Blasi *et al.*, 2009). The usual hosts of *C. psittaci* are birds. However, this pathogen is also able to infect humans and to cause psittacosis, a severe pneumonia (reviewed in Beeckman & Vanrompay, 2009). Similarly, human infection can occur with *C. abortus*, a pathogen usually found in ruminants. Cases have been reported where infection of pregnant women with *C. abortus* led to abortion of the foetus and to sepsis

(Pospischil *et al.*, 2002; Walder *et al.*, 2005). Infections with *C. psittaci* and *C. abortus* are typical zoonotic diseases (Rohde *et al.*, 2010).

### 1.1.2 The chlamydial developmental cycle

Chlamydiae strictly depend on nutrients and energy of the host cells for their growth and multiplication. Therefore these parasites have developed a well adapted intracellular niche, the so-called chlamydial inclusion. The inclusion represents a modified, host membrane derived vacuole in which the chlamydial organisms grow and form new progeny. This represents a convenient way to be protected from host cell defence mechanisms but also to efficiently interact with the host cell for acquisition of nutrients and adenosine triphosphate (ATP).

In mammals the epithelial cell of mucosal surfaces is the primary target cell for infection with members of the family *Chlamydiaceae*. That is why the infections normally occur in the lung, the eye and the genital tract.

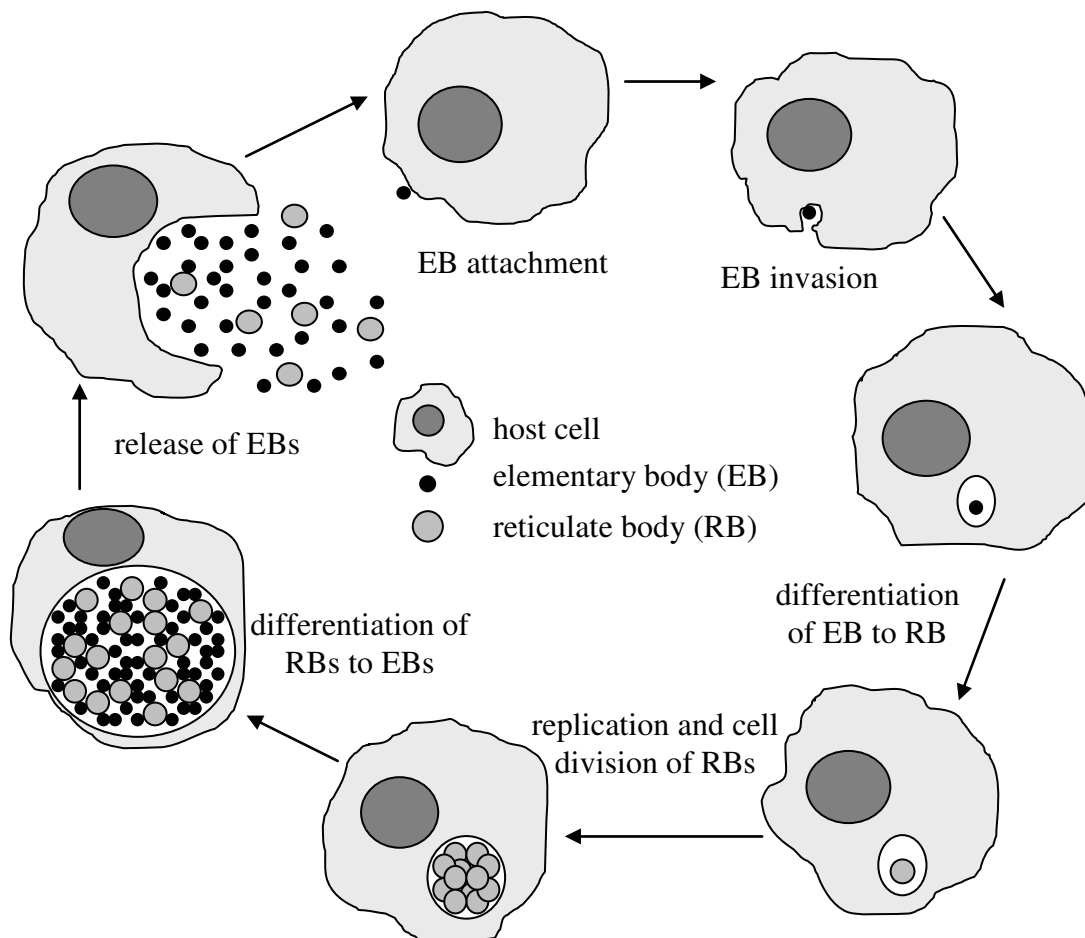


**Fig. 1: The chlamydial developmental cycle.**

Depicted is the replicative infection cycle under optimal growth conditions such as occurring in cell culture.

The replicative developmental cycle of *C. trachomatis* during an active infection starts with the attachment of the extracellular, infectious form, the elementary body (EB; approximately 0.3  $\mu\text{m}$  in size), to the host cell membrane followed by an invasion through endocytosis (Fig. 1). The EB converts to a reticulate body (RB), which is larger (approximately 1.0  $\mu\text{m}$ ) and shows metabolic activity. This RB starts to multiply finally leading to a highly increased number of RBs inside the inclusion. The late phase of the developmental cycle is characterized by an asynchronous re-differentiation of the RBs to EBs. After approximately 48 h the newly formed progeny is released from the host cell and ready for new rounds of infection (reviewed in AbdelRahman & Belland, 2005).

### **1.1.3 Interaction of *Chlamydia* with the host cell**

For optimal growth chlamydiae need to considerably manipulate the host cell in order to escape host defence mechanisms on the one hand and to acquire nutrients and energy from the host cytosol on the other hand. To this purpose chlamydiae secrete different effector proteins into the host cytosol. Results from several studies have shown that chlamydiae possess a type III secretion system (TTSS) and that secretion of many chlamydial proteins into the cytosol and inclusion membrane occurs through this secretion apparatus (Fields *et al.*, 2003; Peters *et al.*, 2007; Stephens *et al.*, 1998).

Active modulation of the host cell already starts during EB attachment as shown by *C. trachomatis* secretion of the translocated actin-recruiting phosphoprotein (TARP) by the TTSS into the host cytosol during this stage (Clifton *et al.*, 2004). After recruitment of actin to the site of chlamydial entry through a process that depends on small GTPases of the Rho family (Balaná *et al.*, 2005; Carabeo *et al.*, 2004; Subtil *et al.*, 2004), TARP directly binds and promotes polymerisation of actin (Jewett *et al.*, 2006). This results in a cytoskeleton rearrangement that is necessary for internalisation of the EB (Carabeo *et al.*, 2002; Jewett *et al.*, 2010). Further interactions with the cytoskeleton that occur later in the development involve recruitment of actin and intermediate filaments to the inclusion through a RhoA-dependent mechanism (Kumar & Valdivia, 2008). This likely serves to build a cytoskeleton scaffold around the inclusion in order to stabilise the intracellular pathogen vacuole (Kumar & Valdivia, 2008). *C. trachomatis* uses also actin polymerisation for release of new progeny from the host cell through extrusion which leaves the host cell intact and, beside cell lysis, represents an alternative mechanism of host cell exit (Hybiske & Stephens, 2007).

To be protected from lysosomal degradation chlamydiae have evolved a mechanism to separate the inclusion from the normal endocytic trafficking pathway very early after host cell invasion. It has been shown that soon after entry the *C. trachomatis* EB moves to the perinuclear region by using dynein to traffic on microtubules to the Microtubule Organising Centre (MTOC) (Clausen *et al.*, 1997; Grieshaber *et al.*, 2003). By this the inclusion is located close to the Golgi apparatus and the chlamydiae now start to recruit host cell sphingolipids and cholesterol from the *trans*-Golgi compartment and from multivesicular bodies (MVBs) to the inclusion (reviewed in Scidmore, 2011). This is an efficient mechanism to disguise the inclusion as an exocytic vesicle in order to escape lysosome fusion (reviewed in Rockey *et al.*, 2002). The comprehensive interaction of chlamydiae with the vesicular trafficking pathway is accompanied by fragmentation of the Golgi apparatus (Heuer *et al.*, 2009), which is the result of cleavage of the structural protein Golgin-84 through the Chlamydial Protease/proteasome-like Activity Factor (CPAF) secreted from the chlamydial inclusion (Christian *et al.*, 2011). This fragmentation is supposed to enhance the transport of lipid-containing Golgi vesicles to the inclusion. Beside sphingolipids and cholesterol, glycerolipids are also acquired by *Chlamydia* and necessary for their growth, however their acquisition occurs independent of the Golgi exocytic pathway (Wylie *et al.*, 1997). Further sources of lipids for chlamydiae represent lipid droplets, which are ER-derived lipid storage organelles and are even taken up into the chlamydial inclusion lumen (Cocchiario *et al.*, 2008; Kumar *et al.*, 2006).

A necessity for interaction with the host cell is the modification of the inclusion membrane with chlamydial proteins called Inc proteins (reviewed in Rockey *et al.*, 2002). Most of them are expressed very early (2 h p.i.) during chlamydial growth and have diverse functions in interaction with the host cell (Shaw *et al.*, 2000 a). For example *C. trachomatis* IncG was found to bind the mammalian protein 14-3-3 $\beta$  that is involved in regulating many host signalling pathways (Scidmore & Hackstadt, 2001). Also, several Inc proteins possess similarities to eukaryotic SNARE proteins that play important roles in vesicle membrane fusion implicating a role in regulating vesicle trafficking (reviewed in Scidmore, 2011). Certain Rab proteins, which are crucial regulators of the vesicular trafficking pathway, are associated with the inclusion membrane, probably by directly or indirectly interacting with Inc proteins (reviewed in Scidmore, 2011). They are supposed to play an important role in directing vesicle trafficking to the inclusion. For example Rab6, Rab11 and Rab14 are necessary for sphingomyelin delivery to the *C. trachomatis* inclusion (Capmany & Damiani, 2010; Rejman Lipinski *et al.*, 2009). Importantly, Rabs that are involved in early

endosome to late endosome trafficking and lysosome fusion, such as Rab 5, Rab 7 and Rab 9, were not found to localise to the chlamydial inclusion (Rzomp *et al.*, 2003). The exclusion of these Rab proteins may be crucial for preventing entry of the chlamydial inclusion into the endosomal pathway in order to escape lysosomal fusion and degradation. Infection of a cell with *C. trachomatis* has further implications for its growth. It is known that *C. trachomatis* inhibits cytokinesis without affecting mitosis thus leading to cells with more than one nucleus (Greene & Zhong, 2003). This could result from the cleavage of cell cycle proteins such as Cyclin B1 through a chlamydial protease secreted into the host cytosol (Balsara *et al.*, 2006 a; Paschen *et al.*, 2008). Chlamydiae also tightly associate with centrosomes which results in supernumerary centrosomes, abnormal spindle poles and defects in chromosome segregation (Grieshaber *et al.*, 2006).

It is well known that chlamydiae inhibit apoptosis and immune defence mechanisms in order to complete their development. Host cell death only seems to be induced late during chlamydial development, but the exact mechanisms still are unclear and do not seem to involve classical apoptotic and necrotic pathways (reviewed in Miyairi & Byrne, 2006 and in Sharma & Rudel, 2009; Yu *et al.*, 2010).

Chlamydiae are also able to interfere with several important host signalling pathways, for example *C. trachomatis* has been shown to interrupt NF- $\kappa$ B signalling, an important host defence and inflammatory pathway, through different mechanisms (Lad *et al.*, 2007 a, Lad *et al.*, 2007 b; Le Negrate *et al.*, 2008).

Thus, chlamydiae have evolved several means to efficiently manipulate the host cell with the primary aims of an intracellular pathogen to promote productive growth and suppress host cell defence mechanisms.

#### **1.1.4 The role of the chlamydial protease CPAF in *Chlamydia* host cell interaction**

A virulence factor that got into the focus of chlamydial research during the last years is CPAF, a serine protease that is secreted into the host cytosol during infection in order to degrade several host proteins (reviewed in Zhong, 2009). This protease is unique to chlamydiae and highly conserved among different chlamydial species (Huang *et al.*, 2008; Zhong *et al.*, 2001). Its name is derived from the observation that the activity of this protease could only be inhibited by the proteasome inhibitor lactacystin, but not by other typical protease or proteasome inhibitors (Zhong *et al.*, 2000). CPAF is secreted in a type II secretion dependent fashion into the inclusion lumen before translocation into the host cytosol (Chen *et al.*, 2010 a). Interestingly, CPAF is produced and translocated as an inactive form

of 70 kDa size. Activation of CPAF occurs in the host cytosol by autocatalytic cleavage of an internal inhibitory segment that binds to the active site of CPAF. This produces an N-terminal fragment of 29 kDa (CPAF<sub>n</sub>) and a C-terminal fragment of 35 kDa (CPAF<sub>c</sub>) that form an enzymatically active heterodimer (Chen *et al.*, 2010 b; Huang *et al.*, 2008).

During the last decade several host proteins were discovered to be cleaved by CPAF. Among them are the transcription factors regulatory factor X 5 (RFX5) and upstream stimulatory factor 1 (USF-1) involved in regulating antigen presentation (Zhong *et al.*, 1999, Zhong *et al.*, 2000), the cytoskeletal intermediate filament proteins vimentin, keratin 8 and keratin 18 (Dong *et al.*, 2004; Kumar & Valdivia, 2008), the lipid antigen presenting glycoprotein CD1d (Kawana *et al.*, 2007), the hypoxia-inducible factor-1 (HIF-1) (Rupp *et al.*, 2007), the Golgi protein Golgin-84 (Christian *et al.*, 2011) and Nectin-1 which is involved in forming adherens and tight junctions between epithelial cells (Sun & Schoborg, 2009). The cleavage of these proteins probably has different functions for the growth of chlamydiae. For example the cleavage of host intermediate filament proteins is supposed to be necessary for rearrangements of the cytoskeleton surrounding and strengthening the chlamydial inclusion in order to allow for size increase during chlamydial growth (Kumar & Valdivia, 2008).

A major role for CPAF has been observed in inhibiting apoptosis, as studies revealed degradation of the pro-apoptotic BH3-only proteins through this protease (Paschen *et al.*, 2008; Pirbhai *et al.*, 2006) thus preventing cytochrome c release from mitochondria. A further role of CPAF in regulating cell death has been observed by degradation of Poly (ADP-ribose) polymerase-1 (PARP-1) and High-mobility group box 1 protein (HMGB-1) (Paschen *et al.*, 2008; Yu *et al.*, 2010). The degradation of HMGB-1 was accompanied by a lack of translocation of this protein from the nucleus into the cytosol, a mechanism that usually occurs during necrosis to promote inflammation (Yu *et al.*, 2010). The role of CPAF in regulating host responses thus seems to be very comprehensive and likely is the result of broad substrate specificity (Huang *et al.*, 2008).

### **1.1.5 Chlamydial persistence**

Chronic chlamydial infections are often associated with severe sequelae like blindness or infertility. In vivo data from clinical studies and experimental animal infections suggest that during chronic infections chlamydiae persist in the host cells for a long time and establish a long-term association with the host (reviewed in Hogan *et al.*, 2004). Since chronic chlamydial infections are difficult to diagnose and to treat and are related to severe

immunopathology, unravelling the characteristics and the eliciting factors of chlamydial persistence is a main topic of chlamydial research. Results from several in vitro studies suggest that chlamydial persistence is generally characterised by aberrant, non-cultivable, but viable, metabolically active bacteria that do not undergo cell division and re-differentiation to EBs (reviewed in Hogan *et al.*, 2004, Wyrick, 2010). It therefore can be considered as a rest in the developmental cycle.

Chlamydial persistence in vitro can be elicited by several factors and is usually reversed to the active, replicative infection state after removal of the eliciting factor (reviewed in Hogan *et al.*, 2004 and Wyrick, 2010). For example it can be induced by nutrient deprivation, antibiotic treatment, iron limitation or herpes simplex virus type-2 (HSV-2) co-infection (Fig. 2).

The so far best studied in vitro persistence model is the IFN- $\gamma$  mediated chlamydial persistence. IFN- $\gamma$  is a cytokine that usually plays an important role in immune eradication of chlamydiae. However, treatment of *Chlamydia*-infected cells with doses of IFN- $\gamma$  that are not high enough to completely inhibit chlamydial growth can lead to persistent growth. It is the result of an elevated expression of the host defence enzyme indoleamine-2,3-dioxygenase (IDO) that degrades the amino acid tryptophan. Because *C. trachomatis* does

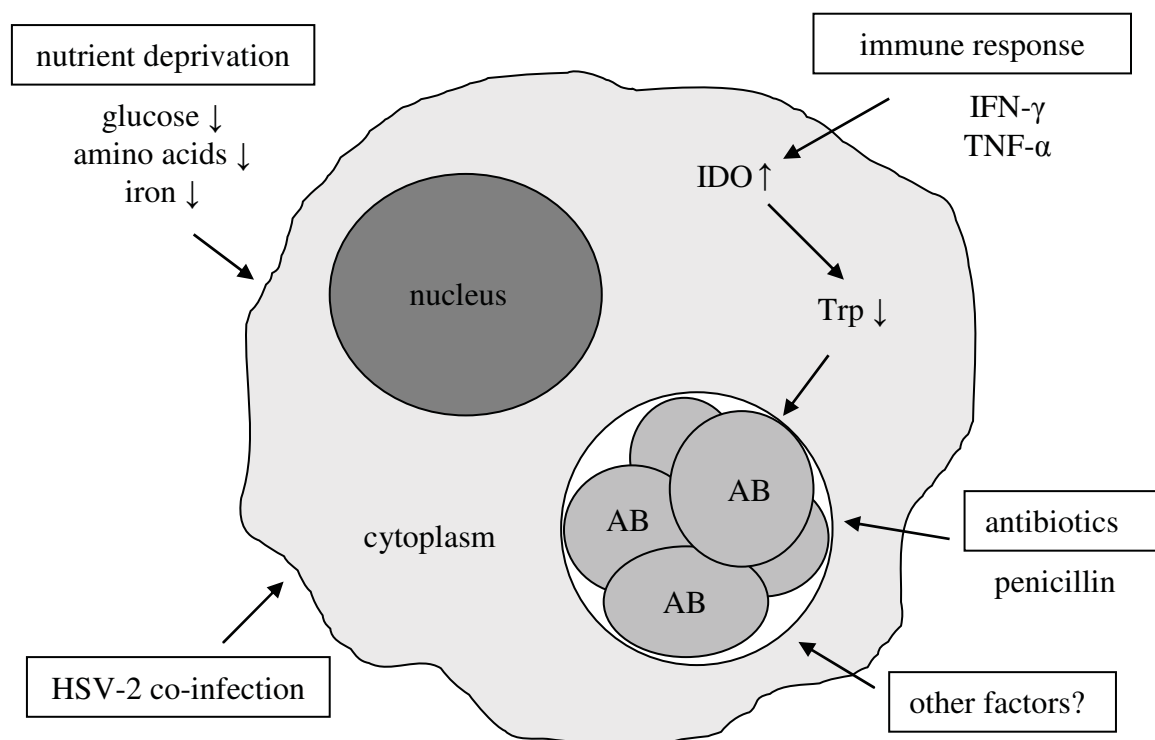


**Fig. 2: Mechanisms of chlamydial persistence induction.**

AB: aberrant chlamydial bodies; TNF- $\alpha$ : tumor necrosis factor alpha; Trp: tryptophan; HSV-2: Herpes simplex virus 2. According to literature reviewed in Hogan *et al.*, 2004 and Wyrick, 2010.

not have a complete set of genes for tryptophan synthesis, intracellular depletion of this essential amino acid leads to starvation and thus persistence of the bacteria (Fig. 2; Beatty *et al.*, 1994 a). However, due to the presence of complete tryptophan synthase subunit A and B (*trpA* and *trpB*) genes, genital strains of *C. trachomatis* are able to use indole in order to produce tryptophan on their own. This is contrary to ocular strains that only encode a truncated form of the tryptophan synthase subunit A. Hence, genital serovars could overcome the IFN- $\gamma$  inhibitory effect by utilising indole that is produced by other bacteria normally residing in the female genital tract (Caldwell *et al.*, 2003; Fehlner-Gardiner *et al.*, 2002). The main characteristics of IFN- $\gamma$  induced chlamydial persistence are small inclusions containing few enlarged, aberrant RBs. They show reduced expression of the major outer membrane protein (MOMP), a main structural component of the chlamydial cell envelope and an antigen that induces a protective antibody response, while expression of the immuno-destructive heat shock protein 60 (HSP60) is maintained (Beatty *et al.*, 1994 a, Beatty *et al.*, 1994 b). In general, most of these characteristics are also found in other in vitro persistence models. Due to the variety of the so far known inducing factors chlamydial persistence probably represents a general stress response against hostile growth conditions (reviewed in Hogan *et al.*, 2004).

### **1.1.6 Immune response to *C. trachomatis* genital infection**

The infection of epithelial cells with *C. trachomatis* results in a pro-inflammatory response that is characterized by secretion of cytokines such as IL-8, CXC-chemokine ligand 1 (CXCL1), granulocyte/monocyte colony-stimulating factor (GM-CSF), IL-6 and IL-1 $\alpha$  (Rasmussen *et al.*, 1997). These cytokines are able to recruit immune effector cells to the site of infection and participate in activation of several immune responses.

Th1 type CD4+ T cells and cytotoxic CD8+ T cells, important members of the adapted immune response, both have very important roles in resolving a chlamydial infection (reviewed in Agrawal *et al.*, 2009; Roan & Starnbach, 2008). By production of IFN- $\gamma$  they can efficiently restrict chlamydial growth. However, the severe pathology that is sometimes observed is considered to be a result of a strong inflammatory response that is also elicited by a high production of IFN- $\gamma$ . Furthermore, an inefficient clearance of chlamydial organisms from the site of infection is supposed to result in chronic infection associated with strong immunopathology which is likely to be induced by inflammation as a result of recurrent chlamydial propagation.

The humoral response also contributes to immunity against chlamydiae by producing antibodies mainly recognizing chlamydial MOMP. Beside their function in direct antigen neutralisation, antibodies obviously play an important role in enhancing the Th1 immune response during chlamydial infection (reviewed in Agrawal *et al.*, 2009)

Because of the involvement of both CD4+ and CD8+ T cells and the restricted knowledge about the immune response mechanisms against human *C. trachomatis* genital infection, no vaccines have been successfully developed to date. The difficult task is to create a vaccine that efficiently protects from chlamydial infection without eliciting a harsh immune response that could lead to destructive immunopathology.

### **1.1.7 *Chlamydia*-induced reactive arthritis**

Genital infection with *C. trachomatis* can elicit an inflammation of the joint known as reactive arthritis. Reactive arthritis occurs as sequela of a bacterial infection, usually caused by *Chlamydia* and enteric bacteria like *Salmonella*, *Shigella*, *Campylobacter* and *Yersinia* (reviewed in Carter & Hudson, 2010). It is not completely clear how the bacteria induce this disease, but it is known that bacterial antigens deposited in the joints probably evoke the inflammation.

In *Chlamydia*-induced reactive arthritis (CiReA) viable chlamydial organisms are transmitted to the joint through circulating monocytes and are able to persist in the synovium for a long time (reviewed in Gérard *et al.*, 2010). Evidence for the persistent infection came from a study that found viable, atypical RBs residing in fibroblasts and macrophages in synovial samples from patients with CiReA (Nanagara *et al.*, 1995). Further examinations revealed the existence of RNA, especially short-lived rRNA transcripts, in such samples indicating that metabolically active and thus viable bacteria reside in the synovial tissue (Gérard *et al.*, 1998 a; Rahman *et al.*, 1992). Expression of the gene encoding MOMP could not be detected in these samples whereas the gene encoding HSP60 was readily expressed (Gérard *et al.*, 1998 a). In vitro studies of chlamydial infection of monocytes correlated with the in vivo data of chlamydial persistence. Chlamydial inclusions within monocytes contained large, aberrant, metabolically active RBs and did not produce EBs indicating the existence of typical persistent forms (Gérard *et al.*, 1998 b; Koehler *et al.*, 1997). Expression of MOMP also was strongly attenuated in these cells (Gérard *et al.*, 1998 b). Obviously, IFN- $\gamma$ -mediated tryptophan depletion through IDO seems not to be the mechanism that induces chlamydial persistence in monocytes (Koehler *et al.*, 1997), and

the inducing factors are still unknown. Major components that may promote a strong inflammation in the joint likely are LPS and HSP60 (reviewed in Zeidler *et al.*, 2004).

In vitro studies on *C. trachomatis* infection of synovial fibroblasts also gave insights into the role of chlamydiae in eliciting reactive arthritis. It has been shown that these cells produce IFN- $\beta$  after infection with *C. trachomatis* (Rödel *et al.*, 1998 a), which upregulates MHCI antigen presentation in *Chlamydia*-infected synovial fibroblasts (Rödel *et al.*, 2002), indicating an important role of these cells in promoting a *Chlamydia*-specific immune response in synovial tissue.

Since antibiotics fail to eradicate the persistent chlamydial infection from the joints (Beutler *et al.*, 1997; reviewed in Gérard *et al.*, 2010) it is important to elucidate the mechanisms and factors that are involved in the immunopathology and the chlamydial persistence during CiReA in order to find efficient ways of treatment.

## **1.2 MHC class I antigen presentation during chlamydial infection**

### **1.2.1 The MHC class I antigen presentation pathway**

The presentation of non-self antigens through major histocompatibility complex (MHC) proteins on the surface of cells is an important part of the immune system to initiate elimination of pathogens and tumour cells. The MHC class I antigen presentation pathway presents antigenic peptides from intracellular sources such as viruses and misfolded proteins to CD8+ T cells that in turn are activated to kill the infected or tumour cell. In contrast, the MHC class II antigen presentation pathway usually presents antigens from exogenous sources to CD4+ T cells. Whereas MHCI antigen presentation is often restricted to professional antigen presenting cells like dendritic cells, macrophages or B cells, principally all cells are able to present antigens by MHCI antigen presentation. MHC class I molecules are glycosylated heterodimers that consist of a heavy chain which has a transmembrane domain and forms the peptide binding groove, and the small accessory protein  $\beta_2$  microglobulin ( $\beta_2$ M). In humans the MHC heavy chains are called human leucocyte antigens (HLA), and there are three major HLA class I genes (HLA-A, -B and -C).

The classical MHCI antigen presentation pathway is depicted in Fig. 3. Newly synthesized MHCI heavy chains are co-translationally translocated through the endoplasmic reticulum (ER) membrane followed by correct folding with the help of the ER-resident chaperones calnexin and binding immunoglobulin protein (BiP). Then the MHCI heavy chains associate with soluble beta-2 microglobulin ( $\beta_2$ M) and enter the peptide loading complex

(PLC) where they are ready to be loaded with peptides. Peptides for MHC I presentation are generated from antigens in the cytosol through the activity of the proteasome and other proteases. These peptides then are transported into the ER through the transporter associated with antigen processing (TAP), which preferentially transports peptides of 8 – 16 amino acids length. Further trimming of the peptides in the ER lumen occurs by the endoplasmic reticulum aminopeptidases 1 (ERAP1) and 2 (ERAP2). They generate peptides of 8 – 10 amino acids length, which is the optimal length for loading on MHC class I molecules. After peptide loading, the MHC I-peptide complexes are transported out of the ER into the Golgi, where further processing of MHC I occurs, and finally reach the cell surface (reviewed in Jensen, 2007, in Schölz & Tampé, 2009 and in Wearsch & Cresswell, 2008). Peptide loading of MHC I molecules is promoted and highly regulated by the PLC, which includes the chaperone calreticulin, the thiol oxidoreductase ERp57, the transmembrane protein tapasin and TAP. Tapasin, ERp57 and calreticulin act together in quality control of peptide loading of MHC I and retain unstable, suboptimally loaded MHC I molecules in the ER. Tapasin further functions in bridging TAP with the other PLC components. TAP belongs to the ATP-binding cassette (ABC) transporter family that uses ATP hydrolysis as energy source for transport of different substrates. It is a heterodimer consisting of the two subunits TAP1 and TAP2 each having a transmembrane domain and a nucleotide binding domain (NBD) (reviewed in Schölz & Tampé, 2009 and in Wearsch & Cresswell, 2008).

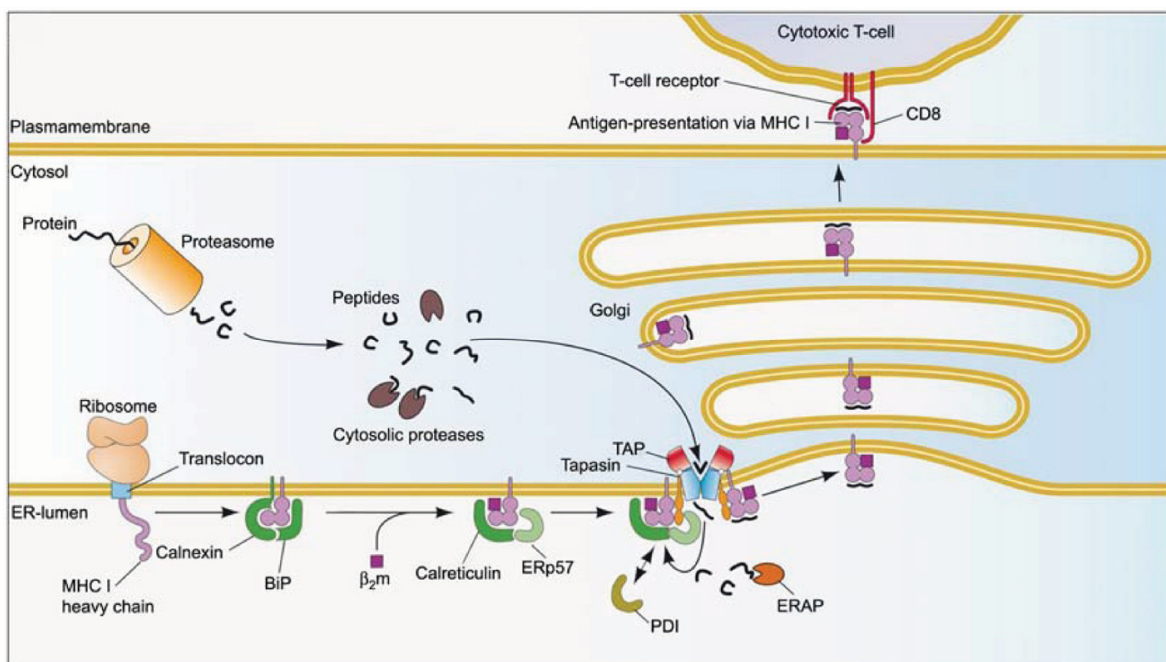


**Fig. 3: The MHC class I antigen presentation pathway.**

(Schölz & Tampé, 2009)

At sites of infection usually the production of type I and type II IFN occurs and contributes to the immune response to intracellular pathogens by upregulation of several defence pathways. This includes the improvement of the MHC class I antigen presentation by upregulating the expression of components of the antigen presentation pathway such as MHC class I heavy chains,  $\beta_2M$ , TAP1 and TAP2. IFNs further activate the expression of special proteasome subunits, namely LMP2 ( $\beta_{1i}$ ), MECL1 ( $\beta_{2i}$ ) and LMP7 ( $\beta_{5i}$ ). Replacement of the constitutive catalytic proteasome subunits  $\beta_1$ ,  $\beta_2$  and  $\beta_5$  by these IFN-inducible subunits results in the so-called immunoproteasome, which generates a different peptide repertoire for presentation to CD8+ T cells during infections in order to improve recognition and eradication of infected cells (reviewed in Sijts & Kloetzel, 2011).

### 1.2.2 MHC class I presentation of chlamydial antigens to CD8+ T cells

Because *Chlamydia* are obligate intracellular bacteria it is conceivable that MHCI antigen presentation of intracellularly processed pathogen-derived peptides to CD8+ T cells would be more efficient for detection and elimination of *Chlamydia*-infected cells than MHCII antigen presentation. Another reason for the importance of the MHCI pathway during eradication of chlamydiae is given by the fact that the main target cell for chlamydial infection is the epithelial cell which like most cells usually only presents peptides via MHCI but not via MHCII. Although many studies in mice indicate that CD4+ T cells play a dominant role in conferring protection against chlamydial infection (for example Magee *et al.*, 1995 and Su & Caldwell, 1995), CD8+ T cell responses were found to essentially participate in resolving chlamydial infection in vivo in mice, and this occurred mainly by secreting TNF- $\alpha$  and IFN- $\gamma$ , cytokines that are known to restrict intracellular chlamydial growth (Igietseme *et al.*, 1994; Ramsey & Rank, 1991; Starnbach *et al.*, 1994; Starnbach *et al.*, 1995). Further, murine CD8+ T cells primed to chlamydial antigens were capable to efficiently kill *Chlamydia*-infected non-haematopoietic cells in an in vitro cytotoxicity assay (Beatty & Stephens, 1994; Starnbach *et al.*, 1995). Both chlamydial and host protein synthesis as well as the secretory pathway were necessary to induce cytotoxicity. Thus, intracellular processing of chlamydial antigens and presentation via MHC class I indeed seem to occur in *Chlamydia*-infected cells. Moreover, a recent study indicated an important role of CD8+ T cells in genital chlamydial infection as CD8+ T cells proliferated in lymph nodes, migrated into the genital mucosa and produced IFN- $\gamma$  in a murine model of genital *C. trachomatis* infection (Roan & Starnbach, 2006). Thus, control of chlamydial infection through MHCI presentation to CD8+ T cells seems to be especially important at primary

infection sites because this would lead to direct elimination of the infected epithelial cells and the restriction of chlamydial growth through cytokines.

Downregulation of MHCI surface expression is a strategy applied by several viruses to escape CD8<sup>+</sup> T cell recognition and to ensure that the infected cell stays intact until the production of new progeny is completed. For *Chlamydia*, which also strictly depend on the intracellular niche for growth and formation of new progeny, evasion of CD8<sup>+</sup> T cell recognition could thus be an important means to complete their development in epithelial cells and to generally escape immune recognition. Indeed, downregulation of MHCI surface expression has been observed in *C. trachomatis* infected epithelial cells by different authors (Hook *et al.*, 2004; Ibane *et al.*, 2011; Zhong *et al.*, 2000). MHCI and  $\beta_2M$  expression were found to be reduced in these cells, and it was hypothesised that this downregulation was the result of CPAF-mediated degradation of RFX5, a transcription factor involved in MHCI and MHCII gene expression (Zhong *et al.*, 2000). However, these findings contradict to other studies mentioned above that found efficient CD8<sup>+</sup> T cell responses during chlamydial infection in vitro and in mice. Furthermore, infection of synovial fibroblasts with *C. trachomatis* resulted in endogenous IFN- $\beta$  production that led to efficient upregulation of MHCI surface expression on these cells throughout the whole developmental cycle (Rödel *et al.*, 2002). This suggests that chlamydial organisms do not interfere with MHCI antigen presentation in this cell type. Interestingly, CD4<sup>+</sup> and CD8<sup>+</sup> T cells proliferating in response to *C. trachomatis* EBs were found in the synovial fluid of patients with CiReA, and the response could be inhibited by antibodies to MHCI and MHCII (Sieper *et al.*, 1991). Furthermore, chlamydial peptides were identified that were presented by HLA-B27 to CD8<sup>+</sup> T cells from infected HLA-B27 transgenic mice, and a response to these epitopes was also detected with CD8<sup>+</sup> T cells from patients with CiReA (Kuon *et al.*, 2001). These studies point to an important role of CD8<sup>+</sup> T cell recognition of MHCI presented chlamydial peptides in the immune response during CiReA.

Less is known about MHCI antigen presentation during chlamydial persistence. It is not yet clear whether chlamydial persistence represents a state where evasion of immune recognition occurs. However, it was found that IFN- $\gamma$  and penicillin induced chlamydial persistence did not affect the lysis of infected cells by CD8<sup>+</sup> T cells suggesting that chlamydiae do not interfere with MHCI surface expression during this growth arrest (Rasmussen *et al.*, 1996). Further studies are needed to clarify the influence of different host cell conditions and chlamydial developmental stages on MHCI antigen presentation in order to get a more detailed picture of CD8<sup>+</sup> T cell immunity to chlamydial infection.

### 1.3 The aim of the present study

The aim of the present study is to clarify whether the MHCI antigen presentation pathway is functional or inhibited during productive and persistent *C. trachomatis* infection, and by which mechanism chlamydial interference with the MHCI antigen presentation pathway occurs. This will help to understand the cellular as well as the immune response to chlamydial infection and chlamydial immune evasion mechanisms in greater detail, which is of vital importance for the development of efficient treatment and vaccination strategies.

Three different infection models were studied and compared: (i) the normal productive chlamydial growth in epithelial cells (designated as active infection), (ii) the atypical, persistent growth of chlamydiae in epithelial cells (persistent infection) using the well-established IFN- $\gamma$  induced persistence model and (iii) the atypical chlamydial growth in fibroblasts, which could represent an alternative host cell type for persistent infection during CiReA and in sublining tissue areas during pelvic inflammatory disease.

The objectives of the present study were as follows:

1. To analyse the atypical growth of *C. trachomatis* in fibroblasts in detail and to compare it with the other two infection models in order to define the role of fibroblasts as a potential host cell for chlamydial infection. This has been done by examination of inclusion morphology, formation of new progeny and chlamydial protein and gene expression analysis. Further, it has been investigated whether IDO is involved in mediating atypical growth of *C. trachomatis* in fibroblasts.
2. To examine whether and how *C. trachomatis* interferes with the MHCI antigen presentation pathway in the different infection models. This has been done by measurement of MHCI expression on the surface of infected cells and by expression analysis of important intracellular components involved in MHCI antigen processing during infection.
3. To analyse if the *Chlamydia*-induced fragmentation of the Golgi apparatus influences MHCI processing and trafficking to the cell surface and to define the role of the chlamydial protease CPAF in interference with the MHCI antigen presentation pathway.

## 2 Material and Methods

### 2.1 Material

#### 2.1.1 Mammalian cells and bacterial strains

BGM cells (from kidney of African Green Monkey)	Friedrich Loeffler Institute of Molecular Pathogenesis, Jena, Germany
<i>Chlamydia trachomatis</i> serovar D strain IC Cal 8	Institute of Ophthalmology, London, UK
HeLa cells CCL-2 (from human cervix)	American Type Culture Collection, Manassas, Virginia, USA
Normal human dermal fibroblasts (from juvenile foreskin)	PromoCell, Heidelberg, Germany

#### 2.1.2 Material

Media, buffers, chemicals, antibodies, nucleic acids and other materials used in the present work are listed in Appendix 6.1.

### 2.2 Methods

#### 2.2.1 Cell culture

HeLa cells and fibroblasts were grown in cell culture flasks with Opti-MEM/10% FCS at 37°C and 5% CO<sub>2</sub>. Culture of BGM cells was done in DMEM/10% FCS. For subculture semi-confluent monolayers were washed with PBS and detached by trypsin/EDTA treatment. Trypsin was inactivated by adding Opti-MEM/10% FCS and cells were collected by centrifugation at 250 x g for 5 min. After resuspension in Opti-MEM/10% FCS cells were seeded into new cell culture flasks. Long-time storage of suspended cells was done in liquid nitrogen at -180°C using medium with 10% FCS containing 14% DMSO as cryo-preserved.

### **2.2.2 Propagation of *C. trachomatis***

Propagation of chlamydial organisms was done in BGM cells. Cells grown in T-25 flasks were infected with  $1 \times 10^7$  inclusion forming units (IFUs) per flask and incubated for 44 – 48 h at 37°C and 5% CO<sub>2</sub>. The chlamydiae were harvested by scraping the cells with a cell scraper into 0.2 M sucrose/2% FCS/PBS. The cells were lysed by sonification to release chlamydial EBs from the cells. To remove cellular debris the suspension was centrifuged at 4,000 x g for 3 min. The supernatant containing EBs was stored in aliquots at -80°C. The suspension was proofed for sterility by streaking a small amount on a Columbia blood agar plate, a chocolate agar plate and a Winkle agar plate and testing it for mycoplasma contamination via PCR. The amount of infectious EBs in the suspension, expressed as IFUs/ml, was determined as described in chapter 2.2.4.

### **2.2.3 Infection procedure**

Confluent cell monolayers were inoculated with chlamydial organisms at a multiplicity of infection (MOI) of 5, if not otherwise indicated, and centrifuged at 4,000 x g for 60 min at 37°C. The inoculum was replaced by cell culture medium with 2% FCS. Cells were incubated for the indicated times at 37°C and 5% CO<sub>2</sub>. For induction of chlamydial persistence in HeLa cells the cell monolayers were pre-treated with 100 U/ml IFN- $\gamma$  48 h before infection. Immediately after centrifugation cells were further treated with 100 U/ml IFN- $\gamma$  in cell culture medium with 2% FCS. For experiments using treatment with IFN- $\beta$  (100 U/ml), IFN- $\gamma$  (100 U/ml), IFNAR antibody (1  $\mu$ g/ml), chloramphenicol (100  $\mu$ g/ml) and cycloheximide (2  $\mu$ g/ml), respectively, the substances were added directly after infection to the culture medium.

### **2.2.4 Determination of inclusion number, IFUs and burst size**

$1 \times 10^5$  cells were seeded in shell vials containing coverslips, and on the next day they got infected with *C. trachomatis* at a MOI of 0.5. After fixation with methanol the chlamydial inclusions were stained with a FITC-conjugated mouse anti-MOMP antibody (MikroTrak *Chlamydia trachomatis* Culture Confirmation Test, Trinity Biotech Plc, Bray, Ireland) according to the manufacturer's instructions. The number of inclusions was determined by counting inclusions on 10 microscopic fields by epifluorescence microscopy. To determine the production of infectious EBs (IFUs), chlamydiae were released from infected monolayers into 0.2 M sucrose/2% FCS/PBS through sonification. The suspension was stored at

-80°C. IFUs were determined by means of titrating different dilutions of the suspension on BGM cell monolayers grown on coverslips and subsequent infection through centrifugation. After fixation and staining at 24 h p.i. the inclusions were counted by epifluorescence microscopy. Each inclusion represented one IFU. Total number of IFUs was determined by including the microscope factor, the dilution factor and the volume of the titrated sample in the calculation. The burst size was determined by dividing the total number of IFUs by the total number of inclusions. The value represents the IFUs produced per inclusion.

### **2.2.5 Preparation of cells for transmission electron microscopy**

Cell monolayers infected with *C. trachomatis* were fixed with 2% glutaraldehyde in 0.1 M sodiumcacodylate buffer for 5 min at RT. Cells were detached by scraping, and incubated for further 30 min with the fixative at RT. The samples were stored at 4°C. Electron microscopy was done by Elisabeth M. Liebler-Tenorio at the Friedrich Loeffler Institute of Molecular Pathogenesis (Jena, Germany) and according to Rödel *et al.* (2012).

Briefly, 1-mm<sup>3</sup> cubes were cut from the cells which had been embedded in 2% agarose before and fixed in 2% osmium tetroxide. Stained ultrathin sections were analysed with a transmission electron microscope (Tecnai 12, FEI, Eindhoven, The Netherlands).

### **2.2.6 Confocal laser scanning microscopy of immunofluorescently stained cells**

For visualisation of the Golgi apparatus and intracellular distribution of MHC I confocal laser scanning microscopy was applied to cells stained with fluorescent dye-conjugated antibodies. Cells grown on coverslips were infected with *C. trachomatis* and incubated for the indicated time points. Then the cells were fixed with 2 % paraformaldehyde/PBS for 20 min, washed three times with PBS and permeabilised with 0.1% Saponin/PBS for 10 min. Blocking occurred by incubation with blocking buffer (3% BSA/0.1% Saponin/PBS) for one hour. The cells were washed three times with 0.1% Saponin/PBS and incubated with rabbit anti-GM130 (Abcam, Cambridge, UK) at a dilution of 1:500 or mouse anti-Golgin-245 (BD Biosciences, Heidelberg, Germany) at a dilution of 1:250 in blocking buffer overnight at 4°C. After washing again three times with 0.1% Saponin/PBS, incubation with the fluorescence-conjugated secondary antibody (Alexa Fluor 633-conjugated goat anti-rabbit IgG or rabbit anti-mouse IgG, Invitrogen, Darmstadt, Germany) at a dilution of 1:1000 in blocking buffer was done for 1 hour in the dark at RT. Thereafter, a second staining step occurred for visualisation of chlamydial inclusions (demonstration of Golgi fragmentation)

or MHCI (co-localisation of MHCI with the Golgi). Chlamydial inclusions were stained with FITC-conjugated mouse anti-MOMP antibody at a dilution of 1:20 (MikroTrak *Chlamydia trachomatis* Culture Confirmation Test, Trinity Biotech Plc, Bray, Ireland). Staining of MHCI occurred with the mouse W6/32 antibody (a gift from Michael Knittler, Friedrich Loeffler Institute Tübingen, Germany) that binds the native form of the MHCI- $\beta_2$ M heterodimer at a dilution of 1:50. The antibody was diluted in blocking buffer and incubated with the cells for one hour at RT. Finally, unbound antibody was removed by three times washing with 0.1% Saponin/PBS. For the visualisation of MHCI a second step of staining was performed through incubation with a fluorescence-conjugated secondary antibody (Alexa Fluor 488 rabbit anti-mouse IgG, Invitrogen, Darmstadt, Germany) diluted in blocking buffer at 1:1000 for 30 min at RT. The coverslips were mounted on a drop of mounting medium (ProLong Gold antifade reagent with DAPI, Invitrogen, Darmstadt, Germany) on a microscope slide. The mounting medium was cured by incubation overnight at RT. Images were generated with the confocal laser scanning microscope LSM 5 (Zeiss, Jena, Germany) using the ZEN software (Zeiss, Jena, Germany) and the following laser and filter options: 405 nm excitation wavelength (405-425 nm Laser Diode, 25 mW) and a 420 – 480 nm bandpass filter for DAPI, 488 nm excitation wavelength (Argon Laser 488 nm, 25 mW) and a 505 – 530 nm bandpass filter for FITC or Alexa Fluor 488, 633 nm excitation wavelength (Helium-neon 633 nm laser, 5 mW) and a 650 nm longpass filter for Alexa Fluor 633.

Co-localisation values were computed by the ZEN software after choosing regions of interest. For examination of Golgi fragmentation cells were categorised in three groups: complete fragmentation, partial fragmentation and no fragmentation. The fragmented Golgi could be distinguished from the normal Golgi by the presence of stained dots irregularly distributed in the cytosol and the absence of a compact Golgi stack. Cells that contained a less compact Golgi stack and some distributed Golgi fragments were considered as having partial fragmentation of the Golgi.

### **2.2.7 RNA isolation and reverse transcription**

RNA was isolated from the cells using the peqGOLD Total RNA Kit (Peqlab, Erlangen, Germany) according to the manufacturer's instructions. The isolation included the digestion of DNA with the peqGOLD DNase I Digest Kit (Peqlab, Erlangen, Germany). Measurement of RNA concentration and purity was carried out with a NanoDrop spectrophotometer using the OD<sub>260</sub>/OD<sub>280</sub> nm absorption ratio. For reverse transcription of the

RNA into cDNA the Reverse Transcription System from Promega (Mannheim, Germany) was used. For a 20 µl reaction the following kit components were mixed: 4 µl MgCl<sub>2</sub>, 2 µl Reverse Transcription Buffer, 2 µl dNTP-Mix, 0.5 µl RNAsin (RNase inhibitor), 1 µl Oligo (dT) primers or 1 µl random primers and 0.5 µl AMV Reverse Transcriptase (containing 15 U). Finally, 10 µl H<sub>2</sub>O containing 1 µg RNA were added, and reverse transcription occurred at 42°C for 30 min. cDNA generated with Oligo (dT) primers was used for analysis of eukaryotic and cDNA made with random primers for analysis of chlamydial gene expression.

### **2.2.8 Analysis of gene expression with real-time quantitative PCR**

PCR was performed using cDNA generated from RNA which has been isolated from mock- or *Chlamydia*-infected cells as described in chapter 2.2.7. Primer pairs were designed using the National Center for Biotechnology Information (NCBI) primer design tool (see Table 7 and Table 8 in Appendix 6.1.5 for primers used in the present study) and synthesised by Jena Bioscience, Jena, Germany. The primers were checked for correct binding and optimum annealing temperature with RT-PCR using GoTaq DNA Polymerase (Promega, Mannheim, Germany) and cDNA as template. The 25 µl RT-PCR reaction mix contained 5 µl GoTaq DNA Polymerase buffer, 0.5 µl of dNTP mix (10 mM), 1 µl forward primer (10 µM), 1 µl reverse primer (10 µM), 0.125 µl GoTaq Polymerase, 1 µl cDNA and 17.4 µl H<sub>2</sub>O. The PCR reaction included a denaturation step at 94°C for 5 min, 30 cycles of 30 s denaturation at 94°C, 30 s annealing and 1 min elongation at 72°C, and finally 10 min extension at 72°C. The PCR product was analysed by electrophoresis on a 1% agarose gel and staining with ethidium bromide.

Real-time PCR was done with the SmartCycler II (Cepheid, Maurens-Scopont, France). The 20 µl PCR reaction mix contained 1x KAPA SYBR FAST qPCR Universal Mastermix (Peqlab, Erlangen, Germany), 1 µl of template and 0.2 µM of each primer. The PCR profile used was the following: initial denaturation at 95°C for 60 s, 45 cycles of denaturation at 95°C for 30 s, primer annealing for 15 s (for the respective temperature see Table 7 and Table 8 in Appendix 6.1.5) and elongation at 72°C for 30 s. The relative quantitation of gene expression was done by calculating the ratio of the expression of the analysed gene relative to the expression of a reference gene (housekeeping gene). GAPDH was chosen as reference gene for human and 16SrRNA for chlamydial genes. The gene expression was calculated from the Cycle Threshold (CT) values of the PCR reactions. Primer efficiencies (E) were determined by performing real-time PCR reactions on different dilutions of one

cDNA sample made of RNA that was isolated from *Chlamydia*-infected HeLa cells. The resulting CT values were plotted against the respective cDNA concentrations giving a linear slope that was used for the calculation of E by using the formula  $E = 10^{-1/\text{slope}}$  (Pfaffl, 2001).

For human gene expression the ratio was calculated using the following formula according to Pfaffl (2001):  $\text{ratio} = E_{\text{target}}^{\Delta\text{CT}_{\text{target}} (\text{control} - \text{treatment})} / E_{\text{reference}}^{\Delta\text{CT}_{\text{reference}} (\text{control} - \text{treatment})}$ . For chlamydial gene expression the relative transcription level was determined with a formula that includes the primer efficiencies of the respective genes modified from Kokab *et al.* (2010):  $\text{relative transcription level} = E^{\Delta\text{CT}} (\text{reference gene}) / E^{\Delta\text{CT}} (\text{target gene})$ . Gene expression values are given as average of three independent experiments.

### **2.2.9 ELISA for IFN- $\beta$ quantitation**

Amounts of secreted IFN- $\beta$  were measured in supernatants of mock- and *Chlamydia*-infected cells with a Human Interferon- $\beta$  ELISA Kit (Invitrogen, Darmstadt, Germany) according to the manufacturer's instructions.

### **2.2.10 siRNA transfection of fibroblasts**

Predesigned siRNAs for knockdown of *IDO* expression were purchased from Qiagen (Hilden, Germany; see Appendix 6.1.5) and used for transfection of fibroblasts at a final concentration of 25 nM according to the Fast-Forward protocol of the HiPerFect transfection reagent, which is composed of cationic and neutral lipids (Qiagen, Hilden, Germany). For six-well plates  $2 \times 10^5$  cells per well were seeded in 2300  $\mu\text{l}$  Opti-MEM with 10% FCS directly before transfection. 750 ng siRNA were diluted in 100  $\mu\text{l}$  Opti-MEM without serum. Then 18  $\mu\text{l}$  HiPerFect was added, and the solution was mixed well. The transfection mixture was incubated at RT for 5-10 min and then added to the 2300  $\mu\text{l}$  cell culture volume drop-wise while swirling the plate. For shell vials  $8 \times 10^4$  cells were seeded in 500  $\mu\text{l}$  Opti-MEM/10% FCS and transfected with a mixture of 100  $\mu\text{l}$  Opti-MEM containing 187.5 ng siRNA and 4.5  $\mu\text{l}$  HiPerFect. Transfection with AllStars Negative Control siRNA (Qiagen, Hilden, Germany) and HiPerFect reagent alone, respectively, using the same amounts as above, was performed as control. The transfected cells were incubated for 48 h at 37°C and 5% CO<sub>2</sub> before infection with chlamydiae. The siRNA knockdown was monitored through confirming downregulation of *IDO* expression by real-time PCR at 72 and 96 h after transfection (24 h and 48 h p.i.).

### **2.2.11 SDS-PAGE and immunoblotting**

The expression of host cell and chlamydial proteins was analysed by SDS-PAGE and immunoblotting. Infected or mock-infected cells grown in six-well plates were detached with a cell scraper into RIPA buffer (see Table 6 in Appendix 6.1.4) for cell lysis. The lysate was incubated for 45 min at 4°C and mixed thoroughly every 10 min. To remove cell debris the lysate was centrifuged at 20,000 x g for 10 min at 4°C. The supernatant containing the proteins was stored at -20°C.

Polyacrylamide gels were casted consisting of a lower resolving gel (with 5, 8, 10 or 12% acrylamide, depending on the size of proteins analysed) and an upper stacking gel with slots (see Table 6 in Appendix 6.1.4). For SDS-PAGE the protein lysate was mixed with the same volume of Laemmli sample buffer (Bio-Rad Laboratories, München, Germany) and boiled for 3 min. In cases where the transmembrane proteins TAP1 and TAP2 should be detected, the lysates were mixed with the same volume of 2x SDS-Urea sample buffer (see Table 6 in Appendix 6.1.4) and shaken for 15 min at RT. The samples and a pre-stained protein standard (Bio-Rad Laboratories, München, Germany) were loaded onto single slots of a polyacrylamide gel covered with Tris/Glycine/SDS-electrophoresis buffer (Bio-Rad Laboratories, München, Germany). To separate the proteins the gel was run at 150 volt until the bromophenol blue line approached the bottom line of the gel.

For immunoblotting the proteins separated in the polyacrylamide gel were transferred on a nitrocellulose membrane (Bio-Rad Laboratories, München, Germany) using a semi-dry blot system (Bio-Rad Laboratories, München, Germany) and Bjerrum-Schafer-Nielsen-transfer buffer (Bjerrum & Schafer-Nielsen, 1986; see Table 6 in Appendix 6.1.4) at 10 volt for 90 – 120 min. The transfer of proteins was verified by incubation of the membrane with Ponceau S staining solution (see Table 6 in Appendix 6.1.4) that led to visualisation of all membrane-bound proteins. Ponceau S was removed by washing with PBS. The membrane was incubated in a blocking buffer containing 2% BSA in TBS-Tween for 2 h in order to allow binding of BSA to regions of the membrane where no protein had bound during the transfer. This step was necessary to prevent unspecific binding of antibody to these regions during the following incubation steps.

Then the membrane was incubated with a primary antibody diluted in blocking buffer overnight at 4°C (see Table 10 in Appendix 6.1.6 for antibodies and the respective dilutions). The membrane was washed three times for 5 min in TBS-Tween. An alkaline phosphatase-conjugated secondary antibody (goat anti-mouse or goat anti-rabbit, Dianova, Hamburg, Germany) diluted in blocking buffer (1:1000) was added and incubated for 2 h

at RT. After a final wash three times for 10 min in TBS-Tween the binding of the secondary antibody was visualised by incubating the membrane in a solution of 5-Bromo-4-chloro-3-indolyl phosphate (BCIP)/Nitro blue tetrazolium (NBT) (Sigma-Aldrich Chemie, München, Germany) which served as substrate for alkaline phosphatase. This enzyme reaction leads to a dark blue colour at antibody-bound protein bands.

Generally, the same volumes of different protein lysates were loaded onto the gel. An antibody binding GAPDH (see Table 10 in Appendix 6.1.6) was used as loading control. The densitometry ratio of the MOMP and HSP60 protein bands was determined by using the ImageJ software (available from <http://rsbweb.nih.gov/ij/>).

### **2.2.12 Flow cytometry**

Surface expression of MHCI on *Chlamydia*-infected cells was analysed by flow cytometry after double immunofluorescence staining of surface MHCI and chlamydial inclusions. *Chlamydia*- and mock-infected cell monolayers grown in six-well plates were detached with 400 µl Trypsin/EDTA per well. 100 µl FCS was added to inactivate trypsin. After addition of 1 ml PBS the suspension was centrifuged at 150 x g for 5 min at 4°C. The pellet was resuspended in 10% FCS/PBS containing the PE-conjugated mouse monoclonal antibody W6/32 binding to native MHCI molecules at a dilution of 1:50 (Santa Cruz Biotechnology, Heidelberg, Germany). After incubation for 30 min at 4°C in the dark the cells were washed once with 1 ml PBS/10% FCS. Then fixation occurred by incubation with 200 µl 2% paraformaldehyde for 10 min at RT. The cells were washed in 1 ml PBS and then permeabilised with 200 µl PBS/0.5% Saponin/0.5% BSA for 30 min at RT. Intracellular staining of chlamydiae was performed by incubation of the cells with 10 µl FITC-conjugated mouse anti-MOMP antibody (MikroTrak *Chlamydia trachomatis* Culture Confirmation Test, Trinity Biotech Plc, Bray, Ireland) in 200 µl PBS/0.5% Saponin/0.5% BSA. After incubation for 30 min at RT the cells were washed with PBS/0.5% Saponin/0.5% BSA and finally resuspended in PBS/0.5% BSA. Fluorescence intensity of 20,000 cells was measured with a FACSCalibur flow cytometer and Cell Quest Software (both from BD Biosciences, Heidelberg, Germany). The cells that were incubated without antibodies and only with PE- or FITC-conjugated IgG, respectively, served as controls to exclude background fluorescence and unspecific antibody binding.

### 2.2.13 Cell-free cleavage assay

In order to analyse whether chlamydial proteases that had been secreted into the cytosol are responsible for degradation of host cell proteins, a cell-free cleavage assay was performed according to Zhong *et al.* (2001) with little modifications. In this enzyme activity assay a purified protein or protein lysate is incubated with the cytosolic extract (CE) isolated from *Chlamydia*-infected cells in order to see if chlamydial proteases present in this CE cleave the protein substrate. The inclusion of protease inhibitors in the buffer used for CE preparation (see Table 6 in Appendix 6.1.4) ensures inhibition of most cellular proteases, but inhibition of the chlamydial protease CPAF does not occur through these inhibitors (Zhong *et al.*, 2000; Zhong *et al.*, 2001).

*Chlamydia*-infected and mock-infected HeLa cells grown in six-well plates were detached at 48 h p.i. by treatment with 400  $\mu$ l trypsin/EDTA per well. Trypsin was inactivated by addition of 100  $\mu$ l FCS and the suspension was filled up with 1 ml PBS. The cells were pelleted by centrifugation at 250 x g for 5 min at 4°C and washed with ice-cold PBS. After a further centrifugation step the pellet was resuspended in 100  $\mu$ l Cell extraction buffer (see Table 6 in Appendix 6.1.4) per well and incubated on ice for 15 min. Preparation of the CE was done applying dounce homogenisation with a conical tissue grinder with 20 times of douncing. This gentle lysis ensures that cells get broken up without lysing the nuclei. The suspension was centrifuged at 1,000 x g for 10 min at 4°C and the supernatant representing the CE was transferred to a new tube. The pellet which contained the nuclei was kept for preparation of the nuclear extract (NE), in case cleavage of nuclear proteins should be analysed. Centrifugation of the CE at 20,000 x g for 15 min at 4°C was done to remove insoluble particles. The NE was prepared after washing the nuclei pellet two times in 1 ml Cell extraction buffer and centrifugation at 1,000 x g for 10 min at 4°C. The nuclei pellet was lysed in 50  $\mu$ l Nuclear extraction buffer (see Table 6 in Appendix 6.1.4) per well and mixed thoroughly. After centrifugation at 20,000 x g for 15 min at 4°C the supernatant was kept for the assay as NE. Since the NE can be only used for detection of nuclear proteins, cell lysate from whole cells was used for the analysis of GM130, Golgin-245 and the TAP2 protein which are proteins located in the Golgi apparatus and the ER membranes, respectively. These cell lysates were made by scraping mock- and *Chlamydia*-infected HeLa cells in 1% Triton-X 100/PBS containing the same protease inhibitors as the Cell extraction buffer. After incubation for 45 min at 4°C and mixing thoroughly every 10 min the samples were centrifuged at 20,000 x g for 10 min and the supernatants were used for the assay. For the assay the CE was mixed with the NE or cell lysate, and the mixture

was incubated for two hours at 37°C. These conditions allow the protein substrate to be cleaved by protease activity. As control CE was incubated with Nuclear Extraction buffer or 1% Triton-X 100/PBS, respectively, and NE was incubated with Cell extraction buffer. To inhibit CPAF activity the CE from infected cells was pre-incubated with the proteasome inhibitor lactacystin (Clasto-Lactacystin  $\beta$ -lactone, Sigma-Aldrich Chemie, München, Germany) for 20 min at 37°C before mixing with substrate and starting the assay. The assay was stopped by transferring the samples onto ice. The samples were analysed by SDS-PAGE and immunoblotting to detect the protein and its cleavage.

#### **2.2.14 Immunoprecipitation of CPAF**

To investigate whether CPAF was responsible for degradation of the examined host proteins the protease was removed from the CE of *Chlamydia*-infected HeLa cells by means of immunoprecipitation followed by analysis of cleavage activity in a cell-free cleavage assay (see chapter 2.2.13). The appropriate amount of CE used for immunoprecipitation was determined in a cell-free cleavage assay where different volumes of CE were used to determine the minimum amount of CE necessary to cause full cleavage of the target protein. It was important to minimise the amount of CPAF in the CE to ensure that most of the CPAF is immunoprecipitated by the antiserum without the need to use huge amounts of antibody. The same amount of CE was used for the other samples in the cell-free cleavage assay. 200  $\mu$ l of the CE from *Chlamydia*-infected cells were pre-cleared by incubation with 1  $\mu$ g mouse IgG and 20  $\mu$ l Protein G PLUS-Agarose (both from Santa Cruz Biotechnology, Heidelberg, Germany) for 30 min at 4°C. The agarose beads were removed by centrifugation at 10,000 x g for 15 min at 4°C. 100  $\mu$ l of the pre-cleared CE were mixed with 5  $\mu$ l CPAF antiserum (a gift from the Institute for Medical Microbiology and Hygiene, University Hospital Ulm, Germany). Another 100  $\mu$ l of the pre-cleared CE were incubated with 5  $\mu$ l mouse IgG, and this sample served as irrelevant antibody control. After incubation overnight at 4°C with gentle agitation 35  $\mu$ l protein G PLUS-Agarose was added and the samples again were incubated overnight at 4°C with gentle agitation. The immunoprecipitate was pelleted by centrifugation at 10,000 x g for 15 min at 4°C. The supernatant, that should contain no CPAF, was used for the cell-free cleavage assay. The immunoprecipitate pellet was washed four times in 1 ml RIPA-buffer (see Table 6 in Appendix 6.1.4), finally mixed with Laemmli sample buffer (Bio-Rad Laboratories, München, Germany) and heated for 3 min at 100°C to dissociate the proteins from the

agarose beads. After another centrifugation step at 10,000 x g for 15 min the supernatant was kept for analysis of the immunoprecipitated CPAF by SDS-PAGE.

### **2.2.15 Endoglycosidase H treatment**

For the Endoglycosidase H (Endo H) cleavage of MHCI cell lysates were made by scraping cells into 1% Triton X-100/PBS containing protease inhibitors (0.1 mM PMSF, 50 µg/ml aprotinin, 2 µg/ml leupeptin). After incubation for 45 min at 4°C with mixing every 10 min the lysates were centrifuged at 20,000 x g for 10 min at 4°C to remove cellular debris. For the assay 10 µl lysate were mixed with 20 µl Endo H reaction buffer (see Table 6 in Appendix 6.1.4) and incubated for 30 min at RT with shaking. Thereafter, 100 U of Endo H (New England Biolabs, Frankfurt am Main, Germany) were added to each sample. The mixtures were incubated overnight at 37°C and finally analysed by SDS-PAGE and immunoblotting. Samples without Endo H treatment were used as controls.

### **2.2.16 Fluorescence in situ hybridisation (FISH)**

FISH was done according to Herold *et al.* (2001) with some modifications. Infected cell monolayers grown on coverslips were fixed with 2% paraformaldehyde for 20 min. After washing three times in PBS and permeabilisation with 0.5% Saponin/PBS for 10 min the coverslips were incubated with prehybridisation buffer (see Table 6 in Appendix 6.1.4) for 15 min at 37°C. Cy3 labelled oligo(dT)<sub>50</sub> (Jena Bioscience, Jena, Germany) was used as probe for hybridisation with poly(A)<sup>+</sup> RNA. The cell monolayers were covered with 0.5 pmol of Cy3 labelled oligo(dT)<sub>50</sub> per µl hybridisation buffer (see Table 6 in Appendix 6.1.4) and incubated in a closed humidity chamber for three hours at 37°C. The following washing steps were applied (each two times for five minutes): 2x saline-sodium citrate (SSC) buffer (see Table 6 in Appendix 6.1.4) containing 20% formamide at 42°C, 2x SSC buffer at 42°C, 1x SSC buffer at RT and PBS at RT. Subsequently, immunofluorescence staining of chlamydiae was performed with a FITC-conjugated mouse anti-MOMP antibody (MikroTrak *Chlamydia trachomatis* Culture Confirmation Test, Trinity Biotech Plc, Bray, Ireland). Briefly, 10 µl of the antibody solution was diluted in 0.5% Saponin/PBS and incubated on the coverslips for one hour at RT. After washing three times with 0.5% Saponin/PBS the coverslips were mounted on microscopy slides with ProLong Gold antifade reagent containing DAPI (Invitrogen, Darmstadt, Germany) and examined with a confocal laser scanning microscope (LSM5, Zeiss, Jena, Germany) using the 543 nm

excitation wavelength (Helium-neon 543 nm laser, 1.2 mW) and the 560 nm longpass filter for Cy3, 488 nm excitation wavelength (Argon Laser 488 nm, 25 mW) and a 505 – 530 nm bandpass filter for FITC and 405 nm excitation wavelength (405-425 nm Laser Diode, 25 mW) and a 420 – 480 nm bandpass filter for DAPI.

### **2.2.17 Sample preparation for two dimensional (2D) gel electrophoresis**

Cells grown in T-25 flasks and infected with *C. trachomatis* at a MOI of 5 were scraped into 250 µl of 0.2 M sucrose/2% FCS/PBS per flask at 24 h p.i. The cell suspensions were collected on ice to inhibit proteases and to prevent a stress response that could result in a change of the chlamydial proteome. Chlamydial organisms were released from the cells by sonification. Then the suspension was stored at -80°C for later use. The preparation of RBs was done by density gradient ultracentrifugation of the cell suspensions according to Caldwell *et al.* (1981). The suspensions were centrifuged at 4,000 x g for 3 min at 4°C to remove cell debris. 24 ml of the supernatant (harvested from 96 T-25 flasks) was filled into a 34 ml quick-seal ultracentrifuge tube (Beckman Coulter, Krefeld, Germany) by means of a peristaltic pump. The density-gradient was generated with different concentrations of iodixanol (Visipaque 320, GE Healthcare, München, Germany). For the first round of ultracentrifugation the tube consisted of the following layers (from top to bottom): 24 ml cell suspension, 2 ml 8%, 3 ml 15% and 5 ml 30% of iodixanol solution. After centrifugation at 40,000 x g for 50 min at 4°C the sediment containing the bacteria was homogenised in 6 ml PBS. The next gradient filled in consisted of 1 ml 8%, 1 ml 15%, 1 ml 30%, 12 ml 36%, 8 ml 40% and 5 ml 47% iodixanol. During the second ultracentrifugation at 50,000 x g for 50 min at 4°C the RBs were collected as a ring in the 36% iodixanol zone and EBs resided between 40 and 47% iodixanol. The RB fraction was transferred to a new ultracentrifuge tube and the remaining iodixanol was removed by washing with PBS and centrifugation at 30,000 x g for 50 min at 4°C. The RB pellet was resuspended in 100 – 200 µl of 50 mM Tris-HCl, pH 7.2 (with 2 mM DTT as protein stabilisator and 100 µg/ml PMSF, 2 µg/ml Leupeptin and 12 µg/ml Aprotinin as protease inhibitors) and sonified followed by incubation for 15 min on ice for lysis.

The proteins were precipitated by TCA/acetone precipitation. Nine volumes of an ice-cold TCA solution (see Table 6 in Appendix 6.1.4) were added to the RB lysate and the sample was thoroughly mixed. After incubation overnight at -20°C and harsh mixing for 30 s the sample was centrifuged at 12,000 x g for 15 min at 4°C. The TCA solution was removed and the pellet washed twice in 1 ml of ice-cold washing solution (see Table 6 in Appendix

6.1.4). After complete removal of the acetone the pellet was allowed to air-dry for 5 min at RT, resuspended in lysis buffer for 2D gel electrophoresis (see Table 6 in Appendix 6.1.4) and incubated for 1 h at RT with mixing every 10 min to solubilise the proteins. After centrifugation at 20,000 x g for 20 min at 16°C the supernatant was transferred to a new tube. Protein concentration was determined according to Bradford *et al.* (1976) with the Bio-Rad Protein assay (Bio-Rad Laboratories, München, Germany) corresponding to the manufacturer's instructions. The RB protein sample was stored at -80°C.

### **2.2.18 2D gel electrophoresis of chlamydial RBs**

2D gel electrophoresis was carried out at the Leibniz Institute for Natural Product Research and Infection Biology in Jena, in cooperation with the department of Molecular and Applied Microbiology. The RB protein samples were separated by 2D gel electrophoresis according to Knemeyer *et al.* (2005) and Grosse *et al.* (2008). The 2D gels were stained with the fluorescent dye SYPRO Ruby Protein Gel Stain (Sigma-Aldrich Chemie, München, Germany) and scanned with a Typhoon multicolour fluorescence and phosphor image scanner (GE Healthcare, Freiburg, Germany) to visualize the proteins. Analysis of the 2D gels and quantitation of the protein spots were done with the Delta 2D software (version 3.4, Decodon, Greifswald, Germany). After isolation of the proteins from the gels and their tryptic digestion the identification of the proteins occurred by mass spectrometry using the MALDI TOF/TOF mass spectrometer Ultraflex I (Bruker Daltonics, Bremen, Germany). This was followed by NCBI database search with the software MASCOT 2.1.0. (Matrix Science, London, UK) using a MASCOT score of  $p = 0.05$  as significance level and the Protein Scape 1.3 software (Protagen, Dortmund, Germany).

### **2.2.19 Statistics**

Average values and standard deviations were determined with Microsoft Excel. To determine if the values are significant from each other a student t-test assuming unequal variances was applied by using Microsoft Excel. P values < 0.05 were considered as statistically significant.

## 3 Results

### 3.1 Characterisation of the persistent-like growth state of *C. trachomatis* in fibroblasts

#### 3.1.1 Comparison of the replication cycle of *C. trachomatis* between epithelial cells and fibroblasts

Fibroblasts could represent another host cell type in vivo in which chlamydiae may replicate after their spread from the infected epithelium to sublining tissue areas. Indeed, chlamydiae have been found inside of fibroblasts in synovial samples from patients with CiReA (Nanagara *et al.*, 1995) and were shown to be able to grow in synovial fibroblasts after in vitro infection (Rödel *et al.*, 1998 a, Rödel *et al.*, 1998 b). However, little is known about the detailed growth behaviour of *C. trachomatis* in fibroblasts as well as the ability of these bacteria to persist inside of these cells. Thus, growth of this organism in this cell type was analysed in more detail and compared with the productive growth in epithelial cells which is the principal host cell type for productive infection of *Chlamydia*.

HeLa cells, a cervix carcinoma cell line, were used as epithelial cell model and human diploid skin fibroblasts, which are primary cells, as fibroblast model for chlamydial infection. Dermal fibroblasts from foreskin were used, because they are easily available from healthy donors. Furthermore, they show similar growth behaviour like synovial fibroblasts (J. Rödel, personal communication). Fig. 4 shows that both HeLa cells and fibroblasts could be successfully infected with *C. trachomatis* as it can be seen by the development of inclusions. An obvious difference between the cell types was the size of inclusions, because inclusions within fibroblasts were much larger (~ 30 x 10 µm at 24 h p.i.) than inclusions within HeLa cells (~ 10 x 10 µm at 24 h p.i.; Fig. 4). Fibroblast inclusions could become very large, with sizes up to 100 µm length and 30 µm width, whereas HeLa cells only contained inclusions of up to 50 µm length and 20 µm width (Fig. 4).

The replication efficiency of chlamydial organisms in both cell types was assessed by quantification of inclusions and intracellular production of new infectious EBs (expressed as IFUs) in shell vials at different time points after infection (Table 1). The amount of inclusion-containing HeLa cells was  $4.7 \times 10^4$  representing 47% of all cells ( $1 \times 10^5$ ) in the culture. This correlates well with the MOI of 0.5 used for this experiment and indicates that HeLa cells are highly susceptible for *C. trachomatis* infection since almost every EB in the inoculum could infect and successfully develop an inclusion in HeLa cells.

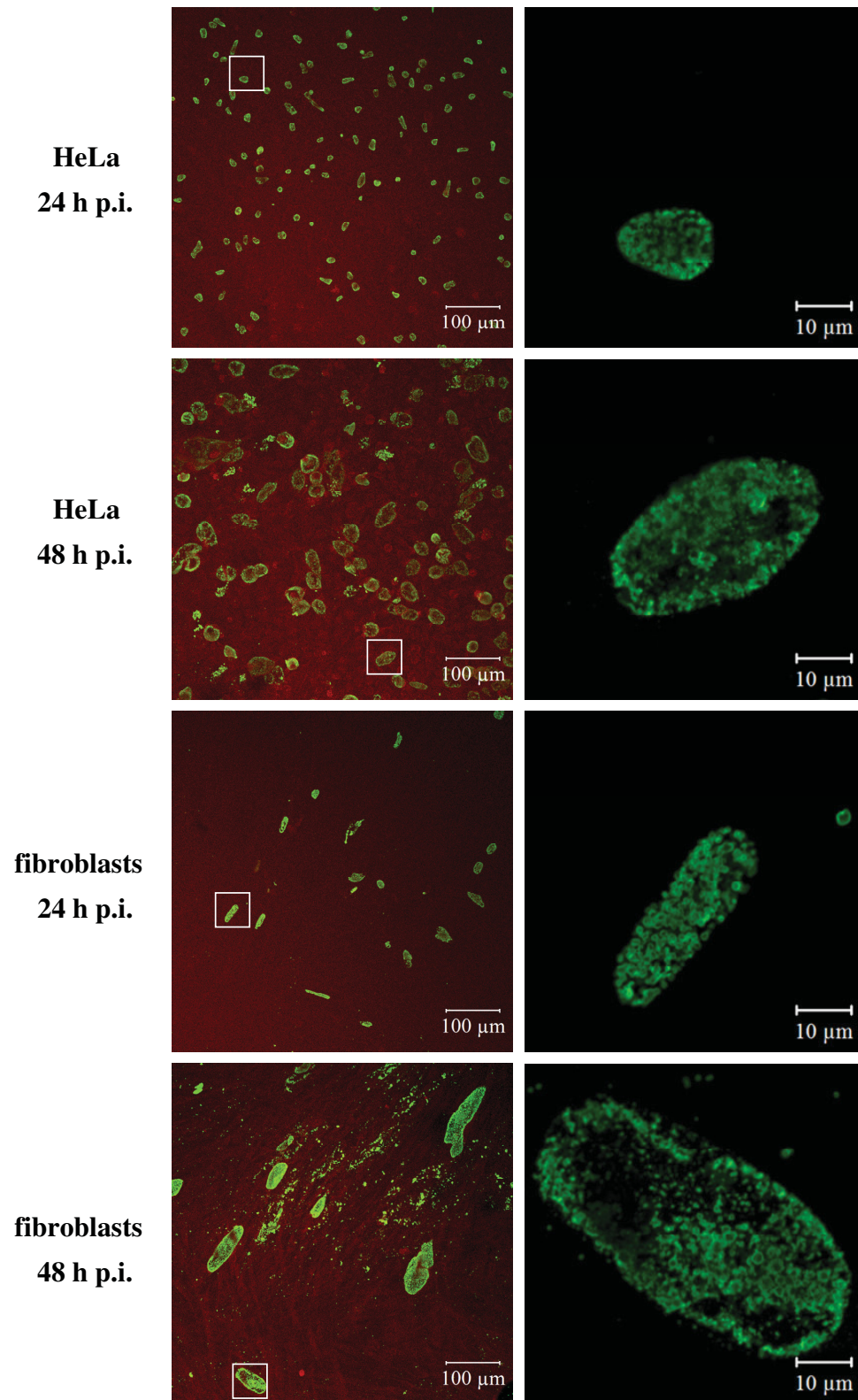


**Fig. 4: Immunofluorescent staining of *C. trachomatis* inclusions in HeLa cells and fibroblasts.**

Chlamydial inclusions in HeLa cells and fibroblasts infected with a MOI of 0.5 were stained with FITC-anti-MOMP (green). Cells were counter-stained with Evans Blue (red). The pictures on the right are detailed pictures of the inclusions on the respective left pictures (marked with a rectangle).

In contrast, infection of fibroblasts with the same inoculum resulted in an inclusion number of only  $2.4 \times 10^3$  which indicates that just 2.4% of all cells were infected. Because the inclusion number in fibroblasts was only 5% of that of HeLa cells (Table 1), it can be concluded that fibroblasts are much less susceptible for infection with *C. trachomatis* than HeLa cells.

The difference was even more pronounced on the level of intracellular EBs (Table 1). The production of infectious progeny at 48 h p.i. was lower in fibroblasts than in HeLa cells by 3 log ranges. Since both the inclusion number and the IFUs in HeLa cells and fibroblasts were different it was important to calculate the burst size (IFUs produced per inclusion) for direct comparison of the chlamydial replication efficiency (Table 1 and Fig. 5). In both cell types only few bacteria converted back from RBs to EBs already at 24 h p.i. In HeLa cells the burst size highly increased from 24 to 48 h p.i. to around 740 EBs per inclusion correlating with the normal time period of 48 h that *C. trachomatis* needs to complete its intracellular multiplication and re-differentiation to EBs.

**Table 1: Replication efficiency of *C. trachomatis* in epithelial cells and fibroblasts: inclusion numbers, IFUs and burst size.**

Cells were infected with *C. trachomatis* at a MOI of 0.5 and the number of inclusions was determined at 24 h p.i. The number of IFUs was determined at 24, 48 and 72 h p.i. The burst size represents the IFUs produced per inclusion. Values are given with standard deviations in brackets and show the mean of five independent experiments in duplicate.

	time p.i.	HeLa	fibroblasts	fibroblasts per-centage of HeLa	p value
<b>Inclusions</b>	24 h	<b><math>4.7 \times 10^4</math></b> ( $9.5 \times 10^3$ )	<b><math>2.4 \times 10^3</math></b> ( $8.9 \times 10^2$ )	5.1%	< 0.0000001
<b>IFUs</b>	24 h	<b><math>2.5 \times 10^5</math></b> ( $1.8 \times 10^5$ )	<b><math>8.5 \times 10^2</math></b> ( $3.9 \times 10^2$ )	0.3%	< 0.0001
	48 h	<b><math>3.4 \times 10^7</math></b> ( $9.4 \times 10^6$ )	<b><math>5.3 \times 10^4</math></b> ( $2.9 \times 10^4$ )	0.2%	< 0.000001
	72 h	<b><math>2.2 \times 10^7</math></b> ( $6.8 \times 10^6$ )	<b><math>3.9 \times 10^4</math></b> ( $1.9 \times 10^4$ )	0.2%	< 0.000005
<b>Burst size</b>	24 h	<b>5.9</b> (5.4)	<b>0.4</b> (0.2)	6.5%	< 0.05
	48 h	<b>743.8</b> (277.2)	<b>22.0</b> (8.0)	3.0%	< 0.00005
	72 h	<b>480.8</b> (159.9)	<b>20.2</b> (14.3)	4.2%	< 0.00001

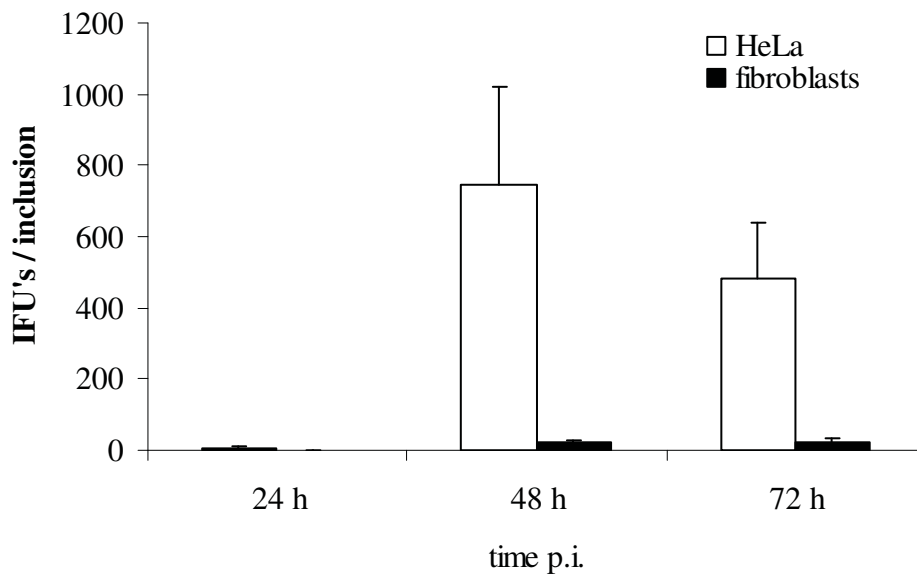


**Fig. 5: Burst size of *C. trachomatis* in epithelial cells and fibroblasts.**

See **Table 1** for description and values.

At 72 h p.i. the number of IFUs in HeLa cells decreased to 480 EBs per inclusion, suggesting that EB release from the cells had occurred between 48 and 72 h p.i. In contrast, in fibroblasts a burst size of only 22 EBs per inclusion could be observed at 48 h p.i. representing only 3% of the amount in HeLa cells. The burst size of *C. trachomatis* in fibroblasts remained at this low level between 48 and 72 h p.i. indicating that there was no delay in the developmental cycle.

Another approach to analyse the development and to evaluate the morphology of chlamydial organisms in more detail is transmission electron microscopy. With this method EBs can be distinguished from RBs by their higher electron density and their smaller size (Matsumoto & Manire, 1970). At 48 h p.i. the inclusions in HeLa cells basically contained EBs (Fig. 6) correlating with the data in Fig. 5. In contrast, in fibroblasts much fewer EBs could be detected and inclusions were mainly filled with RBs. Interestingly, the morphology and size of most of the RBs in fibroblasts was similar to that of RBs in HeLa cells indicating that they rather represent normal RBs than enlarged aberrant bodies (ABs) which are normally found during chlamydial persistence. However, a few ABs were also detectable in fibroblasts. Many of the normal-sized RBs in fibroblast inclusions contained a small electron dense point in their middle indicating a starting re-differentiation to EBs. This form is often found to be described as an intermediate body (IB).

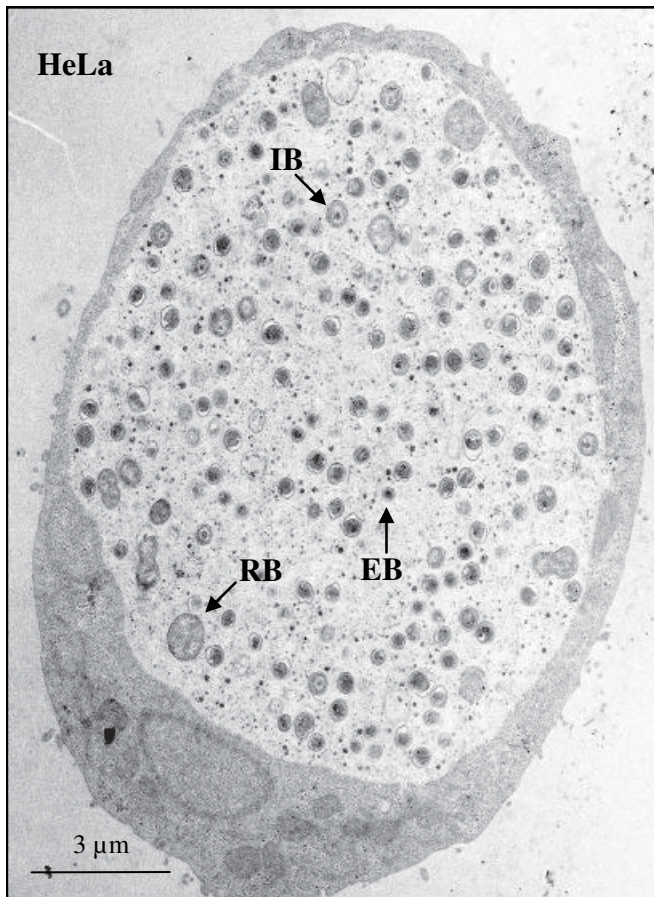
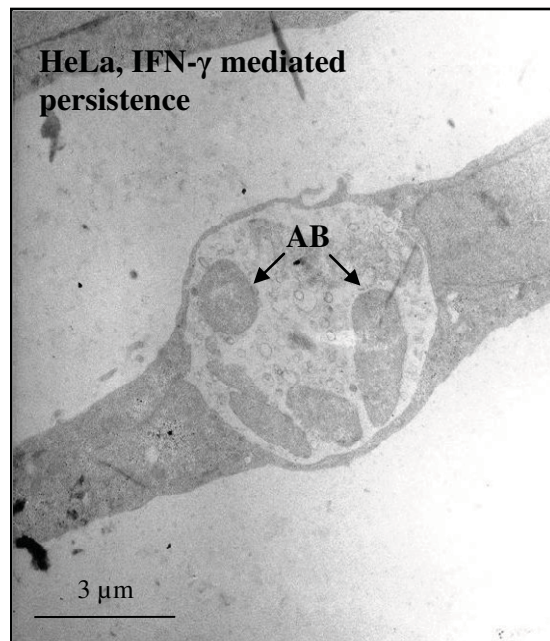
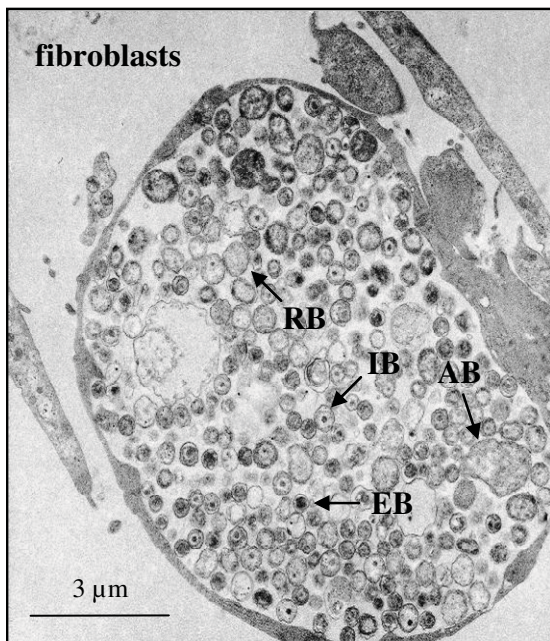


**Fig. 6: *C. trachomatis* inclusions visualised by transmission electron microscopy.**

Depicted in each picture is one cell containing one chlamydial inclusion at 48 h p.i. The picture showing the fibroblast likely represents a cross section of an inclusion. The picture demonstrating the IFN- $\gamma$  mediated persistent infection of a HeLa cell was taken from the publication of Rödel *et al.*, 2012.

RB: reticulate body,  
 EB: elementary body,  
 IB: intermediate body,  
 AB: aberrant body.



For comparison, the morphology of *C. trachomatis* during IFN- $\gamma$  mediated chlamydial persistence in HeLa cells was also analysed. In this model, persistence was induced by incubation of HeLa cells with 100 U/ml IFN- $\gamma$  48 h before infection and ongoing post-infection treatment with IFN- $\gamma$ . The pre-treatment was necessary, because *C. trachomatis* serovar D is less susceptible to the IFN- $\gamma$  inhibitory effect than other *C. trachomatis* serovars, and

inhibition of IFU production only occurs when cells were pre-treated with IFN- $\gamma$  at a minimum concentration of 100 U/ml for 48 h before infection (Morrison, 2000; Yu, 2010). Inclusions that developed during IFN- $\gamma$  mediated persistence in HeLa cells were much smaller than those observed during active infection and contained only few, but very large ABs (Fig. 6). These results suggest that the growth of *C. trachomatis* in fibroblasts also differs from that during IFN- $\gamma$  mediated persistent infection in epithelial cells.

### 3.1.2 *IDO* expression in *C. trachomatis*-infected fibroblasts

In the IFN- $\gamma$  mediated chlamydial persistence model the tryptophan deficiency caused by *IDO* induces the persistent growth state of the chlamydial organisms (Beatty *et al.*, 1994 a). Expression of *IDO* can also be induced by type I IFN (Sanda *et al.*, 2006), and synovial fibroblasts secrete IFN- $\beta$  after infection with *C. trachomatis* which induces *IDO* expression in these cells (Rödel *et al.*, 1998 a, Rödel *et al.*, 1999). Thus, it was assumed that *IDO* could play a role in eliciting the atypical growth state of *C. trachomatis* in fibroblasts.

First, an ELISA was applied to quantify the amount of IFN- $\beta$  in the supernatant of the cells to analyse if dermal fibroblasts also produce IFN- $\beta$  upon infection with *C. trachomatis*. The results reveal that *Chlamydia*-infected dermal fibroblasts, but not HeLa cells, readily produce IFN- $\beta$  after 48 h p.i. (Table 2).

Similar to synovial fibroblasts (Rödel *et al.*, 1998 a, Rödel *et al.*, 1999), *IDO* expression was also highly upregulated after *C. trachomatis* infection of dermal fibroblasts (Fig. 7). To analyse, if the endogenously produced IFN- $\beta$  accounts for this effect, an antibody binding to the type I IFN receptor (IFNAR) was used to block the type I IFN response. Incubation with this antibody abolished the upregulation of *IDO* expression in infected fibroblasts to a large extent (Fig. 7).

**Table 2: IFN- $\beta$  production in HeLa cells and fibroblasts.**

Supernatants taken from infected and mock-infected cells (MOI 0.5) at the indicated time points were used for measuring the amount of secreted IFN- $\beta$  with an ELISA Kit detecting human IFN- $\beta$ . Values are the mean of three independent experiments with standard deviations in brackets.

<i>C. trachomatis</i> infection	HeLa		fibroblasts	
	-	+	-	+
24 h p.i.	-	-	-	-
48 h p.i.	-	-	-	3.5 (3.1) U/ml
72 h p.i.	-	-	-	2.7 (2.0) U/ml

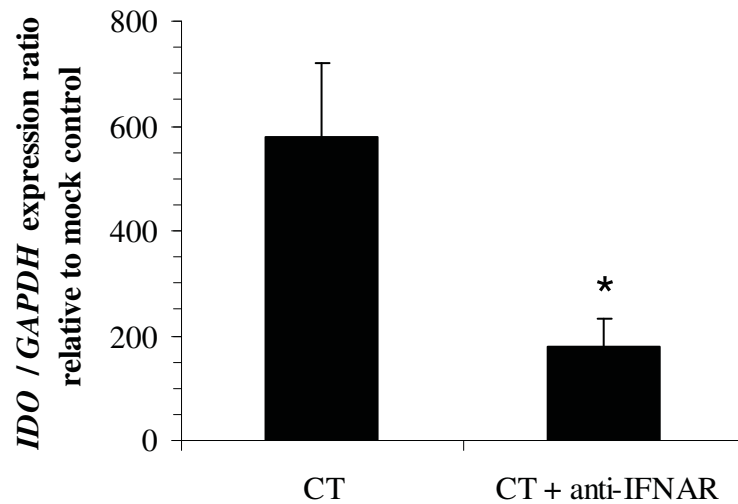


**Fig. 7: Influence of *C. trachomatis* infection on *IDO* gene expression in fibroblasts.**

Gene expression in *C. trachomatis* (CT) infected fibroblasts (MOI 0.5) at 48 h p.i. is depicted as x-fold regulation compared to expression in uninfected cells. Depicted is the average value of three independent experiments with standard deviation as error bar. An antibody binding the type I IFN receptor (anti-IFNAR) was added to the infected culture to neutralize type I IFN activity. \*p < 0.01 compared to value for infected cells without treatment.

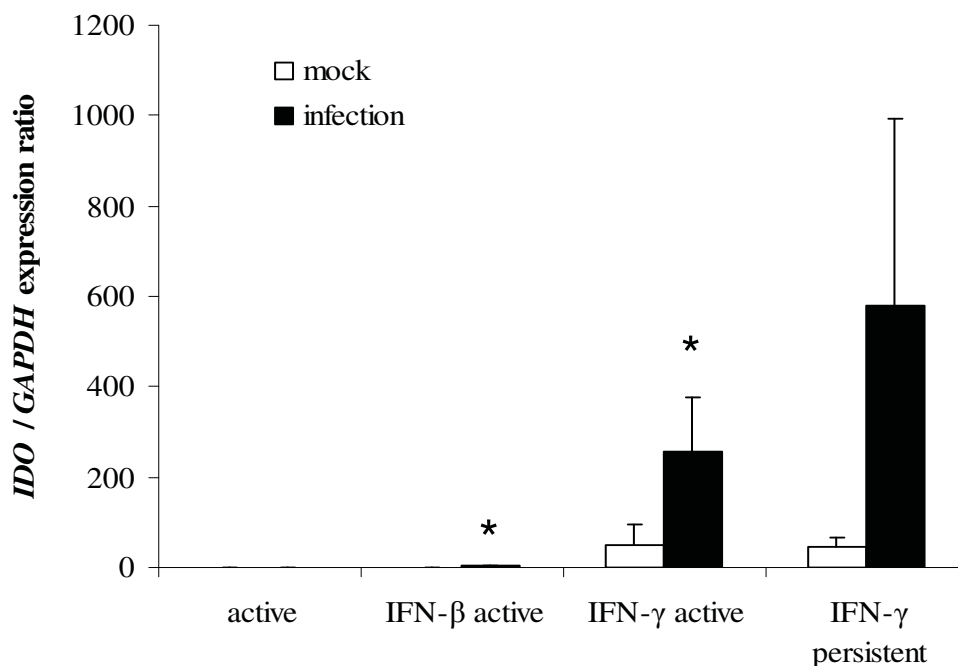


**Fig. 8: Influence of *C. trachomatis* infection on *IDO* gene expression in HeLa cells.**

Gene expression at 48 h p.i. is depicted as x-fold expression change compared to untreated mock-infected cells (\* p < 0.05 shows significant upregulation compared to mock-infected cells in the same infection model). The mean values of three independent experiments with standard deviation as error bars are shown. Cells were either not treated (active infection) or treated with 100 U/ml IFN-β (IFN-β active infection) and 100 U/ml IFN-γ (IFN-γ active infection), respectively. To induce chlamydial persistence IFN-γ treatment started already 48 h before infection (IFN-γ persistent infection).

This result indicates that the infection-induced endogenously produced IFN- $\beta$  strongly contributes to the induction of *IDO* expression after chlamydial infection of fibroblasts. For comparison, the effect of *C. trachomatis* infection on *IDO* expression was also examined in HeLa cells. No upregulation in *IDO* expression could be detected for HeLa cells actively infected with *C. trachomatis* (Fig. 8). Furthermore, the effect of IFN treatment on *IDO* expression in infected HeLa cells was analysed with two other infection models, in which IFN- $\beta$  or IFN- $\gamma$  were added at 0 h p.i. In difference to the IFN- $\gamma$  induced persistence model that required 48 h pre-treatment with IFN- $\gamma$ , the addition of IFN- $\beta$  and IFN- $\gamma$  after infection had no obvious effect on the morphology and growth of *C. trachomatis* serovar D in HeLa cells (data not shown). Thus, these two models are referred to as active infection with IFN- $\beta$  and IFN- $\gamma$  treatment, respectively. In actively infected HeLa cells treated with IFN- $\beta$  or IFN- $\gamma$  there was a significant upregulation of *IDO* expression compared to the respective IFN treated uninfected control. This effect was even more pronounced in the IFN- $\gamma$  mediated persistent infection model, and IFN- $\gamma$  generally was much more potent in eliciting *IDO* expression than IFN- $\beta$ . Thus, *IDO* expression in HeLa cells could only be induced by exogenously added IFN, and the expression level was influenced by the IFN type and by infection with chlamydiae, which seems to induce factors that act synergistically with IFN in upregulating *IDO* expression.

### **3.1.3 Role of IDO in growth inhibition of *C. trachomatis* in fibroblasts**

To examine whether IDO is involved in growth inhibition of *C. trachomatis* in fibroblasts, *IDO* expression was downregulated by siRNA knockdown in infected cells. Fig. 9 displays the efficiency of the knockdown through analysis of *IDO* gene expression in transfected relative to non-transfected cells. Transfection with *IDO* siRNA was very efficient with 91% reduction in gene expression. However, transfection with the transfection reagent alone had also a slight effect on *IDO* expression by 25% reduction, and negative control siRNA even decreased expression to 49%. It is known that siRNAs are able to induce unspecific off-target effects by stimulation of innate immunity (reviewed in Samuel-Abraham & Leonard, 2010). This could explain the observed effects of the transfection controls on *IDO* expression. These effects of transfection itself have to be considered when evaluating the results for *IDO* siRNA knockdown.

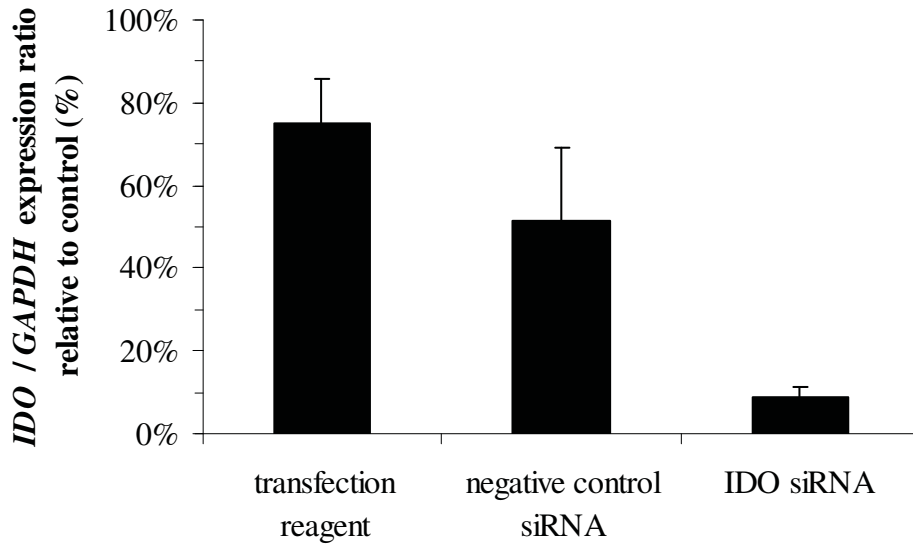


**Fig. 9: Efficiency of *IDO* siRNA knockdown in *C. trachomatis* infected fibroblasts.**

*IDO* gene expression in *Chlamydia*-infected (MOI 0.5), transfected fibroblasts was analysed at 48 h p.i. Depicted is the percentage of gene expression relative to the infected, non-transfected control. The mean values of three independent experiments are shown with standard deviations as error bars.

*IDO* siRNA transfection of fibroblasts led to a significant increase in chlamydial growth as can be seen by a nearly 2-fold increase in the inclusion number (increase from  $6.6 \times 10^3$  [control] to  $10.3 \times 10^4$  [*IDO* siRNA] inclusions) and a 6.2-fold higher production of IFUs (increase from  $2.7 \times 10^4$  [control] to  $16 \times 10^4$  [*IDO* siRNA] IFUs) at 48 h p.i. (Fig. 10).

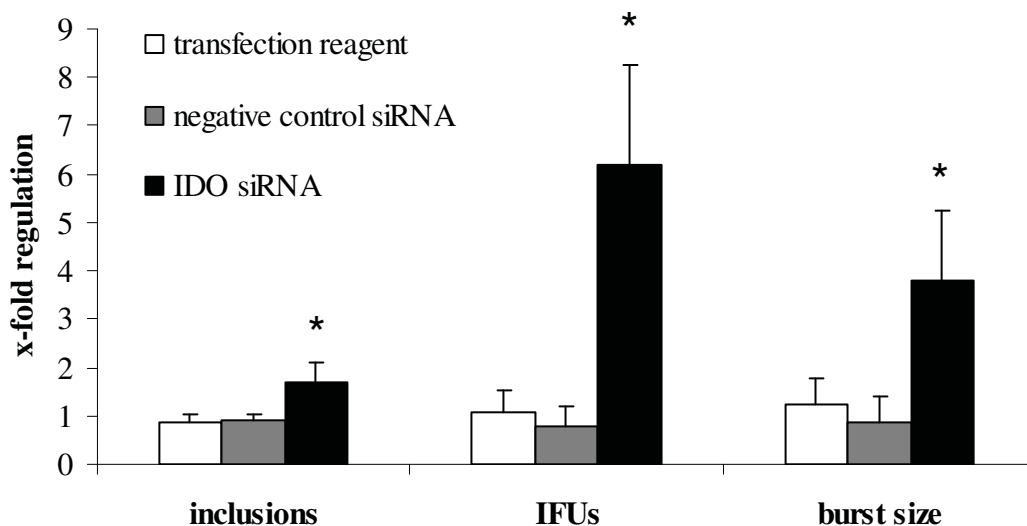


**Fig. 10: Effect of *IDO* siRNA knockdown on *C. trachomatis* growth in fibroblasts.**

The inclusion numbers were calculated 24 h after infection (MOI 0.5) and IFUs were determined at 48 h p.i. Values are expressed as x-fold change of transfected cells relative to the non-transfected control cells. Values are shown as mean of three independent experiments in triplicate with standard deviations as error bars. \* $p < 0.001$  for *IDO* siRNA values compared to negative control siRNA values.

This resulted in a burst size almost 4 times higher than in non-transfected control cells. Although an influence on *IDO* gene expression had been observed in fibroblasts transfected with transfection reagent alone or negative control siRNA, no significant change in chlamydial growth could be detected under these conditions. The results strongly suggest that IDO is involved in inducing the atypical development of *C. trachomatis* in fibroblasts.

### **3.1.4 Expression of selected chlamydial genes in epithelial cells and fibroblasts infected with *C. trachomatis***

To further characterize the atypical developmental cycle of *C. trachomatis* in fibroblasts a comparative proteome analysis of RBs isolated from infected fibroblasts and HeLa cells at 24 h p.i. was used to find chlamydial proteins that are differentially expressed in both cell types (see Appendix 6.2 for results). On the 2D gel of RBs isolated from infected HeLa cells several chlamydial proteins could be identified by mass spectrometry. However, the detection of chlamydial proteins on the 2D gel of RBs from fibroblasts was hampered by co-purification of a huge amount of human proteins, probably due to the low percentage of inclusion-containing cells. Therefore the protein expression differences between the two samples could not be directly compared with each other with this method. Thus, to characterise the differences in the growth of *C. trachomatis* in fibroblasts and HeLa cells gene expression analysis of selected chlamydial genes at different stages of the developmental cycle was performed as another approach.

Most of the genes analysed were downregulated during IFN- $\gamma$  mediated persistent infection compared to active infection of HeLa cells at 48 h p.i. (Fig. 11). These genes included *ompA*, which encodes the MOMP of the chlamydial cell envelope, *dnaA*, encoding a DNA replication protein, *pgsA\_2*, encoding a key enzyme of the glycerophospholipid metabolism, and *omcB*, which encodes the 60 kDa cysteine-rich outer membrane protein that is needed for generating the rigid EB cell wall (Hatch *et al.*, 1986). Further, the expression of *ct858* encoding CPAF was strongly reduced during IFN- $\gamma$  mediated persistence, which is consistent with the recently published results of our group (Rödel *et al.*, 2012). Also, expression of two of the three genes encoding the chlamydial HSP60 (*groEL*, *groEL\_2* and *groEL\_3*) was examined. The gene *groEL\_2* was included in the present work, because Gérard *et al.* (2004) found a significantly higher upregulation of *groEL\_2* expression relative to *groEL* in persistent infection in monocytes than in active infection of HEP-2 cells. Both *groEL* and *groEL\_2* generally showed a lower expression level during IFN- $\gamma$  mediated persistence than during active infection of HeLa cells at later time points.

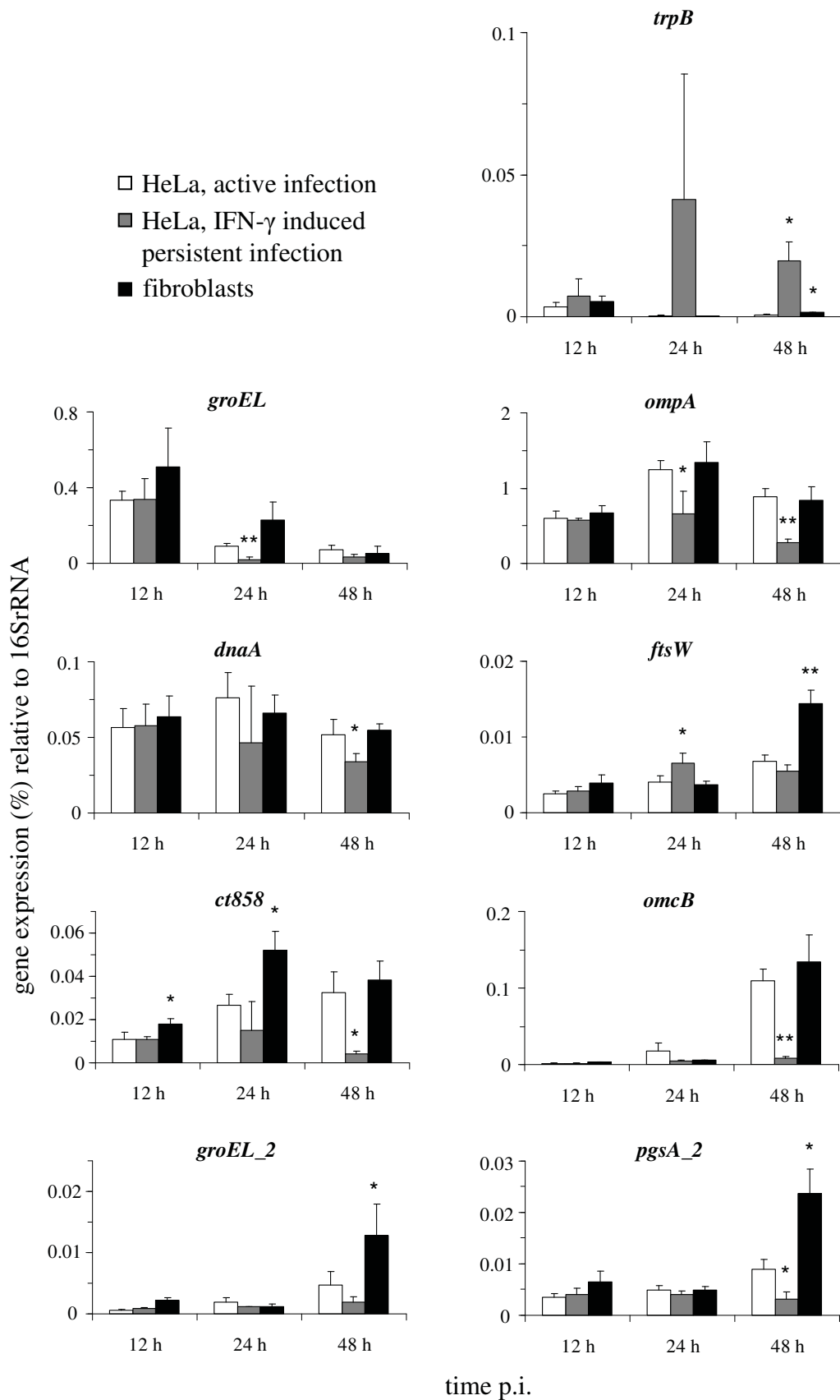


**Fig. 11: Expression of *C. trachomatis* genes in the three different infection models.**

Cells were infected with a MOI of 0.5 for the indicated time points. Significant differences compared to actively infected HeLa cells are indicated with asterisks (\* $p < 0.05$ , \*\* $p < 0.005$ ). The graphs show mean values of three independent experiments with standard deviations as error bars.

In contrast to the above described genes, a decrease in *ftsW* expression during IFN- $\gamma$  mediated persistence compared to active infection of HeLa cells could not be observed. The only gene for which expression was found to be highly upregulated (~ 100-fold at 24 h p.i.) in the IFN- $\gamma$  mediated persistence model relative to the active infection was the gene *trpB*, which encodes the tryptophan synthase subunit  $\beta$ .

Expression of the chlamydial tryptophan synthase subunits encoding genes usually is induced by tryptophan limitation, which is the case after IFN- $\gamma$  activation of IDO leading to degradation of most of the tryptophan in the host cell (Shaw *et al.*, 2000 b).

In contrast to the IFN- $\gamma$  mediated persistent infection of HeLa cells there was no general downregulation of chlamydial gene expression in infected fibroblasts compared to actively infected HeLa cells. Although expression of most of the genes examined was not much differing between these two infection models, some important differences were observed for *ftsW*, *groEL\_2* and *pgsA\_2*. These genes showed a significantly higher expression at 48 h p.i. in infected fibroblasts relative to actively infected HeLa cells. Furthermore, expression of the CPAF encoding *ct858* was higher in infected fibroblasts than during active infection of HeLa cells at 12 and 24 h p.i. *trpB* was the only gene that was characterised by an increased expression in both infected fibroblasts and the IFN- $\gamma$  mediated persistence model relative to actively infected HeLa cells. However, there only was a 2-fold upregulation of *trpB* expression at 48 h p.i. in fibroblasts, which is very low compared to the ~ 30-fold increased expression of this gene at the same time point in the IFN- $\gamma$  mediated persistent infection relative to the active infection of HeLa cells. In contrast to the IFN- $\gamma$  mediated persistence model, expression of the late gene *omcB* was upregulated in infected fibroblasts at 48 h p.i., similar to actively infected HeLa cells. This indicates that growth of chlamydial organisms in fibroblasts occurs in a similar way like active infection in HeLa cells until the late stage of the developmental cycle and is not interrupted at earlier stages like during IFN- $\gamma$  mediated persistence.

Altogether, these results reveal that the expression of chlamydial genes is very different between infected fibroblasts and IFN- $\gamma$  mediated persistence in HeLa cells, especially for *groEL\_2*, *pgsA\_2* and *ct858*, that showed an increased expression in infected fibroblasts and a decreased expression during IFN- $\gamma$  mediated persistence relative to active infection. The gene expression pattern of these two infection models correlates well with the different morphologies of the bacteria observed in the electron microscopic pictures (Fig. 6). It strongly suggests that the development of *C. trachomatis* is quite differently regulated between both cell types due to different host cell conditions.

### 3.1.5 Influence of IDO expression on chlamydial gene expression in fibroblasts infected with *C. trachomatis*

The role of IDO in the atypical development of *C. trachomatis* in fibroblasts was also assessed on the chlamydial gene expression level. For this purpose *IDO* expression was reduced by siRNA knockdown in infected fibroblasts and expression of chlamydial genes was examined relative to expression in infected non-transfected cells at 48 h p.i. (Table 3). With the exception of *dnaA* the genes that were not significantly differentially expressed between infection in fibroblasts and active infection in HeLa cells also revealed no large expression change after *IDO* siRNA knockdown in fibroblasts (*groEL*, *ompA*, *ct858*, *omcB*, compare Table 3 with Fig. 11). This indicates that expression of these genes is not strongly influenced by IDO mediated tryptophan depletion in fibroblasts.

**Table 3: Influence of *IDO* siRNA knockdown on expression of chlamydial genes in fibroblasts.**

Gene expression was monitored in infected (MOI 0.5) fibroblasts at 48 h p.i. and displayed as x-fold expression ratio of transfected cells compared to non-transfected control cells. Values are shown as average of three independent experiments with standard deviations in brackets. For comparison, the x-fold expression ratios of chlamydial genes in infected fibroblasts compared to actively infected HeLa cells at 48 h p.i. are displayed, calculated from the values from the experiment displayed in Fig. 11. Values of genes, for which the *IDO* siRNA knockdown clearly abrogated the observed upregulation in fibroblasts compared to actively infected HeLa cells, are shown in bold.

<b>x-fold expression of <i>C. trachomatis</i> genes normalised to <i>C. trachomatis</i> 16SrRNA expression in transfected fibroblasts relative to fibroblasts without transfection</b>				
	<b>transfection reagent control</b>	<b>negative control siRNA</b>	<b><i>IDO</i> siRNA</b>	<b>fibroblasts vs. HeLa active (see Fig. 11)</b>
<i>groEL</i>	1.08 (0.36)	1.02 (0.03)	1.51 (0.27)	0.77
<i>ompA</i>	1.02 (0.29)	1.27 (0.35)	1.47 (0.13)	0.95
<i>dnaA</i>	1.44 (0.42)	1.17 (0.55)	0.65 (0.19)	1.06
<i>ct858</i>	1.26 (0.55)	0.94 (0.22)	0.74 (0.03)	1.17
<i>omcB</i>	0.97 (0.13)	0.93 (0.08)	1.08 (0.35)	1.23
<i>ftsW</i>	1.41 (0.46)	1.16 (0.61)	<b>0.46</b> (0.41)	<b>2.12</b>
<i>trpB</i>	1.87 (0.27)	1.19 (0.96)	<b>0.72</b> (0.20)	<b>2.20</b>
<i>pgsA_2</i>	1.76 (0.60)	1.06 (0.63)	<b>0.64</b> (0.41)	<b>2.63</b>
<i>groEL_2</i>	1.53 (0.34)	1.11 (0.48)	<b>0.48</b> (0.37)	<b>2.76</b>

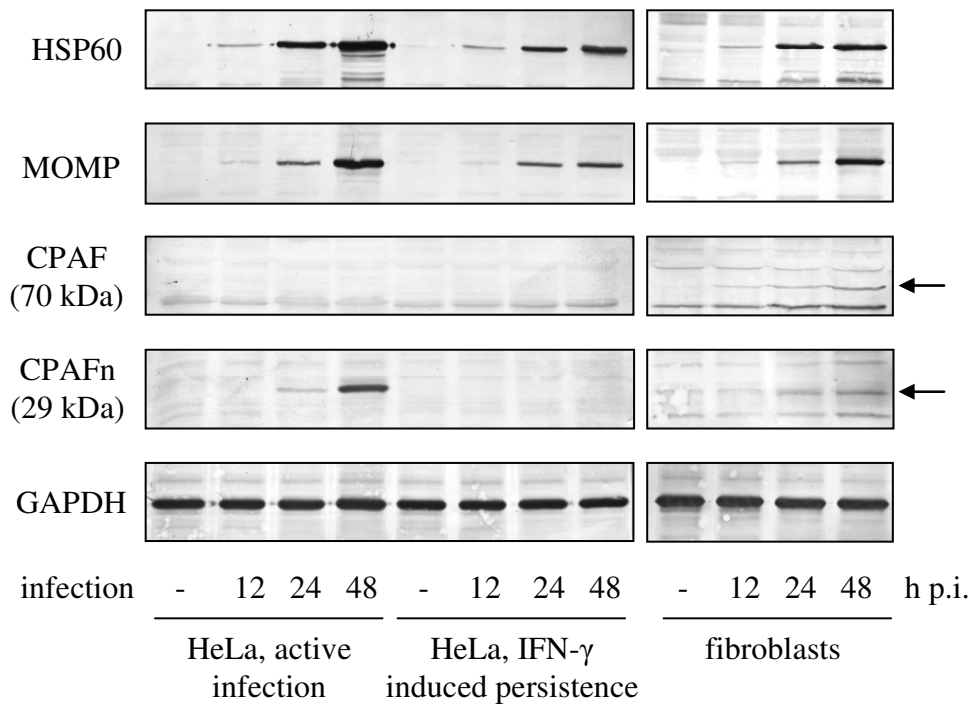
However, for *dnaA* and genes that showed a significantly upregulated expression in fibroblasts relative to active infection in HeLa cells at 48 h p.i. (see Fig. 11) reduced expression was found after *IDO* siRNA knockdown (*ftsW*, *trpB*, *pgsA\_2*, *groEL\_2*, Table 3). This downregulation seemed to abrogate the normally observed differential expression between infected fibroblasts and actively infected HeLa cells (Table 3, values in bold). However, the transfection reagent alone and the negative control siRNA affected also the expression of these genes. Treatment of cells with transfection reagent alone led to their upregulated expression to a different extent, which was less when the cells were transfected with negative control siRNA. Although there was no statistical significance between the values for *IDO* siRNA transfection and the negative control siRNA values, probably due to the low amount of samples, the results are quite convincing because of the downregulation of gene expression after *IDO* siRNA transfection in spite of concomitant upregulated gene expression in the transfection reagent control. Thus, if one considers the *IDO* siRNA values relative to the transfection reagent control values the extent of downregulation would be even larger than the depicted values for *IDO* siRNA knockdown relative to untransfected cells. Hence, there obviously is a tendency to downregulation of those genes that had been upregulated in fibroblasts compared to active infection in HeLa cells when *IDO* expression is inhibited. These results additionally support the hypothesis that *IDO* is involved in mediating an atypical growth of *C. trachomatis* in fibroblasts.

### **3.1.6 Differences in the expression of the chlamydial protease CPAF between active and persistent infection in epithelial cells and in fibroblasts**

Since the present work focused on the *C. trachomatis*-host cell interaction, the expression of the important virulence factor CPAF, which is known to be involved in interference with different host cell functions, was analysed on the protein level in the three infection models and compared with the expression of chlamydial HSP60 and MOMP.

As expected, the 29 kDa N-terminal fragment of the active form of CPAF (CPAFn), which usually is generated by autocleavage after secretion of the 70 kDa inactive form into the host cytosol (Huang *et al.*, 2008), was expressed in readily detectable amounts at the late stage of actively infected HeLa cells (Fig. 12 A). The 70 kDa precursor form of CPAF could not be detected during active infection of HeLa cells. In contrast, during IFN- $\gamma$  mediated persistent infection in HeLa cells neither the 70 kDa nor the 29 kDa form of CPAF could be detected at all. This is consistent with the results on gene expression of the CPAF encoding gene *ct858* that was found to be downregulated in persistently infected

**A**



**B**

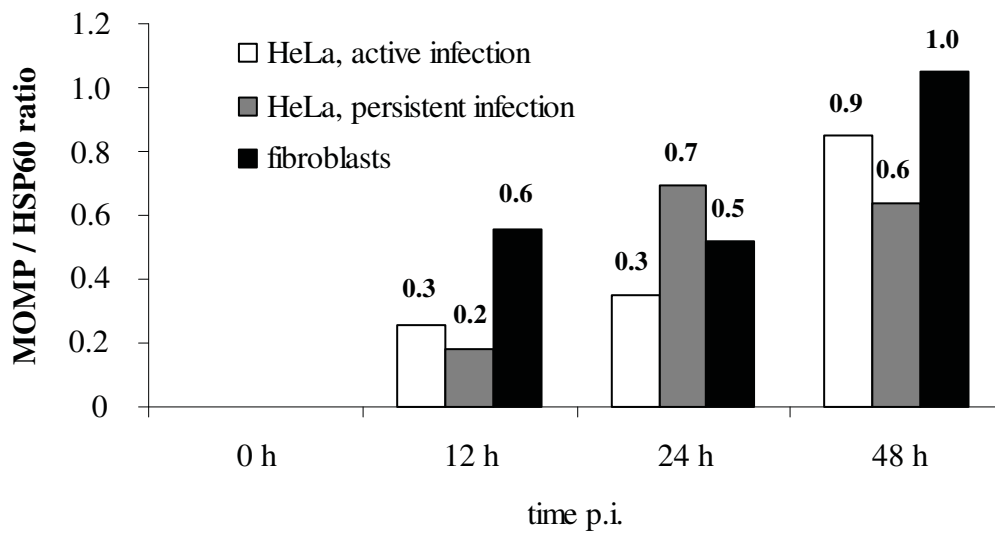


**Fig. 12: Protein expression of chlamydial CPAF, HSP60 and MOMP in the three infection models.**

**A** Depicted are immunoblots of whole cell lysates from *C. trachomatis* infected cells (MOI 0.5) generated at different time points of the chlamydial developmental cycle. CPAF (70 kDa): precursor form of CPAF. CPAFn (29 kDa): N-terminal fragment of proteolytically active CPAF.

**B** MOMP/HSP60 ratio of the immunoblots shown in **A** as measured by densitometry.

relative to actively infected HeLa cells (Fig. 11). Because HSP60 was still expressed in relatively high amounts during IFN- $\gamma$  mediated persistent infection, it can be excluded that the lack of CPAF detection is due to the reduced amount of chlamydial organisms. Also a slight reduction in expression of MOMP relative to HSP60 could be found at 48 h p.i. for this model, as it is known from previous studies (Fig. 12 B, Beatty *et al.*, 1993).

In contrast, *C. trachomatis*-infected fibroblasts showed no decrease in the MOMP/HSP60 ratio compared to actively infected HeLa cells, consistent with the gene expression results in Fig. 11. Although appearing as faint bands, CPAF protein was clearly expressed in infected fibroblasts, but at a much lower level than in actively infected HeLa cells. Both the 70 kDa and the 29 kDa forms were clearly visible at 48 h p.i., however the CPAF antiserum bound also unspecifically to a host cell protein at the size of 29 kDa (see lane of mock-infected fibroblasts in Fig. 12 A) thus interfering with a distinct detection of CPAF in fibroblasts. Nevertheless, the increasing intensity of the band over the time of infection in correlation with the expression of the 70 kDa form suggests that CPAF is expressed in infected fibroblasts.

## **3.2 Influence of *C. trachomatis* infection on the MHC class I antigen presentation pathway**

### **3.2.1 Surface expression of MHC class I in *C. trachomatis* infected cells**

Altered MHCI surface expression can be the result of interference of intracellular pathogens with the antigen processing pathway (reviewed in Antoniou & Powis, 2008). Therefore, the first step in analysis whether *C. trachomatis* interferes also with this pathway was investigation of MHCI surface expression on *Chlamydia*-infected cells using flow cytometry (Fig. 13 and Table 4).

Because not every cell in a *Chlamydia*-infected sample contained an inclusion, differentiation between infected (inclusion-positive) and uninfected (inclusion-negative) cells in the same sample occurred through immunofluorescent staining of chlamydial inclusions and gating into infected and uninfected populations after flow cytometric measurement. Only 10 – 20% of the cells in the *Chlamydia*-infected samples had a fluorescence intensity of inclusion staining that was above that of the cells of the mock-infected sample and could be considered as the infected cell population. This small rate of inclusion-containing cells is shown in Fig. 13 by the presence of the low peak (black) that represents the infected

population. The remaining cells of the *Chlamydia*-infected sample were considered as uninfected cell population.

After 40 h p.i. of active infection of HeLa cells a slight reduction (19%) of surface MHCI was found in the inclusion-positive cell population compared to the inclusion-negative cell population. Treatment of HeLa cells with IFN- $\beta$  and IFN- $\gamma$  generally increased MHCI surface expression. However, there was also a reduction of surface MHCI (23%) in the inclusion-positive population of the actively infected HeLa cells that were treated with IFN- $\beta$ , although the level of surface expression was not reduced to that of the inclusion-positive population without IFN- $\beta$  treatment. This indicates that IFN- $\beta$  efficiently increased MHCI expression not only in mock-infected but also in *Chlamydia*-infected HeLa cells. In both infection models the inclusion-negative population of the infected sample had a lower amount of surface-expressed MHCI than the mock-infected cell sample suggesting a paracrine effect due to soluble mediators.

In the IFN- $\gamma$  induced persistence model MHCI expression was not significantly different between the inclusion-positive and the inclusion-negative cell population of the infected sample (Table 4). However, there was also a general reduction of surface MHCI in the *Chlamydia*-infected sample compared to the mock-infected sample, probably due to paracrine effects.

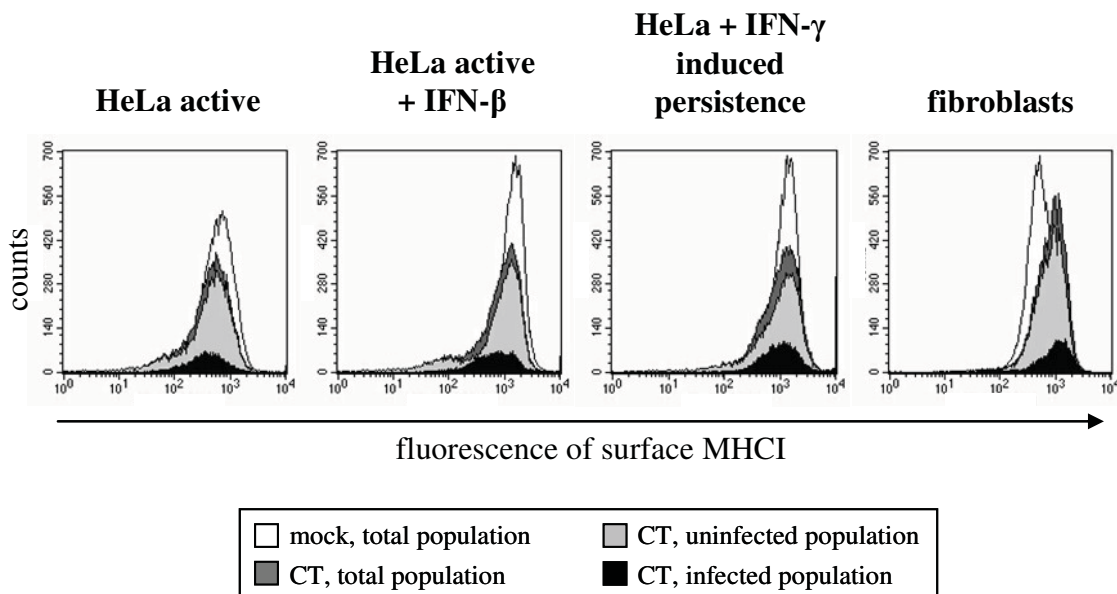


**Fig. 13: Influence of *C. trachomatis* infection on MHCI surface expression.**

Mock-infected (mock) and *C. trachomatis*-infected (CT) cells were prepared for flow cytometry at 40 h p.i. by PE-staining of surface MHCI and FITC-staining of chlamydial inclusions. Gating of the CT-infected sample was done to discriminate between infected and uninfected cell populations. Depicted are representative histograms. See Table 4 for median fluorescence intensity values of MHCI surface expression.

**Table 4: Influence of *C. trachomatis* infection on MHCI surface expression.**

Results of flow cytometry analysis are shown as average values of the median of MHCI fluorescence intensity of three experiments with standard deviations in brackets. <sup>a</sup>  $p < 0.05$  vs. mock total, <sup>b</sup>  $p < 0.05$  vs. CT total, <sup>c</sup>  $p < 0.05$  vs. CT uninfected population. CT: *C. trachomatis*-infected cells.

Average median fluorescence values								
Sample, cell population	HeLa active		HeLa active + IFN- $\beta$		HeLa + IFN- $\gamma$ persistence		fibroblasts	
	values	% of mock	values	% of mock	values	% of mock	values	% of mock
<b>Mock, total</b>	<b>627.5</b> (26.1)	100%	<b>1384.1</b> (48.9)	100%	<b>1330.7</b> (135.1)	100%	<b>433.8</b> (28.0)	100%
<b>CT, total</b>	<b>547.3</b> (50.6)	87%	<b>1039.7</b> (55.7) <sup>a</sup>	75%	<b>1019.6</b> (172.1)	76%	<b>611.8</b> (98.4)	140%
<b>CT, uninfected population</b>	<b>567.4</b> (52.4)	90%	<b>1106.5</b> (79.8) <sup>a</sup>	80%	<b>1035.3</b> (184.6)	77%	<b>584.0</b> (97.2)	134%
<b>CT, infected population</b>	<b>444.0</b> (55.0) <sup>a</sup>	71%	<b>793.7</b> (74.8) <sup>a,b,c</sup>	57%	<b>938.3</b> (156.4)	70%	<b>824.4</b> (84.3) <sup>a</sup>	189%

In contrast, the infection of fibroblasts resulted in an almost 2-fold upregulation of MHCI surface expression (Table 4). An increase in surface MHCI was also found in the inclusion-negative cell population of the *Chlamydia*-infected sample, but to a lower extent. Altogether these results point to a partial interference of chlamydial organisms with the MHCI pathway during active infection. However, the pathway seems to be functional during IFN- $\gamma$  mediated persistence and during infection of fibroblasts.

### 3.2.2 Influence of *C. trachomatis* infection on expression of key proteins involved in MHCI antigen processing and presentation

Some of the strategies that are used by pathogens to interfere with the MHCI antigen presentation pathway are inhibition of the expression or induction of the degradation of proteins involved in antigen processing (reviewed in Antoniou & Powis, 2008). It has been suggested that during *C. trachomatis* infection of epithelial cells CPAF may mediate downregulation of MHCI expression through degradation of the transcription factor RFX5 (Zhong *et al.*, 2000; Zhong *et al.*, 2001). To see whether *C. trachomatis* also interferes with MHCI gene expression during IFN- $\gamma$  mediated persistence and infection of fibroblasts and whether other essential components of the MHCI antigen presentation pathway are

affected a quantitative gene expression analysis was done. Expression was examined for the MHC I encoding genes *HLA-ABC* (ABC referring to the three MHC class I major genes A, B and C), the TAP transporter encoding genes *TAP1* and *TAP2* and the genes *LMP2*, *LMP7* and *MECL1* which encode the three IFN-inducible immunoproteasome subunits.

Table 5 shows the gene expression ratios of *C. trachomatis*-infected cells relative to mock-infected cells for the different infection models. Surprisingly, in contrast to the study of Zhong *et al.* (2000) no significant downregulation of *HLA-ABC* expression could be found in any infection model indicating that there is no specific chlamydial interference with the expression of these genes. The only exception was *LMP2*, which was slightly but statistically significantly downregulated during active infection of HeLa cells. However, in all infection models the expression of *TAP1* and *TAP2* was upregulated after chlamydial infection, although to a lower extent during active infection.

**Table 5: Gene expression of components of the MHC I antigen presentation pathway in *C. trachomatis* infected cells.**

Values are given as x-fold expression change for *Chlamydia*-infected relative to mock-infected cells at 48 h p.i. Fibroblasts were additionally treated with an antibody neutralising type I IFN activity (anti-IFNAR). \* p < 0.05, \*\* p < 0.005 (relative to mock control, for fibroblasts + anti-IFNAR: relative to infected fibroblasts). Depicted are the mean values of three independent experiments with standard deviations in brackets. Significantly different values are marked in bold.

x-fold gene expression normalised to <i>GAPDH</i> expression in infected cells relative to mock-infected cells						
	HeLa active	HeLa active + IFN- $\beta$	HeLa active + IFN- $\gamma$	HeLa IFN- $\gamma$ persistence	fibroblasts	fibroblasts + anti- IFNAR
<i>HLA-ABC</i>	0.96 (0.05)	1.20 (0.17)	0.91 (0.09)	<b>1.68</b> * (0.55)	<b>5.02</b> ** (0.87)	<b>2.80</b> ** (0.64)
<i>TAP1</i>	1.36 (0.06)	<b>1.94</b> * (0.27)	1.39 (0.46)	<b>2.82</b> * (0.23)	<b>8.33</b> * (1.75)	<b>5.29</b> * (0.70)
<i>TAP2</i>	<b>1.42</b> * (0.19)	<b>1.75</b> ** (0.24)	1.33 (0.25)	<b>2.48</b> * (0.75)	<b>6.42</b> * (2.27)	4.69 (2.34)
<i>LMP2</i>	<b>0.77</b> * (0.06)	1.25 (0.10)	0.85 (0.41)	<b>1.77</b> * (0.42)	<b>5.17</b> * (0.20)	3.46 (0.73)
<i>LMP7</i>	0.98 (0.04)	1.26 (0.28)	0.97 (0.31)	<b>2.04</b> * (0.55)	<b>2.87</b> ** (0.50)	2.14 (0.40)
<i>MECL1</i>	1.26 (0.13)	1.48 (0.53)	1.18 (0.38)	1.82 (0.19)	<b>1.74</b> * (0.46)	1.26 (0.32)

In the IFN- $\gamma$  mediated persistence model the expression of almost all genes analysed was significantly upregulated, suggesting that IFN- $\gamma$  interacts synergistically with innate immunity pathways that are induced by the infection thus increasing the expression of proteins involved in the MHCI pathway.

The infection of fibroblasts resulted in a highly upregulated expression of the examined genes, especially for *HLA-ABC*, *TAP1*, *TAP2* and *LMP2*. It was assumed that IFN- $\beta$  secreted after infection of fibroblasts with *C. trachomatis* is responsible for this upregulation. To test this hypothesis the type I IFN activity was neutralised by incubation of infected fibroblasts with an antibody binding to the type I IFN receptor (anti-IFNAR). The inhibition of type I IFN activity reduced the expression of the examined genes in infected fibroblasts (Table 5). However, the degree of reduction differed among the examined genes.

Additionally, the impact of *C. trachomatis* infection on the expression of the corresponding protein products was examined (Fig. 14). As expected, expression of HLA-ABC, TAP1, TAP2 and the immunoproteasome subunits was increased after IFN treatment of HeLa cells. Interestingly, TAP2 was not detectable in actively infected HeLa cells both treated with and without IFN. This is in contrast to the *TAP2* gene expression values that revealed an increased expression of this gene after active chlamydial infection of HeLa cells. These results suggest that the TAP2 protein could be degraded through *C. trachomatis*. Because TAP2 expression was readily detected during IFN- $\gamma$  mediated persistent infection of HeLa cells and after infection of fibroblasts, TAP2 degradation seems to occur only during active but not persistent infection of HeLa cells. Furthermore, there was a slight decrease in HLA-ABC expression during active infection of HeLa cells and a somewhat decreased amount of TAP1 protein after active infection of HeLa cells with IFN- $\beta$  treatment.

Consistent with the strong increase (> 5-fold) of *HLA-ABC*, *TAP1*, *TAP2* and *LMP2* expression in infected fibroblasts (see Table 5), a higher amount of the corresponding proteins could also be detected in the immunoblot (Fig. 14). A similar effect of protein upregulation was seen after IFN- $\beta$  treatment of uninfected fibroblasts. In those cases where gene expression ratios were only up to 3-fold increased (for instance during IFN- $\gamma$  mediated persistent infection of HeLa cells, see Table 5) no distinct upregulation of the corresponding proteins could be detected on the immunoblots, probably due to the less sensitivity of this method compared to real-time PCR analysis.

Because downregulation of surface MHCI during active infection of HeLa cells has been suspected to be the result of RFX5 degradation by CPAF (Zhong *et al.*, 2000, Zhong *et al.*, 2001), the expression of this transcription factor was also analysed under the different

infection conditions in the present study. As expected, RFX5 was readily expressed in uninfected HeLa cells, but the protein could not be detected during active infection of HeLa cells (Fig. 14). However, during IFN- $\gamma$  mediated persistent infection RFX5 expression still could be found, consistent with a previous study that showed inhibition of RFX5 degradation during IFN- $\gamma$  mediated persistence of *C. pneumoniae* (Heuer *et al.*, 2003). In contrast to this, no RFX5 protein at all could be detected in fibroblasts. This suggests that RFX5 is expressed just at low amounts in these cells thus impairing its detection. Because MHCI expression is upregulated in *C. trachomatis*-infected fibroblasts RFX5 seems not to be essential in infection mediated upregulation of MHCI expression in these cells.

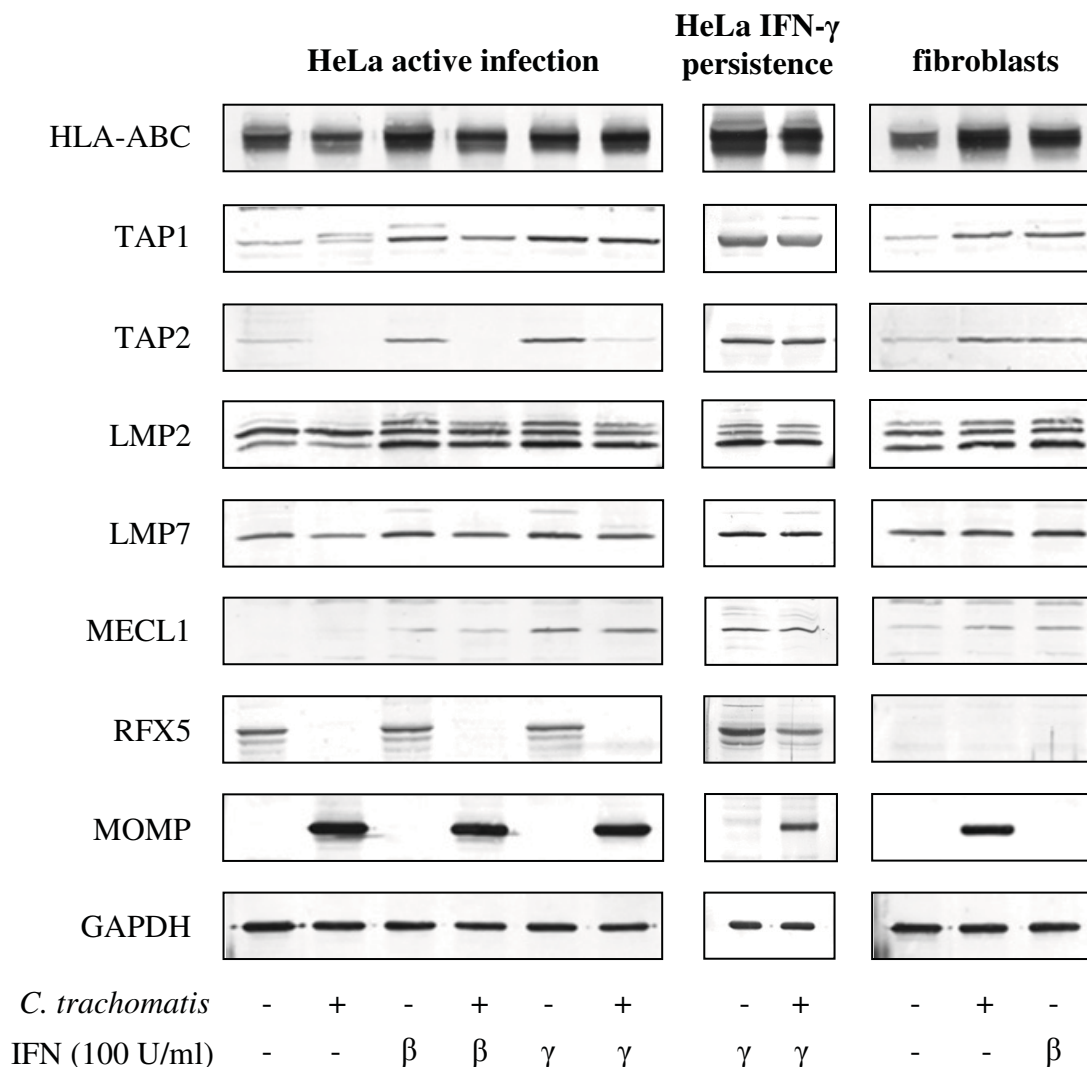


**Fig. 14: Expression of proteins involved in the MHC I antigen presentation pathway in *C. trachomatis* infected cells.**

The proteins were detected by immunoblotting after SDS-PAGE separation of whole cell lysates generated at 48 h p.i.

### 3.2.3 TAP2 degradation during active infection with *C. trachomatis*

To analyse if the diminished TAP2 expression in actively infected HeLa cells (see Fig. 14) was the result of intracellular replication of chlamydial organisms, infected cells were treated with chloramphenicol (Fig. 15). This led to complete inhibition of TAP2 down-regulation. In contrast, treatment of infected cells with cycloheximide did not prevent the reduction in TAP2 expression. This suggests that proliferating chlamydial organisms but not newly synthesized host proteins are responsible for the observed effect.

To see if the reduced TAP2 expression was the result of degradation through a chlamydial protease secreted in the host cytosol, a cell free cleavage assay was performed (Fig. 16). Cell lysate from mock-infected HeLa cells treated with IFN- $\gamma$  was used as substrate, because compared to non-treated cells it contained a higher amount TAP2 that was readily detectable on the immunoblot (see Fig. 14). After performance of the cell-free cleavage assay TAP2 could be only detected in the lysate of mock-infected cells incubated without CE and the mixture of lysate of mock-infected cells with the CE of mock-infected cells. However, it was neither detectable in the lysate generated from *Chlamydia*-infected cells nor in the CEs, as would be expected due to its membrane localisation to the ER. After incubation of the lysate from mock-infected cells with the CE from *Chlamydia*-infected cells the amount of TAP2 protein was highly reduced. This result indicates that a protease active in the host cytosol could be responsible for the degradation of TAP2.

For analysis of the role of CPAF in this event, immunoprecipitation was used to remove the chlamydial protease from the CE of infected cells, and degradation was analysed in the cell-free cleavage assay. If CPAF was responsible for the observed TAP2 degradation, the incubation of this CE with the lysate from mock-infected cells would be expected to result in abrogation of TAP2 degradation.

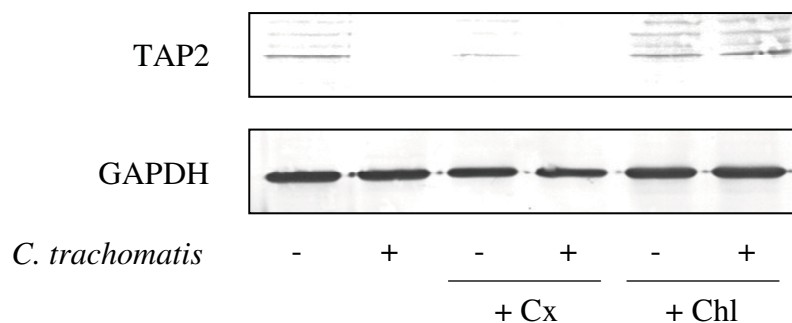


**Fig. 15: Effect of inhibition of eukaryotic and prokaryotic translation on TAP2 expression in HeLa cells actively infected with *C. trachomatis*.**

Immunoblots of lysates from mock- and *Chlamydia*-infected HeLa cells either treated with no inhibitor, 2  $\mu$ g/ml cycloheximide (Cx) or 100  $\mu$ g/ml chloramphenicol (Chl) for 48 h.

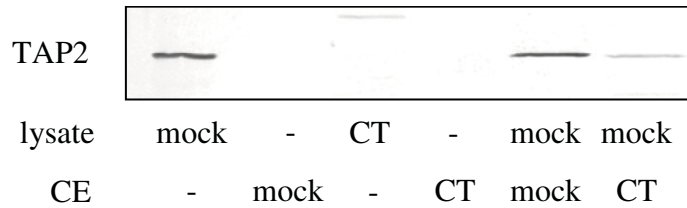


**Fig. 16: Cell-free cleavage assay of TAP2.**

Immunoblot of cell-free cleavage assay samples containing either cytosolic extract (CE) and/or lysate generated from actively infected (CT) or uninfected (mock) HeLa cells at 48 h p.i.

However, detection of the 75 kDa TAP2 in this sample was impaired by the presence of a huge amount of unknown protein that accumulated at the same size like TAP2 and prevented specific binding of the TAP2 antibody (data not shown). This large band was only seen after immunoprecipitation with the CPAF antiserum but not with IgG indicating that it originates from the CPAF antiserum. Because it was assumed that this protein could be serum albumin, attempts to remove this contaminating protein from the sample were made with DEAE sepharose. Yet, this resulted also in removal of TAP2 thus impairing detection (data not shown).

However, treatment of the CE of *Chlamydia*-infected cells with lactacystin, that is known to inhibit CPAF activity (Zhong *et al.*, 2001), could prevent TAP2 degradation in a cell-free cleavage assay in a concentration dependent manner (Fig. 17). Because lactacystin was dissolved in DMSO before usage, treatment with DMSO alone was used as control to exclude that the effect was due to the solvent.

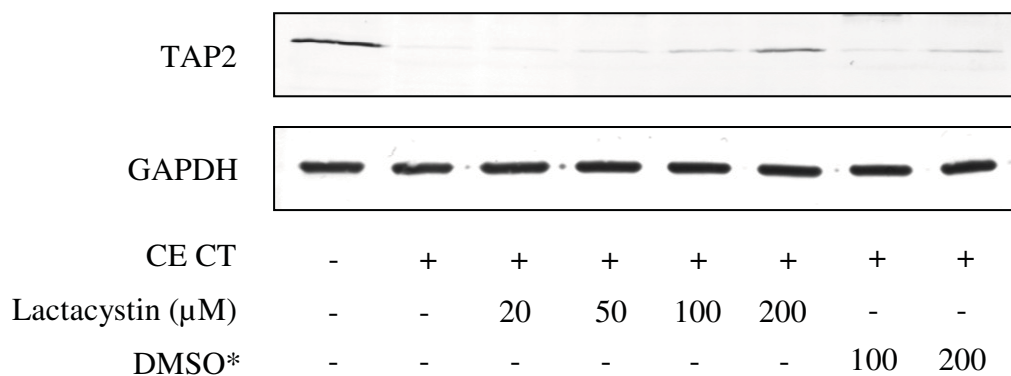


**Fig. 17: Impact of inhibition of CPAF activity with lactacystin on the degradation of TAP2.**

Immunoblot of a cell free-cleavage assay that was performed by incubating the lysate of mock-infected HeLa cells with the CE of actively infected (CT) HeLa cells as source of cleavage activity. Cell lysate alone was used as control. Lactacystin inhibitor was added to the mixtures at the indicated concentrations. Because lactacystin was solved in DMSO, the solvent was added alone and served as control. \*The respective lactacystin concentrations are indicated, and the same volume of DMSO was added instead of lactacystin.

Although DMSO partially inhibited degradation of TAP2 at an amount that was equal to the volume used for 200  $\mu$ M lactacystin, the effect of DMSO in inhibiting cleavage was much less than that of lactacystin.

These results suggest that *C. trachomatis* specifically degrades TAP2, probably through the activity of CPAF, which could serve as a mechanism to interfere with the MHC I antigen presentation pathway.

### **3.3 Role of Golgi fragmentation in the downregulated MHC I surface expression in actively *C. trachomatis* infected epithelial cells**

#### **3.3.1 Fragmentation of the Golgi apparatus in *C. trachomatis* infected cells**

It has been shown that the infection with *C. trachomatis* leads to fragmentation of the Golgi apparatus (Heuer *et al.*, 2009). It was hypothesized that this fragmentation may result in incorrect MHC class I processing thus contributing to the decreased surface MHC I expression observed in actively infected HeLa cells (Table 4).

Golgi fragmentation was examined by immunofluorescent staining of the *cis*-Golgi protein GM130 and the *trans*-Golgi protein Golgin-245 in *C. trachomatis* infected cells (Fig. 18). Fragmentation of the Golgi apparatus did rarely occur in actively infected HeLa cells after 24 h p.i. (Fig. 18 A). However, it was readily detected after 48 h in most of the inclusion-containing HeLa cells for both the *cis*-Golgi and the *trans*-Golgi compartments. Golgi fragments seemed to localise near to or around the chlamydial inclusion, as has been already demonstrated by Heuer *et al.*, 2009.

During IFN- $\gamma$  mediated chlamydial persistence in HeLa cells a complete fragmentation of the *cis*-Golgi compartment at 48 h p.i. was detected only in few of the inclusion-positive cells (Fig. 18 B), most of them showed only a partial fragmentation by GM130 staining. In contrast, a complete fragmentation of the *trans*-Golgi in connection with an arrangement of Golgin-245 containing Golgi fragments around the chlamydial inclusion was found at 48 h p.i. in most inclusion-containing cells of this model.

In fibroblasts a low percentage of the inclusion-positive cells exhibited complete fragmentation of both the *cis*- and *trans*-Golgi compartment, whereas partial fragmentation was also observed in the majority of these cells (Fig. 18 C).

These results suggest that fragmentation of the Golgi compartments occurs in all three models, although to a much lesser extent in fibroblasts and for the *cis*-Golgi in IFN- $\gamma$  mediated chlamydial persistence.

**A** HeLa, active infection

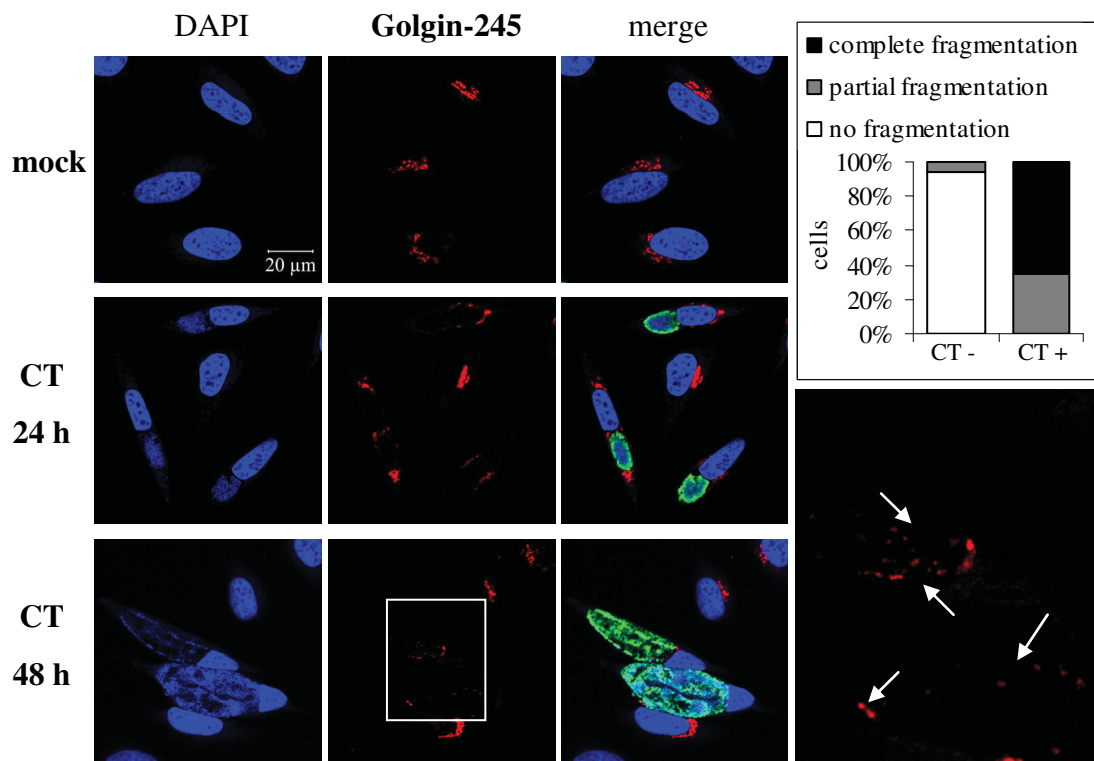
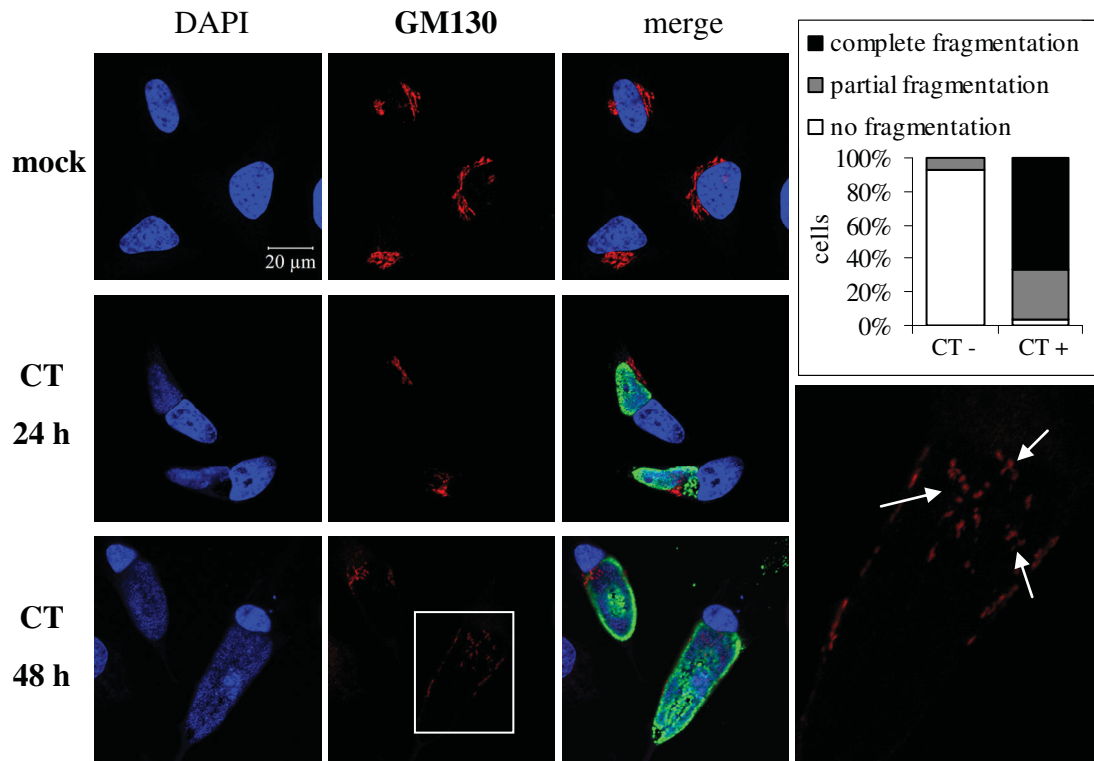
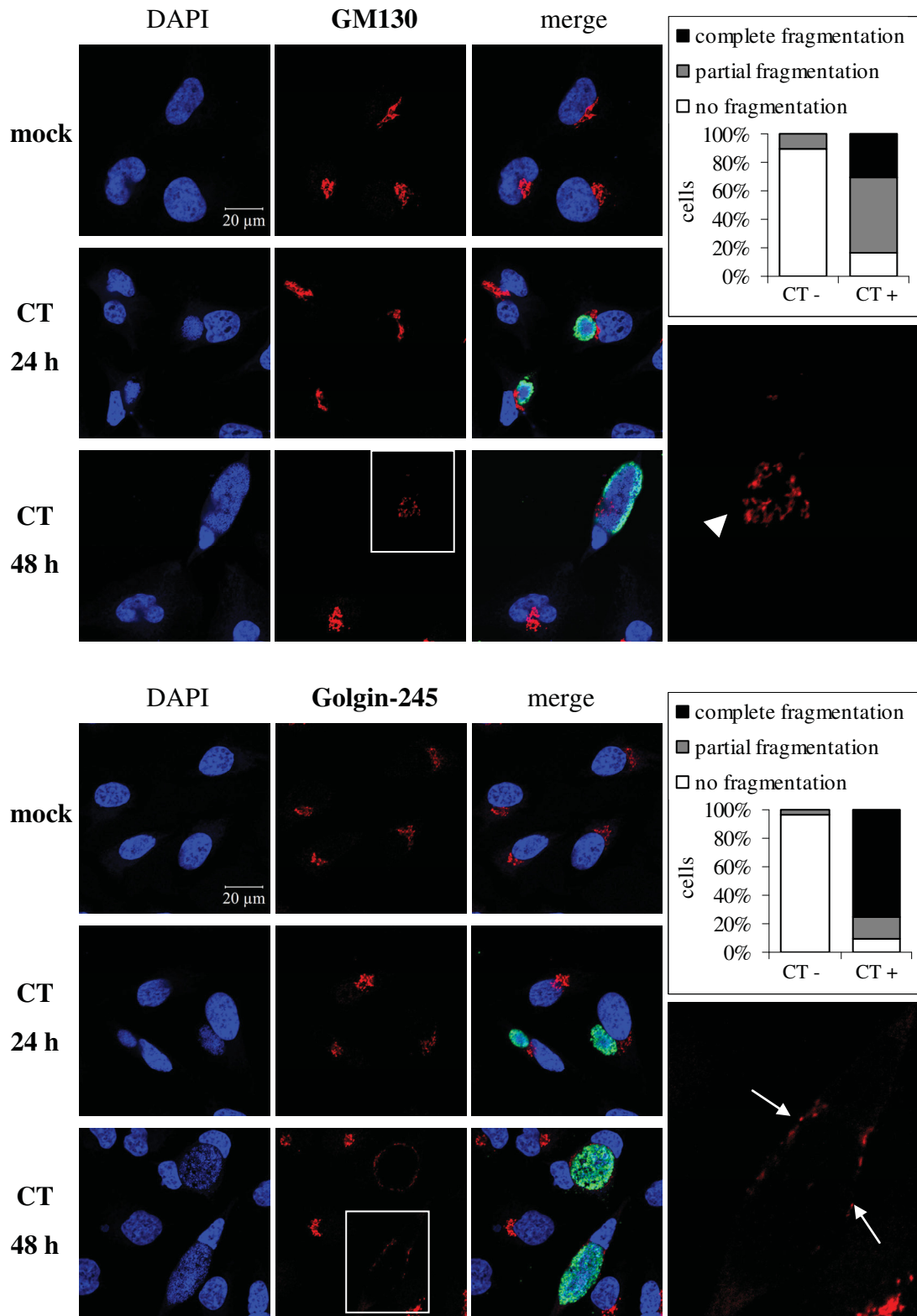


**Fig. 18: Immunofluorescent staining of Golgi proteins in *C. trachomatis* infected cells.**

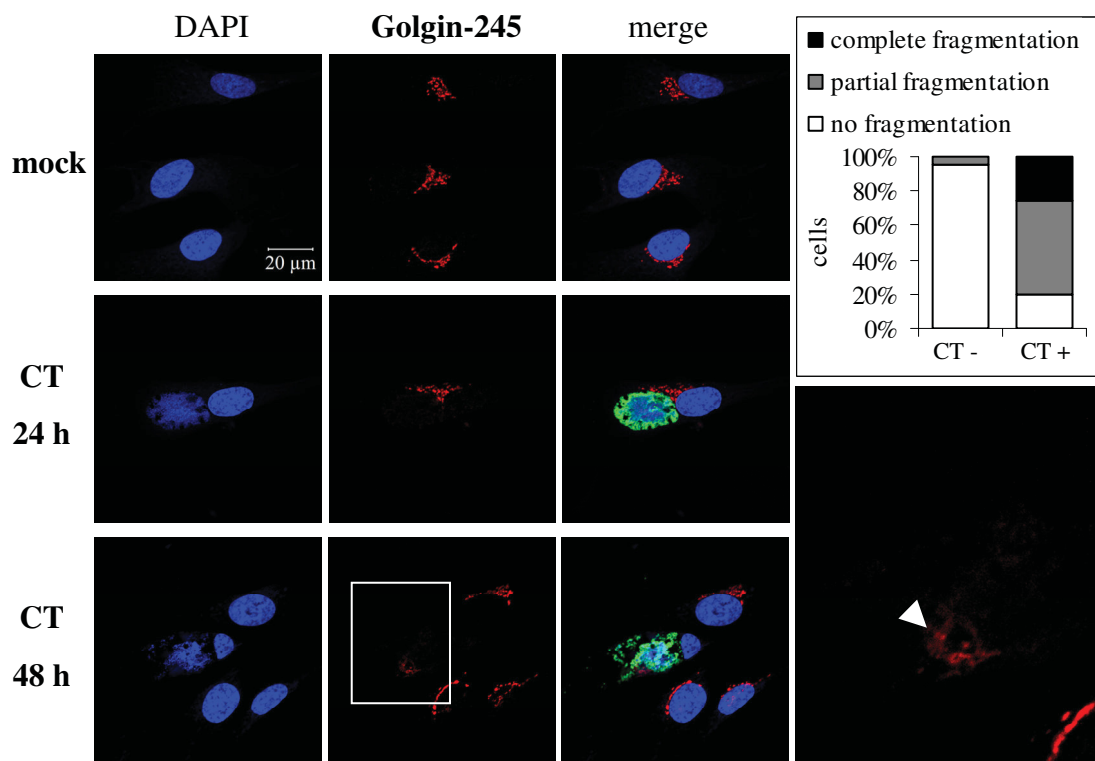
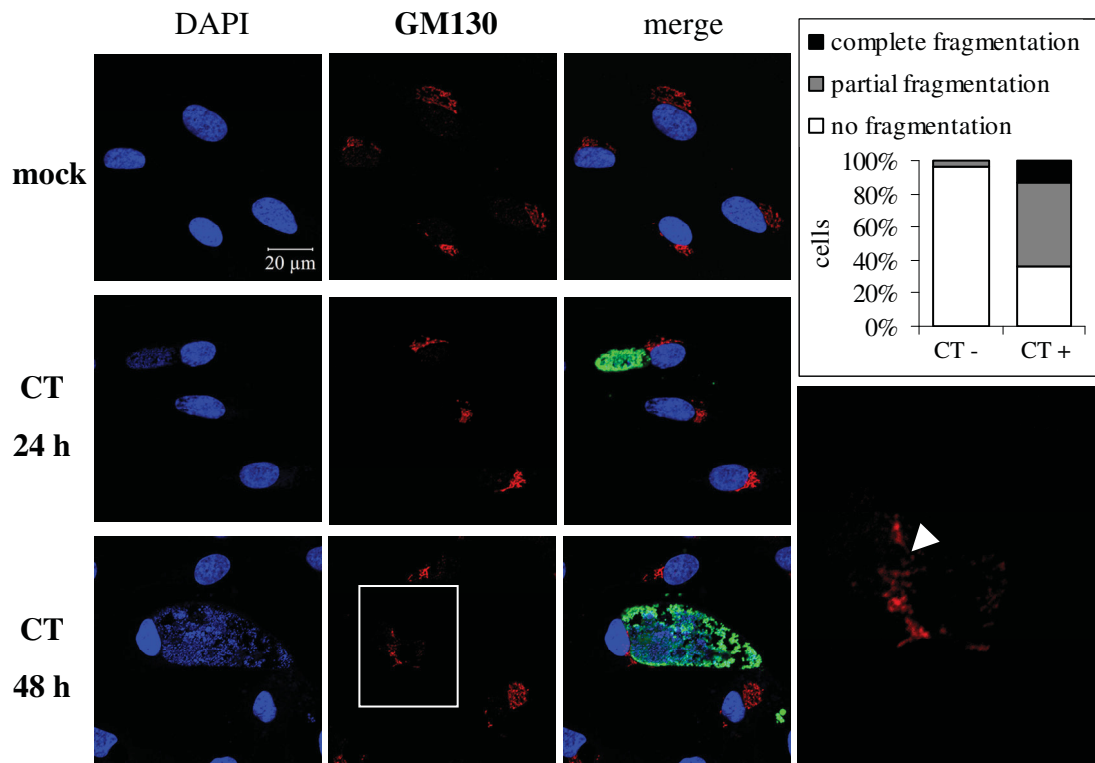
The Golgi apparatus (red) of mock-infected (48 h p.i.) and *Chlamydia*-infected (CT) cells (MOMP, green) was stained during active infection of HeLa cells (A), IFN- $\gamma$  induced persistent infection of HeLa cells (B) and infection of fibroblasts (C) with an antibody binding the *cis*-Golgi protein GM130 (upper panels) and

## B HeLa, IFN- $\gamma$ persistent infection



with an antibody specific for the *trans*-Golgi protein Golgin-245 (lower panels), respectively. A magnified section showing the Golgi of infected cells at 48 h p.i. is shown on the right. Fragmented Golgi is marked with an arrow and partial fragmented Golgi is marked with an arrowhead. The percentage of inclusion-negative (CT -) and inclusion-positive (CT +) cells ( $n = 20$ ) showing either complete, partial or no fragmentation of the Golgi apparatus is depicted for each model and Golgi protein at 48 h p.i. in the graphs.

**C fibroblasts**



### 3.3.2 Degradation of GM130 and Golgin-245 during active *C. trachomatis* infection

It was demonstrated recently that Golgin-84 cleavage by CPAF is responsible for Golgi fragmentation (Christian *et al.*, 2011). Thus, it would be interesting to know whether GM130 and Golgin-245 are also degraded during chlamydial infection which could have severe effects on the Golgi processing of MHCI. Indeed, detection of these proteins by immunoblotting revealed a drastically reduced amount of both proteins after active infection of HeLa cells (Fig. 19). However, the expression of GM130 was also reduced in persistently infected HeLa cells and in infected fibroblasts compared to uninfected cells, although to a lower extent. In contrast, Golgin-245 expression was not affected by chlamydial infection in the IFN- $\gamma$  mediated persistence model. Interestingly, a 2-fold increase in Golgin-245 protein was observed in infected fibroblasts.

To examine if chlamydial organisms were responsible for the reduced expression of GM130 and Golgin-245 observed in Fig. 19 during active infection chloramphenicol was added to infected HeLa cells in order to inhibit the growth of chlamydial organisms (Fig. 20). This prevented the observed downregulation indicating that proliferating chlamydial organisms are needed.

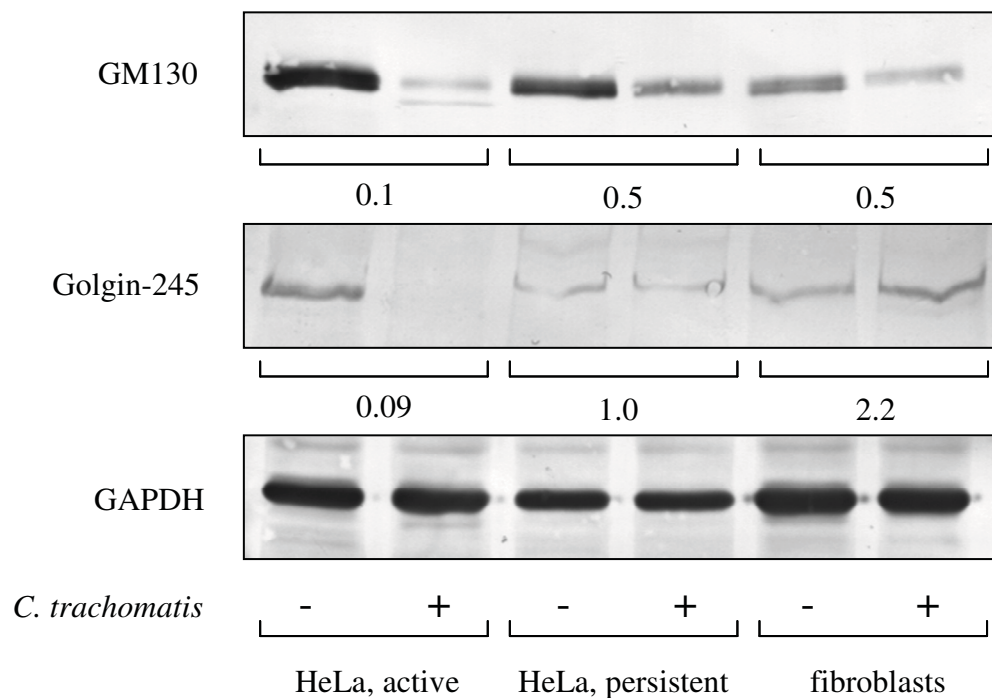


**Fig. 19: Expression of GM130 and Golgin-245 after infection with *C. trachomatis*.**

Immunoblots were made with cell lysates generated from *Chlamydia*- and mock-infected cells at 48 h p.i. Densitometry ratios are depicted for infected cells vs. uninfected cells normalised to GAPDH.

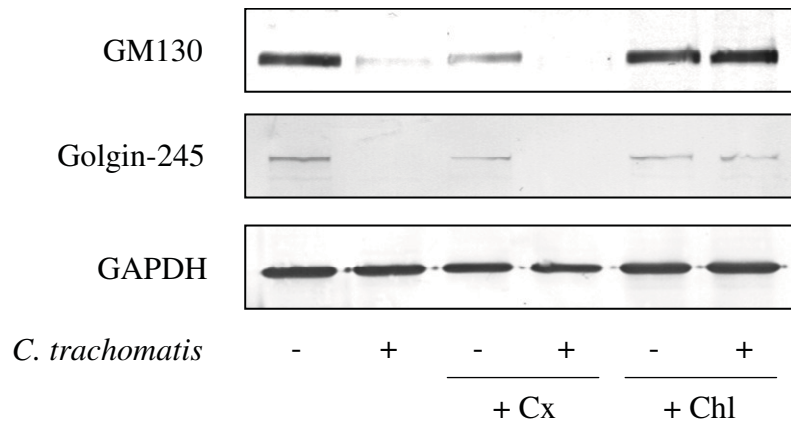


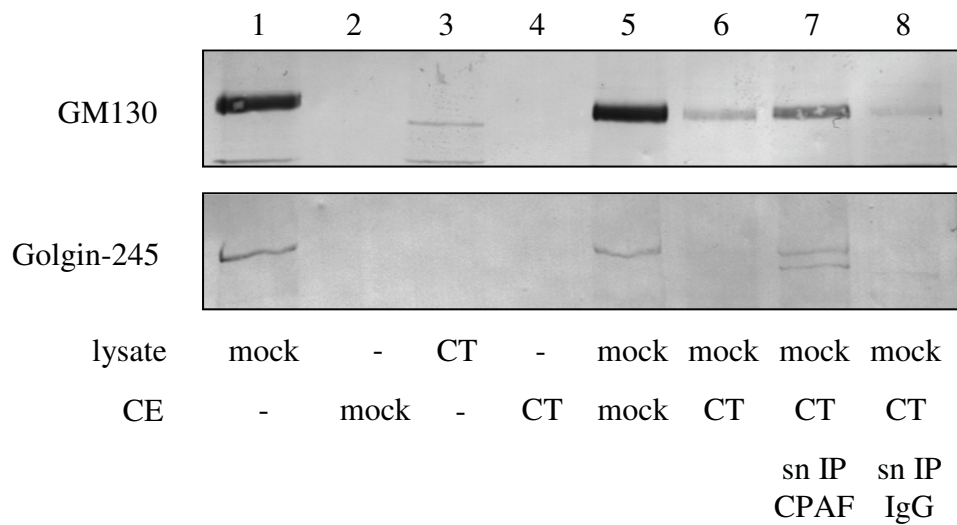
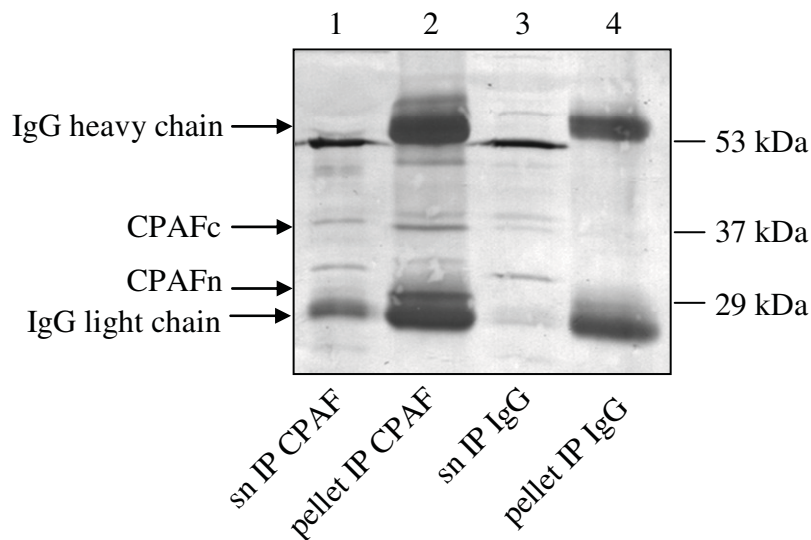
**Fig. 20: Effect of inhibition of eukaryotic and prokaryotic translation on GM130 and Golgin-245 expression in *C. trachomatis* infected cells.**

See Fig. 15 for description. Cx: cycloheximide, Chl: chloramphenicol.

In contrast, treatment of infected cells with cycloheximide, an inhibitor of eukaryotic protein translation, did not prevent the downregulation of GM130 and Golgin-245. Thus, the results point to a *Chlamydia*-mediated degradation of both proteins that could be mediated by a protease secreted into the host cytosol.

### 3.3.3 Role of CPAF in degradation of GM130 and Golgin-245

Because it has been found recently that Golgin-84 is a target protein for CPAF cleavage (Christian *et al.*, 2011), it was assumed that CPAF could also be responsible for the degradation of GM130 and Golgin-245. A cell-free cleavage assay was applied in which whole cell lysates of mock-infected HeLa cells were used as a substrate containing both Golgi proteins. This substrate was incubated with CEs from mock- or actively *Chlamydia*-infected HeLa cells which were used as source of the enzymatic activity. Both Golgi proteins were readily detected in the cell lysates of mock-infected cells (Fig. 21 A, lane 1). The proteins were not observed in the CEs (Fig. 21 A, lane 2 and 4) and in the lysates of *Chlamydia*-infected cells (Fig. 21 A, lane 3). The incubation of mock-cell lysate with the CE from infected cells resulted in degradation of GM130 and Golgin-245 (Fig. 21 A, lane 6). In contrast, no disappearance of protein was seen when CE from mock-infected cells was used instead (Fig. 21 A, lane 5). This indicates that the protease responsible for degradation of the two Golgi proteins resides in the host cytoplasm.

**A****B**

**Fig. 21: Role of CPAF in degradation of GM130 and Golgin-245 during active chlamydial infection.**

**A** Immunoblot showing the cell-free cleavage assay of samples containing cytosolic extract (CE) and/or lysate generated from actively infected (CT) or uninfected (mock) HeLa cells at 48 h p.i. sn IP CPAF: CPAF was removed from the CE prior to the assay by immunoprecipitation with CPAF antiserum. sn IP IgG: Immunoprecipitation control with unspecifically binding mouse IgG.

**B** Immunoprecipitation of CPAF was verified by immunoblotting. The 29 kDa N-terminal fragment (CPAFn) and the 34 kDa C-terminal fragment (CPAFc) of CPAF were found in the immunoprecipitation pellet of the sample incubated with CPAF-antiserum but not in the pellet of the IgG control sample. The IgG heavy chains (50 kDa) and light chains (25 kDa) of the CPAF antiserum and control IgG antibody were readily detectable. sn: supernatant, IP: immunoprecipitation.

In order to examine the role of CPAF in this event the protease was removed from the CE of infected cells by immunoprecipitation with CPAF antiserum. The 29 kDa N-terminal fragment (CPAFn) and the 34 kDa C-terminal fragment (CPAFc) could be readily detected in the pellet of the CPAF immunoprecipitation sample (Fig. 21 B, lane 2), but not in the pellet of the sample with unspecific mouse IgG for immunoprecipitation (Fig. 21 B, lane 4). CPAF was not found in the supernatant of the CPAF immunoprecipitation sample (Fig. 21 B, lane 1). Unexpectedly, it was also not detectable in the supernatant of the control IgG immunoprecipitation sample (Fig. 21 B, lane 3). Because diluted CE was used in order to achieve a maximal removal of CPAF from the CE by immunoprecipitation, it therefore is likely that the concentration of CPAF protein in the CE was too low to be detected by immunoblotting. However, CPAF concentration was high enough to promote degradation of target proteins (Fig. 21 A, lane 6). The removal of CPAF from the CE of infected cells resulted in reduced degradation of GM130 and Golgin-245 when the immunoprecipitation supernatant was incubated with the mock-cell lysate (Fig. 21 A, lane 7). However, there was no total inhibition which could be explained by incomplete removal of CPAF from the CE during immunoprecipitation leading to remaining residual CPAF activity in the CE. This is also supported by the appearance of a second band of lower size when Golgin-245 was detected indicating that the protein is partially cleaved at a side near to the C- or N-terminus. As a control, degradation was not reduced by immunoprecipitation with mouse IgG (Fig. 21 A, lane 8).

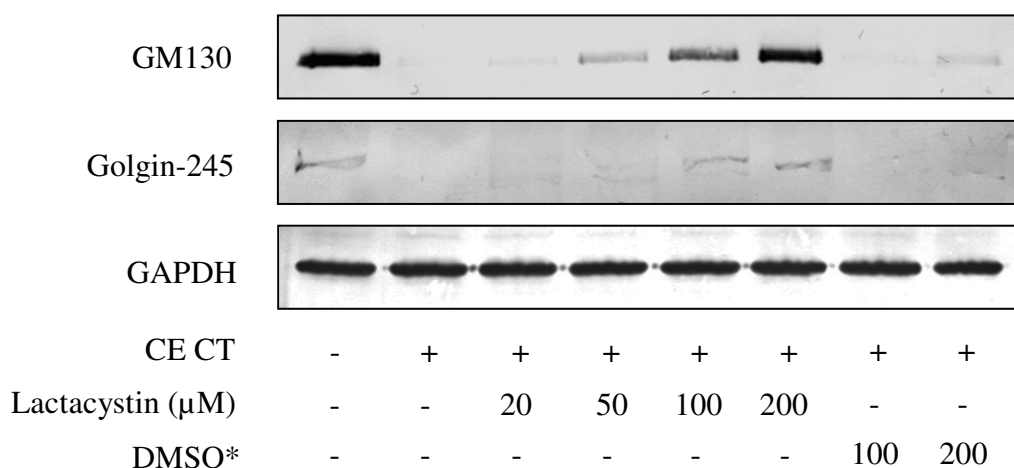


**Fig. 22: Impact of inhibition of CPAF activity with lactacystin on cleavage of GM130 and Golgin-245.**

See Fig. 17 for description.

Furthermore, the degradation of GM130 and Golgin-245 was inhibited when the CE from infected cells was treated with the CPAF inhibitor lactacystin (Fig. 22). The inhibitory effect increased with higher doses of the compound. DMSO alone only had a marginal inhibitory effect on the degradation.

Altogether, both experiments strongly indicate that CPAF degrades GM130 and Golgin-245 in the host cytosol of *Chlamydia*-infected cells.

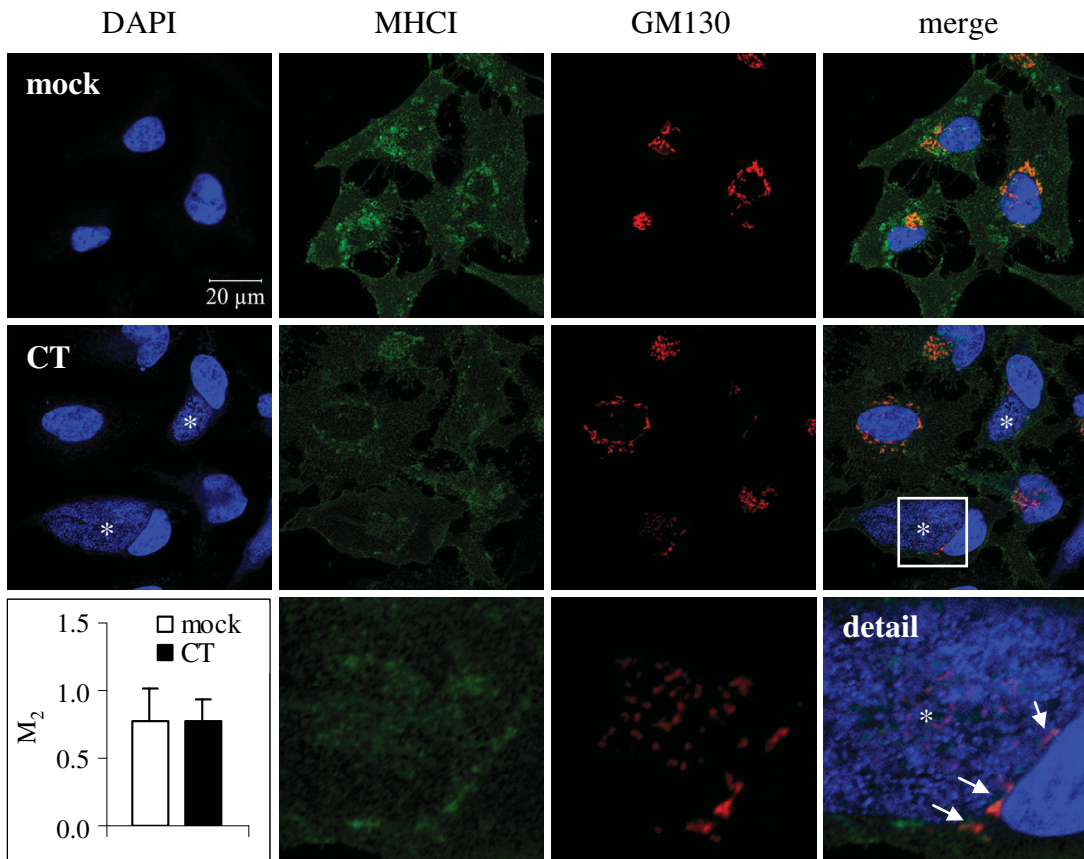
### 3.3.4 MHCI co-localisation with GM130 in *C. trachomatis* infected cells

The fragmentation of the Golgi and degradation of Golgi proteins by chlamydiae is expected to have severe impacts on the function of the Golgi apparatus as a sorting and posttranslational modification compartment. To analyse the consequences of this pathogen-host interaction for the MHCI processing immunofluorescent staining of GM130 and MHCI was used to see if MHCI molecules still localise to the Golgi compartment after infection with *C. trachomatis*. Furthermore, analysis of this co-localisation was important to see whether MHCI transport from ER to the Golgi was affected due to the degradation of TAP2 which may result in a defect of peptide-loading associated with a retention of MHCI molecules to the ER.

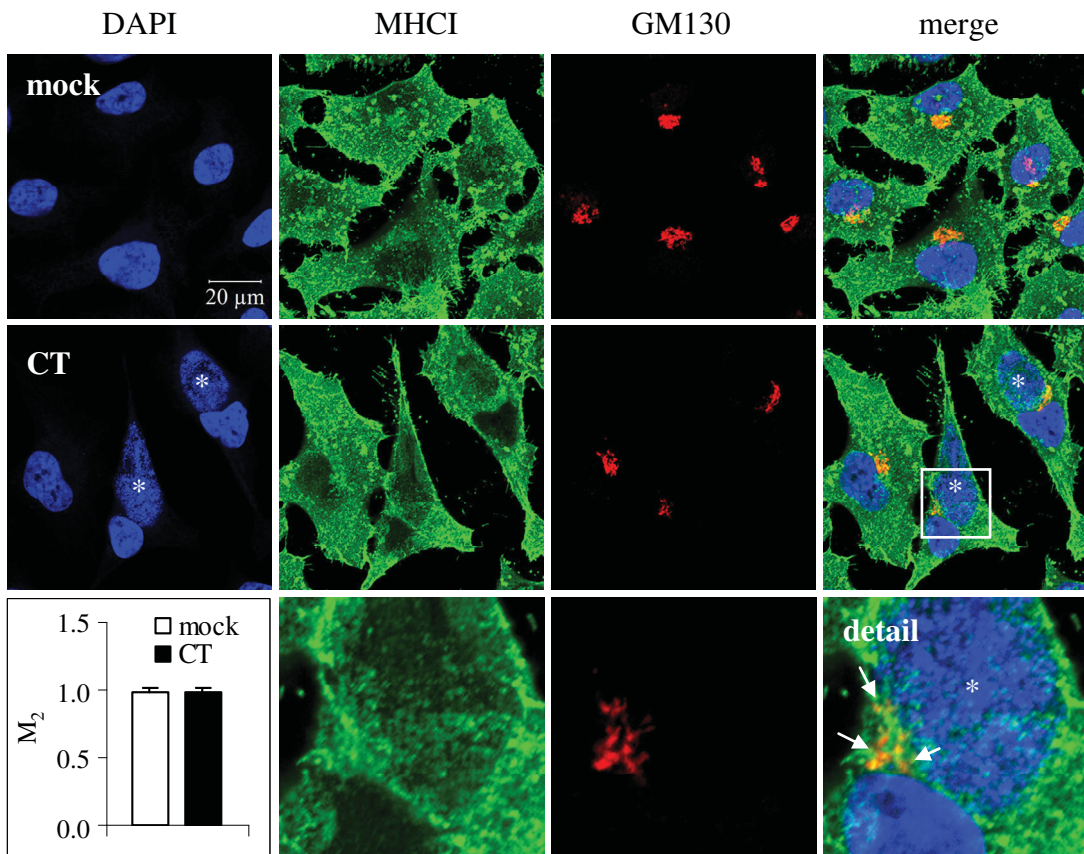
In uninfected HeLa cells most of the intracellular MHCI localised to the Golgi (Fig. 23). The fragmentation of the Golgi to mini-stacks in actively infected HeLa cells and the low intensity of MHCI staining due to the low expression of MHCI in these cells made it difficult to detect co-localisation of MHCI with the Golgi. Nevertheless, a stronger staining intensity of MHCI seemed to occur in regions of the inclusion-containing cells where GM130 was stained indicating that MHCI can reach the Golgi compartment despite its fragmentation. The detection of co-localisation of MHCI with GM130 during IFN- $\gamma$  mediated persistence was hampered because of the highly increased MHCI staining intensity due to enhanced MHCI expression elicited by IFN- $\gamma$  treatment. Here, MHCI was evenly distributed in the whole cell including the Golgi apparatus. In fibroblasts the localisation of MHCI to the Golgi was very well detectable. Although infected fibroblasts showed a higher overall MHCI staining intensity than uninfected fibroblasts most of the MHCI could be clearly detected in the Golgi compartment.

To get a more precise picture, the co-localisation was quantified by defining regions of interests (ROIs) that were drawn around the Golgi compartment and calculating co-localisation coefficients. The co-localisation coefficient  $M_2$  describes the percentage of the red pixel (GM130) co-localising with green pixel (MHCI).

### HeLa, active infection



### HeLa, IFN- $\gamma$ mediated persistent infection



## fibroblasts

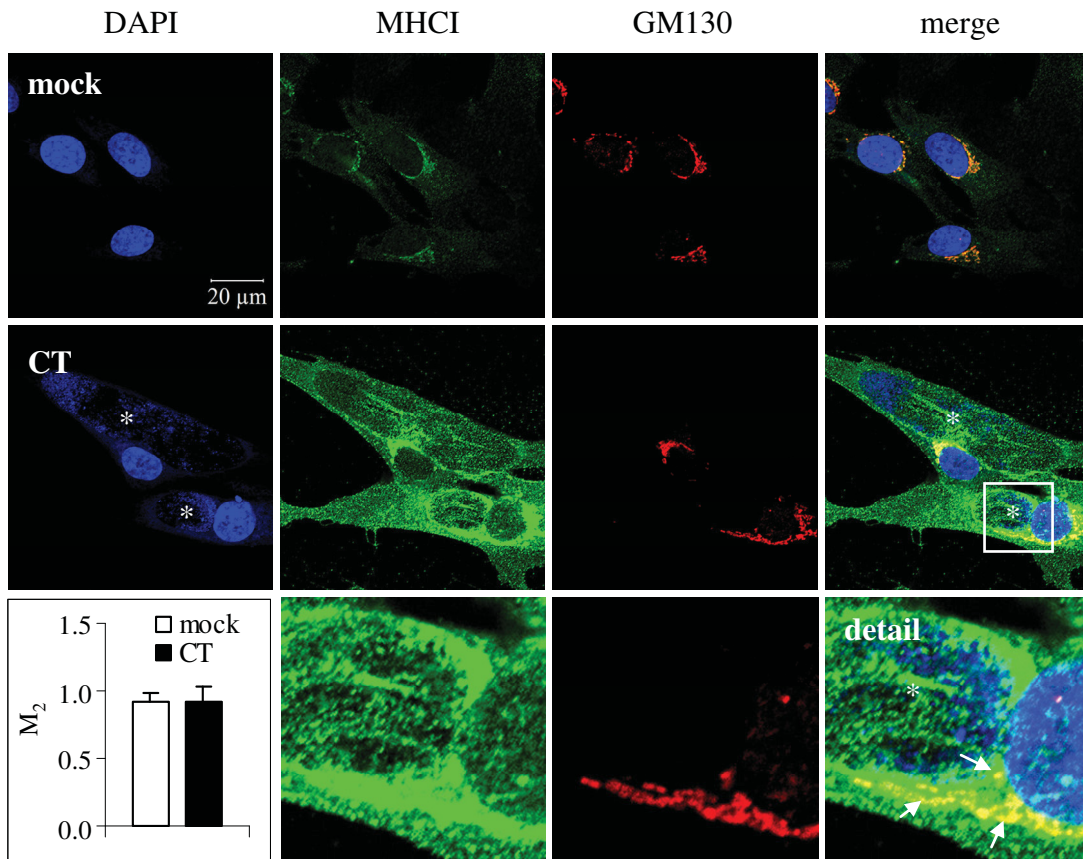


**Fig. 23: Co-localisation of MHCI with the Golgi apparatus during chlamydial infection.**

Immunofluorescent staining of the Golgi was done with an antibody binding to GM130 (red). Chlamydial organisms were stained by DAPI (blue) and inclusions are marked with a white asterisk. The same intensity adjustment was used for all samples in order to allow direct comparison of MHCI staining intensity between the three infection models. The third row of each panel shows a detailed picture of the Golgi region of an infected cell (marked with a square). White arrows indicate areas of co-localisation. The graph shows the average co-localisation coefficient  $M_2$  for ROIs from each 15 uninfected (mock) and 15 cells containing inclusions (CT).  $M_2$  represents the number of red pixel (Golgi) co-localising with green pixel (MHCI).

The values were nearly the same between infected and uninfected cells in each model (graphs in Fig. 23). Actively infected HeLa cells only had ~70% of GM130-associated pixel co-localised with MHCI-associated pixel, whereas the other two models showed almost 100% co-localisation of these two proteins. This discrepancy can be explained by the different intensities of the MHCI staining, which was less in the actively infected HeLa cell model than in the other two models resulting in less pixel that could co-localise with the GM130-associated pixels. The results suggest that transport and localisation of MHCI to the Golgi is not influenced by chlamydial infection.

### 3.3.5 Change in sensitivity of MHCI molecules to Endoglycosidase H cleavage after active infection with *C. trachomatis*

Treatment of cell lysates with Endo H was used as another method to examine if MHCI molecules reached the Golgi compartment of infected cells and were processed to mature MHCI. Endo H cleaves asparagine-linked high-mannose type oligosaccharide chains from glycoproteins. This type of carbohydrate residue usually becomes attached to MHCI and other glycoproteins in the ER rendering the proteins sensitive to Endo H cleavage. After reaching the *medial*-Golgi these glycan residues get modified by  $\alpha$ -mannosidase II leading to resistance of the protein to Endo H cleavage. Endo H sensitive, immature MHCI molecules are distinguished from Endo H resistant, mature MHCI by their lower molecular weight due to removal of the glycan residues (Freeze & Kranz, 2010).

In uninfected HeLa cells both Endo H resistant and sensitive MHCI molecules were observed indicating a functional maturation of MHCI (Fig. 24). In contrast, only Endo H resistant but no Endo H sensitive MHCI molecules could be detected after active infection of HeLa cells. This suggests that active chlamydial infection leads to a reduction of MHCI molecules in the ER. Additionally, active infection of HeLa cells led to a strong decrease in the total MHCI protein amount. This reduction is more prominent than on the immunoblot in Fig. 14, and the differences could be explained by the usage of different lysis buffers for both experiments. For Endo H treatment only Triton-X 100 was used for lysis whereas RIPA buffer, containing additionally deoxycholic acid and SDS for better solubilisation and denaturation of proteins, was used generally for sample preparation for immunoblotting (see chapter 2.2.11 and 2.2.15). Together with the observed lack of Endo H sensitive MHCI forms this result suggests that there is an interference with the MHCI processing pathway. The same Endo H cleavage pattern as seen during active infection was also detectable during active infection with additional IFN- $\beta$  and IFN- $\gamma$  treatment, respectively. However, a faint Endo H sensitive band appeared under IFN- $\gamma$  treatment of actively infected cells indicating some inhibitory effect of IFN- $\gamma$  on the chlamydial interference with MHCI processing. In persistently infected HeLa cells and in infected fibroblasts both Endo H sensitive and Endo H resistant MHCI molecules were present, with a similar amount of Endo H sensitive forms in both mock-infected and *Chlamydia*-infected cells in both models. This suggests that under these conditions the MHCI antigen processing pathway is functional and not manipulated by chlamydial organisms, which correlates well with the MHCI surface expression data (Table 4).

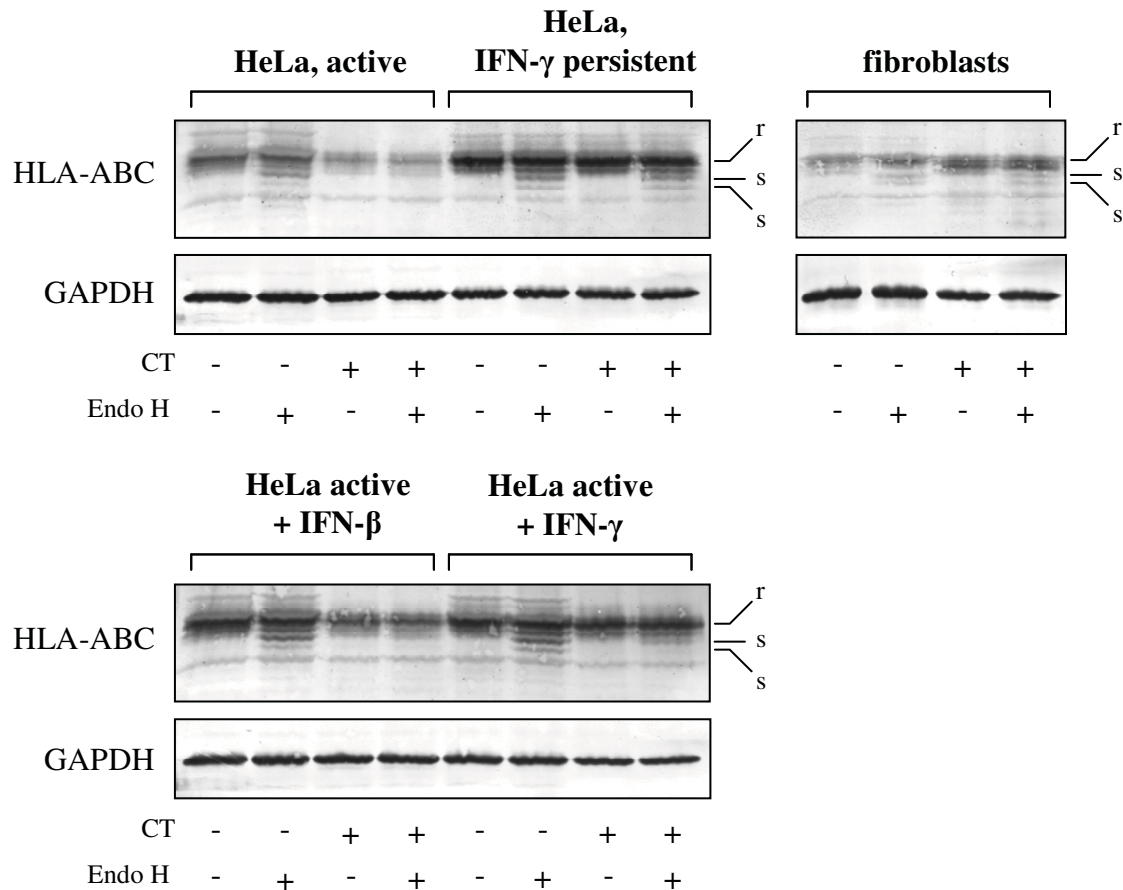


**Fig. 24: Differences in sensitivity of MHCI molecules to cleavage with Endo H between the different infection models.**

Lysates from *Chlamydia*-infected and mock-infected cells were generated at 48 h p.i. and treated with or without Endo H. Endo H resistant (r) and sensitive (s) forms of MHCI were detected after immunoblotting with an antibody binding HLA-ABC. CT: *C. trachomatis*.

### 3.4 *C. trachomatis* mediated degradation of the host cell mRNA export factor NXF1

#### 3.4.1 Influence of active *C. trachomatis* infection on NXF1 expression in HeLa cells

During analysis of expression of proteins involved in antigen presentation an accidental discovery revealed that the host cell mRNA export factor NXF1 (nuclear RNA export factor 1) gets degraded in actively *Chlamydia*-infected HeLa cells. This discovery was the result of usage of a commercially available TAP1 antibody which was applied in order to analyse TAP1 expression in *Chlamydia*-infected cells. In fact, it turned out that this antibody represents an antibody clone specific for NXF1.

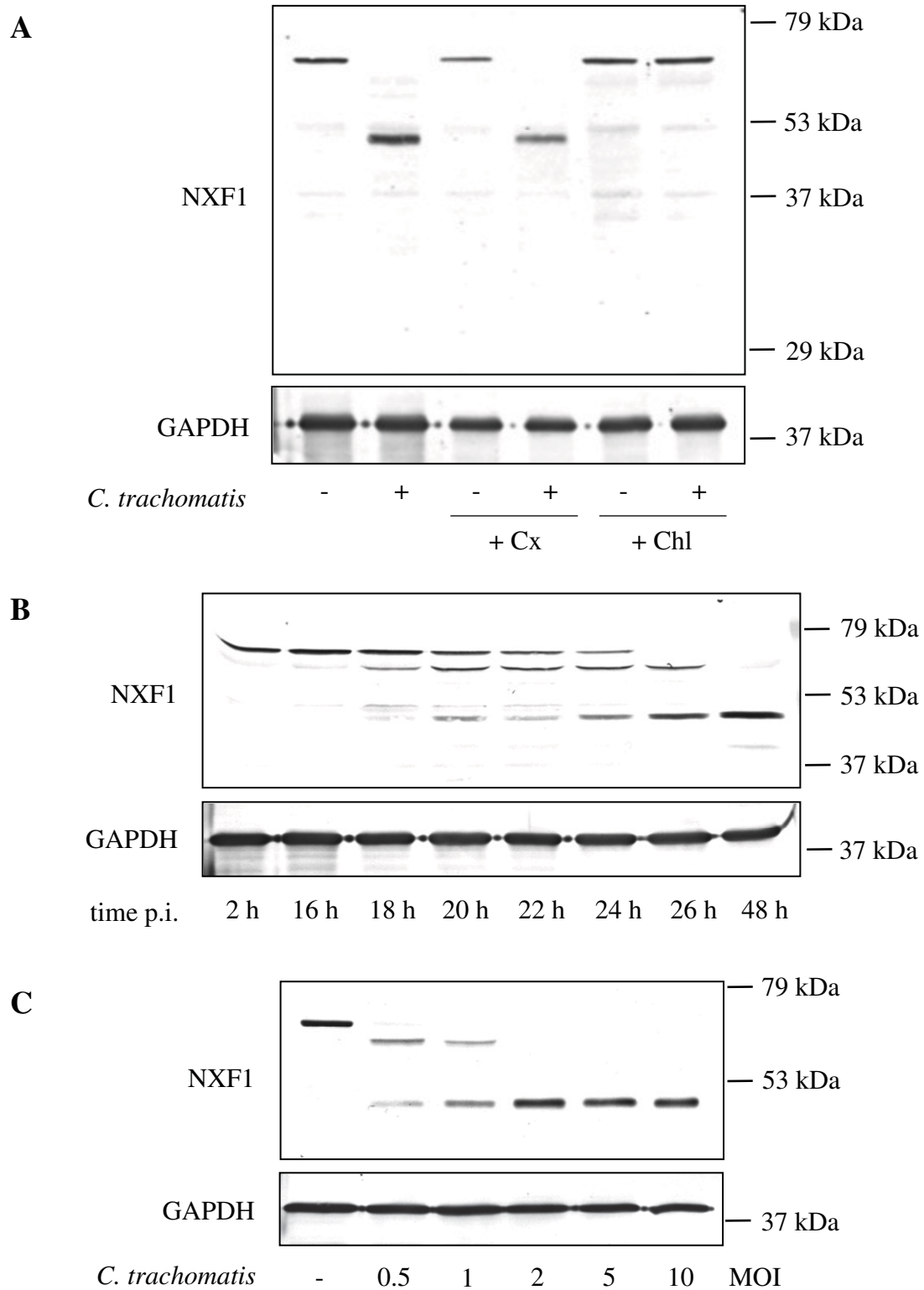


**Fig. 25: NXF1 is degraded upon active *C. trachomatis* infection in HeLa cells.**

Immunoblots of HeLa cell lysates.

**A** Mock- and *Chlamydia*-infected cells were either not treated or treated with cycloheximide (Cx, 2  $\mu$ g/ml) and chloramphenicol (Chl, 100  $\mu$ g/ml), respectively, and analysed at 48 h p.i.

**B** *Chlamydia*-infected cells were incubated for different time points.

**C** Different infectious doses (MOI) of *C. trachomatis* were used for infection, and cells were harvested at 48 h p.i.

It was found that the expression of NXF1 was drastically reduced after active chlamydial infection of HeLa cells (Fig. 25 A). The 70 kDa band, which represents NXF1, disappeared after 48 h of infection and a prominent band of 47 kDa appeared instead suggesting that NXF1 got cleaved. Treatment with the eukaryotic protein translation inhibitor cycloheximide did not affect the degradation of NXF1 in infected cells. This excludes the possibility that host cell proteins newly synthesized after chlamydial infection account for the degradation of NXF1. When *Chlamydia*-infected cells were treated with chloramphenicol the degradation of NXF1 was totally inhibited. These results suggest that a chlamydial protease is responsible for the cleavage of NXF1.

The degradation of NXF1 started during the mid-cycle of chlamydial development as it can be seen by the appearance of a 61 kDa cleavage product at 16 hours p.i. (Fig. 25 B). The 70 kDa band representing the NXF1 full-length protein disappeared over the time and could not be detected anymore at 26 hours p.i. The 61 kDa fragment was further cleaved to a 47 kDa fragment because only the 47 kDa band could be detected at 48 hours p.i.

The degree of NXF1 degradation correlated with the infectious dose of *C. trachomatis* as it is shown in Figure Fig. 25 C. At 48 h p.i. the 61 kDa band could only be detected at lower doses. However, with higher infectious doses the amount of the 47 kDa cleavage product increased. The result suggests that the stronger proteolytical activity at higher infectious doses is due to an increased amount of inclusion-containing cells in which NXF1 got degraded.

### **3.4.2 The role of CPAF in degradation of NXF1**

It was assumed that the degradation of NXF1 could be a result of the cleavage activity of a chlamydial protease secreted into the host cytosol during infection. To test this hypothesis a cell-free cleavage assay was applied in a similar approach as described in chapter 3.2.3 and Fig. 16. However, instead of whole cell lysate only nuclear extract (NE) from mock-infected HeLa cells was used as a substrate, because NXF1 is mainly located in the nucleus (Kang & Cullen, 1999). The NXF1 protein could not be detected at all in the CEs, and the NE of infected cells contained only the cleavage products of NXF1 (Fig. 26). When the NE of mock-infected cells was incubated with the CE of *Chlamydia*-infected cells the typical 47 kDa cleavage band of NXF1 could be seen. As expected, incubation of the NE of mock-infected cells with the CE of mock-infected cells left the substrate uncleaved.

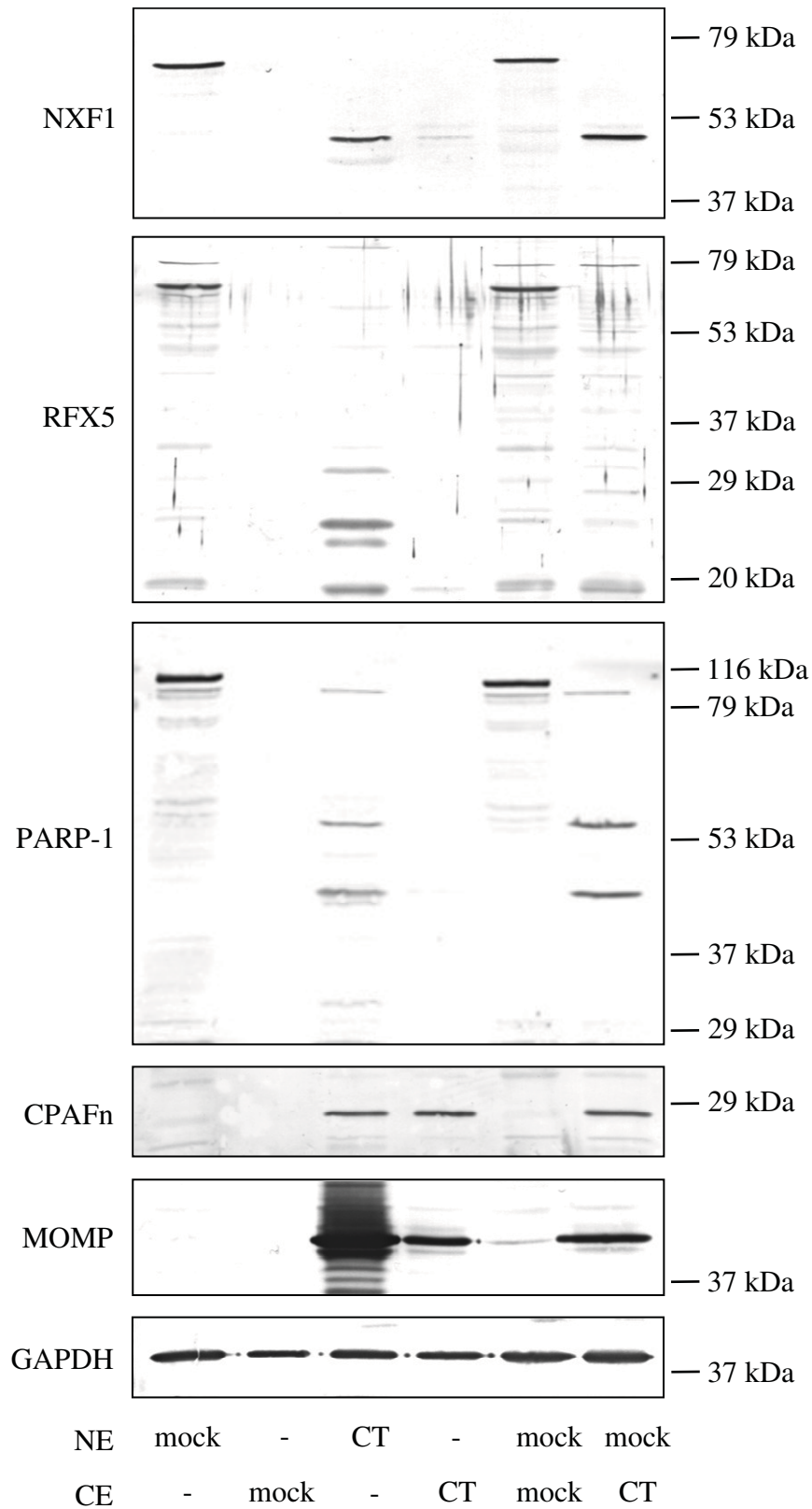


**Fig. 26: Cleavage of NXF1 and other nuclear proteins in a cell-free cleavage assay.**

Immunoblots of cell-free cleavage assay samples containing either cytosolic extract (CE) and/or nuclear extract (NE) of uninfected (mock) or actively infected (CT) HeLa cells at 48 h p.i. Proteins detected were the nuclear proteins NXF1, RFX5, PARP-1 and the chlamydial proteins CPAF and MOMP. CPAFn: N-terminal fragment of CPAF.

There are other nuclear proteins, for example RFX5 and PARP-1, which are known to be degraded by *C. trachomatis* through the activity of CPAF (Paschen *et al.*, 2008; Yu *et al.*, 2010; Zhong *et al.* 2001). As control, the cleavage of both proteins was analysed and could be detected in immunoblots of the cell-free cleavage assay in the NE of *Chlamydia*-infected cells and after incubation of the NE from mock-infected cells with the CE from *Chlamydia*-infected cells (Fig. 26).

During the preparation of the extracts of infected cells most of the chlamydial organisms are expected to be contained in the NE due to co-purification of whole chlamydial inclusions with the nuclei after centrifugation of the CE that was prepared by limited douncing to keep the inclusions intact (Chen *et al.*, 2009). This was analysed by detecting MOMP which revealed that most of the protein was present in the NE of infected cells (Fig. 26). A smaller fraction of MOMP was detected in the CE of infected cells suggesting a contamination with chlamydial organisms due to too strong homogenisation which may lead to rupture of the inclusions and/or that MOMP is also located outside the inclusion as has been described previously (Giles *et al.*, 2006; Giles & Wyrick, 2008). Beside its presence in the NE of infected cells the proteolytically active N-terminal fragment of the chlamydial protease CPAF (CPAFn) was also found in the CE of *Chlamydia*-infected cells correlating with the secretion of this protease into the host cytosol. Because the amount of CPAF relative to MOMP was much smaller in the NE than in the CE of infected cells, the presence of CPAF in the CE likely is the result of secretion of the protease into the host cytosol.

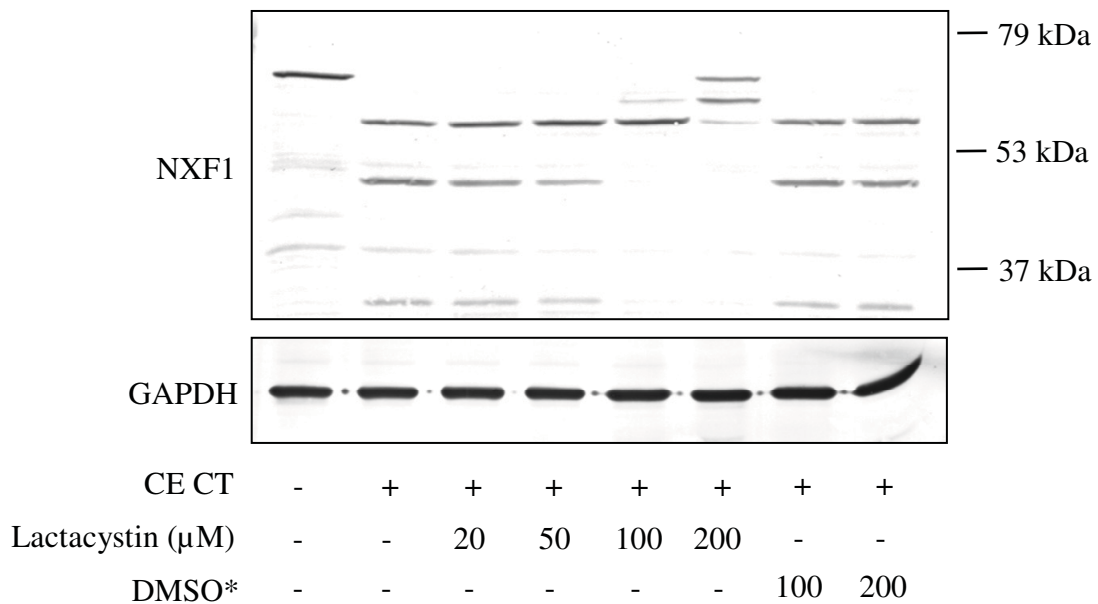


**Fig. 27: Effect of inhibition of CPAF with lactacystin on NXF1 cleavage.**

See Fig. 17 for description. NE of mock-infected cells containing NXF1 was used as substrate.

CPAFn and GAPDH, which served as loading control, are expected to be present only in the CE but not in the NE due to their cytosolic localisation. However, both proteins could also be detected in the NE of both mock-infected and *Chlamydia*-infected cells. This likely is the result of a contamination of the NE with CE from the same lysate during the preparation of the NE. Furthermore, the homogenisation may have been not rigorous enough to lyse all cells in the preparation leading the presence of some whole cells in the NE. Nevertheless, this contamination of NE with CE has no influence on the results, since the NE only served as substrate for cleavage. Rather, it is important that the CE is not contaminated with NE to show the presence of CPAF and proteolytic activity in the cytosol.

To examine if NXF1 is cleaved by CPAF, again CPAF was removed from the CE of infected cells by immunoprecipitation. However, it was not possible to detect NXF1 in the sample of NE mixed with the supernatant of CPAF immunoprecipitation due to interference of a contaminating 70 kDa serum protein band with antibody detection, the same phenomenon as described in chapter 3.2.3 (data not shown). When the CPAF inhibitor lactacystin was added to the CE of infected cells at a concentration of 200  $\mu$ M, the cleavage of NXF1 in a cell-free cleavage assay was strongly reduced (Fig. 27). This suggests that CPAF is the protease that is responsible for the degradation of NXF1 in *Chlamydia*-infected cells.

### **3.4.3 Analysis of NXF1 degradation during IFN- $\gamma$ mediated chlamydial persistence and chlamydial infection of fibroblasts**

Because CPAF expression is downregulated during IFN- $\gamma$  mediated chlamydial persistence in HeLa cells (Fig. 11 and Fig. 12), it would be expected that under these conditions NXF1 degradation would be reduced. As displayed in Fig. 28 cleavage of NXF1 was strongly reduced during IFN- $\gamma$  mediated persistent infection of HeLa cells whereas the protein got completely degraded during active infection. Further, it was examined whether NXF1 degradation occurred in *Chlamydia*-infected fibroblasts. Although intact NXF1 could be still detected during infection, the amount was reduced and the 61 kDa cleavage product appeared (Fig. 28). This suggests that NXF1 is at least in part degraded during infection of fibroblasts. However, in contrast to actively infected HeLa cells no smaller cleavage products could be detected suggesting that less cleavage of NXF1 occurs due to a reduced CPAF activity during infection of fibroblasts. These results indicate that *C. trachomatis* mediated NXF1 degradation is strongly reduced during IFN- $\gamma$  mediated persistence and during infection of fibroblasts.

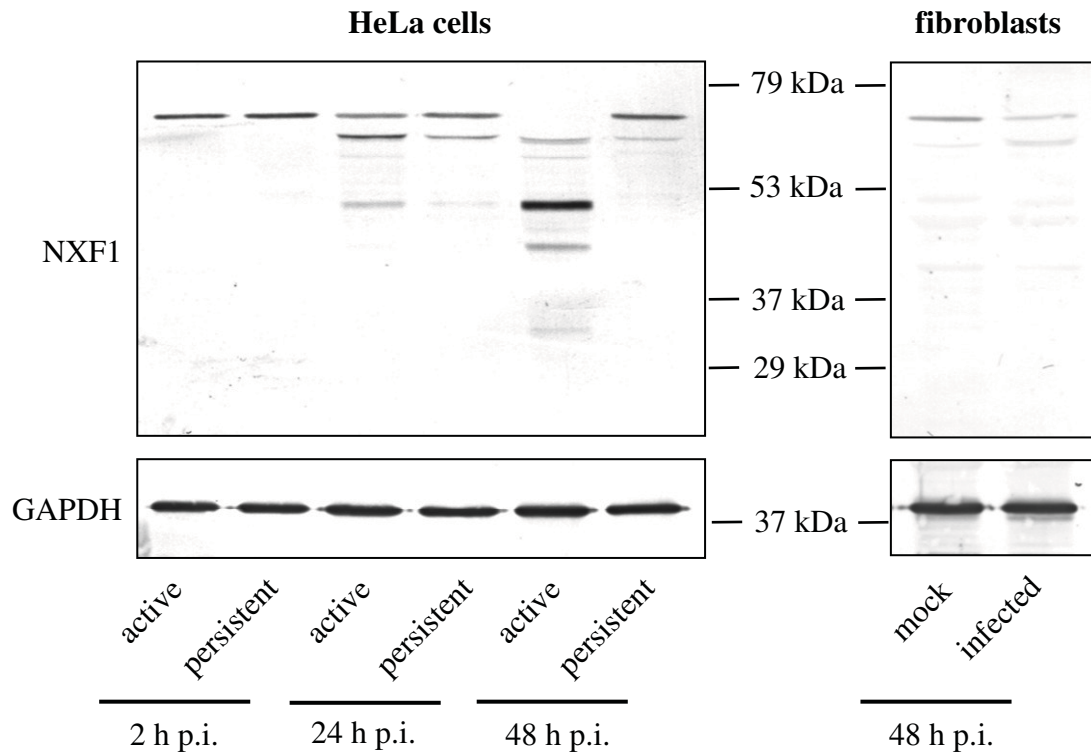


**Fig. 28: Degradation of NXF1 during IFN- $\gamma$  mediated persistent infection and in infected fibroblasts.**

Immunoblots of lysates from cells incubated for the indicated time points after active and IFN- $\gamma$  mediated persistent *C. trachomatis* infection of HeLa cells as well as mock- and *C. trachomatis*-infection of fibroblasts.

### 3.4.4 Examination of poly(A)+ RNA distribution in *Chlamydia*-infected cells

It was assumed that the degradation of NXF1 in *Chlamydia*-infected cells would lead to an impaired transport of cellular mRNA out of the nucleus. Thus, to analyse whether poly(A)+ RNA accumulates in the nuclei of *C. trachomatis*-infected HeLa cells FISH was used as a method for detection of poly(A)+ RNA with fluorescence microscopy. Most of the nuclei of inclusion-containing cells exhibited a higher fluorescence intensity of poly(A)+ RNA than the nuclei of uninfected cells (Fig. 29). However, some parts of the cytoplasm in proximity to the nucleus showed also increased staining indicating a general upregulation of poly(A)+ RNA synthesis in *Chlamydia*-infected cells. Nevertheless, the results suggest that poly(A)+ RNA accumulates in the nuclei of *Chlamydia*-infected cells due to an impaired cellular mRNA export as a result of NXF1 degradation through the chlamydial protease CPAF.

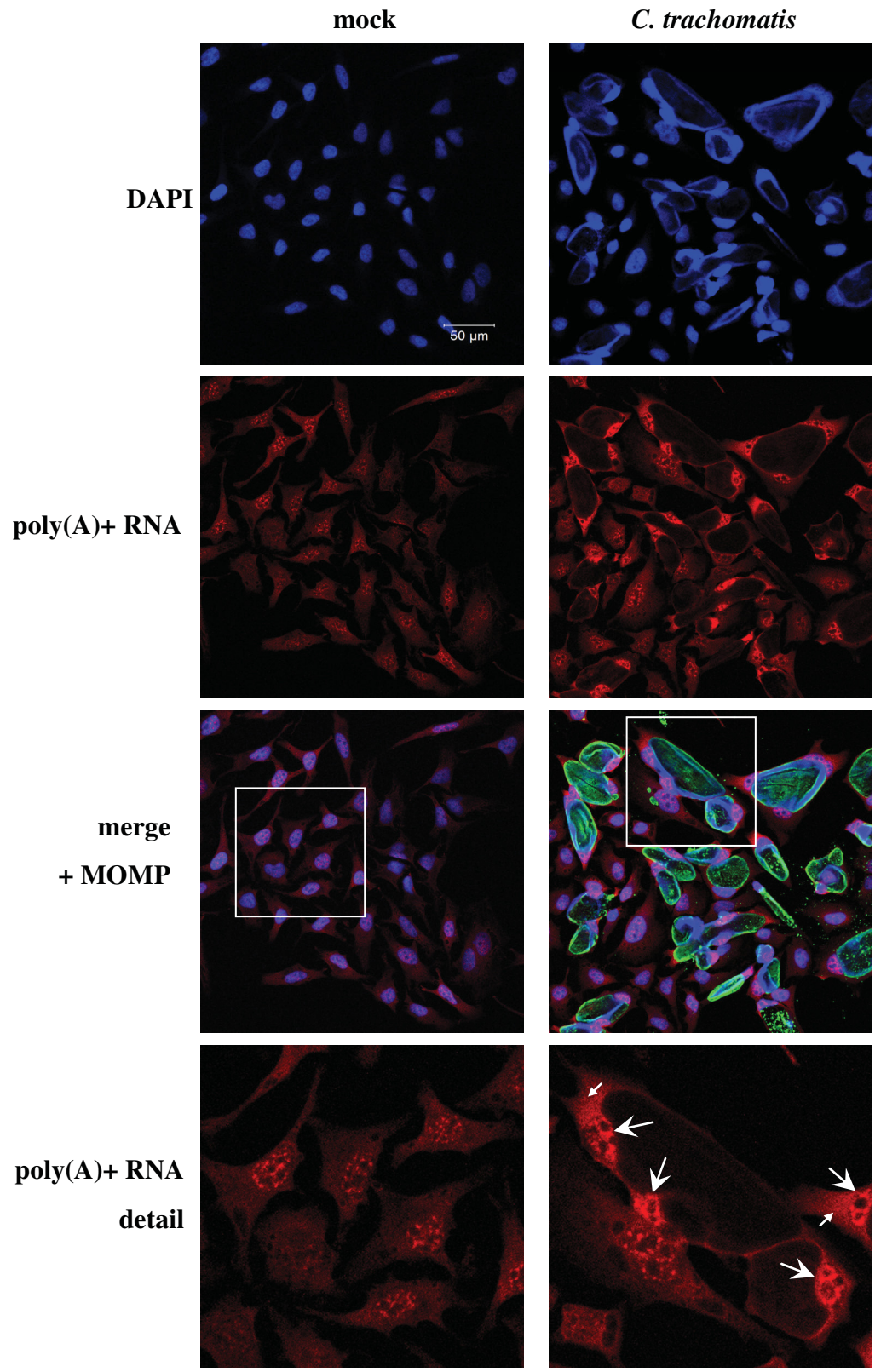


**Fig. 29: Influence of *C. trachomatis* infection on intracellular distribution of poly(A)+ RNA.**

Confocal laser scanning microscopy images of mock- and actively *Chlamydia*-infected HeLa cells at 48 h p.i. after immunofluorescent staining. Cell nuclei were stained with DAPI (blue) and chlamydial inclusions with an antibody detecting MOMP (green). Poly(A)+ RNA was detected by FISH using a Cy3-labeled oligo(dT)<sub>50</sub> probe (red). Nuclei (large arrows) and some areas of the cytoplasm (small arrows) of *Chlamydia*-infected cells showed increased poly(A)+ RNA fluorescence intensity.

## 4 Discussion

In the present study the interaction of *C. trachomatis* with the host cell MHC I antigen presentation pathway was analysed and compared with regard to three different infection models (active infection of HeLa cells, IFN- $\gamma$  mediated persistence of HeLa cells, infection of fibroblasts) in order to elucidate whether and at which step *C. trachomatis* interferes with this pathway and how this is influenced by chlamydial persistence.

In the first part of the present study the growth of *C. trachomatis* in fibroblasts was characterised to find out whether this cell type could generally function as a host cell for chlamydial growth. In fibroblasts *C. trachomatis* displayed a strongly reduced EB production, when compared to active infection of HeLa cells, which suggests that the bacteria are able to persist in this cell type. However, chlamydial growth in fibroblasts differed also from IFN- $\gamma$  mediated persistent infection of HeLa cells in chlamydial morphology and gene expression. Because infection of fibroblasts led to IDO expression through endogenous IFN- $\beta$  production, the role of IDO in causing the atypical chlamydial growth was also assessed. siRNA mediated knockdown of *IDO* expression resulted in increased production of progeny indicating that IDO is involved in mediating atypical chlamydial growth in fibroblasts.

The second part of the present work covered the interaction of *C. trachomatis* with the MHC I antigen presentation pathway. The expression of MHC I on the cell surface was only slightly downregulated during active infection of HeLa cells, indicating that there is some chlamydial interference but no total inhibition of this pathway. Analysing components of the MHC I pathway revealed that the antigen transporter subunit TAP2 was degraded during active infection, probably through the chlamydial protease CPAF.

Further, the examination of the influence of *Chlamydia*-induced Golgi fragmentation on MHC I processing revealed that MHC I molecules are present in the fragmented Golgi of actively infected HeLa cells. However, tracking of MHC I molecules from the ER to the Golgi may be reduced after active infection due to interference at a step in the ER as indicated through the absence of Endo H sensitive MHC I molecules. Because TAP2 degradation, altered MHC I processing and reduced MHC I surface expression only occurred during active but not persistent and fibroblast infection, it is suggested that TAP2 degradation may be responsible for the surface MHC I downregulation during active infection.

Additionally, it was found that the Golgi proteins GM130 and Golgin-245 are degraded by CPAF during active infection, and accidentally, the human mRNA export factor NXF1 was

also discovered as another target for chlamydial cleavage. Degradation of these proteins generally was strongly reduced during persistent and fibroblast infection. This correlated with decreased expression of proteolytically active CPAF in these infection models. The results show that the ability of chlamydiae to interfere with host cell pathways such as the MHCI pathway depends on the growth state of chlamydiae which is influenced by the host cell conditions such as the cell type or the presence of immunomodulatory factors.

#### **4.1 Persistent growth of *C. trachomatis* in fibroblasts**

The epithelial cell represents the typical chlamydial host cell type that promotes productive infection. Also other cell types are known in which *Chlamydia* are able to grow, such as macrophages, monocytes, fibroblasts and dendritic cells among others (Gervassi *et al.*, 2004 a; Manor & Sarov, 1986; Rödel *et al.*, 1998 a). Direct evidence that fibroblasts and macrophages could promote chlamydial growth in vivo came from a study which showed that viable chlamydial organisms reside in these cell types in the joints of patients with chronic CiReA (Nanagara *et al.*, 1995). This suggests that fibroblasts and macrophages could serve as a reservoir of chlamydiae during chronic chlamydial infection and thus could represent host cells for persistent infection. So far, the chlamydial growth and inclusion formation has been well described for monocytes, macrophages and dendritic cells, revealing that chlamydiae are able to persist in these cell types (Koehler *et al.*, 1997; Manor & Sarov, 1986; Rey-Ladino *et al.*, 2007). Successful chlamydial in vitro infection of fibroblasts has been reported for synovial fibroblasts (Rödel *et al.*, 1998 a), dermal fibroblasts (Baumert *et al.*, 2009) and even gingival fibroblasts (Rizzo *et al.*, 2008), suggesting that fibroblasts generally promote chlamydial growth independently of their organ origin. However, not much is known about the detailed growth behaviour of chlamydiae in fibroblasts. Thus, the first part of the present work was dedicated to the detailed characterisation of the *C. trachomatis* growth in fibroblasts.

##### **4.1.1 Chlamydial growth arrest in fibroblasts at the stage of RB-to-EB re-differentiation**

The establishment of chlamydial persistence in vitro is known to be induced by different factors and host conditions (reviewed in Hogan *et al.*, 2004). All of the known chlamydial persistence models have in common that new progeny is abrogated or strongly reduced, and in most of these models enlarged but viable chlamydial forms (ABs) are present in the

inclusions. Here, the IFN- $\gamma$  mediated chlamydial persistence model, in which chlamydial growth is restricted through IDO-mediated tryptophan depletion (Beatty *et al.*, 1994 a), was used for comparison with chlamydial infection of fibroblasts, because it represents one of the most-well studied persistence models.

Like in other persistence models a highly reduced production of EBs was found during infection of fibroblasts when compared with actively infected HeLa cells, which suggests that fibroblast infection could represent another model for chlamydial persistence. However, the comparison of chlamydial growth in fibroblasts with the IFN- $\gamma$  mediated chlamydial persistence model revealed important differences. First, instead of being reduced in size chlamydial inclusions appeared much larger in fibroblasts than in the IFN- $\gamma$  mediated persistence model, and they exceeded even the size of inclusions during active infection of HeLa cells, probably because fibroblasts themselves are larger than HeLa cells. Second, inclusions within fibroblasts rarely contained enlarged ABs, instead apparently normal RBs and IBs were the pre-dominant bacterial forms and were present in much higher number than the few ABs in the IFN- $\gamma$  mediated persistence model. Third, the analysis of chlamydial gene expression in infected fibroblasts revealed no downregulation, when compared to actively infected HeLa cells, but even upregulation of the expression of some genes at the late stage of infection (48 h p.i.), whereas during IFN- $\gamma$  mediated persistent infection most genes were downregulated at this stage. Furthermore, an attenuated protein ratio of MOMP to HSP60, which is a hallmark of IFN- $\gamma$  mediated chlamydial persistence (Beatty *et al.*, 1993), has not been found in infected fibroblasts. Thus, the atypical chlamydial growth in fibroblasts seems to be very different from other known persistence models. However, the chlamydial growth in fibroblasts differed also considerably from that in active infection by the presence of a high number of RBs and IBs and a low production of EBs at 48 h p.i., indicating that the developmental cycle is not completed in fibroblasts at that time point. A possible explanation would be a delay in RB to EB differentiation. However, the amount of EBs produced in fibroblasts did not increase but rather remained at the same level at 96 and 120 h p.i. (data not shown), excluding this possibility. The presence of RBs and IBs at the late stage of the developmental cycle therefore rather indicates an arrest of chlamydial growth at the stage shortly before RB-to-EB differentiation, resulting in the inability to produce EBs and supporting the hypothesis of chlamydial persistence in fibroblasts. This persistence is different from the IFN- $\gamma$  mediated persistence model because it lacks aberrant chlamydial forms, a small inclusion size, a low number of chlamydial

organisms and a general downregulation of chlamydial gene expression, which all seems to be more typical for an arrest at an earlier stage of chlamydial growth.

#### **4.1.2 Different efficiencies of IFN to induce *IDO* expression between the three infection models**

Previous work of our group showed that *C. trachomatis* infection of synovial fibroblasts led to induction of interferon regulatory factor 1 (IRF-1) and the interferon-stimulated gene factor 3 $\gamma$  (ISGF3 $\gamma$ ) expression, thus indicating an activation of intracellular defence pathways that contributed to the IFN- $\beta$  expression observed after chlamydial infection of these cells (Rödel *et al.*, 1998 a; Rödel *et al.*, 1999). Furthermore, *IDO* expression was detected in infected synovial fibroblasts, and this was partially mediated by endogenously produced IFN- $\beta$  (Rödel *et al.*, 1999). In the present study it was shown that *C. trachomatis* infection of dermal fibroblasts leads also to IFN- $\beta$  production, which in part contributed to an upregulation of *IDO* expression as revealed by a reduced expression after neutralisation of type I IFN activity. However, because this neutralisation did not lead to a decrease in *IDO* expression to the level of uninfected fibroblasts, other factors that are activated after chlamydial infection may contribute to and synergistically act with IFN- $\beta$  in increasing *IDO* expression. Similarly, infection of HeLa cells led to activation of factors that together with IFN synergistically increased *IDO* expression. Such factors could be cytokines, such as IL-1, which is produced by *Chlamydia*-infected cells (Rasmussen *et al.*, 1997) and known to increase *IDO* expression in HeLa cells treated with IFN- $\gamma$  (Babcock & Carlin, 2000).

Interestingly, the level of *IDO* expression was similar between infected fibroblasts and the IFN- $\gamma$  mediated persistently infected HeLa cells. When HeLa cells were treated with an amount of recombinant IFN- $\beta$  that exceeded the amount of endogenous IFN- $\beta$  produced by infected fibroblasts, *IDO* expression was still very low in comparison to infected fibroblasts. This could be due to differences in efficiencies between recombinant IFN- $\beta$  and naturally produced IFN- $\beta$  on the one hand and the usage of different cell types which could have differential susceptibilities to IFN- $\beta$  on the other hand. For many cell lines strong *IDO* activity has only been reported to be induced by IFN- $\gamma$  but not or only marginally by type I IFN (Byrne *et al.*, 1986; Ozaki *et al.*, 1988; Takikawa *et al.*, 1988). In the present work, a similar response to both IFN types could be detected for HeLa cells. However, the highly increased *IDO* expression in fibroblasts after chlamydial infection shows that the induction of *IDO* through low amounts of endogenously produced IFN- $\beta$  seems to be very efficient in fibroblasts.

### 4.1.3 Role of IDO in chlamydial persistence in fibroblasts

IFN- $\gamma$  is regarded as the main factor that induces expression of human IDO, an enzyme that converts L-tryptophan to N-formyl L-kynurenine, thus depleting the intracellular tryptophan pool. IDO-mediated tryptophan depletion represents an effective innate immune mechanism to control infections with intracellular pathogens like *Chlamydia*, *Toxoplasma gondii* and different viruses (reviewed in King & Thomas, 2007). It is also well known to induce chlamydial persistence (reviewed in Hogan *et al.*, 2004).

Because synovial fibroblasts were shown to express IDO upon chlamydial infection (Rödel *et al.*, 1999), IDO mediated tryptophan depletion might be responsible for the chlamydial growth arrest in fibroblasts. Indeed, the results of the present study show that IDO is involved in mediating chlamydial persistence in fibroblasts, as a 4-fold increase in burst size was found after *IDO* siRNA knockdown in infected fibroblasts, which correlates to around 80 EBs per inclusion. Also, the chlamydial gene expression after *IDO* siRNA knockdown in fibroblasts was altered to a state that was more similar to that in actively infected HeLa cells. However, the burst size in actively infected HeLa cells was still 9 to 10 times higher than the burst size in infected fibroblasts after *IDO* siRNA transfection. Therefore, it can be assumed that the effect of IDO on the inhibition of chlamydial growth is much lower in fibroblasts than in the IFN- $\gamma$  mediated persistence model. This is supported by the expression of *trpB* which was found to be highly upregulated during IFN- $\gamma$  mediated persistence, but only slightly increased in infected fibroblasts. *trpB* expression is a good indicator of the level of tryptophan depletion in infected cells and thus for IDO activity, because *trpB* transcription is repressed in the presence and activated in the absence of tryptophan (Wood *et al.*, 2003). Interestingly, the upregulation of *trpB* expression started later in infected fibroblasts than in the IFN- $\gamma$  mediated persistence model. This further suggests that tryptophan starvation followed by inhibition of chlamydial growth occurs at a late stage of chlamydial growth and correlates with the hypothesis of an arrest of chlamydial growth in fibroblasts just before RB-to-EB differentiation. Furthermore, there may be a later onset of IDO expression in these cells, because chlamydial infection first leads to the production of IFN- $\beta$  which in turn induces *IDO* expression. This results in a longer duration until the initiation of IDO synthesis, than would be the case when adding IFN to the cells directly after infection. In contrast, tryptophan depletion could occur at earlier time points and thus more efficiently in the IFN- $\gamma$  mediated persistence model due to pre-treatment with IFN- $\gamma$ .

Another possible reason for the discrepancies between the persistence in fibroblasts and the IFN- $\gamma$  mediated persistence in epithelial cells could be differences in the degree of IDO induction due to distinct efficiencies and concentrations of the IFN in each model. Indeed, it has been shown that the degree of the atypical morphology of the chlamydial forms depends on the concentration of IFN- $\gamma$  or the level of amino acid deprivation (Harper *et al.*, 2000; Jones *et al.*, 2001). However, in the present study a similar level of *IDO* expression in both infection of fibroblasts and IFN- $\gamma$  mediated persistent infection of HeLa cells was found, indicating a similar efficiency of the endogenously produced IFN- $\beta$  and the exogenously added IFN- $\gamma$  in IDO activation. Thus, a late onset of *IDO* expression could more likely be responsible for the lower effect of IDO on inhibition of chlamydial growth in fibroblasts compared to the IFN- $\gamma$  mediated persistence. However, treatment of HeLa cells with IFN- $\gamma$  after infection did not result in chlamydial persistence. Because of this and because of the results of the *IDO* siRNA knockdown it is suggested that IDO mediated tryptophan depletion is only one factor contributing to persistence induction in fibroblasts, and that additional factors are involved.

It has been reported that IFN- $\gamma$  treatment of cells can also lead to intracellular iron depletion (Byrd & Horwitz, 1993). IFN- $\alpha$  induced inhibition of *C. trachomatis* growth in HeLa cells could be reversed both by tryptophan and iron addition (Ishihara *et al.*, 2005), suggesting that IFN exerts its inhibitory effect on *Chlamydia* by a combination of tryptophan and iron depletion. Another mechanism that is known to restrict growth of intracellular pathogens is the IFN induction of inducible nitric oxide synthase (iNOS) that produces nitric oxide to eradicate pathogens (reviewed in Chakravorty & Hensel, 2003). However, in the present work iNOS expression has not been detected after chlamydial infection of fibroblasts (data not shown), and iNOS has been implicated in restriction of chlamydial growth basically in murine, but not in human cells (Roshick *et al.*, 2006).

Similar to fibroblasts *C. trachomatis* infection of monocytes results in chlamydial persistence without addition of any exogenous factors (Schmitz *et al.*, 1993). Treatment of infected monocytes with tryptophan or antibodies neutralising TNF- $\alpha$ , IFN- $\alpha$  or IFN- $\gamma$  did not abrogate the persistence (Koehler *et al.*, 1997). However, IDO expression is upregulated in *Chlamydia*-infected monocytes (Krausse-Opatz *et al.*, 2007), and microarray data revealed an increased expression of IFN- $\gamma$  and other cytokines (Schradler *et al.*, 2007). This suggests that although IDO is readily expressed upon chlamydial infection of monocytes, probably through endogenously produced cytokines, other factors are involved in the persistence in monocytes. Due to the manifold cytokine expression and activation of diverse

intracellular pathways it is conceivable that several factors may contribute and synergistically act in inhibiting chlamydial growth in infection of monocytes as well as fibroblasts.

#### **4.1.4 Comparison of chlamydial gene expression in fibroblasts with other persistence models**

In most persistence models, such as the IFN- $\gamma$  mediated, amino acid depletion, iron deficiency, monocyte and the HSV-2 co-infection persistence model, the expression of MOMP was attenuated, suggesting that it is a general feature of chlamydial persistence (Belland *et al.*, 2003; Deka *et al.*, 2006; Gérard *et al.*, 1998 b; Goellner *et al.*, 2006; Jones *et al.*, 2001; Timms *et al.*, 2009). However, no MOMP downregulation has been observed in infected fibroblasts. Therefore, the phenomenon seems not to apply to all persistence models. Also in the penicillin persistence model no decrease of MOMP expression could be detected (Cevenini *et al.*, 1988; Goellner *et al.*, 2006; Nicholson & Stephens, 2002).

Furthermore, the downregulation of the expression of the 60 kDa cysteine-rich outer membrane protein OmcB has been observed for the penicillin persistence and several other chlamydial persistence models (Beatty *et al.*, 1993; Belland *et al.*, 2003, Cevenini *et al.*, 1988; Goellner *et al.*, 2006; Jones *et al.*, 2001; Nicholson & Stephens, 2002). Decreased expression of late genes like *omcB* seems to point to a growth arrest during early stages of the chlamydial developmental cycle. However, similar to active infection in HeLa cells, *omcB* expression in *Chlamydia*-infected fibroblasts was highly upregulated at the late stage. This suggests a normal chlamydial development in fibroblasts until the late stage. Cysteine-rich proteins like OmcB are incorporated into the chlamydial cell wall at the late stage to form the rigid EBs (Hatch *et al.*, 1986). Since EBs are rarely formed in fibroblasts, it is tempting to speculate that despite proper *omcB* transcription reduced protein synthesis of cysteine-rich proteins could occur by low availability of the amino acid cysteine. Indeed, cysteine seems to be essential for chlamydial RB-to-EB differentiation, as its depletion was reported to reduce the formation of new EBs (Allan *et al.*, 1985). In contrast, cysteine seems not to be essential for the development of normal inclusions and RBs (Allan & Pearce, 1983). Thus, a low intracellular cysteine pool could be a potential inducing factor for the observed atypical chlamydial development in fibroblasts.

A general hallmark of chlamydial persistence seems to be the inhibition of chlamydial cell division, as was found by the attenuated expression of proteins involved in this process in several persistence models (Belland *et al.*, 2003; Byrne *et al.*, 2001; Gérard *et al.*, 2001; Goellner *et al.*, 2006; Klos *et al.*, 2009). Surprisingly, expression of the gene encoding the

cell division protein FtsW was highly upregulated in fibroblasts, when compared to active infection at the late stage of the developmental cycle. Thus, in contrast to other persistence models bacterial multiplication appears not to be inhibited in fibroblasts, which is in correlation with the electron microscopy observations that revealed a high number of RBs in fibroblasts. The higher *ftsW* expression in infected fibroblasts compared to actively infected HeLa cells at 48 h p.i. suggests that the RBs within fibroblasts continue to undergo cell division instead of re-differentiating to EBs. Because fibroblasts are larger than HeLa cells the increased *ftsW* expression could further be explained by more space available inside the cell, which may result in higher cell division rates.

Interestingly, instead of a downregulation an upregulation of *ftsW* expression was found in the IFN- $\gamma$  induced persistence model at 24 h p.i., which is in contrast to a previous study (Belland *et al.*, 2003). Although the present work is very similar to this study in using the same cells and serovar, a higher concentration and longer pre-treatment of IFN- $\gamma$  as well as another cell culture medium with different nutrient composition was used in the present study. This shows that persistence induction is very sensitive to different culture conditions. Furthermore, differences in conditions for gene expression analysis could account for the observed discrepancies. A similar difference in results as for *ftsW* expression was observed for the expression of *pgsA\_2*, encoding a protein involved in phospholipid synthesis, which was found to be downregulated during IFN- $\gamma$  induced persistent infection, whereas its expression was upregulated in the study of Belland *et al.* (2003). However, in that study gene expression was only measured at 24 h p.i., but not at 48 h p.i. Like *ftsW*, the expression of *pgsA\_2* was highly upregulated in fibroblasts indicating that an enhanced metabolism and availability of nutrients could lead to increased cell division. Chlamydiae are known to acquire host lipids for incorporation into the bacterial cell and inclusion membrane (reviewed in Scidmore, 2011). The upregulation of *pgsA\_2* in infected fibroblasts could thus also be explained by the larger inclusion size, because an increasing inclusion membrane surface area would need more lipids to be acquired from the host cell and to be altered to bacterial phospholipids.

One particularly interesting observation was the highly increased expression of *groEL\_2* (also called *ct604*), encoding one of three HSP60 proteins, at the late stage of fibroblast infection. An upregulated expression of this gene was found in *C. trachomatis* infected monocytes, indicating that it plays an important role in persistent infection (Gérard *et al.*, 2004). This is supported by another study that showed a larger amount of this protein in iron deficiency mediated chlamydial persistence (LaRue *et al.*, 2007). Importantly,

*groEL\_2* expression was also found to be upregulated in synovial samples from patients with CiReA (Gérard *et al.*, 2004). The finding of increased *groEL\_2* expression in fibroblasts thus strengthens the hypothesis that this HSP60 form plays an important immunopathological role during *in vivo* persistence of chlamydiae, because HSP60 is supposed to contribute to the severe immunopathology observed during chlamydial infection. On the other hand, increased expression of this protein could simply represent a specific stress response to unfavourable growth conditions.

#### **4.1.5 Expression of the chlamydial protease CPAF in fibroblasts**

The chlamydial protease CPAF represents an important virulence factor during chlamydial infection. The present work revealed that CPAF was severely attenuated in the IFN- $\gamma$  mediated persistence model both at the transcriptional and the translational level, which has also been described recently (Rödel *et al.*, 2012). Downregulation of CPAF expression had also been observed in *C. psittaci* persistence induced by IFN- $\gamma$  treatment or iron depletion (Goellner *et al.*, 2006). It has been reported that expression of genes encoding the type III secretion system is attenuated during IFN- $\gamma$  mediated chlamydial persistence (Slepenkin *et al.*, 2003), indicating that translocation of chlamydial effector proteins could be severely reduced under these conditions. Although CPAF is translocated through the type II secretion pathway (Chen *et al.*, 2010 a), secretion of the protease into the cytoplasm was also found to be inhibited during IFN- $\gamma$  or iron deficiency mediated persistence (Heuer *et al.*, 2003). This correlated with an abrogation of RFX5 degradation (Heuer *et al.*, 2003), a host transcription factor normally cleaved by CPAF during active infection (Zhong *et al.*, 2000). In the present study an inhibition of the degradation of RFX5 and other host proteins that are cleaved by CPAF was observed also during IFN- $\gamma$  mediated chlamydial persistence, which indicates that CPAF has no strong activity during persistent infection, thus reducing the ability of chlamydiae to manipulate the host cell. Interestingly, gene expression of CPAF was not diminished during infection of fibroblasts, and it even showed an increase at early stages when compared to active infection of HeLa cells. However, no or only reduced degradation of CPAF substrates has been observed in fibroblasts. Interestingly, in contrast to actively infected HeLa cells the 70 kDa precursor protein of CPAF could be readily detected in infected fibroblasts. Because the precursor usually is processed as soon as it is translocated into the host cytosol, the result suggests an accumulation of the precursor protein in fibroblast inclusions due to a reduced translocation into the host cytosol. This is supported by the lower amount of the active 29 kDa N-terminal CPAF form in

infected fibroblasts compared to HeLa cells. Another possibility could be that translocation readily occurs while autoprocesing of CPAF could be inhibited in the cytosol of fibroblasts due to suboptimal host cell conditions.

## **4.2 Impact of chlamydial infection on MHC class I antigen presentation**

The presentation of intracellularly processed chlamydial antigens via MHCI to CD8+ T cells is important for the recognition and elimination of infected cells, especially of infected epithelial cells since they represent host cells for chlamydial multiplication and primary sites of chlamydial infection. However, *Chlamydia* have evolved mechanisms to escape immune defence in order to survive and finish their development inside the host cell. One such mechanism could be the downregulation of MHCI surface expression in order to escape recognition by CD8+ T cells. Indeed, the downregulation of surface MHCI has been found in *C. trachomatis* infected epithelial cells (Hook *et al.*, 2004; Ibane *et al.*, 2011; Zhong *et al.*, 2000). In the present study, a reduction of surface MHCI has also been detected in HeLa cells infected with *C. trachomatis*, however, compared to the above studies, there was only a slight decrease of surface MHCI expression in these cells.

Downregulation of MHCI surface expression is a general mechanism applied by different viruses to escape CD8+ T cell mediated killing. This is achieved through endocytosis of MHCI from the cell surface, retention of MHCI in the ER or Golgi, proteasomal degradation of MHCI heavy chains and/or inhibition of TAP-mediated peptide transport (reviewed in Antoniou & Powis, 2008). Interestingly, TAP generally seems to be a very popular target for viral interference with MHCI antigen presentation as several viruses have been found to inhibit peptide transport through TAP (reviewed in Antoniou & Powis, 2008). *Chlamydia* also seem to possess the ability to inhibit TAP-mediated peptide transport, as chlamydial degradation of TAP2 has been found in the present work, which likely may lead to inhibition of peptide loading of MHCI and may be responsible for the observed surface MHCI downregulation during active infection of HeLa cells.

Furthermore, because *Chlamydia* induce Golgi fragmentation (Heuer *et al.*, 2009) it was assumed that this has also an influence on MHCI processing and transport to the cell surface. However, no clear evidence of an inhibition of MHCI trafficking due to Golgi fragmentation has been observed, because inhibition of MHCI transport already seems to occur at the ER in actively *Chlamydia*-infected HeLa cells due to TAP2 degradation.

#### 4.2.1 Expression of the TAP transporter and immunoproteasome subunits in *Chlamydia*-infected cells

*Chlamydia* are confined to an intracellular vacuole and do not get access to the ER and Golgi lumen as easy as viral proteins that are produced by the host protein translation machinery and often travel through the secretory route. Hence, an efficient way for *Chlamydia* to interfere with the MHC I pathway would likely be the attack of components of the MHC I pathway that are exposed to the host cytosol through chlamydial effector proteins secreted into the host cytosol. Thus, the TAP transporter and immunoproteasome subunits were analysed as potential targets by examination of their gene and protein expression.

Some viruses, for example HIV-1 and CMV, are known to interfere with the assembly of the immunoproteasome (Gavioli *et al.*, 2004, Miller *et al.*, 2000), a proteasome which contains different catalytic subunits that generate an altered peptide repertoire during infection and inflammation. Interestingly, the intracellular parasite *Trypanosoma cruzi* is also able to downregulate the IFN- $\gamma$  induction of immunoproteasome expression (Bergeron *et al.*, 2008). In contrast to these studies, it was found, that the expression of the immunoproteasome subunits LMP7 and MECL1 was not affected by *Chlamydia*. Only the gene expression of LMP2 was significantly downregulated after active chlamydial infection of HeLa cells. However, since this downregulation was less than 2-fold, and as no reduction in LMP2 protein expression could be detected in these cells, it is concluded that this slightly reduced LMP2 expression may have no functional relevance for the MHC I pathway. This suggests that inflammation-induced formation of the immunoproteasome is not compromised by *Chlamydia*, thus leading to the proper generation of a different peptide repertoire which is known to increase the efficiency of MHC I presentation (reviewed in Sijts & Kloetzel, 2011).

When analysing the expression of the TAP transporter subunits, TAP1 but no TAP2 protein could be detected after active chlamydial infection of HeLa cells, although gene expression of TAP2 was not decreased. This disappearance of TAP2 protein was mediated by chlamydial degradation of TAP2, probably through the chlamydial protease CPAF. TAP2 expression was even slightly, but significantly, upregulated in actively infected HeLa cells without and with IFN- $\beta$  treatment indicating a compensation for the decreased TAP2 protein by upregulating synthesis of new TAP2 as a possible feedback mechanism. Interestingly, a slight reduction of TAP1 protein has also been found in infected HeLa cells treated with IFN- $\beta$ , and concomitantly TAP1 gene expression was significantly increased

in these cells. This phenomenon was not seen in IFN- $\gamma$  treated and non-treated actively infected cells, suggesting that TAP1 is not directly attacked by *Chlamydia*. It rather indicates that TAP1 is less stable in cells treated with IFN- $\beta$  than in cells treated with IFN- $\gamma$  or without treatment, which could be the case if TAP2 is degraded and cannot bind to and stabilise TAP1. Because most of the TAP1 in the IFN-treated cells is supposed to be newly generated due to the IFN treatment, instability of TAP1 may only affect newly synthesized TAP1 and thus might rather occur in IFN-treated cells. The differences between IFN- $\beta$  and IFN- $\gamma$  could be explained by a general stabilising effect of IFN- $\gamma$  on the MHC I pathway components, because IFN- $\gamma$  was shown to increase the stability of MHC I by improving quality control and slowing maturation of MHC I in the ER (Fromm & Ehrlich, 2001).

In contrast to active infection of HeLa cells, no TAP2 degradation has been found during persistent infection of HeLa cells and infection of fibroblasts. In both models, there was even an increased gene expression of HLA-ABC, TAP1, TAP2 and the immunoproteasome subunits after chlamydial infection. In fibroblasts this effect was partially mediated through type I IFN, as became apparent after neutralising the type I IFN response. However, because the effect of type I IFN neutralisation on gene expression was not the same for all genes analysed, other factors seem to be activated after chlamydial infection that could also increase the expression of certain MHC I related genes in fibroblasts to different levels. In addition, the potential of IFN- $\beta$  to upregulate gene expression could differ between these genes. Factors that get activated after chlamydial infection and could act synergistically with IFN- $\gamma$  in upregulating gene expression of MHC I components could also be responsible for the increased gene expression observed during IFN- $\gamma$  persistent infection of HeLa cells.

#### **4.2.2 Role of RFX5 in MHC I antigen presentation in *Chlamydia*-infected cells**

Up to now, only one potential mechanism of chlamydial interference with MHC I surface expression has been documented, namely the degradation of RFX5 through CPAF (Zhong *et al.*, 2000; Zhong *et al.* 2001). RFX5 is part of the regulatory factor complex (RFX) that is necessary for MHC II gene expression and also involved in transcription initiation of the MHC I genes (reviewed in van den Elsen *et al.*, 1998).

In contrast to the study of Zhong *et al.* (2000), no decreased expression of the MHC I encoding genes *HLA-ABC* has been observed in the present study, and there was only a slightly reduced amount of HLA-ABC protein product after active chlamydial infection of HeLa cells despite the degradation of RFX5 in these cells. Because of this, it was assumed

that RFX5 generally does not play any essential role in regulating MHCI gene expression upon chlamydial infection. Rather, redundant factors might exist that could bind to the MHCI promoter and activate MHCI transcription also in the absence of RFX5. The MHCI promoter contains different upstream elements that regulate gene expression, and different factors such as IRF-1, ISGF3 and NF- $\kappa$ B may bind to the promoter and could be sufficient to activate MHCI gene expression (Chang *et al.*, 1992; Nielsch *et al.*, 1991). Thus, it could be possible that increased expression of these factors during chlamydial infection could compensate for the RFX5 deficiency. This would also explain why an upregulation of MHCI expression was found during infection of fibroblasts despite a very low RFX5 expression that was not detectable by immunoblotting. In *C. trachomatis*-infected fibroblasts IFN- $\beta$  induction of ISGF3 $\gamma$  has been shown to lead to increased MHCI expression (Rödel *et al.*, 2002), in addition an elevated expression of IRF-1 was also found in these cells (Rödel *et al.*, 1999). Since these factors are involved in binding to the MHCI promoter, their increased expression in fibroblasts could be sufficient to enhance MHCI gene transcription despite low RFX5 expression.

#### **4.2.3 Differences in interference of *C. trachomatis* with MHC class I antigen presentation during active and persistent infection**

In contrast to actively infected HeLa cells, no interference with the MHCI presentation pathway was observed during IFN- $\gamma$  mediated persistence and fibroblast infection, as a downregulation of surface MHCI and a degradation of TAP2 was not detected under these conditions. Infected fibroblasts showed high upregulation of the MHCI pathway components through endogenously produced IFN- $\beta$  which explains the increased MHCI surface expression in these cells. This is consistent with the previous finding of MHCI upregulation in synovial fibroblasts after *C. trachomatis* infection, which was shown to be mediated by *Chlamydia*-induced endogenous IFN- $\beta$  production (Rödel *et al.*, 2002).

Furthermore, the trafficking of MHCI from the ER to the Golgi was similar to mock-infected cells during persistence and fibroblast infection as revealed by the presence of both Endo H sensitive and resistant forms. Thus, it seems that under host conditions where chlamydial growth is aberrant, such as in fibroblasts and IFN- $\gamma$  induced chlamydial persistence, MHCI antigen presentation is functional and not manipulated by chlamydial organisms. In part this could be explained by the strongly reduced CPAF expression and degradation of TAP2, respectively, which have been observed in persistently infected HeLa cells and in infected fibroblasts. Thus, during persistent chlamydial growth host cell

pathways such as MHCI antigen presentation may be functional due to a reduced CPAF activity. These results are consistent with a previous study that showed efficient CD8+ T cell mediated lysis of *C. trachomatis*-infected cells in which persistence was induced by IFN- $\gamma$  and penicillin, respectively (Rasmussen *et al.*, 1996).

Apart from the differences in MHCI surface expression between actively and persistently *Chlamydia*-infected HeLa cells, there was a general MHCI downregulation that appeared also on inclusion-negative HeLa cells in both actively and persistently infected cell cultures. This is consistent with a previous study (Ibana *et al.*, 2011) and probably the result of a soluble factor secreted by infected HeLa cells that influences the MHCI surface expression on uninfected neighbour cells. In contrast, this phenomenon could not be observed in the infected fibroblast culture, because fibroblasts increased their MHCI surface expression upon infection due to secretion of IFN- $\beta$ . Thus, MHCI surface expression could be influenced by different cytokines making it difficult to evaluate the real situation and the role of MHCI presentation in vivo.

#### **4.2.4 Correlation of CPAF expression with chlamydial interference with MHCI antigen presentation**

In the present study, a slight MHCI downregulation on the surface of actively infected HeLa cells was observed. As the results indicate that CPAF is responsible for degradation of TAP2, interference with MHCI expression might thus depend on the expression of CPAF. Therefore, MHCI expression and killing of infected cells by CD8+ T cells might be functional during chlamydial persistence, as described in the previous chapter. However, it might also be functional during the early chlamydial growth stage during active infection, since CPAF expression starts at later stages and degradation of substrates is not detected before 13 hours p.i. (Dong *et al.*, 2004). This is consistent with the observation that efficient activation of CD8+ T cells in response to the chlamydial class I accessible protein-1 (Cap1), which is known to be recognised by *Chlamydia*-specific CD8+ T cells (Fling *et al.*, 2001), occurred between 8 and 24 h p.i. (Balsara *et al.*, 2006 b) correlating with the time of *cap1* expression. Other studies examining CD8+ T cell responses to *Chlamydia*-infected cells in vitro showed efficient CD8+ T cell mediated cytotoxic killing of cells that were actively or persistently infected for 24 h (Beatty & Stephens, 1994; Rasmussen *et al.*, 1996). Another study revealed a surface MHCI staining on *C. trachomatis* infected cells at 18 h p.i. that was similar to that of mock-infected cells, and that same study found comparable Endo H digestion results for infected and uninfected cells at 24 h p.i. (Scidmore *et*

*al.*, 1996). However, all of these studies did not analyse CD8+ T cell cytotoxicity or MHCI expression in actively infected cells at later time points of *C. trachomatis* infection. As it is assumed that interference with MHCI antigen presentation correlates with CPAF activity, it would be expected that an inhibition of MHCI antigen presentation does not occur before 24 h p.i., which would explain the functional MHCI expression and CD8+ T cell lysis of actively infected cells at 24 h p.i. However, the findings of the present study clearly suggest that MHCI antigen presentation is compromised during active infection, but still functional during IFN- $\gamma$  induced persistence at later time points (40 h p.i.).

The hypothesis that interference with MHCI starts late during the developmental cycle is further supported by the finding that MHCI surface expression was only slightly reduced in actively infected HeLa cells. If blocking of MHCI trafficking would already occur at earlier stages of infection, a more drastic surface MHCI downregulation would be expected at 40 h p.i. This suggests that residual MHCI from early stages of infection, where normal MHCI trafficking is expected to occur, can still be detected at the cell surface. Cells that have severely reduced MHCI surface expression are usually recognised and eliminated by natural killer (NK) cells. Indeed, an induction of a NK cell response accompanied by IFN- $\gamma$  production was detected in response to *Chlamydia*-infected epithelial cells and started between 18 and 24 h p.i. (Hook *et al.*, 2004), and this response depended on chlamydial but not on host protein synthesis. This further supports the hypothesis that interference with the MHCI antigen presentation pathway starts during later stages of chlamydial growth, when sufficient CPAF activity is available in the host cytosol.

#### **4.2.5 Degradation of TAP2 through *C. trachomatis***

The degradation of TAP2 through a chlamydial protease, probably CPAF, is particularly interesting, since this is the first description of an attack of the TAP transporter through an intracellular pathogen residing in a host vacuole. TAP is an essential component of the MHCI antigen presentation pathway, because cell lines deficient for one or both subunits of the peptide transporter have a reduced level of surface MHCI expression and unstable MHCI molecules that are mostly retained in the ER (Cerundolo *et al.*, 1990; Kelly *et al.*, 1992; Powis *et al.*, 1991; Spies & DeMars, 1991; Townsend *et al.*, 1989; van Kaer *et al.*, 1992). Hence, interference with the function of TAP is a good strategy to block MHCI traffic to the cell surface and thus is applied by several viruses. For example, the ICP47 protein of HSV-1 is an efficient substrate inhibitor of TAP by binding to the peptide binding domain with high affinity (Ahn *et al.*, 1996; Früh *et al.*, 1995; Hill *et al.*, 1995;

Tomazin *et al.* 1996). Likewise, Epstein-Barr virus (EBV) and human CMV are able to prevent ATP binding to TAP (Hewitt *et al.*, 2001; Hislop *et al.*, 2007; Kyritsis *et al.*, 2001). Degradation of the TAP transporter has also been described in virus-infected cells, for example upon murine  $\gamma$ -herpesvirus-68 infection (Boname *et al.*, 2004; Boname *et al.*, 2005), however, this occurs through directing the TAP proteins to the host proteasome.

It would be interesting to know at which sites of the TAP2 protein cleavage occurs in *Chlamydia*-infected cells. TAP is a typical ABC transporter made of the two subunits TAP1 and TAP2 that each contains a large transmembrane domain for anchoring in the ER membrane and an NBD at the C-terminus that is located in the cytosol (reviewed in Lankat-Buttgereit & Tampé, 2002). Because of the inaccessibility of the membrane-located transmembrane domain it is unlikely that CPAF cleaves in this region. However, parts of the protein that are exposed to the cytosol, such as the NBD, would be potential cleavage sites, as CPAF activity normally is detected in the host cytosol (Zhong *et al.*, 2001). Although TAP1 and TAP2 possess similar NBDs, some parts, especially the core NBDs and the C-terminal tails, have reduced homology (Bouabe & Knittler, 2003), making it possible that CPAF cleaves in such regions which would explain the specific cleavage only of TAP2, but not of TAP1. Interestingly, the monoclonal antibodies that were used in the present work both recognise the C-terminal region of TAP1 and TAP2, respectively (van Endert *et al.*, 1994). If the C-terminal region of TAP2, which the antibody binds to, would be cleaved off by CPAF, it would be likely to interfere with detection of TAP2 by either destroying the antibody epitope or by generating fragments that are too small to be detected by immunoblotting. Indeed, no cleavage fragment in the cell-free cleavage assay could be observed, which thus makes it likely that CPAF attacks the NBD of TAP2.

Cleavage of the NBD of TAP2 would be expected to be sufficient to inactivate the function of the peptide transporter, since ATP binding is absolutely necessary for peptide transport (Androlewicz *et al.*, 1993) and both NBDs of the TAP transporter are necessary for the transporter function (Alberts *et al.*, 2001; Daumke & Knittler, 2001). It has been shown that the C-terminal tail of the NBD of TAP2 is essential for ATP binding and the peptide transport function (Bouabe & Knittler, 2003; Ehses *et al.*, 2005). Thus, removal of the C-terminal tail from TAP2 would be sufficient to inhibit ATP-binding to TAP2 and peptide transport into the ER in *Chlamydia*-infected cells.

Through Endo H digestion of total MHCI in actively infected HeLa cells only Golgi-resident Endo H-resistant, but no ER-resident Endo H-sensitive forms, could be detected. This is surprising, because in TAP-deficient cells most of the MHCI remained Endo H-

sensitive due to their retention in the ER as empty (peptide-receptive) molecules (Garstka *et al.*, 2007; Grandea *et al.*, 2000). The lack of ER-resident MHCI in actively infected HeLa cells could be explained by either downregulated synthesis of new MHCI heavy chains and/or rapid degradation of the ER-resident MHCI molecules. Indeed, a slight decrease in the protein amount was found in these cells, although this was less visible in the normal immunoblot and more obvious in the Endo H experiment. This decrease in MHCI heavy chain protein cannot be explained by decreased transcription, as there was no significant downregulation of *HLA-ABC* gene expression. Furthermore, during active infection with IFN- $\gamma$  treatment no protein downregulation could be found and a few Endo H-sensitive bands occurred, which could either be due to an inhibitory effect on *Chlamydia*, thus reducing interference with MHCI antigen presentation, or, which is more

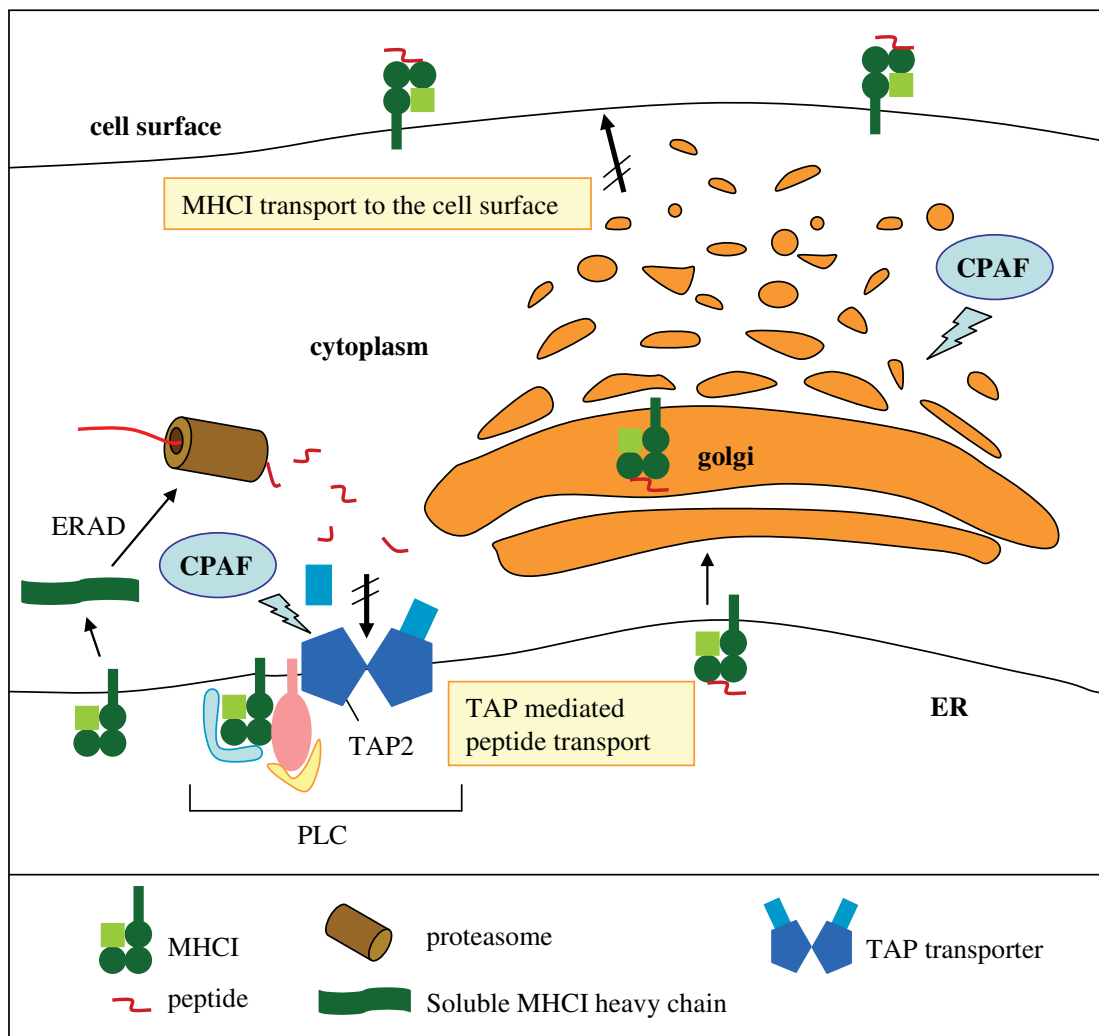


**Fig. 30: Hypothetical model of *C. trachomatis* interference with the MHC class I antigen presentation pathway.**

The possible influence of TAP2 degradation on the TAP-mediated peptide transport and MHCI stability and the potential effect of Golgi protein degradation on MHCI surface trafficking are outlined.

likely, due to a strongly increased synthesis of TAP2 and other components which would allow peptide-loading of a few MHCI molecules as a result of incomplete chlamydial degradation of TAP2.

Furthermore, IFN- $\gamma$  is known to stabilise MHCI molecules by improving peptide loading quality control (Fromm & Ehrlich, 2001). Thus, degradation of empty MHCI would be the most plausible explanation for the observed effect during active infection. Indeed, increased ER-associated proteasomal degradation (ERAD) of misfolded or unstable MHCI heavy chains was observed in cells that lack normal assembly of MHCI molecules such as in  $\beta_2M$  or TAP deficient cells (Hughes *et al.*, 1997). Moreover, the enzymes involved in ERAD of MHCI heavy chains have been identified recently (Burr *et al.*, 2011). Thus, it is hypothesised that newly synthesized MHCI chains are rapidly degraded in *Chlamydia*-infected cells due to a defect in TAP-mediated peptide delivery from the cytosol as a consequence of TAP2 degradation. A hypothetical model visualising the mechanisms that *C. trachomatis* may apply to interfere with the MHCI antigen presentation pathway is displayed in Fig. 30.

#### **4.2.6 Role of Golgi fragmentation and Golgi protein degradation in inhibition of intracellular MHCI trafficking in actively *Chlamydia*-infected cells**

It has been reported that in cells infected with African Swine Fever Virus the Golgi got fragmented, which resulted in reduced MHCI surface expression (Netherton *et al.*, 2006). Because it is known that *Chlamydia* are also able to induce fragmentation of the Golgi apparatus through CPAF-mediated degradation of Golgin-84 (Christian *et al.*, 2011; Heuer *et al.*, 2009), it was assumed that this could also have a negative impact on processing and transport of MHCI molecules through the Golgi to the cell surface and thus might contribute to the reduced MHCI surface expression during active chlamydial infection.

Similar to the study of Heuer *et al.* (2009) a complete fragmentation of the Golgi during active *C. trachomatis* infection of HeLa cells was also found in the present study by immunofluorescence staining of GM130 and Golgin-245. Additionally, it was shown that the *cis*-Golgi protein GM130 and the *trans*-Golgi protein Golgin-245 got degraded through CPAF during active infection of HeLa cells. Thus, beside Golgin-84 two other golgins are substrates of CPAF cleavage. This suggests that all golgins may be cleaved by CPAF which would assure that not only the *cis*-Golgi, but all sub-compartments of the Golgi could undergo fragmentation during chlamydial infection, provided that degradation of the golgins is leading to Golgi fragmentation in a similar way like cleavage of Golgin-84. This

hypothesis is supported by the finding that depletion of Golgin-245 and other *trans*-Golgi network (TGN) golgins resulted in fragmentation of the TGN (Derby *et al.*, 2007; Yoshino *et al.*, 2003).

Although there was a complete Golgi fragmentation during active chlamydial infection, the immunofluorescence staining of GM130 and MHCI revealed no reduced localisation of MHCI to the Golgi in inclusion-containing cells compared to non-infected cells. Furthermore, examination of the Endo H cleavage pattern of MHCI during active chlamydial infection of HeLa cells showed that MHCI that is resistant to Endo H cleavage and thus localised to post-ER compartments is still present in these cells, although to a reduced amount. These results indicate that MHCI is not excluded from the Golgi compartment despite Golgi fragmentation. Since no Endo H sensitive MHCI was found upon active chlamydial infection, which indicates that MHCI is not present in the ER, it would be expected that no MHCI could be delivered from the ER to the Golgi. Thus, the Golgi-resident MHCI in these cells could represent MHCI that has reached the Golgi during earlier stages of infection at which chlamydial interference with the MHCI antigen presentation pathway had not yet occurred. This is supported by the finding of a reduced amount of Endo H resistant MHCI in actively infected cells when compared to uninfected cells, indicating a decrease in the Golgi-resident MHCI amount due to the lack of delivery of MHCI from the ER. Cells infected with certain viruses were shown to accumulate MHCI in the Golgi due to interruption of transport of MHCI from the Golgi to the cell surface or endocytosis of surface MHCI (Abendroth *et al.*, 2001; Greenberg *et al.*, 1998). However, an increased amount of MHCI in the Golgi of actively *Chlamydia*-infected HeLa cells could not be observed indicating that there is no accumulation of MHCI in this compartment. This further supports the hypothesis that no MHCI is delivered from the ER to the Golgi at later stages of infection. As explained in the previous chapter this lack of ER-resident MHCI could be due to interruption of the MHCI antigen presentation pathway already at the stage of ER, likely through degradation of newly synthesised MHCI as a consequence of *Chlamydia*-mediated TAP2 cleavage.

Due to this lack of delivery of MHCI to the Golgi it is difficult to evaluate the impact of *Chlamydia*-induced Golgi fragmentation on the MHCI trafficking. However, Golgi fragmentation may serve as a second, additional mechanism to inhibit MHCI trafficking to the cell surface (Fig. 30). The finding of Golgin-245 degradation in actively *Chlamydia*-infected HeLa cells is particularly interesting, because the TGN-resident Golgin-245 seems to be necessary for the vesicle transport to the plasma membrane (Yoshino *et al.*, 2003).

Moreover, a role for Golgin-245 in regulating the MHCI transport from the Golgi to the plasma membrane has been suggested (Brémond *et al.*, 2009).

Additionally, fragmentation of the *trans*-Golgi could have a negative effect on recycling of MHCI molecules from the cell surface. Indeed, it has been found that MHCI recycling from the plasma membrane requires the Rab GTPases Rab22a and Rab11 (Weigert *et al.*, 2004), and it is known that Rab11 is recruited to the chlamydial inclusion (Rzomp *et al.*, 2003). Thus, *Chlamydia* could also interfere with MHCI recycling from the cell surface by recruitment of Rab11 which would not be available anymore for the MHCI recycling.

Alternative ways of peptide-loading could also be inhibited in *Chlamydia*-infected cells as a result of *trans*-Golgi fragmentation. For example, proprotein convertase 7 (PC7), that resides in the TGN and usually is involved in post-translational modification, is able to generate peptides that can be loaded on unstable MHCI molecules and by this partially rescues the surface expression in cells with defective PLC quality control (Leonhardt *et al.*, 2010). In *Chlamydia*-infected cells the function of PC7 as a second quality control could be compromised due to the fragmentation of the TGN as a result of degradation of Golgi proteins such as Golgin-245. This is supported by the observation that depletion of Golgin-245 from the TGN resulted in dispersal of the TGN, with concomitant reduction of protein cleavage by the proprotein convertase furin (Yoshino *et al.*, 2003).

#### **4.2.7 Golgi fragmentation and Golgi protein degradation during chlamydial persistence and fibroblast infection**

In contrast to the results of actively infected HeLa cells, during IFN- $\gamma$  induced persistence and in infected fibroblasts the Golgi was only partially fragmented in the majority of inclusion-containing cells. The only exception was the *trans*-Golgi compartment which was completely fragmented in the majority of persistently infected HeLa cells, similar to active infection. Although Golgi fragmentation occurred during these persistent conditions, MHCI trafficking was not compromised as there was no reduced MHCI surface expression after infection, MHCI still localised to the Golgi of inclusion-containing cells, and the Endo H cleavage pattern of MHCI was not different between mock-infected and infected cells. Thus, the results suggest that partial Golgi fragmentation does not seem to have any effect on the traffic of MHCI in these cells. In fact, the functional MHCI trafficking could be explained by the absence of degradation of Golgin-245 in persistently infected HeLa cells and infected fibroblasts, because Golgin-245 is necessary for the *trans*-Golgi transport function (Yoshino *et al.*, 2003) and involved in MHCI transport to the cell surface

(Brémond *et al.*, 2009). In contrast to this, GM130, which is not essential for ER to Golgi transport, but instead is important for correct glycosylation of proteins in the *cis*-Golgi (Nakamura, 2010), still was degraded during persistent and fibroblasts infection, although to a lesser extent than during active infection leading to only 50% reduction in the protein level. Thus, it could be possible that MHCI trafficking is functional, while MHCI processing may be incomplete in persistently infected cells. This is supported by the finding that Golgi fragmentation by *Chlamydia* does not interfere with the delivery of glycoproteins to the cell surface, but does affect the processing of glycoproteins in the Golgi as indicated by an increased amount of premature glycoproteins containing an N-acetyl-D-glucosamine chain on the cell surface (Heuer *et al.*, 2009).

Interestingly, the expression of Golgin-245 was upregulated after chlamydial infection of fibroblasts. It could be possible that this upregulation is a result of the increased transport enquiry for MHCI to ensure rapid elevation of MHCI surface expression. Indeed, Golgin-245 vesicles were shown to increase transport of TNF- $\alpha$  to the cell surface in macrophages after stimulation with LPS (Lieu *et al.*, 2008). Thus, a logical consequence would be to coordinate the increased synthesis of surface located proteins with an upregulation of the respective Golgi proteins involved in their transport to the cell surface.

#### **4.2.8 Other mechanisms of *C. trachomatis* to escape immune recognition by T cells**

It has been described recently that *C. trachomatis* infected macrophages induce apoptosis of T cells, and this was in part mediated by TNF- $\alpha$  secretion (Jendro *et al.*, 2000; Jendro *et al.*, 2004). T cell apoptosis represents another mechanism of how *Chlamydia*-infected cells could escape killing by CD8<sup>+</sup> T cells. This could lead to decreased numbers of CD8<sup>+</sup> T cells which may reduce the rate of lysis of infected non-haematopoietic cells. On the other hand, TNF- $\alpha$  was shown to strongly enhance MHCI surface expression on *Chlamydia*-infected fibroblasts (Rödel *et al.*, 2002), which could increase the probability to be detected by CD8<sup>+</sup> T cells.

CD8<sup>+</sup> T cells are known to induce killing of infected cells through induction of apoptosis. However, chlamydiae inhibit apoptosis through different mechanisms (reviewed in Sharma & Rudel, 2009), and CPAF is known to be involved in this inhibition through degradation of the pro-apoptotic BH3-only proteins (Pirbhai *et al.*, 2006). It has been shown that granzyme B, Fas and TNF- $\alpha$  mediated apoptosis, which are applied by CD8<sup>+</sup>T cells in order to kill target cells, are inhibited in *Chlamydia*-infected cells (Fan *et al.*, 1998).

Hence, chlamydial inhibition of apoptosis may represent a very important and potent mechanism for preventing CD8+ T cell mediated killing of the infected host cell.

*C. trachomatis* has not only developed mechanisms to escape the recognition by CD8+ T cells. The pathogen was shown also to degrade upstream stimulatory factor 1 (USF-1), a transcription factor necessary for MHCII gene expression, through CPAF (Zhong *et al.*, 1999; Zhong *et al.*, 2001). This is expected to suppress MHCII surface expression, which would result in less recognition of *Chlamydia*-infected cells by CD4+ cells. Indeed, Zhong *et al.* (1999) observed a specific inhibition of IFN- $\gamma$ -inducible MHCII surface expression in *Chlamydia*-infected epithelial cells.

Beside the MHCI and MHCII antigen presentation pathways, there is a third pathway of antigen presentation, which is specific for the presentation of self or foreign lipids to immune cells and involves the glycoprotein class CD1 as antigen presenting molecules. Similar to MHCI molecules, CD1 molecules consist of a membrane-binding anchor and an antigen binding domain and are associated with  $\beta_2M$ . They bind amphiphilic lipids, such as glycolipids, and expose the hydrophilic moiety of the lipids at the cell surface for recognition by T cell receptors. There are two groups of CD1 molecules: group 1 CD1 (CD1a, CD1b, CD1c) molecules which present lipids to CD1 specific T cells and group 2 CD1 molecules (CD1d) which present lipids to natural killer T (NKT) cells (reviewed in Schiefner & Wilson, 2009). Interestingly, in *Chlamydia*-infected epithelial cells CD1d was found to be a target of CPAF resulting in reduced CD1d surface expression (Kawana *et al.*, 2007). Thus, CPAF seems to interfere with different antigen presentation pathways underlining its importance as a virulence factor. It has been shown recently that invariant NKT cells may play an important role in protective immunity to CiReA by enhancing the CD4+ and CD8+ T cell response (Bharhani *et al.*, 2009). This was demonstrated with CD1d knockout mice that had a more severe disease than wild type mice, as well as by a lessened severity of the disease through the activation of a NKT cell response. Because CPAF expression and associated degradation of different host proteins was found to be strongly reduced during infection of fibroblasts, it would be interesting to know if CPAF-mediated cleavage of CD1d is also inhibited in fibroblasts, because this would result in a functional CD1d surface expression similar to the functional MHCI surface expression. This could further underline the importance of infected fibroblasts as antigen-presenting cells during CiReA.

#### **4.2.9 Chlamydial proteins that may elicit a CD8+ T cell response and their different expression during active and persistent infection**

Since *Chlamydia* are separated and protected from the host cytosol through residing in a modified host cell derived vacuole, the question arises how the host proteasome machinery gets access to chlamydial proteins. Certain chlamydial antigens, such as LPS, MOMP, Cap1 and IncA were detected outside the chlamydial inclusion (Brown *et al.*, 2002; Giles *et al.*, 2006) and thus could serve as potential antigens for MHCI presentation.

An efficient CD8+ T cell response has already been shown to be elicited by MOMP and Cap1 derived peptides, respectively (Fling *et al.*, 2001; Kim *et al.*, 2000). Furthermore, OmcB was shown to be a candidate for MHCI presentation (Gervassi *et al.*, 2004 b). Since expression of MOMP and the OmcB encoding gene was downregulated during IFN- $\gamma$  induced chlamydial persistence, but not in *Chlamydia*-infected fibroblasts, one might speculate that a protective CD8+ T cell response regarding these proteins could occur to fibroblasts, but not to persistently infected epithelial cells. In general, since expression of many chlamydial genes is reduced during IFN- $\gamma$  induced persistence several proteins might not gain access to the host cytosol under these conditions. It would be interesting to know if there are any chlamydial proteins that are processed for MHCI presentation during IFN- $\gamma$  induced persistence, and which that may be.

Interestingly, the chlamydial HSP60 proteins GroEL\_2 and GroEL\_3, but not GroEL\_1 were detected in vesicles everting from the inclusion (Giles *et al.*, 2006). Because an increased gene expression of GroEL\_2 was found during the infection of fibroblasts in the present study, and GroEL\_2 expression was also upregulated during infection of monocytes (Gérard *et al.*, 2004), it will be a future task to examine whether this protein is also processed to peptides that get presented on the cell surface via MHCI and whether by this it may play a special role in promoting severe immunopathology during chronic chlamydial infection, such as during CiReA.

#### **4.2.10 Role of CPAF mediated golgin degradation in *Chlamydia*-host cell interaction**

It has been reported recently that Golgin-84 is degraded through CPAF (Christian *et al.*, 2011). In the present study it was discovered that another two golgins, GM130 and Golgin-245, are also cleaved through CPAF. Golgins are Golgi proteins with large coiled-coil domains reaching into the cytoplasm (reviewed in Goud & Gleeson, 2010), and because of this cytoplasmic exposure CPAF probably gets access easily to these proteins. Indeed,

Heuer *et al.* (2009) observed that the cleavage occurred in the N-terminal coiled-coil domain, thus this domain could be a general target for CPAF cleavage.

In contrast to the results of the present study, Heuer *et al.* (2009) suggested that GM130 is not degraded by *Chlamydia*, because the immunoblot ratio of GM130 to tubulin was not changed during infection. However, the expression of both GM130 and tubulin decreased during the infection time course, and it cannot be excluded that tubulin expression was also affected by chlamydial infection. This could explain the different interpretation of the GM130 expression results by Heuer *et al.* (2009) in contrast to the findings of the present work where GAPDH was used as loading control.

Golgi fragmentation is necessary for chlamydial growth as has been shown by a strongly reduced progeny formation when fragmentation was inhibited (Heuer *et al.*, 2009). Since *Chlamydia* acquires sphingomyelin and cholesterol from the Golgi (Carabeo *et al.*, 2003; Hackstadt *et al.*, 1996), fragmentation of Golgi might facilitate this process. CPAF mediated cleavage of Golgin-84 was shown to be responsible for the fragmentation of the Golgi apparatus (Christian *et al.*, 2011; Heuer *et al.*, 2009). Since knockdown of GM130 did not result in *cis*-Golgi fragmentation (Heuer *et al.*, 2009), it is proposed that the degradation of golgins may also have other functions. *Chlamydia* are known to recruit Rab proteins to the inclusion in order to interact with vesicle trafficking (Rzomp *et al.*, 2003). This probably serves as a mechanism to acquire vesicles containing proteins and lipids from the host cell. Golgins are well known to bind Rab proteins and probably serve as docking sites for vesicle trafficking (reviewed in Goud & Gleeson, 2010). Hence, chlamydial degradation of golgins may prevent binding of Rab proteins to the Golgi, thus facilitating their recruitment to the inclusion membrane. One Rab protein that is found to be localised at the inclusion is Rab1 (Rzomp *et al.*, 2003), and Rab1 is known to bind to GM130 and to Golgin-84 (reviewed in Ramirez & Lowe, 2009). Moreover, Rab1 is the only Rab protein required for the anterograde cargo transport from the ER through the Golgi (reviewed in Barr, 2009). Thus, degradation of GM130 and Golgin-84 could prevent binding of Rab1 to the Golgi, which may direct Rab1 vesicles everting from the ER to Rab binding inclusion membrane proteins. This is supported by the recent discovery of a *C. pneumoniae* inclusion membrane protein, which shares sequence similarity with Rab effector proteins such as Golgin-84 and GM130, and which was also shown to interact with Rab1, Rab10 and Rab11 (Cortes *et al.*, 2007).

The Golgi apparatus and the centrosome, the main MTOC of the cell, are in close proximity to each other, because the centrosome regulates the morphology of the Golgi through

generation of microtubules reaching through the cell. This association might be important for the directional protein transport in polarised cells and for the migration of cells (reviewed in Sütterlin & Colanzi, 2010). Rapidly after the invasion of host cells *Chlamydia* travel to the peri-Golgi region on microtubules in a dynein-dependent manner (Clausen *et al.*, 1997; Grieshaber *et al.*, 2003). By this, *Chlamydia* might be able also to interact with the centrosome. Indeed, *C. trachomatis* was shown to influence centrosome assembly leading to supernumerary centrosomes, to a defect in mitotic spindle formation and to abnormal chromosome segregation, which suggests a possible role in cancer development (Grieshaber *et al.*, 2006). Although the morphology of the centrosomes in *Chlamydia*-infected cells appeared normal, they contained premature centrioles, and an abnormal centrosome number was detected from 30 h p.i. on (Johnson *et al.*, 2009). This interaction of *Chlamydia* with the centrosome was not necessary for chlamydial growth, and the generation of such supernumerary centrosomes depended on the host cell centrosome duplication machinery (Johnson *et al.*, 2009). It has been reported that GM130 is involved in regulating the centrosome function and assembly during interphase, because the depletion of GM130 resulted in aberrant supernumerary centrosomes, a defect in microtubule nucleation and inhibition of cell division, which led to cell death through arrest in mitosis (Kodani & Sütterlin, 2008). Thus, GM130 degradation through CPAF could be an important process involved in the abnormal centrosome amplification in *Chlamydia*-infected cells. Furthermore, GM130 has been shown to be required for microtubule nucleation at the Golgi apparatus (Rivero *et al.*, 2009), an event that is necessary for maintaining Golgi morphology, cell polarisation and migration (Efimov *et al.*, 2007; Miller *et al.*, 2009). Hence, *Chlamydia*-mediated GM130 degradation could be an important event for abrogating polarised protein secretion and cell migration in order to reduce cytokine secretion and expression of surface-exposed molecules on polarised cells which could affect immune recognition. Recently, other gram-negative pathogens, such as enteropathogenic *E. coli* (EPEC), enterohaemorrhagic *E. coli* (EHEC) and *Shigella flexneri* have also been found to induce Golgi fragmentation and reduce protein secretion, probably by secretion of the TTSS protein EspG into the host cytosol, which interacted with GM130 and induced destabilisation of microtubules (Clements *et al.*, 2011; Tomson *et al.*, 2005). Therefore, interfering with the GM130 function might generally be an efficient strategy of some bacterial pathogens to manipulate multiple host cell functions for which this Golgi protein is necessary.

### **4.3 *C. trachomatis* mediated degradation of the host cell mRNA export factor NXF1**

An intriguing, accidental discovery of the present study has been the *Chlamydia*-induced cleavage of NXF1, which probably also involves CPAF. NXF1 belongs to the NXF protein family that is conserved among eukaryotic organisms (reviewed in Stutz & Izaurralde, 2003). It forms a heterodimer together with the small protein p15, and this heterodimer functions as a transport receptor for the export of most of the poly(A)<sup>+</sup> RNA from the nucleus to the cytoplasm (Wiegand *et al.*, 2002). Transcription, processing and nuclear export of mRNA are tightly associated and controlled in the nucleus through many different proteins. After its transcription the nascent mRNA is associated with many proteins of distinct functions resulting in the formation of a so-called messenger ribonucleoprotein (mRNP) complex. This mRNP complex is exported into the cytoplasm mainly through the mRNA export receptor NXF1/p15, which binds to it through recognition of other bound proteins and recruits the mRNP to the nuclear pore complex (NPC). The NXF1/p15 associates with certain proteins of the NPC, the nucleoporins, which results in translocation of the mRNP through the nuclear pore into the cytoplasm through an ATP-dependent mechanism involving several other proteins located at the cytoplasmic face of the NPC. After the translocation through the nuclear pore, NXF1/p15 is released from the mRNP and transported back into the nucleus (reviewed in Carmody & Wenthe, 2009).

In *Drosophila melanogaster* cells depletion of NXF1 led to strong accumulation of poly(A)<sup>+</sup> RNA in the nucleus with concomitant inhibition of protein synthesis (Herold *et al.*, 2001; Wiegand *et al.*, 2002). FISH of poly(A)<sup>+</sup> RNA in mammalian cells normally reveals equal distribution of mRNA in the cytoplasm and speckled nuclear mRNA signals. However, when mRNA export is impaired the nuclear speckles show increased staining intensity (Tokunaga & Tani, 2008). Using the same approach of FISH an enhanced fluorescence intensity of poly(A)<sup>+</sup> RNA in the nuclei of *Chlamydia*-infected HeLa cells has also been observed in the present study, which suggests a nuclear accumulation of poly(A)<sup>+</sup> RNA as a result of the degradation of NXF1. Interestingly, a stronger fluorescence signal in the cytoplasmic area near the nucleus of infected cells was also detected, which could represent cellular mRNA located at the ER for translation. An increased cytoplasmic poly(A)<sup>+</sup> RNA amount would point to an upregulated mRNA synthesis in the nucleus. However, if the nuclear export of bulk mRNA is blocked as a result of NXF1 degradation, then the question would be how this mRNA enters the

cytoplasm. It remains to be elucidated if this increased cytoplasmic mRNA amount is a result of transport through a redundant mRNA export pathway or if it is remaining mRNA from an earlier infection stage, at which NXF1 was not yet degraded and host cell transcription was still enhanced. This is supported by the fact that mammalian mRNA is very stable (Tokunaga & Tani, 2008).

Several viruses are known that use nuclear export pathways to export their RNA from the nucleus to the cytosol, which is necessary for their propagation (reviewed in Fontoura *et al.*, 2005). This is mediated by certain viral proteins that interact with components of the export pathway. On the other hand, this manipulation can also influence the export of cellular mRNAs, thus leading to an inhibition of the antiviral response (reviewed in Fontoura *et al.*, 2005). Examples for viruses that use the NXF1 export pathway are type D retroviruses (Grüter *et al.*, 1998), HSV-1 (Koffa *et al.*, 2001), EBV (Juillard *et al.*, 2009) and adenovirus (Yatherajam *et al.*, 2011). So far, this is the first description of an intracellular bacterial pathogen to interact with this pathway. The interesting question arising is that of why *C. trachomatis* does interfere with the NXF1 mRNA export pathway. The most likely explanation could be a general inhibition of cellular defence pathways through inhibition of protein synthesis as a consequence of compromised mRNA delivery to the cytosol. Since the NXF1 degradation was observed at a late stage of infection, normal host cell protein synthesis should not be compromised at early time points. At late time points *Chlamydia* would be expected to have a higher need for nutrients from the host cell, because of the increasing number of bacterial organisms. Thus, as suggested by Zhong (2009), degradation of several host proteins, including NXF1, through CPAF could deliver additional essential amino acids to the inclusion. This is a hypothesis that would generally explain the broad substrate specificity of CPAF. Inhibition of poly(A)+ RNA export would additionally have the advantage of availability of higher amounts of ATP for *Chlamydia* due to the inhibition of the host protein translation machinery, which usually requires huge amounts of energy. Thus, *Chlamydia* could benefit from interference with the cellular mRNA export from the nucleus in several ways.

#### **4.4 Summary and outlook**

In the present study the MHCI antigen presentation pathway has been studied during active and persistent chlamydial infection as well as during fibroblast infection, which also seems to represent another type of persistent infection characterised by a different chlamydial growth and gene expression profile than the IFN- $\gamma$  mediated chlamydial persistence. It

could be shown that *C. trachomatis* interferes with MHCI antigen presentation only during active, but not during persistent infection of HeLa cells and during fibroblast infection. The important antigen transporter component TAP2 was degraded by *C. trachomatis* only during active HeLa cell infection, which may be responsible for the reduced MHCI expression observed on the surface of these cells. Also, the Golgi fragmentation and CPAF-mediated cleavage of the two Golgi proteins GM130 and Golgin-245 during active infection, which was strongly reduced during persistent and fibroblast infection, might contribute to inhibit trafficking of MHCI from the ER to the cell surface as a second step of chlamydial interference with the MHCI antigen presentation pathway.

The present study further underlines the importance of the chlamydial protease CPAF as a multi-functional virulence factor that is involved in the degradation of different host proteins leading to disruption of several host cell pathways. It has been found that CPAF is involved in the cleavage of the Golgi proteins GM130 and Golgin-245, and is likely to play a role in the degradation of TAP2 and the mRNA export factor NXF1. The importance of CPAF for chlamydial development and pathogenesis is pronounced by the finding of a strong reduction of its expression and enzyme activity during chlamydial persistence, which reduces the ability of *Chlamydia* to interfere with host cell functions such as for example MHCI antigen presentation.

Future studies will reveal how host cell functions are affected by the CPAF-mediated degradation of the proteins analysed in the present study. The functionality of the peptide transporter TAP should be examined as well as the intracellular processing and trafficking of MHCI in the ER and Golgi. Likewise, the identification of peptides presented by MHCI on the host cell surface during chlamydial persistence and fibroblast infection could give more insight if the processing of chlamydial proteins efficiently occurs under these conditions. Cytotoxic effects of *Chlamydia*-specific CD8<sup>+</sup> T cells on actively and persistently infected epithelial cells should be measured at later time points of infection (after 24 h p.i.) in order to see whether CD8<sup>+</sup> T cell activation in response to *Chlamydia*-infected cells is reduced at late infection stages as a result of diminished expression of surface MHCI.

Furthermore, as the present results of GM130 degradation point to an interference of *Chlamydia* with the centrosome function, the role of this event in centrosome multiplication, assembly and chromosome segregation should be investigated. An interesting new field of *Chlamydia*-host cell interaction has been opened by the discovery of degradation of NXF1. Interference of *Chlamydia* with the cellular mRNA export as well as with the host cell transcription and translation machinery should be examined in detail to find out

why *Chlamydia* interfere with this pathway and what the consequences are for the host cell function.

The ability of *Chlamydia* to grow well in fibroblasts, but with compromised conversion to EBs, represents another kind of chlamydial persistence which is distinct from the persistence models known so far. Further work needs to be done to identify other factors beside IDO that are involved in the induction of chlamydial persistence in fibroblasts. Analyses of the role of fibroblasts in chlamydial infection, especially during CiReA, as well as the role of specifically expressed chlamydial proteins will add to our knowledge about the importance of this host cell type for chlamydial pathogenesis and persistent infection in vivo.

The results of the present study will help to understand chlamydial persistence, *Chlamydia*-host cell interaction and MHCI antigen presentation during chlamydial infection. This is important to find new therapeutical targets and to develop an efficient vaccine strategy in order to combat chronic chlamydial infections.

## 5 References

- AbdelRahman, Y. M., Belland, R. J.** 2005. The chlamydial developmental cycle. *FEMS Microbiol. Rev.* 29 (5): 949-959.
- Abendroth, A., Lin, I., Slobedman, B., Ploegh, H., Arvin, A. M.** 2001. Varicella-Zoster virus retains major histocompatibility complex class I proteins in the Golgi compartment of infected cells. *J. Virol.* 75 (10): 4878-4888.
- Agrawal, T., Vats, V., Salhan, S., Mittal, A.** 2009. The mucosal immune response to *Chlamydia trachomatis* infection of the reproductive tract in women. *J. Reprod. Immunol.* 83 (1-2): 173-178.
- Ahn, K., Meyer, T. H., Uebel, S., Sempé, P., Djaballah, H., Yang, Y., Peterson, P. A., Früh, K., Tampé, R.** 1996. Molecular mechanism and species specificity of TAP inhibition by herpes simplex virus protein ICP47. *EMBO J.* 15 (13): 3247-3255.
- Alberts, P., Daumke, O., Deverson, E. V., Howard, J. C., Knittler, M. R.** 2001. Distinct functional properties of the TAP subunits coordinate the nucleotide-dependent transport cycle. *Curr. Biol.* 11 (4): 242-251.
- Allan, I., Pearce, J. H.** 1983. Amino acid requirements of strains of *Chlamydia trachomatis* and *C. psittaci* growing in McCoy cells: relationship with clinical syndrome and host origin. *J. Gen. Microbiol.* 129 (7): 2001-2007.
- Allan, I., Hatch, T. P., Pearce, J. H.** 1985. Influence of cysteine deprivation on chlamydial differentiation from reproductive to infective life-cycle forms. *J. Gen. Microbiol.* 131 (12): 3171-3177.
- Androlewicz, M. J., Anderson, K. S., Cresswell, P.** 1993. Evidence that transporters associated with antigen processing translocate a major histocompatibility complex class I-binding peptide into the endoplasmic reticulum in an ATP-dependent manner. *Proc. Natl. Acad. Sci. USA* 90 (19): 9130-9134.
- Antoniou, A. N., Powis, S. J.** 2008. Pathogen evasion strategies for the major histocompatibility complex class I assembly pathway. *Immunology* 124 (1): 1-12.
- Babcock, T. A., Carlin, J. M.** 2000. Transcriptional activation of indoleamine dioxygenase by interleukin 1 and tumor necrosis factor  $\alpha$  in interferon-treated epithelial cells. *Cytokine* 12 (6): 588-594.
- Balaná, M. E., Niedergang, F., Subtil, A., Alcover, A., Chavrier, P., Dautry-Varsat, A.** 2005. ARF6 GTPase controls bacterial invasion by actin remodelling. *J. Cell Sci.* 118: 2201-2210.
- Balsara, Z. R., Misaghi, S., Lafave, J. N., Starnbach, M. N.** 2006 a. *Chlamydia trachomatis* infection induces cleavage of the mitotic cyclin B1. *Infect. Immun.* 74 (10): 5602-5608.
- Balsara, Z. R., Roan, N. R., Steele, L. N., Starnbach, M. N.** 2006 b. Developmental regulation of *Chlamydia trachomatis* Class I Accessible Protein-1, a CD8+ T cell antigen. *J. Infect. Dis.* 193 (10): 1459-1463.
- Barr, F. A.** 2009. Rab GTPase function in Golgi trafficking. *Semin. Cell Dev. Biol.* 20 (7): 780-783.
- Baumert, J., Schmidt, K. H., Eitner, A., Straube, E., Rödel, J.** 2009. Host cell cytokines induced by *Chlamydia pneumoniae* decrease the expression of interstitial collagens and fibronectin in fibroblasts. *Infect. Immun.* 77 (2): 867-876.
- Beatty, W. L., Byrne, G. I., Morrison, R. P.** 1993. Morphologic and antigenic characterization of interferon  $\gamma$ -mediated persistent *Chlamydia trachomatis* infection in vitro. *Proc. Natl. Acad. Sci. USA* 90 (9): 3998-4002.
- Beatty, P. R., Stephens, R. S.** 1994. CD8+ T lymphocyte-mediated lysis of *Chlamydia*-infected L cells using an endogenous antigen pathway. *J. Immunol.* 153 (10): 4588-4595.
- Beatty, W. L., Belanger, T. A., Desai, A. A., Morrison, R. P., Byrne, G. I.** 1994 a. Tryptophan depletion as a mechanism of gamma interferon-mediated chlamydial persistence. *Infect. Immun.* 62 (9): 3705-3711.
- Beatty, W. L., Morrison, R. P., Byrne, G. I.** 1994 b. Immunoelectron-microscopic quantitation of differential levels of chlamydial proteins in a cell culture model of persistent *Chlamydia trachomatis* infection. *Infect. Immun.* 62 (9): 4059-4062.
- Beekman, D. S., Vanrompay, D. C.** 2009. Zoonotic *Chlamydia psittaci* infections from a clinical perspective. *Clin. Microbiol. Infect.* 15 (1): 11-17.

- Belland, R. J., Nelson, D. E., Virok, D., Crane, D. D., Hogan, D., Sturdevant, D., Beatty, W. L., Caldwell, H. D.** 2003. Transcriptome analysis of chlamydial growth during IFN- $\gamma$ -mediated persistence and reactivation. *Proc. Natl. Acad. Sci. USA* 100 (26): 15971-15976.
- Bergeron, M., Blanchette, J., Rouleau, P., Olivier, M.** 2008. Abnormal IFN- $\gamma$ -dependent immunoproteasome modulation by *Trypanosoma cruzi*-infected macrophages. *Parasite Immunol.* 30 (5): 280-292.
- Beutler, A. M., Hudson, A. P., Whittum-Hudson, J. A., Salameh, W. A., Gerard, H. C., Branigan, P. J., Schumacher, H. R. Jr.** 1997. *Chlamydia trachomatis* can persist in joint tissue after antibiotic treatment in chronic Reiter's syndrome/reactive arthritis. *J. Clin. Rheumatol.* 3 (3): 125-130.
- Bharhani, M. S., Chiu, B., Na, K. S., Inman, R. D.** 2009. Activation of invariant NKT cells confers protection against *Chlamydia trachomatis*-induced arthritis. *Int. Immunol.* 21 (7): 859-870.
- Bjerrum, O. J., Schafer-Nielsen, C.** 1986. Analytical Electrophoresis. Dunn, M. J. (editor). Page 315. Verlag Chemie, Weinheim.
- Blasi, F., Tarsia, P., Aliberti, S.** 2009. *Chlamydomytila pneumoniae*. *Clin. Microbiol. Infect.* 15 (1): 29-35.
- Boname, J. M., de Lima, B. D., Lehner, P. J., Stevenson, P. G.** 2004. Viral degradation of the MHC class I peptide loading complex. *Immunity* 20 (3): 305-317.
- Boname, J. M., May, J. S., Stevenson, P. G.** 2005. The murine gamma-herpesvirus-68 MK3 protein causes TAP degradation independent of MHC class I heavy chain degradation. *Eur. J. Immunol.* 35 (1): 171-179.
- Bouabe, H., Knittler, M. R.** 2003. The distinct nucleotide binding states of the transporter associated with antigen processing (TAP) are regulated by the nonhomologous C-terminal tails of TAP1 and TAP2. *Eur. J. Biochem.* 270 (22): 4531-4546.
- Bradford, M. M.** 1976. A rapid and sensitive method for the quantitation of microgram quantities of protein utilizing the principle of protein-dye binding. *Anal. Biochem.* 72: 248-252.
- Brémond, A., Meynet, O., Mahiddine, K., Coito, S., Tichet, M., Scotlandi, K., Breitmayer, J. P., Gounon, P., Gleeson, P. A., Bernard, A., Bernard, G.** 2009. Regulation of HLA class I surface expression requires CD99 and p230/golgin-245 interaction. *Blood* 113 (2): 347-357.
- Brown, W. J., Skeiky, Y. A., Probst, P., Rockey, D. D.** 2002. Chlamydial antigens colocalize within IncA-laden fibers extending from the inclusion membrane into the host cytosol. *Infect. Immun.* 70 (10): 5860-5864.
- Burr, M. L., Cano, F., Svobodova, S., Boyle, L. H., Boname, J. M., Lehner, P. J.** 2011. HRD1 and UBE2J1 target misfolded MHC class I heavy chains for endoplasmic reticulum-associated degradation. *Proc. Natl. Acad. Sci. USA* 108 (5): 2034-2039.
- Burton, M. J., Mabey, D. C.** 2009. The global burden of trachoma: a review. *PLoS Negl. Trop. Dis.* 3 (10): e460.
- Byrd, T. F., Horwitz, M. A.** 1993. Regulation of transferrin receptor expression and ferritin content in human mononuclear phagocytes. Coordinate upregulation by iron transferrin and downregulation by interferon gamma. *J. Clin. Invest.* 91 (3): 969-976.
- Byrne, G. I., Lehmann, L. K., Kirschbaum, J. G., Borden, E. C., Lee, C. M., Brown, R. R.** 1986. Induction of tryptophan degradation in vitro and in vivo: a  $\gamma$ -interferon-stimulated activity. *J. Interferon Res.* 6 (4): 389-396.
- Byrne, G. I., Ouellette, S. P., Wang, Z., Rao, J. P., Lu, L., Beatty, W. L., Hudson, A. P.** 2001. *Chlamydia pneumoniae* expresses genes required for DNA replication but not cytokinesis during persistent infection of HEp-2 cells. *Infect. Immun.* 69 (9): 5423-5429.
- Caldwell, H. D., Kromhout J., Schachter J.** 1981. Purification and partial characterization of the major outer membrane protein of *Chlamydia trachomatis*. *Infect. Immun.* 31 (3): 1161-1176.
- Caldwell, H. D., Wood, H., Crane, D., Bailey, R., Jones, R. B., Mabey, D., Maclean, I., Mohammed, Z., Peeling, R., Roshick, C. et al.** 2003. Polymorphisms in *Chlamydia trachomatis* tryptophan synthase genes differentiate between genital and ocular isolates. *J. Clin. Invest.* 111 (11): 1757-1769.
- Capmany, A., Damiani, M. T.** 2010. *Chlamydia trachomatis* intercepts Golgi-derived sphingolipids through a Rab14-mediated transport required for bacterial development and replication. *PLoS ONE* 5 (11): e14084.

- Carabeo, R. A., Grieshaber, S. S., Fischer, E., Hackstadt, T.** 2002. *Chlamydia trachomatis* induces remodelling of the actin cytoskeleton during attachment and entry into HeLa cells. *Infect. Immun.* 70 (7): 3793-3803.
- Carabeo, R. A., Mead, D. J., Hackstadt, T.** 2003. Golgi-dependent transport of cholesterol to the *Chlamydia trachomatis* inclusion. *Proc. Natl. Acad. Sci. USA* 100 (11): 6771-6776.
- Carabeo, R. A., Grieshaber, S. S., Hasenkrug, A., Dooley, C., Hackstadt, T.** 2004. Requirement for the Rac GTPase in *Chlamydia trachomatis* invasion of non-phagocytic cells. *Traffic* 5 (6): 418-425.
- Carey, A. J., Beagley, K. W.** 2010. *Chlamydia trachomatis*, a hidden epidemic: effects on female reproduction and options for treatment. *Am. J. Reprod. Immunol.* 63 (6): 576 – 586.
- Carmody, S. R., Wenthe, S. R.** 2009. mRNA nuclear export at a glance. *J. Cell Sci.* 122: 1933-1937.
- Carter, J. D., Hudson, A. P.** 2010. The evolving story of *Chlamydia*-induced reactive arthritis. *Curr. Opin. Rheumatol.* 22 (4): 424-430.
- Cerundolo, V., Alexander, J., Anderson, K., Lamb, C., Cresswell, P., McMichael, A., Gotch, F., Townsend, A.** 1990. Presentation of viral antigen controlled by a gene in the major histocompatibility complex. *Nature* 345 (6274): 449-452.
- Cevenini, R., Donati, M., La Placa, M.** 1988. Effects of penicillin on the synthesis of membrane proteins of *Chlamydia trachomatis* LGV2 serotype. *FEMS Microbiol. Letters* 56: 41-46.
- Chang, C. H., Hammer, J., Loh, J. E., Fodor, W. L., Flavell, R. A.** 1992. The activation of major histocompatibility complex class I genes by interferon regulatory factor-1 (IRF-1). *Immunogenetics* 35 (6): 378-384.
- Chakravorty, D., Hensel, M.** 2003. Inducible nitric oxide synthase and control of intracellular bacterial pathogens. *Microbes Infect.* 5 (7): 621-627.
- Chen, D., Chai, J., Hart, P. J., Zhong, G.** 2009. Identifying catalytic residues in CPAF, a *Chlamydia*-secreted protease. *Arch. Biochem. Biophys.* 485 (1): 16-23.
- Chen, D., Lei, L., Lu, C., Flores, R., DeLisa, M. P., Roberts, T. C., Romesberg, F. E., Zhong, G.** 2010 a. Secretion of the chlamydial virulence factor CPAF requires the Sec-dependent pathway. *Microbiology* 156: 3031-3040.
- Chen, D., Lei, L., Flores, R., Huang, Z., Wu, Z., Chai, J., Zhong, G.** 2010 b. Autoprocessing and self-activation of the secreted protease CPAF in *Chlamydia*-infected cells. *Microb. Pathog.* 49 (4): 164-173.
- Christian, J. G., Heymann, J., Paschen, S. A., Vier, J., Schauenburg, L., Rupp, J., Meyer, T. F., Häcker, G., Heuer, D.** 2011. Targeting of a chlamydial protease impedes intracellular bacterial growth. *PLoS Pathog* 7 (9): e1002283.
- Clausen, J. D., Christiansen, G., Holst, H. U., Birkelund, S.** 1997. *Chlamydia trachomatis* utilizes the host cell microtubule network during early events of infection. *Mol. Microbiol.* 25 (3): 441-449.
- Clements, A., Smollett, K., Lee, S. F., Hartland, E. L., Lowe, M., Frankel, G.** 2011. EspG of enteropathogenic and enterohemorrhagic *E. coli* binds the Golgi matrix protein GM130 and disrupts the Golgi structure and function. *Cell. Microbiol.* 13 (9): 1429-1439.
- Clifton, D. R., Fields, K. A., Grieshaber, S. S., Dooley, C. A., Fischer, E. R., Mead, D. J., Carabeo, R. A., Hackstadt, T.** 2004. A chlamydial type III translocated protein is tyrosine-phosphorylated at the site of entry and associated with recruitment of actin. *Proc. Natl. Acad. Sci. USA* 101 (27): 10166-10171.
- Cocchiaro, J. L., Kumar, Y., Fischer, E. R., Hackstadt, T., Valdivia, R. H.** 2008. Cytoplasmic lipid droplets are translocated into the lumen of the *Chlamydia trachomatis* parasitophorous vacuole. *Proc. Natl. Acad. Sci. USA* 105 (27): 9379-9384.
- Cortes, C., Rzomp, K. A., Tvinnereim, A., Scidmore, M. A., Wizel, B.** 2007. *Chlamydia pneumoniae* inclusion membrane protein Cpn0585 interacts with multiple Rab GTPases. *Infect. Immun.* 75 (12): 5586-5596.
- Daumke, O., Knittler, M. R.** 2001. Functional asymmetry of the ATP-binding-cassettes of the ABC transporter TAP is determined by intrinsic properties of the nucleotide binding domains. *Eur. J. Biochem.* 268 (17): 4776-4786.

- Deka, S., Vanover, J., Dessus-Babus, S., Whittimore, J., Howett, M. K., Wyrick, P. B., Schoborg, R. V.** 2006. *Chlamydia trachomatis* enters a viable but non-cultivable (persistent) state within herpes simplex virus type 2 (HSV-2) co-infected host cells. *Cell. Microbiol.* 8 (1): 149-162.
- Derby, M. C., Lieu, Z. Z., Brown, D., Stow, J. L., Goud, B., Gleeson, P. A.** 2007. The *trans*-Golgi network golgin, GCC185, is required for endosome-to-Golgi transport and maintenance of Golgi structure. *Traffic* 8 (6): 758-773.
- Dong, F., Su, H., Huang, Y., Zhong, Y., Zhong, G.** 2004. Cleavage of host keratin 8 by a *Chlamydia*-secreted protease. *Infect. Immun.* 72 (7): 3863-3868.
- Efimov, E., Kharitonov, A., Efimova, N., Loncarek, J., Miller, P. M., Andreyeva, N., Gleeson, P., Galjart, N., Maia, A. R., McLeod, I. X. et al.** 2007. Asymmetric CLASP-dependent nucleation of non-centrosomal microtubules at the *trans*-Golgi network. *Dev. Cell.* 12 (6): 917-930.
- Ehnes, S., Leonhardt, R. M., Hansen, G., Knittler, M. R.** 2005. Functional role of C-terminal sequence elements in the transporter associated with antigen processing. *J. Immunol.* 174 (1): 328-339.
- Fan, T., Lu, H., Hu, H., Shi, L., McClarty, G. A., Nance, D. M., Greenberg, A. H., Zhong, G.** 1998. Inhibition of apoptosis in *Chlamydia*-infected cells: Blockade of mitochondrial cytochrome c release and caspase activation.
- Fehlner-Gardiner, C., Roshick, C., Carlson, J. H., Hughes, S., Belland, R. J., Caldwell, H. D., McClarty, G.** 2002. Molecular basis defining human *Chlamydia trachomatis* tissue tropism. A possible role for tryptophan synthase. *J. Biol. Chem.* 277 (30): 26893-26903.
- Fields, K. A., Mead, D. J., Dooley, C. A., Hackstadt, T.** 2003. *Chlamydia trachomatis* type III secretion: evidence for a functional apparatus during early-cycle development. *Mol. Microbiol.* 48 (3): 671-683.
- Fling, S. P., Sutherland, R. A., Steele, L. N., Hess, B., D'Orazio, S. E., Maisonneuve, J., Lampe, M. F., Probst, P., Starnbach, M. N.** 2001. CD8+ T cells recognize an inclusion membrane-associated protein from the vacuolar pathogen *Chlamydia trachomatis*. *Proc. Natl. Acad. Sci. USA* 98 (3): 1160-1165.
- Fontoura, B. M., Faria, P. A., Nussenzeig, D. R.** 2005. Viral interactions with the nuclear transport machinery: discovering and disrupting pathways. *IUBMB Life* 57 (2): 65-72.
- Freeze, H. H., Kranz, C.** 2010. Endoglycosidase and glycoamidase release of N-linked glycans. *Curr. Protoc. Protein Science Suppl.* 62: Unit 12.4.
- Fromm, S. V., Ehrlich, R.** 2001. IFN- $\gamma$  affects both the stability and the intracellular transport of class I MHC complexes. *J. Interferon Cytokine Res.* 21 (4): 199-208.
- Früh, K., Ahn, K., Djaballah, H., Sempé, P., van Endert, P. M., Tampé, R., Peterson, P. A., Yang Y.** 1995. *Nature* 375 (6530): 415-418.
- Garstka, M., Borchert, B., Al-Balushi, M., Praveen, P. V., Kühl, N., Majoul, I., Duden, R., Springer, S.** 2007. Peptide-receptive major histocompatibility complex class I molecules cycle between endoplasmic reticulum and *cis*-Golgi in wild-type lymphocytes. *J. Biol. Chem.* 282 (42): 30680-30690.
- Gavioli, R., Gallerani, E., Fortini, C., Fabris, M., Bottoni, A., Canella, A., Bonaccorsi, A., Marastoni, M., Micheletti, F., Cafaro, A. et al.** 2004. HIV-1 Tat protein modulates the generation of cytotoxic T cell epitopes by modifying proteasome composition and enzymatic activity. *J. Immunol.* 173 (6): 3838-3843.
- Gérard, H. C., Branigan, P. J., Schumacher, H. R. Jr., Hudson, A. P.** 1998 a. Synovial *Chlamydia trachomatis* in patients with reactive arthritis / Reiter's syndrome are viable but show aberrant gene expression. *J. Rheum.* 25 (4): 734-742.
- Gérard, H. C., Köhler, L., Branigan, P. J., Zeidler, H., Schumacher, H. R., Hudson, A. P.** 1998 b. Viability and gene expression in *Chlamydia trachomatis* during persistent infection of cultured human monocytes. *Med. Microbiol. Immunol.* 187 (2): 115-120.
- Gérard, H. C., Krauß-Opatz, B., Wang, Z., Rudy, D., Rao, J. P., Zeidler, H., Schumacher, H. R., Whittum-Hudson, J. A., Köhler, L., Hudson, A. P.** 2001. Expression of *Chlamydia trachomatis* genes encoding products required for DNA synthesis and cell division during active versus persistent infection. *Mol. Microbiol.* 41 (3): 731-741.
- Gérard, H. C., Whittum-Hudson, J. A., Schumacher, H. R., Hudson, A. P.** 2004. Differential expression of three *Chlamydia trachomatis* hsp60-encoding genes in active vs. persistent infections. *Microb. Pathog.* 36 (1): 35-39.

- Gérard, H. C., Whittum-Hudson, J. A., Carter, J. D., Hudson, A. P.** 2010. The pathogenic role of *Chlamydia* in spondyloarthritis. *Curr. Opin. Rheumatol.* 22 (4): 363-367.
- Gervassi, A., Alderson, M. R., Suchland, R., Maisonneuve, J. F., Grabstein, K. H., Probst, P.** 2004 a. Differential regulation of inflammatory cytokine secretion by human dendritic cells upon *Chlamydia trachomatis* infection. *Infect. Immun.* 72 (12): 7231-7239.
- Gervassi, A. L., Grabstein, K. H., Probst, P., Hess, B., Alderson, M. R., Fling, S. P.** 2004 b. Human CD8+ T cells recognize the 60-kDa cysteine-rich outer membrane protein from *Chlamydia trachomatis*. *J. Immunol.* 173 (11): 6905-6913.
- Giles, D. K., Whittimore, J. D., LaRue, R. W., Raulston, J. E., Wyrick, P. B.** 2006. Ultrastructural analysis of chlamydial antigen-containing vesicles everting from the *Chlamydia trachomatis* inclusion. *Microbes Infect.* 8 (6): 1579-1591.
- Giles, D. K., Wyrick, P. B.** 2008. Trafficking of chlamydial antigens to the endoplasmic reticulum of infected epithelial cells. *Microbes Infect.* 10 (14-15): 1494-1503.
- Goellner, S., Schubert, E., Liebler-Tenorio, E., Hotzel, H., Saluz, H. P., Sachse, K.** 2006. Transcriptional response patterns of *Chlamydomytila psittaci* in different in vitro models of persistent infection. *Infect. Immun.* 74 (8): 4801-4808.
- Goud, B., Gleeson, P. A.** 2010. TGN golgins, Rabs and cytoskeleton: regulating the Golgi trafficking highways. *Trends Cell Biol.* 20 (6): 329-336.
- Grande III, A. G., Golovina, T. N., Hamilton, S. E., Sriram, V., Spies, T., Brutkiewicz, R. R., Harty, J. T., Eisenlohr, L. C., Van Kaer, L.** 2000. Impaired assembly yet normal trafficking of MHC class I molecules in *Tapasin* mutant mice. *Immunity* 13 (2): 213-222.
- Greenberg, M. E., Iafrate, A. J., Skowronski, J.** 1998. The SH3 domain-binding surface and an acidic motif in HIV-1 Nef regulate trafficking of class I MHC complexes. *EMBO J.* 17 (10): 2777-2789.
- Greene, W., Zhong, G.** 2003. Inhibition of host cell cytokinesis by *Chlamydia trachomatis* infection. *J. Infect.* 47 (1): 45-51.
- Grieshaber, S. S., Grieshaber, N. A., Hackstadt, T.** 2003. *Chlamydia trachomatis* uses host cell dynein to traffic to the microtubule-organizing center in a p50 dynamitin-independent process. *J. Cell Science* 116: 3793-3802.
- Grieshaber, S. S., Grieshaber, N. A., Miller, N., Hackstadt, T.** 2006. *Chlamydia trachomatis* causes centrosomal defects resulting in chromosomal segregation abnormalities. *Traffic* 7 (8): 940-949.
- Grosse, C., Heinekamp, T., Kniemeyer, O., Gehrke, A., Brakhage, A. A.** 2008. Protein kinase A regulates growth, sporulation, and pigment formation in *Aspergillus fumigatus*. *Appl. Environ. Microbiol.* 74 (15): 4923-33.
- Grüter, P., Taberner, C., von Kobbe, C., Schmitt, C., Saavedra, C., Bachi, A., Wilm, M., Felber, B. K., Izaurralde, E.** 1998. TAP, the human homolog of Mex67p, mediates CTE-dependent RNA export from the nucleus. *Mol. Cell* 1 (5): 649-659.
- Hackstadt, T., Rockey, D. D., Heinzen, R. A., Scidmore, M. A.** 1996. *Chlamydia trachomatis* interrupts an exocytic pathway to acquire endogenously synthesized sphingomyelin in transit from the Golgi apparatus to the plasma membrane. *EMBO J.* 15 (5): 964-977.
- Harper, A., Pogson, C. I., Jones, M. L., Pearce, J. H.** 2000. Chlamydial development is adversely affected by minor changes in amino acid supply, blood plasma amino acid levels, and glucose deprivation. *Infect. Immun.* 68 (3): 1457-1464.
- Hatch, T. P., Miceli, M., Sublett, J. E.** 1986. Synthesis of disulfide-bonded outer membrane proteins during the developmental cycle of *Chlamydia psittaci* and *Chlamydia trachomatis*. *J. Bacteriol.* 165 (2): 379-385.
- Herold, A., Klymenko, T., Izaurralde, E.** 2001. NXF1/p15 heterodimers are essential for mRNA nuclear export in *Drosophila*. *RNA* 7 (12): 1768-1780.
- Heuer, D., Brinkmann, V., Meyer, T. F., Szczepek, A. J.** 2003. Expression and translocation of chlamydial protease during acute and persistent infection of the epithelial HEp-2 cells with *Chlamydomytila (Chlamydia) pneumoniae*. *Cell. Microbiol.* 5 (5): 315-322.
- Heuer, D., Rejman Lipinski, A., Machuy, N., Karlas, A., Wehrens, A., Siedler, F., Brinkmann, V., Meyer, T. F.** 2009. *Chlamydia* causes fragmentation of the Golgi compartment to ensure reproduction. *Nature* 457: 731-735.

- Hewitt, E. W., Gupta, S. S., Lehner, P. J.** 2001. The human cytomegalovirus gene product US6 inhibits ATP binding by TAP. *EMBO J.* 20 (3): 387-396.
- Hill, A., Jugovic, P., York, I., Russ, G., Bennink, J., Yewdell, J., Ploegh, H., Johnson, D.** 1995. Herpes simplex virus turns off the TAP to evade host immunity. *Nature* 375 (6530): 411-415.
- Hislop, A. D., Rensing, M. E., van Leeuwen, D., Pudney, V. A., Horst, D., Koppers-Lalic, D., Croft, N. P., Neefjes, J. J., Rickinson, A. B., Wiertz, E. J.** 2007. A CD8+ T cell immune evasion protein specific to Epstein-Barr virus and its close relatives in Old World primates. *J. Exp. Med.* 204 (8): 1863-1873.
- Hobolt-Pedersen, A. S., Christiansen, G., Timmerman, E., Gevaert, K., Birkelund, S.** 2009. Identification of *Chlamydia trachomatis* CT621, a protein delivered through the type III secretion system to the host cell cytoplasm and nucleus. *FEMS Immunol. Med. Microbiol.* 57 (1): 46-58.
- Hogan, R. J., Mathews, S. A., Mukhopadhyay, S., Summersgill, J. T., Timms, P.** 2004. Chlamydial persistence: beyond the biphasic paradigm. *Infect. Immun.* 72 (4): 1843-1855.
- Hook, C. E., Telyatnikova, N., Goodall, J. C., Braud, V. M., Carmichael, A. J., Wills, M. R., Gaston J. S.** 2004. Effects of *Chlamydia trachomatis* infection on the expression of natural killer (NK) cell ligands and susceptibility to NK cell lysis. *Clin. Exp. Immunol.* 138 (1): 54-60.
- Huang, Z., Feng, Y., Chen, D., Wu, X., Huang, S., Wang, X., Xiao, X., Li, W., Huang, N., Gu, L., Zhong, G., Chai, J.** 2008. Structural basis for activation and inhibition of the secreted *Chlamydia* protease CPAF. *Cell Host Microbe* 4 (6): 529-542.
- Hughes, E. A., Hammond, C., Cresswell, P.** 1997. Misfolded major histocompatibility complex class I heavy chains are translocated into the cytoplasm and degraded by the proteasome. *Proc. Natl. Acad. Sci. USA* 94 (5): 1896-1901.
- Hybiske, K., Stephens, R. S.** 2007. Mechanisms of host cell exit by the intracellular bacterium *Chlamydia*. *Proc. Natl. Acad. Sci. USA* 104 (27): 11430-11435.
- Ibana, J. A., Schust, D. J., Sugimoto, J., Nagamatsu, T., Greene, S. J., Quayle, A. J.** 2011. *Chlamydia trachomatis* immune evasion via downregulation of MHC class I surface expression involves direct and indirect mechanisms. *Infect. Dis. Obstet. Gynecol.*, published online.
- Igietseme, J. U., Magee, D. M., Williams, D. M., Rank, R. G.** 1994. Role for CD8+ T cells in antichlamydial immunity defined by *Chlamydia*-specific T-lymphocyte clones. *Infect. Immun.* 62 (11): 5195-5197.
- Ishihara, T., Aga, M., Hino, K., Ushio, C., Taniguchi, M., Iwaki, K., Ikeda, M., Kurimoto, M.** 2005. Inhibition of *Chlamydia trachomatis* growth by human interferon- $\alpha$ : mechanisms and synergistic effect with interferon- $\gamma$  and tumor necrosis factor- $\alpha$ . *Biomed. Res.* 26 (4): 179-185.
- Jendro, M. C., Deutsch, T., Körber, B., Köhler, L., Kuipers, J. G., Krausse-Opatz, B., Westermann, J., Raum, E., Zeidler, H.** 2000. Infection of human monocyte-derived macrophages with *Chlamydia trachomatis* induces apoptosis of T cells: a potential mechanism for persistent infection. *Infect. Immun.* 68 (12): 6704-6711.
- Jendro, M. C., Fingerle, F., Deutsch, T., Liese, A., Köhler, L., Kuipers, J. G., Raum, E., Martin, M., Zeidler, H.** 2004. *Chlamydia trachomatis*-infected macrophages induce apoptosis of activated T cells by secretion of tumor necrosis factor- $\alpha$  in vitro. *Med. Microbiol. Immunol.* 193 (1): 45-52.
- Jensen, P. E.** 2007. Recent advances in antigen processing and presentation. *Nat. Immunol.* 8 (10): 1041-1048.
- Jewett, T. J., Fischer, E. R., Mead, D. J., Hackstadt, T.** 2006. Chlamydial TARP is a bacterial nucleator of actin. *Proc. Natl. Acad. Sci. USA* 103 (42): 15599-15604.
- Jewett, T. J., Miller, N. J., Dooley, C. A., Hackstadt, T.** 2010. The conserved Tarp actin binding domain is important for chlamydial invasion. *PLoS Pathogens* 6 (7), e1000997.
- Johnson, K. A., Tan, M., Sütterlin, C.** 2009. Centrosome abnormalities during a *Chlamydia trachomatis* infection are caused by dysregulation of the normal duplication pathway. *Cell. Microbiol.* 11 (7): 1064-1073.
- Jones, M. L., Gaston, J. S., Pearce, J. H.** 2001. Induction of abnormal *Chlamydia trachomatis* by exposure to interferon- $\gamma$  or amino acid deprivation and comparative antigenic analysis. *Microb. Pathog.* 30 (5): 299-309.

- Juillard, F., Hiriart, E., Sergeant, N., Vingtdeux-Didier, V., Drobecq, H., Sergeant, A., Manet, E., Gruffat, H.** 2009. Epstein-Barr virus protein EB2 contains an N-terminal transferable nuclear export signal that promotes nucleocytoplasmic export by directly binding TAP/NXF1. *J. Virol.* 83 (24): 12759-12768.
- Kang, Y., Cullen, B. R.** 1999. The human Tap protein is a nuclear mRNA export factor that contains novel RNA-binding and nucleocytoplasmic transport sequences. *Genes Dev.* 13 (9): 1126-1139.
- Kawana, K., Quayle, A. J., Ficarra, M., Ibane, J. A., Shen, L., Kawana, Y., Yang, H., Marrero, L., Yavagal, S., Greene, S. J. et al.** 2007. CD1d degradation in *Chlamydia trachomatis*-infected epithelial cells is the result of both cellular and chlamydial proteasomal activity. *J. Biol. Chem.* 282 (10): 7368-7375.
- Kelly, A. Powis, S. H., Kerr, L. A., Mockridge, I., Elliott, T., Bastin, J., Uchanska-Ziegler, B., Ziegler, A., Trowsdale, J., Townsend, A.** 1992. Assembly and function of the two ABC transporter proteins encoded in the human major histocompatibility complex. *Nature* 355 (6361): 641-644.
- Kim, S. K., Devine, L., Angevine, M., DeMars, R., Kavathas, P. B.** 2000. Direct detection and magnetic isolation of *Chlamydia trachomatis* major outer membrane protein-specific CD8+ CTLs with HLA class I tetramers. *J. Immunol.* 165 (12): 7285-7292.
- King, N. J., Thomas, S. R.** 2007. Molecules in focus: Indoleamine 2,3-dioxygenase. *Int. J. Biochem. Cell Biol.* 39 (12): 2167-2172.
- Klos, A., Thalmann, J., Peters, J., Gérard, H. C., Hudson, A. P.** 2009. The transcript profile of persistent *Chlamydophila (Chlamydia) pneumoniae* in vitro depends on the means by which persistence is induced. *FEMS Microbiol. Lett.* 291 (1): 120-126.
- Kniemeyer, O., Lessing, F., Scheibner, O., Hertweck, C., Brakhage, A. A.** 2005. Optimisation of a 2-D gel electrophoresis protocol for the human-pathogenic fungus *Aspergillus fumigatus*. *Curr. Genet.* 49: 178-89.
- Kodani, A., Sütterlin, C.** 2008. The Golgi protein GM130 regulates centrosome morphology and function. *Mol. Biol. Cell* 19 (2): 745-753.
- Koehler, L., Nettelbreker, E., Hudson, A. P., Ott, N., Gérard, H. C., Branigan, P. J., Schumacher, H. R., Drommer, W., Zeidler, H.** 1997. Ultrastructural and molecular analyses of the persistence of *Chlamydia trachomatis* (serovar K) in human monocytes. *Microb. Pathog.* 22 (3): 133-142.
- Koffa, M. D., Clements, J. B., Izaurrealde, E., Wadd, S., Wilson, S. A., Mattaj, I. W., Kuersten, S.** 2001. Herpes simplex virus ICP27 protein provides viral mRNAs with access to the cellular mRNA export pathway. *EMBO J.* 20 (20): 5769-5778.
- Kokab, A., Jennings, R., Eley, A., Pacey, A. A., Cross N. A.** 2010. Analysis of modulated gene expression in a model of interferon- $\gamma$ -induced persistence of *Chlamydia trachomatis* in Hep-2 cells. *Microb. Pathog.* 49 (5): 217-25.
- Krausse-Opatz, B., Busmann, A., Tammen, H., Menzel, C., Möhring, T., Le Yondre, N., Schmidt, C., Schulz-Knappe, P., Zeidler, H., Selle, H., Köhler, L.** 2007. Peptidomic analysis of human peripheral monocytes persistently infected by *Chlamydia trachomatis*. *Med. Microbiol. Immunol.* 196 (2): 103-114.
- Kumar, Y., Cocchiaro, J., Valdivia, R. H.** 2006. The obligate intracellular pathogen *Chlamydia trachomatis* targets host lipid droplets. *Curr. Biol.* 16 (16): 1646-1651.
- Kumar, Y., Valdivia, R. H.** 2008. Actin and intermediate filaments stabilize the *Chlamydia trachomatis* vacuole by forming dynamic structural scaffolds. *Cell Host Microbe* 4 (2): 159-169.
- Kuon, W., Holzhütter, H. G., Appel, H., Grolms, M., Kollnberger, S., Traeder, A., Henklein, P., Weiss, E., Thiel, A., Lauster, R. et al.** 2001. Identification of HLA-B27-restricted peptides from the *Chlamydia trachomatis* proteome with possible relevance to HLA-B27-associated diseases. *J. Immunol.* 167 (8): 4738-4746.
- Kyritsis, C., Gorbulev, S., Hutschenreiter, S., Pawlitschko, K., Abele, R., Tampé, R.** 2001. Molecular mechanism and structural aspects of transporter associated with antigen processing inhibition by the cytomegalovirus protein US6. *J. Biol. Chem.* 276 (51): 48031-48039.
- Lad, S. P., Li, J., da Silva Correia, J., Pan, Q., Gadwal, S., Ulevitch, R. J., Li, E.** 2007 a. Cleavage of p65/RelA of the NF- $\kappa$ B pathway by *Chlamydia*. *Proc. Natl. Acad. Sci. USA* 104 (8): 2933-2938.
- Lad, S. P., Yang, G., Scott, D. A., Wang, G., Nair, P., Mathison, J., Reddy, V. S., Li, E.** 2007 b. Chlamydial CT441 is a PDZ domain-containing tail-specific protease that interferes with the NF- $\kappa$ B pathway of immune response. *J. Bacteriol.* 189 (18): 6619-6625.

- Lankat-Buttgereit, B., Tampé, R.** 2002. The transporter associated with antigen processing: function and implications in human diseases. *Physiol. Rev.* 82 (1): 187-204.
- LaRue, R. W., Dill, B. D., Giles, D. K., Whittimore, J. D., Raulston, J. E.** 2007. Chlamydial Hsp60-2 is iron responsive in *Chlamydia trachomatis* serovar E-infected human endometrial epithelial cells in vitro. *Infect. Immun.* 75 (5): 2374-2380.
- Le Negrate, G., Krieg, A., Faustin, B., Loeffler, M., Godzik, A., Krajewski, S., Reed, J. C.** 2008. *ChlaDub1* of *Chlamydia trachomatis* suppresses NF- $\kappa$ B activation and inhibits I $\kappa$ B $\alpha$  ubiquitination and degradation. *Cell. Microbiol.* 10 (9): 1879-1892.
- Leonhardt, R. M., Fiegl, D., Rufer, E., Karger, A., Bettin, B., Knittler, M. R.** 2010. Post-endoplasmic reticulum rescue of unstable MHC class I requires proprotein convertase PC7. *J. Immunol.* 184 (6): 2985-2998.
- Lieu, Z. Z., Lock, J. G., Hammond, L. A., La Gruta, N. L., Stow, J. L., Gleeson, P. A.** 2008. A *trans*-Golgi network golgin is required for the regulated secretion of TNF in activated macrophages in vivo. *Proc. Natl. Acad. Sci. USA* 105 (9): 3351-3356.
- Magee, D. M., Williams, D. M., Smith, J. G., Bleicker, C. A., Grubbs, B. G., Schachter, J., Rank, R. G.** 1995. Role of CD8 T cells in primary *Chlamydia* infection. *Infect. Immun.* 63 (2): 516-521.
- Manor, E., Sarov, I.** 1986. Fate of *Chlamydia trachomatis* in human monocytes and monocyte-derived macrophages. *Infect. Immun.* 54 (1): 90-95.
- Matsumoto, A., Manire, G. P.** 1970. Electron microscopic observations on the effects of penicillin on the morphology of *Chlamydia psittaci*. *J. Bacteriol.* 101 (1): 278-285.
- Miller, D. M., Zhang, Y., Rahill, B. M., Kazor, K., Rofagha, S., Eckel, J. J., Sedmak, D. D.** 2000. Human cytomegalovirus blocks interferon- $\gamma$  stimulated up-regulation of major histocompatibility complex class I expression and the class I antigen processing machinery. *Transplantation* 69 (4): 687-690.
- Miller, P. M., Folkmann, A. W., Maia, A. R., Efimova, N., Efimov, A., Kaverina, I.** 2009. Golgi-derived CLASP-dependent microtubules control Golgi organization and polarized trafficking in motile cells. *Nat. Cell. Biol.* 11 (9): 1069-1080.
- Miyairi, I., Byrne, G. I.** 2006. *Chlamydia* and programmed cell death. *Curr. Opin. Microbiol.* 9(1): 102-108.
- Morrison, R. P.** 2000. Differential sensitivities of *Chlamydia trachomatis* strains to inhibitory effects of gamma interferon. *Infect. Immun.* 68 (10): 6038-6040.
- Nakamura, N.** 2010. Emerging new roles of GM130, a *cis*-Golgi matrix protein, in higher order cell functions. *J. Pharmacol. Sci.* 112 (3): 255-264.
- Nanagara, R., Li, F., Beutler, A., Hudson, A., Schumacher, H. R. Jr.** 1995. Alteration of *Chlamydia trachomatis* biologic behavior in synovial membranes. Suppression of surface antigen production in reactive arthritis and Reiter's syndrome. *Arthritis Rheum.* 38 (10): 1410-1417.
- Netherton, C. L., McCrossan, M. C., Denyer, M., Ponnambalam, S., Armstrong, J., Takamatsu, H. H., Wileman, T. E.** 2006. African Swine Fever Virus causes Microtubule-Dependent cispersal of the *trans*-Golgi network and slows delivery of membrane protein to the plasma membrane. *J. Virol.* 80 (22): 11385-11392.
- Nicholson, T., Stephens, R. S.** 2002. Chlamydial genomic transcriptional profile for penicillin-induced persistence. In: Schachter, J., Christiansen, G., Clarke, I. N., *et al.* (editors). *Chlamydial infections. Proceedings of the Tenth International Symposium on Human Chlamydial Infections.* San Francisco, CA: International Chlamydia Symposium, 2002: 611-614.
- Nielsen, U., Zimmer, S. G., Babiss, L. E.** 1991. Changes in NF- $\kappa$ B and ISGF3 DNA binding activities are responsible for differences in MHC and  $\beta$ -IFN gene expression in Ad5- versus Ad12-transformed cells. *EMBO J.* 10 (13): 4169-4175.
- Ozaki, Y., Edelstein, M. P., Duch, D. S.** 1988. Induction of indoleamine 2,3-dioxygenase: A mechanism of the antitumor activity of interferon  $\gamma$ . *Proc. Natl. Acad. Sci. USA* 85 (4): 1242-1246.
- Paschen, S. A., Jan, G. C., Vier, J., Schmidt, F., Walch, A., Ojcius, D. M., Häcker, G.** 2008. Cytotoxicity of *Chlamydia* is largely reproduced by expression of a single chlamydial protease. *J. Cell Biol.* 182 (1): 117-127.
- Peters, J., Wilson, D. P., Myers, G., Timms, P., Bavoil, P. M.** 2007. Type III secretion à la *Chlamydia*. *Trends Microbiol.* 15 (6): 241-251.

- Pfaffl, M. W.** 2001. A new mathematical model for relative quantification in real-time RT-PCR. *Nucleic Acids Res.* 29 (9): e45.
- Pirbhai, M., Dong, F., Zhong, Y., Pan, K. Z., Zhong, G.** 2006. The secreted protease factor CPAF is responsible for degrading pro-apoptotic BH3-only proteins in *Chlamydia trachomatis*-infected cells. *J. Biol. Chem.* 281 (42): 31495-31501.
- Pospischil, A., Thoma, R., Hilbe, M., Grest, P., Gebbers, J. O.** 2002. Abortion in woman caused by caprine *Chlamydia abortus* (*Chlamydia psittaci* serovar 1). *Swiss Med. Wkly.* 132 (5-6): 64-66.
- Powis, S. J., Townsend, A. R., Deverson, E. V., Bastin, J., Butcher, G. W., Howard, J. C.** 1991. Restoration of antigen presentation to the mutant cell line RMA-S by an MHC-linked transporter. *Nature* 354 (6354): 528-531.
- Rahman, M. U., Cheema, M. A., Schumacher, H. R., Hudson, A. P.** 1992. Molecular evidence for the presence of chlamydia in the synovium of patients with Reiter's syndrome. *Arthritis Rheum.* 35 (5): 521-529.
- Ramirez, I. B., Lowe, M.** 2009. Golgins and GRASPs: holding the Golgi together. *Semin. Cell Dev. Biol.* 20 (7): 770-779.
- Ramsey, K. H., Rank, R. G.** 1991. Resolution of chlamydial genital infection with antigen-specific T-lymphocyte lines. *Infect. Immun.* 59 (3): 925-931.
- Rasmussen, S. J., Timms, P., Beatty, P. R., Stephens, R. S.** 1996. Cytotoxic-T-lymphocyte-mediated cytolysis of L cells persistently infected with *Chlamydia* spp. *Infect. Immun.* 64 (6): 1944-1949.
- Rasmussen, S. J., Eckmann, L., Quayle, A. J., Shen, L., Zhang, Y. X., Anderson, D. J., Fierer, J., Stephens, R. S., Kagnoff, M. F.** 1997. Secretion of proinflammatory cytokines by epithelial cells in response to *Chlamydia* infection suggests a central role for epithelial cells in chlamydial pathogenesis. *J. Clin. Invest.* 99 (1): 77-87.
- Rejman Lipinski, A., Heymann, J., Meissner, C., Karlas, A., Brinkmann, V., Meyer, T. F., Heuer, D.** 2009. Rab6 and Rab11 regulate *Chlamydia trachomatis* development and Golgin-84-dependent Golgi fragmentation. *PLoS Pathog.* 5 (10): e1000615.
- Rey-Ladino, J., Jiang, X., Gabel, B. R., Shen, C., Brunham, R. C.** 2007. Survival of *Chlamydia muridarum* within dendritic cells. *Infect. Immun.* 75 (8): 3707-3714.
- Rivero, S., Cardenas, J., Bornens, M., Rios, R. M.** 2009. Microtubule nucleation at the cis-side of the Golgi apparatus requires AKAP450 and GM130. *EMBO J.* 28 (8): 1016-1028.
- Rizzo, A., Paolillo, R., Lanza, A. G., Guida, L., Annunziata, M., Carratelli, C. R.** 2008. *Chlamydia pneumoniae* induces interleukin-6 and interleukin-10 in human gingival fibroblasts. *Microbiol. Immunol.* 52 (9): 447-454.
- Roan, N. R., Starnbach, M. N.** 2006. Antigen-specific CD8+ T cells respond to *Chlamydia trachomatis* in the genital mucosa. *J. Immunol.* 177 (11): 7974-7979.
- Roan, N. R., Starnbach, M. N.** 2008. Immune-mediated control of *Chlamydia* infection. *Cell. Microbiol.* 10 (1): 9-19.
- Rockey, D. D., Scidmore, M. A., Bannantine, J. P., Brown, W. J.** 2002. Proteins in the chlamydial inclusion membrane. *Microbes Infect.* 4 (3): 333-340.
- Rödel, J., Groh, A., Vogelsang, H., Lehmann, M., Hartmann, M., Straube, E.** 1998 a. Beta interferon is produced by *Chlamydia trachomatis*-infected fibroblast-like synoviocytes and inhibits gamma interferon-induced HLA-DR expression. *Infect. Immun.* 66 (9): 4491-4495.
- Rödel, J., Straube, E., Lungershausen, W., Hartmann, M., Groh, A.** 1998 b. Secretion of cytokines by human synoviocytes during in vitro infection with *Chlamydia trachomatis*. *J. Rheumatol.* 25 (11): 2161-2168.
- Rödel, J., Groh, A., Hartmann, M., Schmidt, K. H., Lehmann, M., Lungershausen, W., Straube, E.** 1999. Expression of interferon regulatory factors and indoleamine 2,3-dioxygenase in *Chlamydia trachomatis*-infected synovial fibroblasts. *Med. Microbiol. Immunol.* 187 (4): 205-212.
- Rödel, J., Vogelsang, H., Prager, K., Hartmann, M., Schmidt, K. H., Straube, E.** 2002. Role of interferon-stimulated gene factor 3 $\gamma$  and beta interferon in HLA class I enhancement in synovial fibroblasts upon infection with *Chlamydia trachomatis*. *Infect. Immun.* 70 (11): 6140-6146.

- Rödel J., Große C., Yu H., Wolf K., Otto G.P., Liebler-Tenorio E., Forsbach-Birk V., Straube E.** 2012. Persistent *Chlamydia trachomatis* infection of HeLa cells mediates apoptosis resistance through a *Chlamydia* protease-like activity factor-independent mechanism and induces High mobility group box 1 release. *Infect. Immun.* 80 (1): 195-205.
- Rohde, G., Straube, E., Essig, A., Reinhold, P., Sachse, K.** 2010. Chlamydial zoonoses. *Dtsch. Arztebl. Int.* 107 (10): 174-180.
- Roshick, C., Wood, H., Caldwell, H. D., McClarty, G.** 2006. Comparison of gamma interferon-mediated antichlamydial defense mechanisms in human and mouse cells. *Infect. Immun.* 74 (1): 225-238.
- Rupp, J., Gieffers, J., Klinger, M., van Zandbergen, G., Wrase, R., Maass, M., Solbach, W., Deiwick, J., Hellwig-Burgel, T.** 2007. *Chlamydia pneumoniae* directly interferes with HIF-1 $\alpha$  stabilization in human host cells. *Cell. Microbiol.* 9 (9): 2181-2191.
- Rzomp, K. A., Scholtes, L. D., Briggs, B. J., Whittaker, G. R., Scidmore, M. A.** 2003. Rab GTPases are recruited to chlamydial inclusions in both a species-dependent and species-independent manner. *Infect. Immun.* 71 (10): 5855-5870.
- Samuel-Abraham, S., Leonard, J. N.** 2010. Staying on message: design principles for controlling nonspecific responses to siRNA. *FEBS J.* 277 (23): 4828-4836.
- Sanda, C., Weitzel, P., Tsukahara, T., Schaley, J., Edenberg, H. J., Stephens, M. A., McClintick, J. N., Blatt, L. M., Li, L., Brodsky, L., Taylor, M. W.** 2006. Differential gene induction by type I and type II interferons and their combination. *J. Interferon & Cytokine Res.* 26 (7): 462-472.
- Schiefner, A., Wilson, I. A.** 2009. Presentation of lipid antigens by CD1 glycoproteins. *Curr. Pharm. Des.* 15 (28): 3311-3317.
- Schmitz, E., Nettelbreker, E., Zeidler, H., Hammer, M., Manor, E., Wollenhaupt, J.** 1993. Intracellular persistence of chlamydial major outer-membrane protein, lipopolysaccharide and ribosomal RNA after non-productive infection of human monocytes with *Chlamydia trachomatis* serovar K. *J. Med. Microbiol.* 38 (4): 278-285.
- Schölz, C., Tampé, R.** 2009. The peptide-loading complex – antigen translocation and MHC class I loading. *Biol. Chem.* 390 (8): 783-794.
- Schrader, S., Klos, A., Hess, S., Zeidler, H., Kuipers, J. G., Rihl, M.** 2007. Expression of inflammatory host genes in *Chlamydia trachomatis*-infected human monocytes. *Arthritis Res. Ther.* 9 (3): R54.
- Scidmore, M. A., Fischer, E. R., Hackstadt, T.** 1996. Sphingolipids and glycoproteins are differentially trafficked to the *Chlamydia trachomatis* inclusion. *J. Cell Biol.* 134 (2): 363-374.
- Scidmore, M. A., Hackstadt, T.** 2001. Mammalian 14-3-3 $\beta$  associates with the *Chlamydia trachomatis* inclusion membrane via its interaction with IncG. *Mol. Microbiol.* 39 (6): 1638-1650.
- Scidmore, M. A.** 2011. Recent advances in *Chlamydia* subversion of host cytoskeletal and membrane trafficking pathways. *Microbes Infect.* 13 (6): 527-535.
- Sharma, M., Rudel, T.** 2009. Apoptosis resistance in *Chlamydia*-infected cells: a fate worse than death? *FEMS Immunol. Med. Microbiol.* 55 (2): 154-161.
- Shaw, E. I., Dooley, C. A., Fischer, E. R., Scidmore, M. A., Fields, K. A., Hackstadt, T.** 2000 a. Three temporal classes of gene expression during the *Chlamydia trachomatis* developmental cycle. *Mol. Microbiol.* 37 (4): 913-925.
- Shaw, A. C., Christiansen, G., Roepstorff, P., Birkelund, S.** 2000 b. Genetic differences in the *Chlamydia trachomatis* tryptophan synthase  $\alpha$ -subunit can explain variations in serovar pathogenesis. *Microbes Infect.* 2 (6): 581-592.
- Sieper, J., Kingsley, G., Palacios-Boix, A., Pitzalis, C., Treharne, J., Hughes, R., Keat, A., Panayi, G. S.** 1991. Synovial T lymphocyte-specific immune response to *Chlamydia trachomatis* in Reiter's disease. *Arthritis Rheum.* 34 (5): 588-598.
- Sijts, E. J., Kloetzel, P. M.** 2011. The role of the proteasome in the generation of MHC class I ligands and immune responses. *Cell. Mol. Life Sci.* 68 (9): 1491-1502.
- Slepenkin, A., Motin, V., de la Maza, L. M., Peterson, E. M.** 2003. Temporal expression of type III secretion genes of *Chlamydia pneumoniae*. *Infect. Immun.* 71 (5): 2555-2562.

- Spies, T., DeMars, R.** 1991. Restored expression of major histocompatibility class I molecules by gene transfer of a putative peptide transporter. *Nature* 351 (6324): 323-324.
- Starnbach, M. N., Bevan, M. J., Lampe, M. F.** 1994. Protective cytotoxic T lymphocytes are induced during murine infection with *Chlamydia trachomatis*. *J. Immunol.* 153 (11): 5183-5189.
- Starnbach, M. N., Bevan, M. J., Lampe, M. F.** 1995. Murine cytotoxic T lymphocytes induced following *Chlamydia trachomatis* intraperitoneal or genital tract infection respond to cells infected with multiple serovars. *Infect. Immun.* 63 (9): 3527-3530.
- Stary, G. Stary, A.** 2008. Lymphogranuloma venereum outbreak in Europe. *J. Dtsch. Dermatol. Ges.* 6 (11): 935-939.
- Stephens, R. S., Kalman, S., Lammel, C., Fan, J., Marathe, R., Aravind, L., Mitchell, W., Olinger, L., Tatusov, R. L., Zhao, Q. et al.** 1998. Genome Sequence of an obligate intracellular pathogen of humans: *Chlamydia trachomatis*. *Science* 282: 754-759.
- Stutz, F., Izaurralde, E.** 2003. The interplay of nuclear mRNP assembly, mRNA surveillance and export. *Trends Cell Biol.* 13 (6): 319-327.
- Su, H., Caldwell, H. D.** 1995. CD4+ T cells play a significant role in adoptive immunity to *Chlamydia trachomatis* infection of the mouse genital tract. *Infect. Immun.* 63 (9): 3302-3308.
- Subtil, A., Wyplosz, B., Balan, M. E., Dautry-Varsat, A.** 2004. Analysis of *Chlamydia caviae* entry sites and involvement of Cdc42 and Rac activity. *J. Cell Sci.* 117: 3923-3933.
- Sun, J., Schoborg, R. V.** 2009. The host adherens junction molecule nectin-1 is degraded by chlamydial protease-like activity factor (CPAF) in *Chlamydia trachomatis*-infected genital epithelial cells. *Microbes Infect.* 11 (1): 12-19.
- Sütterlin, C., Colanzi, A.** 2010. The Golgi and the centrosome: building a functional partnership. *J. Cell Biol.* 188 (5): 621-628.
- Takikawa, O., Kuroiwa, T., Yamazaki, F., Kido, R.** 1988. Mechanism of interferon- $\gamma$  action. Characterization of indoleamine 2,3-dioxygenase in cultured human cells induced by interferon- $\gamma$  and evaluation of the enzyme-mediated tryptophan degradation in its anticellular activity. *J. Biol. Chem.* 263 (4): 2041-2048.
- Timms, P., Good, D., Wan, C., Theodoropoulos, C., Mukhopadhyay, S., Summersgill, J., Mathews, S.** 2009. Differential transcriptional responses between the interferon- $\gamma$ -induction and iron-limitation models of persistence for *Chlamydia pneumoniae*. *J. Microbiol. Immunol. Infect.* 42 (1): 27-37.
- Tokunaga, K., Tani, T.** 2008. Monitoring mRNA export. *Curr. Protoc. Cell Biol.* Chapter 22 Unit 22.13.
- Tomazin, R., Hill, A. B., Jugovic, P., York, I., van Endert, P., Ploegh, H. L., Andrews, D. W., Johnson, D. C.** 1996. Stable binding of the herpes simplex virus ICP47 protein to the peptide binding site of TAP. *EMBO J.* 15 (13): 3256-3266.
- Tomson, F. L., Viswanathan, V. K., Kanack, K. J., Kanteti, R. P., Straub, K. V., Menet, M., Kaper, J. B., Hecht, G.** 2005. Enteropathogenic *Escherichia coli* EspG disrupts microtubules and in conjunction with Orf3 enhances perturbation of the tight junction barrier. *Mol. Microbiol.* 56 (2): 447-464.
- Townsend, A., Öhlén, C., Bastin, J., Ljunggren, H. G., Foster, L., Kärre, K.** 1989. Association of class I major histocompatibility heavy and light chains induced by viral peptides. *Nature* 340 (6233): 443-448.
- van den Elsen, P. J., Gobin, S. J., van Eggermond, M. C., Peijnenburg, A.** 1998. Regulation of MHC class I and II gene transcription: differences and similarities. *Immunogenetics* 48 (3): 208-221.
- van Endert, P. M., Tampé, R., Meyer, T. H., Tisch, R., Bach, J. F., McDevitt, H. O.** 1994. A sequential model for peptide binding and transport by the transporters associated with antigen processing. *Immunity* 1 (6): 491-500.
- Van Kaer, L., Ashton-Rickardt, P. G., Ploegh, H. L., Tonegawa, S.** 1992. *TAP1* mutant mice are deficient in antigen presentation, surface class I molecules, and CD4-8+ T cells. *Cell* 71 (7): 1205-1214.
- Walder, G. Hotzel, H., Brezinka, C. Gritsch, W., Tauber, R., Würzner, R., Ploner, F.** 2005. An unusual cause of sepsis during pregnancy: recognizing infection with *Chlamydophila abortus*. *Obstet. Gynecol.* 106 (5 Pt. 2): 1215-1217.
- Wearsch, P. A., Cresswell, P.** 2008. The quality control of MHC class I peptide loading. *Curr. Opin. Cell Biol.* 20 (6): 624-631.

- Weigert, R., Yeung, A. C., Li, J., Donaldson, J. G.** 2004. Rab22a regulates the recycling of membrane proteins internalized independently of clathrin. *Mol. Biol. Cell* 15 (8): 3758-3770.
- Wiegand, H. L., Coburn, G. A., Zeng, Y., Kang, Y., Bogerd, H. P., Cullen, B. R.** 2002. Formation of Tap/NXT1 heterodimers activates Tap-dependent nuclear mRNA export by enhancing recruitment to nuclear pore complexes. *Mol. Cell. Biol.* 22 (1): 245-256.
- Wood, H., Fehlner-Gardner, C., Berry, J., Fischer, E., Graham, B., Hackstadt, T., Roshick, C., McClarty, G.** 2003. Regulation of tryptophan synthase gene expression in *Chlamydia trachomatis*. *Mol. Microbiol.* 49 (5): 1347-1359.
- Wylie, J. L., Hatch, G. M., McClarty, G.** 1997. Host cell phospholipids are trafficked to and then modified by *Chlamydia trachomatis*. *J. Bacteriol.* 179 (23): 7233-7242.
- Wyrick, P. B.** 2010. *Chlamydia trachomatis* persistence in vitro: an overview. *J. Infect. Dis.* 201 (Suppl. 2): S88-S95.
- Yatherajam, G., Huang, W., Flint, S. J.** 2011. Export of adenoviral late mRNA from the nucleus requires the Nxf1/Tap export receptor. *J. Virol.* 85 (4): 1429-1438.
- Yoshino, A., Bieler, B. M., Harper, D. C., Cowan, D. A., Sutterwala, S., Gay, D. M., Cole, N. B., McCaffery, J. M., Marks, M. S.** 2003. A role for GRIP domain proteins and/or their ligands in structure and function of the trans Golgi network. *J. Cell Sci.* 116: 4441-4454.
- Yu, H., Schwarzer, K., Förster, M., Kniemeyer, O., Forsbach-Birk, V., Straube, E., Rödel, J.** 2010. Role of high-mobility group box 1 protein and poly(ADP-ribose) polymerase 1 degradation in *Chlamydia trachomatis*-induced cytopathicity. *Infect. Immun.* 78 (7): 3288-3297.
- Yu, H.** 2010. Modulation of host death by *Chlamydia trachomatis*: the role of the *Chlamydia*-specific protease CPAF. Dissertation, Friedrich Schiller University Jena.
- Zeidler, H., Kuipers, J., Köhler, L.** 2004. Chlamydia-induced arthritis. *Curr. Opin. Rheumatol.* 16 (4): 380-392.
- Zhong, G., Fan, T., Liu, L.** 1999. *Chlamydia* inhibits interferon  $\gamma$ -inducible major histocompatibility complex class II expression by degradation of upstream stimulatory factor 1. *J. Exp. Med.* 189 (12): 1931-1937.
- Zhong, G., Liu, L., Fan, T., Fan, P., Ji, H.** 2000. Degradation of transcription factor RFX5 during the inhibition of both constitutive and interferon  $\gamma$ -inducible major histocompatibility complex class I expression in *Chlamydia*-infected cells. *J. Exp. Med.* 191 (9): 1525-1534.
- Zhong, G., Fan, P., Ji, H., Dong, F., Huang, Y.** 2001. Identification of a chlamydial protease-like activity factor responsible for the degradation of host transcription factors. *J. Exp. Med.* 193 (8): 935-42.
- Zhong, G.** 2009. Killing me softly: chlamydial use of proteolysis for evading host defenses. *Trends Microbiol.* 17 (10): 467-474.

## 6 Appendix

### 6.1 Material

#### 6.1.1 Chemicals

Acetic acid	VWR, Dresden, Germany
Acetone	VWR, Dresden, Germany
40% Acrylamide/Bis Solution, 37.5:1	Bio-Rad Laboratories, München, Germany
Agarose, LE, Analytical Grade	Promega, Mannheim, Germany
Ammonium persulfate (APS)	Sigma-Aldrich Chemie, München, Germany
Bromophenol blue	Amresco, Solon, Ohio, USA
Chloramphenicol	Roth, Karlsruhe, Germany
3-[(3-Cholamidopropyl)dimethylammonio]-1-propanesulfonate (CHAPS)	GE Healthcare Europe, München, Germany
Cycloheximide	Serva Electrophoresis, Heidelberg, Germany
DAPI	Invitrogen, Darmstadt, Germany
Diethylaminoethyl (DEAE) sepharose	Pharmacia Fine Chemicals/Amersham Biosciences, Uppsala, Sweden
Deoxycholic acid	Sigma-Aldrich Chemie, München, Germany
Dextran sulphate sodium salt from <i>Leuconostoc</i> spp.	Sigma-Aldrich Chemie, München, Germany
Dimethyl sulfoxide (DMSO)	Sigma-Aldrich Chemie, München, Germany
Disodium phosphate dihydrate	Roth, Karlsruhe, Germany
Dithiothreitol (DTT)	Roth, Karlsruhe, Germany
Ethanol	VWR, Dresden, Germany
Ethidium bromide	Roth, Karlsruhe, Germany
Formamide	Roth, Karlsruhe, Germany
8% Glutaraldehyde solution grade I	Sigma-Aldrich Chemie, München, Germany
Glycerol	Roth, Karlsruhe, Germany
Glycine	Bio-Rad Laboratories, München, Germany
HiPerFect Transfection Reagent	Qiagen, Hilden, Germany
4-(2-Hydroxyethyl)-1-piperazineethanesulfonic acid (HEPES)	Serva Electrophoresis, Heidelberg, Germany
Clasto-Lactacystin $\beta$ -lactone	Sigma-Aldrich Chemie, München, Germany
Leupeptin	Serva Electrophoresis, Heidelberg, Germany
Magnesium chloride (MgCl <sub>2</sub> )	Merck, Darmstadt, Germany

β-mercaptoethanol	Ferak Berlin, Berlin, Germany
Methanol	VWR, Dresden, Germany
Paraformaldehyde	Sigma-Aldrich Chemie, München, Germany
Pharmalyte, broad range pH 3-10, 25 ml	GE Healthcare Europe, München, Germany
Phenylmethylsulfonyl fluoride (PMSF)	Serva Electrophoresis, Heidelberg, Germany
Ponceau S	Amresco, Solon, Ohio, USA
Potassium chloride (KCl)	Merck, Darmstadt, Germany
Potassium dihydrogen phosphate	Merck, Darmstadt, Germany
ProLong Gold antifade reagent with DAPI	Invitrogen, Darmstadt, Germany
Saponin	Sigma-Aldrich Chemie, München, Germany
Sigma FAST BCIP/NBT	Sigma-Aldrich Chemie, München, Germany
Sodiumcacodylate Trihydrate	Sigma-Aldrich Chemie, München, Germany
Sodium chloride (NaCl)	Sigma-Aldrich Chemie, München, Germany
Sodium dodecyl sulphate (SDS)	Sigma-Aldrich Chemie, München, Germany
Sodium-ethylenediaminetetraacetic acid (Na-EDTA)	Amresco, Solon, Ohio, USA
Sodium-ethylene glycol tetraacetic acid (Na-EGTA)	Roth, Karlsruhe, Germany
Sodium hydroxide (NaOH)	Roth, Karlsruhe, Germany
Sucrose	Roth, Karlsruhe, Germany
Tetramethylethyldiamin (TEMED)	Bio-Rad Laboratories, München, Germany
Thiourea	Sigma-Aldrich Chemie, München, Germany
Trichloroacetic acid (TCA)	Merck, Darmstadt, Germany
Tris(hydroxymethyl)methylamine (Tris)	Amresco, Solon, Ohio, USA
Tris/Hydrochloride (Tris/HCl)	Promega, Mannheim, Germany
Trisodium citrate dihydrate	Roth, Karlsruhe, Germany
Triton X-100	Serva Electrophoresis, Heidelberg, Germany
Urea	GE Healthcare Europe, München, Germany

### 6.1.2 Kits

Bio-Rad Protein Assay	Bio-Rad Laboratories, München, Germany
Human Interferon-β ELISA Kit	Fujirebio inc., Invitrogen, Darmstadt, Germany
KAPA SYBR FAST qPCR Universal Mastermix	Peqlab, Erlangen, Germany
peqGOLD Total RNA Kit	Peqlab, Erlangen, Germany
peqGOLD DNase I Digest Kit	Peqlab, Erlangen, Germany
Reverse Transcription System	Promega, Mannheim, Germany

### 6.1.3 Proteins, enzymes and standards

AmpliSize™ Molecular Ruler, 50-2,000 bp	Bio-Rad Laboratories, München, Germany
Aprotinin, from bovine lung	Sigma-Aldrich Chemie, München, Germany
BSA	Sigma-Aldrich Chemie, München, Germany
Endoglycosidase H	New England Biolabs, Frankfurt am Main, Germany
FCS	ReliaTech, Wolfenbüttel, Germany
GoTaq DNA Polymerase	Promega, Mannheim, Germany
Prestained SDS-PAGE Standards, broad range	Bio-Rad Laboratories, München, Germany
Protein G PLUS-Agarose	Santa Cruz Biotechnology, Heidelberg, Germany
Recombinant human IFN-β	PromoCell, Germany
Recombinant human IFN-γ	ReliaTech, Wolfenbüttel, Germany

### 6.1.4 Buffers and media

Dulbecco's Modified Eagle Medium (DMEM) liquid medium with stable glutamine, with 3.7 g/l NaHCO <sub>3</sub> , with 4.5 g/l D-glucose	Biochrom AG, Berlin, Germany
Laemmli sample buffer	Bio-Rad Laboratories, München, Germany
Opti-MEM® I Reduced Serum Medium with GlutaMAX™ I	Invitrogen, Darmstadt, Germany
Resolving Gel Buffer (1.5 M Tris-HCl, pH 8.8)	Bio-Rad Laboratories, München, Germany
Stacking Gel Buffer (0.5 M Tris-HCl, pH 6.8)	Bio-Rad Laboratories, München, Germany
SYPRO Ruby Protein Gel Stain	Sigma-Aldrich Chemie, München, Germany
50x Tris-acetate-EDTA (TAE) Electrophoresis Buffer	Fermentas, St. Leon-Rot, Germany
TBS, with Tween 20, pH 8.0	Sigma-Aldrich Chemie, München, Germany
10x Tris/glycine/SDS	Bio-Rad Laboratories, München, Germany
1.5 M Tris-HCl pH 8.8	Bio-Rad Laboratories, München, Germany
1.5 M Tris-HCl pH 6.8	Bio-Rad Laboratories, München, Germany
Trypsin/EDTA solution (0.05%/0.02%)	Biochrom AG, Berlin, Germany
Visipaque 320	GE Healthcare Europe, München, Germany

**Table 6: Composition of buffers and solutions**

<b>buffer</b>	<b>composition</b>
Cell extraction buffer	20 mM HEPES-NaOH (pH 7.5) 10 mM KCl 1,5 mM MgCl <sub>2</sub> 1 mM Na-EDTA 1 mM Na-EGTA 1 mM DTT (add immediately before use) Protease inhibitors: 0,1 mM PMSF 2 µg/ml aprotinin 10 µg/ml leupeptin
Endo H reaction buffer	50 mM Sodium citrate, pH 5.5 7% β-mercaptoethanol 0.01% SDS
Hybridisation buffer	10% dextran sulphate in prehybridisation buffer
Lysis buffer for 2D gel electrophoresis	7 M Urea 2 M Thiourea 4% CHAPS 10 mM DTT 2% Pharmalyte 3-10
Nuclear extraction buffer	0.5 mM NaCl 1% Triton X-100 20 mM Tris (pH 8.0)
PBS	137 mM NaCl 2.7 mM KCl 8.1 mM Disodium phosphate dihydrate 1.5 mM Potassium dihydrogen phosphate
Ponceau S staining solution	0.2% Ponceau S 1% acetic acid
Prehybridisation buffer	2x SSC buffer containing: 20% formamide 0.2% BSA 1 mg/ml yeast transfer RNA
Radioimmunoprecipitation assay (RIPA) buffer (Cell lysis buffer for immunoblotting)	0.15 M NaCl 50 mM Tris/HCl 1% deoxycholic acid 1% Triton X-100 0.1% SDS Protease inhibitors: 0.1 mM PMSF 50 µg/ml aprotinin 2 µg/ml leupeptin

<b>buffer</b>	<b>composition</b>
Resolving gel	375 mM Tris-HCl pH 8.8 0.1% SDS 0.05% APS 0.05% TEMED 5, 8, 10 or 12% acrylamide (depending on the size of proteins analysed)
2x SDS-Urea sample buffer	4% SDS 2.4 M urea 20% glycerol 125 mM Tris 7% $\beta$ -mercaptoethanol some bromophenol blue crystals
2x SSC buffer	30 mM sodium citrate 300 mM sodium chloride
Stacking gel	187.5 M Tris-HCl pH 6.8 0.05% SDS 0.025% APS 0.1% TEMED 2% acrylamide
TCA solution	15% TCA 22 mM DTT solved in acetone
Transfer buffer for immunoblotting (according to Bjerrum & Schafer-Nielsen, 1986)	48 mM Tris 39 mM glycine 20% methanol
Washing solution for TCA/acetone precipitation	20 mM DTT solved in 90% acetone

### 6.1.5 Nucleic acids

AllStars Negative Control siRNA	Qiagen, Hilden, Germany
Cy3 labelled oligo(dT) <sub>50</sub>	Jena Bioscience, Jena, Germany
Hs_INDO_10 FlexiTube siRNA (gene accession number: NM_002164)	Qiagen, Hilden, Germany
Hs_IFNB1_1 FlexiTube siRNA (gene accession number: NM_002176)	Qiagen, Hilden, Germany
Mycoplasma positive control DNA (16S rRNA fragment from Mycoplasma bovis)	in-house generation
Transfer ribonucleic acid from baker's yeast	Sigma-Aldrich Chemie, München, Germany

All primers were synthesized by and purchased from Jena Bioscience, Jena, Germany.

**Table 7: Primer for human genes**

target gene	protein product	sequence 5' - 3'	product size	annealing temperature	primer efficiency E
<i>GAPDH</i>	Glyceraldehyde-3-phosphate dehydrogenase	tcaagtggggcgcgatgctggc tgggggcatcagcagagggg	135 bp	64 °C	1.99
<i>HLA-A, -B and -C</i>	MHCI molecule encoded by major HLA genes A, B and C	ctgagtgctggggccctg cccacttctggaagggtc	133 bp	54 °C	2.00
<i>IDO1</i>	Indoleamine 2,3-dioxygenase	gtgatgctggcctcgggaa ttggctgctggcttcagga	117 bp	63 °C	1.96
<i>LMP7</i>	immunoproteasome $\beta$ type subunit 8	ggcctgctggccaaggaat gagaggcccatgccccggta	120 bp	65 °C	1.98
<i>LMP2</i>	immunoproteasome $\beta$ type subunit 9	ggggaggtgggtgcttcct acgtgatcacctgcatgtatagggc	140 bp	64 °C	2.00
<i>MECL1</i>	immunoproteasome $\beta$ type subunit 10	gctccgggggcaatgtggac gcgccagacctcttcacgg	101 bp	64 °C	1.99
<i>TAP 1</i>	Transporter associated with antigen processing subunit 1	gcagctcatggagaaaaagg gaaaaggaggagatggag	108 bp	58 °C	1.95
<i>TAP 2</i>	Transporter associated with antigen processing subunit 2	caggcctgtgctcaaggggc ttctgcagcagggcagccac	108 bp	63 °C	1.99

**Table 8: Primer for *C. trachomatis* D genes**

target gene	protein product	sequence 5' - 3'	product size	annealing temperature	primer efficiency E
<i>16S rRNA</i>	-	cggtatacggagggtgcta ctacgcattcaccgctaca	176 bp	60°C	2.00
<i>ct858</i>	CPAF	cggagggtctttccgcgct tccaaggaggcggctctga	139 bp	60°C	1.99
<i>dnaA</i>	Chromosomal replication initiation protein	gcctttgaaaactggattgc gcgtttgatctctgcaaca	189 bp	56 °C	1.98
<i>ftsW</i>	Cell division protein	ttggacttggtatcgcttc tagccaacgcttagctccat	153 bp	58 °C	2.00

target gene	protein product	sequence 5' - 3'	product size	annealing temperature	primer efficiency E
<i>groEL</i>	Hsp60 chaperone GroEL	ccagcaaaactgctgacaaa tgctccagctgttacattgc	101 bp	55 °C	1.82
<i>groEL_2</i>	Hsp60 chaperone Ct604	cggaaacaggaacggtagaa aatcacaagcgggtgtttcc	131 bp	54°C	1.88
<i>omcB</i>	60 kDa cysteine-rich outer membrane protein	agcacgaccacgtttaagcgga accaaggaacagcaacagctcgt	167 bp	62°C	1.97
<i>ompA</i>	MOMP	aatttcagatgggtgccaag ccactggtggctcctaagt	190 bp	57 °C	1.98
<i>pgsA_2</i>	CDP-diacylglycerol- glycerol-3-phosphate 3-phosphatidyl- transferase	cctcacgttcacacaacctccg cgcatagcgtacgcaaagtgt	98 bp	62°C	1.90
<i>trpB</i>	Tryptophan synthase subunit β	tgagtcaggacgagcctttt atgtgcgagagcatgtgaag	121 bp	56°C	1.89

**Table 9: Primer for detection of mycoplasma contamination**

target gene	sequence 5' - 3'	product size	annealing temperature
<i>16S rRNA</i>	ccagactcctacgggaggca tgcgagcatactactcaggc	560 bp	55°C

### 6.1.6 Antibodies

**Table 10: Primary antibodies**

target	name/clone	origin	company/source	Application/dilution
<i>C. trachomatis</i> CPAF	CPAF antiserum	mp	Institute for Medical Microbiology and Hygiene, University Hospital Ulm, Germany	Immunoprecipitation (5 µl per reaction), Immunoblot (1:2000)
GAPDH	FL-335	rp	Santa Cruz Biotechnology, Heidelberg, Germany	Immunoblot (1:1000) (loading control)
GM130	EP892Y	rm	Abcam, Cambridge, UK	Immunofluorescence (1:500), Immunoblot (1:2000)

<b>target</b>	<b>name/clone</b>	<b>origin</b>	<b>company/source</b>	<b>Application/dilution</b>
Golgin-245 (p230)	15/p230 trans Golgi	mm	BD Biosciences, Heidelberg, Germany	Immunofluorescence (1:250), Immunoblot (1:250)
HLA-ABC	LY5.1	mm	Anogen, Mississauga, Canada	Immunoblot (1:1000)
<i>C. trachomatis</i> HSP60	A57-B9	mm	Acris Antibodies, Herford, Germany	Immunoblot (1:1000)
IFNAR	MMHAR-2	mm	Millipore, Schwalbach, Germany	Neutralisation of type I IFN activity in cell culture (1 µg/ml)
LMP2	H-200	rp	Santa Cruz Biotechnology, Heidelberg, Germany	Immunoblot (1:1000)
LMP7	1B3	mm	Abnova, Heidelberg, Germany	Immunoblot (1:500)
MECL1	H-70	rp	Santa Cruz Biotechnology, Heidelberg, Germany	Immunoblot (1:1000)
<i>C. trachomatis</i> MOMP	1297/142	mm	Acris Antibodies, Herford, Germany	Immunoblot (1:1000)
<i>C. trachomatis</i> MOMP	MikroTrak <i>Chlamydia</i> <i>trachomatis</i> Culture Confirmation Test (FITC conjugated)	mm	Trinity Biotech Plc, Bray, Ireland	Immunofluorescence (1:20), Flow cytometry (1:100)
MHCI (native)	W6/32 (PE/unconju- gated)	mm	PE-conjugated: Santa Cruz Biotechnology, Heidelberg, Germany; unconjugated: Friedrich Loeffler Institute Tübingen, Germany	Flow cytometry (1:50), Immunofluorescence (1:50)
NXF1 (TAP)	53H8	mm	Abcam, Cambridge, UK	Immunoblot (1:2000)
PARP-1	Anti-Poly- (ADP- Ribose)- Polymerase	rp	Roche Applied Science, Mannheim, Germany	Immunoblot (1:2000)
RFX5	Anti-RFX5	rp	BioMol, Hamburg, Germany	Immunoblot (1:1000)

target	name/clone	origin	company/source	application
TAP1	148.3 (van Endert <i>et al.</i> , 1994)	mm	Friedrich Loeffler Institute Tübingen, Germany	Immunoblot (1:1000)
TAP2	435.3 (van Endert <i>et al.</i> , 1994)	mm	Friedrich Loeffler Institute Tübingen, Germany	Immunoblot (1:1000)
unspecific	normal mouse IgG	mp	Santa Cruz Biotechnology, Heidelberg, Germany	Immunoprecipitation (irrelevant antibody control; 5 µl per reaction)
unspecific	FITC- and PE- conjugated mouse IgG	mp	Dianova, Hamburg, Germany	Flow cytometry (1:200)

mm: mouse monoclonal, mp: mouse polyclonal, rm: rabbit monoclonal, rp: rabbit polyclonal

## Secondary antibodies

Affinity Pure Goat anti-mouse IgG (H+L), alkaline phosphatase conjugated	Dianova, Hamburg, Germany
Affinity Pure Goat anti-rabbit IgG (H+L), alkaline phosphatase conjugated	Dianova, Hamburg, Germany
Alexa Fluor 633 goat anti-rabbit IgG (H+L)	Invitrogen, Darmstadt, Germany
Alexa Fluor 488 rabbit anti-mouse IgG (H+L)	Invitrogen, Darmstadt, Germany
Alexa Fluor 633 rabbit anti-mouse IgG (H+L)	Invitrogen, Darmstadt, Germany

## 6.1.7 Material

25 cm <sup>2</sup> and 75 cm <sup>2</sup> cell culture flasks	Greiner Bio-One, Frickenhausen, Germany
6 well and 24 well cell culture plates	Greiner Bio-One, Frickenhausen, Germany
Cell scrapers	Nunc, Langenselbold, Germany
Chocolate agar	in-house production
Columbia Blood agar	in-house production
Extra Thick Blot Paper	Bio-Rad Laboratories, München, Germany
Immobiline DryStrip gels	GE Healthcare Europe, München, Germany
Nitrocellulose Membrane, 0.45 µm	Bio-Rad Laboratories, München, Germany
Smart Cycler 25 µl tubes	Peqlab, Erlangen, Germany
Ultracentrifuge Tubes, Quick-Seal, Polyallomer, 33 ml	Beckman Coulter, Krefeld, Germany
Winkle agar	in-house production

### 6.1.8 Devices

Branson Sonifier 250	Branson Ultrasonics, Dietzenbach, Germany
Centrifuge Rotanta 460 RS	Hettich, Tuttlingen, Germany
Confocal laser scanning microscope LSM 5 Exciter	Zeiss, Jena, Germany
Epifluorescence microscope Axioskop	Zeiss, Jena, Germany
Ettan DALT System	GE Healthcare Europe, München, Germany
FACSCalibur flow cytometer	BD Biosciences, Heidelberg, Germany
IPGphor II	GE Healthcare Europe, München, Germany
MALDI TOF/TOF mass spectrometer Ultraflex I	Bruker Daltonics, Bremen
Mini-PROTEAN Tetra Electrophoresis System	Bio-Rad Laboratories, München, Germany
MTP anchor chip 384	Bruker Daltonics, Bremen
NanoDrop ND-1000 Spectrophotometer	Peqlab, Erlangen, Germany
Optima™ L-80 XP Ultracentrifuge with SW 32 T rotor	Beckman Coulter, Krefeld, Germany
SmartCycler II	Cepheid, Maurens-Scopont, France
Spectrophotometer Ultraspec 2000	GE Healthcare Europe, München, Germany
Tissue grinder, conical	Bel-Art, Pequannock, New Jersey, USA
Trans-Blot SD Semi-Dry Transfer Cell	Bio-Rad Laboratories, München, Germany
TRIO-Thermoblock	Biometra, Göttingen, Germany

### 6.1.9 Software

CellQuest Pro Version 4.0.2	BD Biosciences, Heidelberg, Germany
Delta 2D, version 3.4	Decodon, Greifswald, Germany
ImageJ	Open source software from <a href="http://rsbweb.nih.gov/ij/">http://rsbweb.nih.gov/ij/</a>
Labscan software 5	GE Healthcare Europe, München, Germany
MASCOT interface (MASCOT 2.1.0)	Matrix Science, London, UK
Protein Scape 1.3	Protagen, Dortmund, Germany
Smart Cycler Dx Software	Cepheid, Maurens-Scopont, France
ZEN Software 2009	Zeiss, Jena, Germany

## 6.2 Comparative 2D gel electrophoresis of chlamydial RB proteins from infected HeLa cells and fibroblasts

A comparative proteome analysis of RBs isolated from infected HeLa cells and fibroblasts at 24 h p.i. was done to identify proteins that are differentially regulated between both cell types. The RBs were isolated from the cells through density gradient ultracentrifugation and protein samples were generated as described in chapter 2.2.17. The RB proteins were separated by their isoelectric point (pI) and molecular weight through 2D gel electrophoresis. The gel of RB proteins from HeLa cells is depicted in Fig. 31 and the gel of RB proteins from fibroblasts in Fig. 32. Proteins identified by mass spectrometry (MS) are indicated. The most abundant protein was MOMP, and could be readily detected both on the HeLa and fibroblast gel. Due to co-purification of human proteins during the ultracentrifugation step and the low infectivity rate of fibroblasts the protein sample of RBs isolated from fibroblasts contained mainly human proteins (as identified by MS) which masked the detection of chlamydial proteins. Thus, it was not possible to compare the two samples with each other for detecting differential expression. However, the gel of RBs isolated from HeLa cells and the plentiful detected proteins show that it is principally possible to generate a 2D gel from purified RBs, which are more fragile than the rigid EBs. Thus, in situations where the growth of *Chlamydia* should be compared under different conditions a comparative proteome analysis using isolated RBs could be a more exact tool in examining chlamydial protein expression than treating cells with cycloheximide and marking chlamydial proteins with radioactive amino acids, because cycloheximide inhibits host cell protein synthesis and thus could influence the host cell condition.

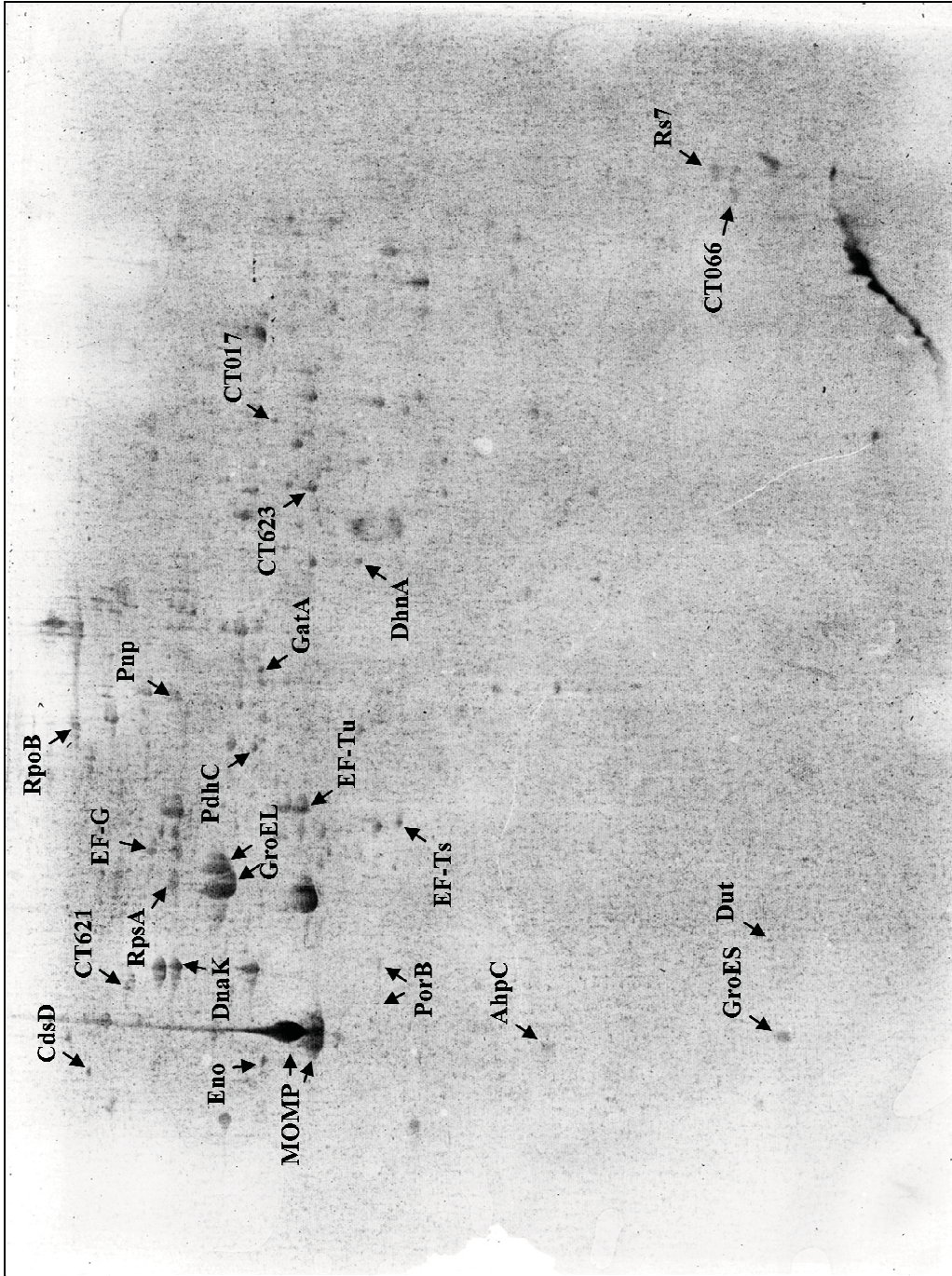
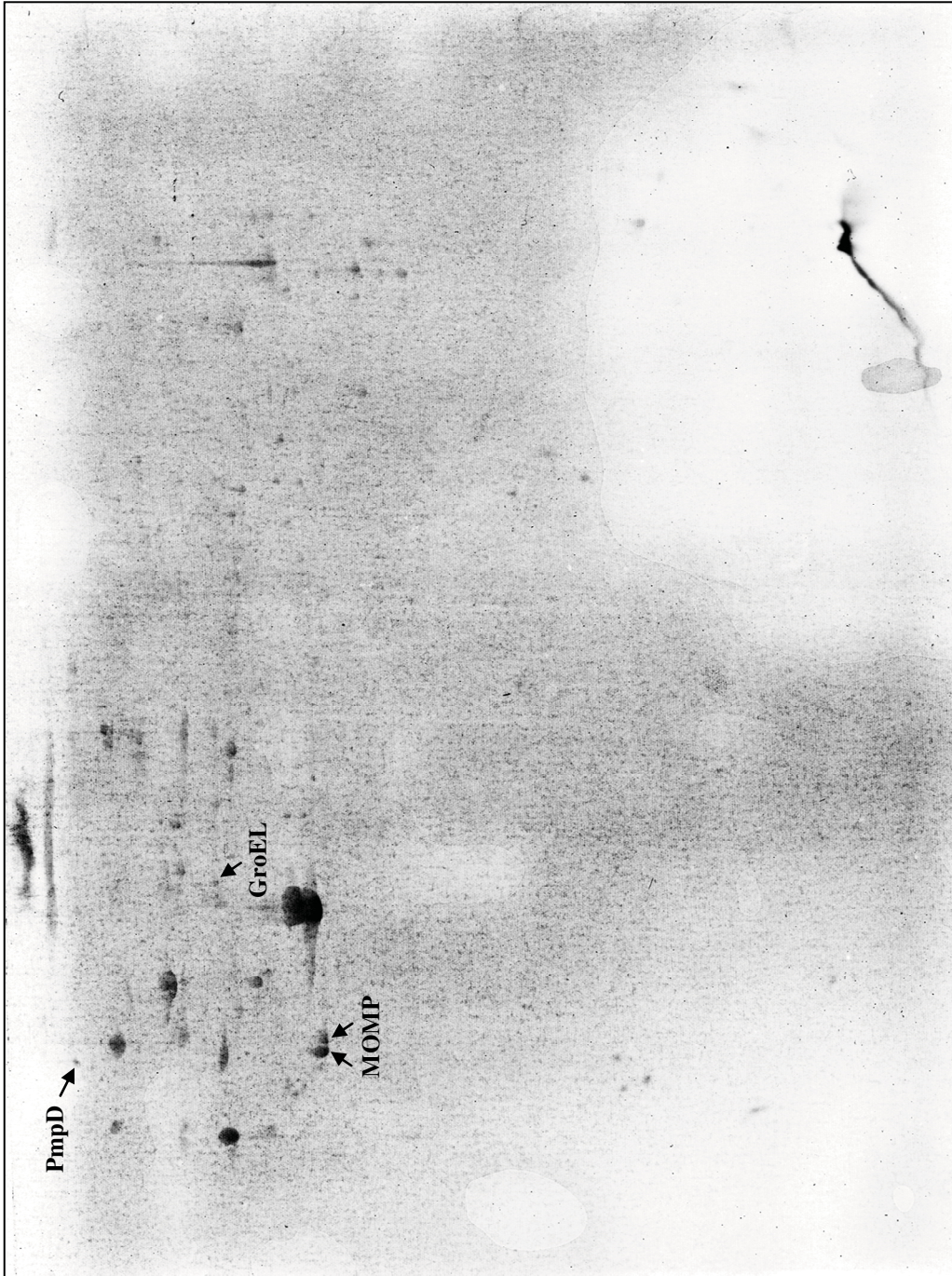


Fig. 31: 2D gel of purified proteins from RBs grown in HeLa cells for 24 h.



**Fig. 32: 2D gel of purified proteins from RBs grown in fibroblasts for 24 h.**

**Table 11: Proteins from HeLa gel identified with MS (\*MS/MS)**

<b>name</b>	<b>protein description</b>	<b>identified MS matches</b>	<b>accession number</b>	<b>theoretical MW (kDa)</b>	<b>Mascot Score</b>	<b>sequence coverage (%)</b>
<b>AhpC</b>	thioredoxin peroxidase	CT D/UW-3/CX	gil15605333	21.70	77	54.87
<b>CdsD</b>	Phosphopeptide binding protein; predicted inner membrane ring protein of TTSS; homologue to YscD	CT 70 CT D(s)2923	gil255349053 gil255507271	89.59 89.58	216 216	59.59 59.59
<b>CT017</b>	hypothetical protein	Ctra70_00090 (CT 70) CT017 (CT D/UW-3/CX)	gil255348379 gil15604735	47.70 47.76	102 117	45.73 46.65
<b>CT066</b>	hypothetical protein	CT D/UW-3/CX	gil15604785	17.94	32.8	52.23
<b>CT621</b>	hypothetical protein; TTSS secreted into cytosol and nucleus (Hobolt-Pedersen <i>et al.</i> , 2009)	G9768_03260 (CT G/9768) CT621 (CT D/UW-3/CX) CTL0885 (CT 434/Bu) CTDEC_0621 (CT D-EC) Ctra70_03315 (CT 70) CTB_6251 (CT B/TZ1A828/OT)	gil296436157 gil15605352 gil166154836 gil297748751 gil255349003 gil237804971	92.57 92.65 92.57 93.22 92.68 92.63	97.2 103 98.2 94.4 147 91.3	47.24 45.31 42.31 45.04 51.32 43.63
<b>CT623</b>	hypothetical protein	CHLPN 76 kD protein-like (CT A/HAR-13) CT D/UW-3/CX*	gil76789362 gil15605354	49.99 48.34	41.8 117.5	26.91 7.18
<b>DhnA</b>	fructose-bisphosphate aldolase	CT D/UW-3/CX*	gil15604935	37.96	102.3	5.75
<b>DnaK</b>	molecular chaperone DnaK, heat shock protein 70	75 kD membrane protein (CT)* <i>C. muridarum</i> Nigg CT D/UW-3/CX	gil144555 gil270285464 gil15605121	70.45 70.53 70.78	181.48 85.5 104	7.82 41.37 48.48
<b>Dut</b>	Deoxyuridine 5'-triphosphate nucleotide-hydrolase	CT D/UW-3/CX <i>C. muridarum</i> Nigg CT D/UW-3/CX	gil15605013 gil7190605 gil15605013	15.33 16.22 15.33	63.78 61.8 78.1	25.52 54.19 77.24
<b>EF-G</b>	Elongation factor G	CT 70	gil255348805	76.49	117	45.39
<b>EF-Ts</b>	Elongation factor Ts	CT A/HAR-13 CT D/UW-3/CX* CT D(s)2923	gil76789419 gil15605412 gil255507286	30.78 30.86 30.76	95 27.59 107	63.12 3.90 67.73

		CT	gil46370964	21.93	98.3	78.71
<b>EF-Tu</b>	elongation factor Tu	CT D/UW-3/CX	gil15605043	43.27	91.2	51.52
<b>Eno</b>	phosphopyruvate hydratase, enolase	CT 434/Bu CT D/UW-3/CX	gil166154802 gil15605316	45.41 45.41	45.2 45.2	44.58 37.50
<b>GatA</b>	aspartyl/glutamyl-tRNA amidotransferase subunit A	CT D/UW-3/CX	gil15604721	53.55	80.20	50.51
<b>GroEL</b>	Chaperonin GroEL, heat shock protein 60	Heat shock protein ( <i>C. muridarum</i> )* chaperonin GroEL (CT A/HAR-13) chaperonin homologue ( <i>C. psittaci</i> )* chaperonin GroEL (CT 6276) groE (CT)*	gil402333 gil76788825 gil7240534 gil255310911 gil144505	58.11 58.08 44.97 58.10 58.03	94.63 57.30 106.95 89.50 43.98	6.80 23.7 3.36 36.03 2.21
<b>GroES</b>	Co-Chaperonin 10	CT*	gil1589856	10.65	121.78	18.56
<b>MOMP</b>	major outer membrane protein	CT CT CT CT CT CT CT CT CT CT D/UW-3/CX CT D(s)2923 CT CT	gil209363151 gil209363125 gil209363119 gil61696984 gil11561792 gil209363153 gil209363119 gil11561792 gil15605414 gil255507288 gil209363119 gil209363153	39.37 39.42 39.41 33.51 41.42 39.37 39.41 41.42 42.41 42.48 39.41 39.37	97 108 108 83.60 78.50 95.30 107 75.5 95.2 94 85.7 99.6	58.68 62.53 61.71 66.34 60.52 66.67 66.67 49.61 51.15 51.15 43.25 49.86
<b>PdhC</b>	branched-chain alpha-keto acid dehydrogenase subunit E2	CT D/UW-3/CX* CT 434/Bu	gil15604968 gil166154458	46.29 46.37	69.99 81.30	3.50 37.76
<b>Pnp</b>	polynucleotide phosphorylase/polyadenylase	CT D/UW-3/CX	gil15605577	75.45	70.4	32.66
<b>PorB</b>	outer membrane protein B	CT D/UW-3/CX* CT D/UW-3/CX*	gil15605446 gil15605446	37.37 37.37	28.65 36.18	4.41 3.82
<b>RpoB</b>	DNA-directed RNA polymerase subunit beta	CT 434/Bu	gil166154525	139.97	205	29.87
<b>RpsA</b>	30S ribosomal protein S1	CT E/11023	gil296438403	63.46	110	30.93
<b>Rs7</b>	30S ribosomal protein S7	<i>C. muridarum</i> Nigg	gil15835337	17.80	72	52.23

**Table 12: Proteins from fibroblast gel identified with MS (\*MS/MS)**

<b>name</b>	<b>protein description</b>	<b>identified MS matches</b>	<b>accession number</b>	<b>theoretical MW (kDa)</b>	<b>Mascot Score</b>	<b>sequence coverage (%)</b>
<b>GroEL</b>	Chaperonin GroEL, heat shock protein 60	CT 6276	gil255310911	58.10	110	39.52
<b>MOMP</b>	major outer membrane protein	CT* CT D(s)2923 CT CT CT CT CT CT CT CT D/UW-3/CX CT CT CT CT D(s)2923 CT CT D/UW-3/CX CT	gil40719 gil255507288 gil11561792 gil38683387 gil38683369 gil168478744 gil168478718 gil168478732 gil15605414 gil61696984 gil38683369 gil168478718 gil255507288 gil168478744 gil15605414 gil11561792	42.51 42.48 41.42 34.00 38.70 41.43 41.43 41.34 42.41 33.51 38.70 41.43 42.48 41.43 42.41 41.42	137.6 128 92.2 89.5 95.6 94.5 105 94.6 117 93.3 105 116 143 105 132 102	8.91 61.83 60.52 63.49 63.33 61.82 61.98 62.24 61.83 65.05 63.33 61.98 61.83 61.82 61.83 60.52
<b>PmpD</b>	polymorphic outer membrane protein D	CT 70 CT D-EC	gil255349213 gil297748940	160.47 161.63	110 72.4	27.19 21.59

## 7 Acknowledgement

### Danksagung

Ich möchte Herrn Prof. Dr. Eberhard Straube herzlich dafür danken, dass er mir die Möglichkeit gegeben hat, diese Dissertation am Institut für Medizinische Mikrobiologie des Universitätsklinikums Jena anzufertigen. Dies ermöglichte mir die Bearbeitung eines äußerst interessanten Themengebietes. Außerdem danke ich ihm dafür, dass er immer für Fragen jeglicher Art zur Verfügung stand und mich auf allen Ebenen während meiner Promotionsphase freundlich unterstützte.

Herrn PD Dr. Jürgen Rödel gilt mein größter Dank für die Bereitstellung dieses sehr interessanten Promotionsthemas, für die intensive Betreuung während meiner Promotion und seine freundliche Unterstützung. Außerdem danke ich ihm für die vielen konstruktiven, hilfreichen Vorschläge und Diskussionen, die mir während der Erstellung dieser Arbeit sehr viel geholfen und zu meiner wissenschaftlichen Weiterentwicklung beigetragen haben.

Bei Herrn PD Dr. Micheal Knittler sowie Dorothee Fiegl bedanke ich mich außerdem für die schöne, erfahrungsreiche Zeit während meines Forschungsaufenthaltes in Tübingen, für die vielen interessanten Gespräche sowie für die Bereitstellung der MHCI-, TAP1- und TAP2-Antikörper.

Meinen Kollegen am Institut für Medizinische Mikrobiologie danke ich sehr für die wunderbare Atmosphäre und für die unvergesslichen Erlebnisse. Hier möchte ich insbesondere Katharina Wolf, Hangxing Yu, Svea Sachse, Katja Schwarzer, Katrin Prager, Jürgen Baumert und Beate Hermann für die vielen konstruktiven Gespräche, für ihre Hilfsbereitschaft und die gemeinsamen schönen und humorvollen Momente im Laboralltag danken, die immer für eine gute Stimmung und freundschaftliche Verhältnisse sorgten.

Weiterhin gilt mein bester Dank Dr. Martin Förster für die Unterstützung bei den Durchflusszytometrie-Experimenten, für das Korrekturlesen dieser Arbeit sowie für die vielen hilfreichen, freundschaftlichen Hinweise für deren Erstellung. Mein Dank gilt auch Herrn Dr. Olaf Kniemeyer für die Möglichkeit, die Proteomanalyse in seinem Labor am HKI in Jena durchzuführen, Frau Prof. Dr. Elisabeth Liebler-Tenorio für die Erstellung der Elektronenmikroskopie-Aufnahmen sowie Frau Dr. Vera Forsbach-Birk für die freundliche Bereitstellung des CPAF-Antiserums.

Außerdem danke ich Herrn Dr. Carsten Thoms als Manager der Graduiertenschule JSMC für die sehr gute Betreuung seitens der JSMC. Großer Dank gilt auch der JSMC für die finanzielle Unterstützung sowie für die soziale und wissenschaftliche Vernetzung mit anderen JSMC-Studenten und Instituten in Jena.

Des Weiteren danke ich meiner langjährigen Freundin Ulrike Ellguth-Malakhov von Herzen für das Korrekturlesen auf Grammatik und sonstige fehlerhafte Ausdrücke der englischen Sprache.

Mein herzlichster Dank gilt meinem Lebenspartner John Ebert und meiner ganzen Familie, deren Liebe, Ermutigung und Unterstützung mir immer sehr viel Kraft und Motivation gaben und mir als Lebensgrundlage für die Zeit während der Promotion unentbehrlich erschienen.

## 8 Curriculum vitae

Christina Große

born 10<sup>th</sup> January 1982 in Jena

1988 – 1989	Johann-Gottlieb-Fichte-Oberschule, Jena, Grundschule
1989 – 1992	Heinrich-Heine-Schule, Jena, Grundschule
1992 – 2000	Staatliches Gymnasium am Anger, Jena
10/2000 – 05/2007	Study of biology at the Friedrich-Schiller-University Jena Subjects: Microbiology, Medical Microbiology, Genetics
01/2004 – 06/ 2004	Erasmus student at the Imperial College London, UK (ERASMUS/SOCRATES-Programm)
03/2006 – 05/2007	Diploma thesis at the Leibniz Institute for Natural Product Research and Infection Biology e.V. Hans-Knöll-Institute, Jena, Department for Molecular and Applied Microbiology Topic: „Die Proteinkinase A von <i>Aspergillus fumigatus</i> : Identifizierung potentieller Zielproteine“
10/2007 – 04/2011	Member of the Institute for Medical Microbiology, University Hospital Jena
since 03/2008	PhD fellow of the excellence graduate school „Jena School for Microbial Communication“
since 09/2011	Research fellow at the Junior Research Group “Novel Diagnostic Tools for Culture-Independent Sepsis Pathogen Detection” at the Center for Sepsis Control and Care, University Hospital Jena

## 9 Publications

### 9.1 Journal publications

**Grosse, C., Heinekamp, T., Kniemeyer, O., Gehrke, A., Brakhage, A. A.** 2008. Protein Kinase A regulates Growth, Sporulation, and Pigment Formation in *Aspergillus fumigatus*. Appl. Environ. Microbiol. 74 (15): 4923-33.

**Rödel, J., Große, C., Yu, H., Wolf, K., Otto, G. P., Liebler-Tenorio, E., Forsbach-Birk, V., Straube, E.** 2012. Persistent *Chlamydia trachomatis* infection of HeLa cells mediates apoptosis resistance through a *Chlamydia* protease-like activity factor-independent mechanism and induces High mobility group box 1 release. Infect. Immun. 80 (1): 195-205.

### 9.2 Conference contributions

**Poster:** Differences in the developmental cycle of *Chlamydia trachomatis* within epithelial cells and fibroblasts. 6th meeting of the European Society of Chlamydia Research, Aarhus, Denmark, 2008.

**Talk:** Differences in the developmental cycle of *Chlamydia trachomatis* within epithelial cells and fibroblasts. 7th German *Chlamydia* Workshop, Lübeck, Germany, 2009.

**Poster:** The role of type I interferon for enhancing the MHC class I antigen presentation pathway in *Chlamydia*-infected cells. 8th German *Chlamydia* Workshop, Munich, Germany, 2010.

**Poster:** *Chlamydia*-host cell interaction – differences during active and persistent infection. MiCom2010, Jena, 2010.

**Talk:** Degradation of the cellular mRNA export factor NXF1 by *Chlamydia trachomatis*. 9th German *Chlamydia* Workshop, Ascona, Switzerland, 2011.

## **10 Statement**

### **10.1 Selbständigkeitserklärung**

Hiermit erkläre ich, dass ich die vorliegende Arbeit selbstständig und nur unter Verwendung der angegebenen Hilfsmittel und Literaturquellen angefertigt habe. Ich habe alle Dienstleistungen und Materialien, die ich von Dritten erhalten habe, ordnungsgemäß als solche gekennzeichnet.

Jena, den 28.03.2012

Christina Große

### **10.2 Erklärung zur Dissertation**

Hiermit erkläre ich, dass ich die vorliegende Dissertationsschrift noch nicht als Prüfungsarbeit für eine staatliche oder andere Prüfungen eingereicht habe. Des Weiteren versichere ich, dass ich bisher noch keinen Antrag zur Eröffnung des Promotionsverfahrens an einer anderen Hochschule eingereicht habe. Ich versichere, dass ich nicht die Hilfe eines Promotionsberaters in Anspruch genommen habe und dass Dritte keine geldwerte Leistungen für Arbeiten, die im Zusammenhang mit dem Inhalt dieser Dissertation stehen, von mir erhalten haben. Die geltende Promotionsordnung der Biologisch-Pharmazeutischen Fakultät der FSU Jena ist mir bekannt.

Jena, den 28.03.2012

Christina Große